CANNABINOID 2 RECEPTOR-BASED MODULATION OF THE IMMUNE RESPONSE IN EXPERIMENTAL MODELS OF CNS INJURY

by

Yan Burkovskiy

Submitted in partial fulfilment of the requirements

for the degree of Doctor of Philosophy

at

Dalhousie University

Halifax, Nova Scotia

May 2019

DEDICATION PAGE

This thesis is dedicated to my colleagues, friends, and family who have encouraged and supported me throughout this degree.

TABLE OF CONTENTS

LIST OF TABLES

LIST OF FIGURES

ABSTRACT

One of the most important outcome-limiting medical risks after an acute CNS injury, such as stroke, spinal cord or traumatic brain injury, is an increased susceptibility to infections. This dysregulation of the immune system has been termed CNS injury-induced immunodeficiency syndrome (CIDS). The underlying mechanisms that are responsible for CIDS are still not elucidated but are hypothesized to be promoted by the injured brain. The endocannabinoid system (ECS) is responsible for key homeostatic functions in both the CNS and immune system. Local upregulation of the ECS occurs following CNS injury and represents an adaptive mechanism to limit neuroinflammation. It has been shown that activation of CB2Rs causes an immunosuppressive effect, suggesting that CB2R activity may contribute to peripheral immunosuppression after CNS injury. The work in this dissertation investigated whether CB2R modulation can prevent or reduce the severity of CIDS.

Experimental CNS injury was induced in C57Bl/6 mice via two models – (1) an intracerebral injection of the vasoconstrictor peptide, endothelin-1 (ET-1) and (2) surgical hypoxia-ischemia. The immune response to bacterial endotoxin was studied 24 hours after the CNS injury by intravital microscopy (IVM) to assess leukocyte recruitment in the peripheral (gut), as well as in local (brain) microcirculation. Neurological impairment and brain infarct volume were evaluated across treatment groups. Circulating cytokine and adhesion molecule levels were also assessed. CB2R expression in peripheral tissue was measured with qRT-PCR.

Results suggest that pharmacological manipulation of the CB2R may present a viable therapeutic approach – early CB2R activation with HU308 reduced brain injury size and ameliorated the immune function, whereas late CB2R inhibition with AM630 reduced the severity of immune suppression. In conclusion, CB2R modulation may prevent CIDS in acute CNS injury by reducing the initial damage to the brain or to directly improve the immune activity in cases where CIDS is already physiologically established. Future studies should focus on investigating various time points throughout the onset of CIDS, as well as on elucidation of the pathways involved in CIDS onset to identify the optimal treatment targets and time window for the proposed CB2R modulation therapies.

LIST OF ABBREVIATIONS USED

2-AG 2-arachidonoylglycerol

AA arachidonic acid

AC adenylate cyclase

ACEA arachidonyl-2'-chloroethylamide

ACPA arachidonyl-cyclopropylamide

AEA N-arachidonoylethanolamine

AM630 6-Iodopravadoline

AMP adenosine monophosphate

ANOVA analysis of variance

AP anterior-posterior

APC antigen presenting cells

BBB blood-brain barrier

BDNF brain-derived growth factor

BSA bovine serum albumin

CACF Carleton animal care facility

cAMP cyclic adenosine monophosphate

CASP colon ascendens stent peritonitis

CB1 cannabinoid receptor 1

CB2 cannabinoid receptor 2

CBC cannabichromene

CBD cannabidiol

CBG cannabigerol

CBN cannabinol

CIDS CNS injury-induced immunodeficiency syndrome

CNS central nervous system

COX-2 cyclooxygenase-2

cPLA2 cytosolic phospholipase A2

CREB cAMP response-binding protein

CT cycle threshold

DAGL diacylglycerol lipase

DMSO dimethyl sulfoxide

DV dorsal-ventral

ECS endocannabinoid system

ERK extracellular signal regulated kinases

ET-1 endothelin-1

FAAH fatty acid amide hydrolase

FABP fatty acid binding proteins

FACS fluorescence-activated cell sorting

FCD functional capillary density

FDA food and drug administration

FITC fluorescein isothiocyanate

GPCRs G protein coupled receptors

HAI hospital-acquired infections

HI hypoxia-ischemia

HIS hyperspectral imaging

HPA hypothalamus-pituitary-adrenal axis

I.P. intraperitoneal

I.V. intravenous

ICAM intercellular adhesion molecule

IFN-γ interferon-γ

IKK IκB kinase

IL interleukin

IVM intravital microscopy

JAM junctional adhesion molecules

JNK c-Jun NH2-terminal kinase

LBP LPS-binding protein

LFA-1 lymphocyte function associated antigen-1

LOX lipoxygenase

LPS lipopolysaccharide

MAGL monoacylglycerol lipase

MAPK mitogen activated protein kinase

MHC major histocompatibility complex

ML medial-lateral

NAPE-PLD N-acyl phosphatidylethanolamine

NF-κB nuclear factor κB

NGF nerve growth factor

NK natural killer

NMDA N-methyl-D-aspartate

NO nitric oxide

NOD nucleotide-binding oligomerization domain

OBT open bench top

PAMP pathogen associated molecular pattern

PASS preventive antibiotics in stroke study

PAT preventative antibiotic treatment

PECAM platelet endothelial cell adhesion molecule

PKA protein kinase A

PLC phospholipase C

PND postnatal day

PPAR peroxisome proliferator-activated receptor γ

PRR Pattern recognition receptor

PSGL-1 P-selectin glycoprotein ligand-1

qRT-PCR quantitative reverse transcriptase polymerase chain reaction

RAGE receptor for advanced glycation end products

RCCA right common carotid artery

RIG-1 retinoic acid-inducible gene-1-like receptors

S.C. subcutaneous

SCI spinal cord injury

TACE TNFa-converting enzyme

TBI traumatic brain injury

TEM transendothelial cell migration

TGF-β transforming growth factor β

TLR toll like receptor

TNFα tumor necrosis factor-α

TTC tetrazolium chloride

VCAM vascular cellular adhesion molecule

VLA-4 very late antigen-4

Δ9-THC Δ9-tetrahydrocannabinol

ACKNOWLEDGEMENTS

First, I would like to thank my supervisor Dr. Christian Lehmann for providing me with his guidance, expertise, support and patience throughout my degree. The skills that I have learned from my mentor are life-long instruments which I will continue to use in both professional and personal aspects of life.

It would be very hard to progress as far as I did without Dr. Juan Zhou and her immense contribution in teaching me the surgical and research skills throughout my path.

My advisory committee members – Dr. Melanie Kelly, Dr. Ryan Pelis and Dr. Morgan Langille have been very helpful in providing the guidance, feedback and pushing me forward in the direction that challenged me.

I also extend great appreciation to Dr. Easton and Dr. Warford for their technical expertise and for providing the stereotaxic equipment for one of the experimental models used in my work.

It would be very difficult to do the research without a very supportive and friendly lab environment with great members, these people have left a great impression on me, as well as have helped me grow both as a person and as a researcher - Dr. Tom Toguri, Dr. Joel Sardinha, Maral Aali, Taylor Thorburn, Sara Whynot, Nancy McGrath, Patricia Colp, Suzanne Pearce and many others.

Finally, a special acknowledgement is given to the mice that went through the experimental protocols and ultimately made this research possible.

Chapter 1: Introduction

1.1. Foreword

This thesis focuses on examining the role of the endocannabinoid system (ECS) in regulating the systemic immune response after central nervous system (CNS) injury. The experimental work evaluates an immunopharmacological approach targeting the cannabinoid 2 receptor (CB2R), with special consideration to time-sensitivity and time-dependability of post CNS injury pathophysiology. The thesis follows a standard format, where each section in the introduction presents important theory and concepts essential for the understanding of the aims, objectives and findings of my research. This is followed by the central hypothesis, along with a brief explanation of the main objectives that have been explored with my experimental work. Next, I present a brief overview of experimental *in vivo* models used to generate the data in this thesis. I then describe the materials and methods used to obtain and analyze the experimental evidence, followed by the presentation of acquired data. Finally, I present a balanced discussion and critical evaluation of the experimental findings, as well as their implications for the field. I conclude by discussing a pilot project that branched from my research and potential future directions.

1.2. CNS injury – Definition & Epidemiology

The CNS consists of the brain and spinal cord and receives the "central" in its name due to its important role in the body as a regulator and coordinator of body's functions. CNS injury is an umbrella term that includes multiple and potentially debilitating conditions, such as stroke, spinal

cord injury (SCI) or traumatic brain injury (TBI). CNS injury can be acquired via physical impact trauma, such as in the case of TBI or can result from a closed-head hemorrhage, such as in the case of hemorrhagic stroke. Loss of blood supply to a certain region of the brain causes an ischemic injury, such as in the case of ischemic stroke. Spinal cord injury varies not only in the type of impact but also in the level of injury, as it dramatically changes the severity of impairment and its derived neurological complications.

Functional impairments from CNS damage depend upon the severity, mode and the anatomical location of the injury. Statistically, stroke represents a major cause of death and disability in many countries. Epidemiologically, stroke represents a significant challenge as the absolute number of stroke cases, along with those living or dying from consequences of stroke has been steadily increasing. In 2013, globally, there were 25.7 million stroke survivors with 6.5 million deaths from stroke (Feigin et al., 2015). The majority of the stroke burden was associated with developing countries, accounting for nearly 73% of all stroke-related deaths (Venketasubramanian et al., 2017). The estimated direct and indirect costs of stroke care in United States alone has been estimated at nearly $70 billion for 2009 alone (Brown et al., 2006; Demaerschalk et al., 2010). Stroke inflicts a heavy societal toll as it is the leading cause of chronic disability, second leading cause of vascular dementia (Pendlebury & Rothwell, 2009) and the fourth leading cause of death in the US (Roger et al., 2011). While a large body of research focuses on stroke treatment and prevention, a significant portion of research is focused on the resulting pathophysiological complications after the brain injury, which are associated with neurological impairment, reduction of quality of life and worsening of patient outcome. The incidence of stroke increases with age, doubling for every single decade after age 55 (Ovbiagele & Nguyen-Huynh, 2011). To put that in perspective, in the 35 to 44 cohort, the incidence of

stroke is 30-120 out of 100,000 per year, whereas the 65 to 74 cohort carries an incidence that is 670-970 out of 100,000 per year (Roger et al., 2011).

TBI also represents a major public health issue and a socioeconomic problem globally. TBI can be incredibly complex with multiple underlying pathologies and is generally defined as an alternation in brain activity caused by an external force (Menon et al., 2010). TBI can be caused by a wide range of etiologies – automobile accidents, falls, assaults and many others (Hazeldine et al., 2015a). In terms of numbers, TBI resulted in over 177,000 admissions in one year in UK, 1.7 million cases of TBI in US, with 52,000 fatalities (Hazeldine et al., 2015a).

SCI is a major detrimental event that results in dramatic alterations in sensory, motor and/or autonomic function, impacting physical, psychological, as well as social well-being (Furlan et al., 2011). The socioeconomic burden of SCI is rather substantial, as the required level of medical care is usually acute, with many secondary complications in patients (Krueger et al., 2013). In Canada, the estimated economic burden per individual with SCI can range from $1.5 million (incomplete paraplegia) to $3.0 million (complete paraplegia) (Krueger et al., 2013). Combined, the estimated annual economic burden of new 1389 SCI patients is estimated at $2.67 billion (Krueger et al., 2013). An attempt that tried to put together a SCI data repository revealed that the global prevalence of SCI is 236-1009 per million (Cripps et al., 2011). The same data set, predictably shows that good SCI prognosis is usually associated with being in a developed country, whereas SCI in Sub-Saharan Africa, along with being the highest level of violence-related SCI in the world, is also is likely to be a fatal condition within a year (Cripps et al., 2011). In summary, acute CNS injury and the resulting neurological and functional

complications are both serious medical and socioeconomic challenges that require immediate attention from preclinical and clinical research fields.

1.3. The Immune System

Knowing the purpose and function of the immune system is crucial to understanding the resulting pathophysiology after CNS injury. The immune system can be defined as the collection of cells, tissues and molecules responding to inflammation and infections (Abbas et al., 2014). The principal function of the immune system, which drives many of the described physiological responses and is impaired by the resulting pathophysiology after CNS injury, is to prevent infections and to remove established infections. Life-threatening outcomes of defective or compromised immune response only highlight the vast importance of the immune system. Vaccination or stimulation of the immune response against pathogens is one of the most effective methods used to protect individuals against infections and has led to the world-wide eradication of smallpox, the only disease that has been eliminated by human intervention (Abbas et al., 2014). The function of the immune system extends well beyond infectious disease. Growth of some tumors is prevented by an immune response, an exploited property by novel approaches in cancer therapy, some of which involve stimulating the immune response against tumor cells (Abbas et al., 2014). Once the infection is neutralized or a tumor has been prevented from growing, the resulting cell mass needs to be cleared and the area repaired. The immune system is involved in that as well, adding clearance of dead cells and tissue repair initiation to its functional repertoire. (Abbas et al., 2014). Beneficial roles of the immune system are many, which is the reason why abnormal immune function is the cause of a multitude of inflammatory

diseases with staggering morbidity and mortality across the globe. Even a normally functioning immune system can be a significant barrier for some organ transplantation patients and be the deciding factor to the life-saving procedure being a success or a failure. For example, the rejection of newly transplanted organ begins via recognition by the immune system, which treats the foreign cells as an invading tissue, compromising the outcome of the performed procedure. Immune cells, or rather the molecules they produce, are also extremely useful in clinical practice. For example, antibodies, which are proteins manufactured by the immune cells are widely used in medical research and testing. Antibodies have been tuned to block or eliminate pathogens and are used for treatment of a variety of immunological disorders and diseases, including cancer (Abbas et al., 2014). This briefly outlines the importance of the immune system and its deep integration into many physiological functions. However, to further understand the complexity of the immune system, we need to dive into major components of the immune system, immune signaling pathways and the role of various immune cells.

1.3.1. Inflammation

Inflammation is the result of organism's response to pathogens, infection or tissue damage. The main purpose of such a response is to avoid damage, begin tissue repair and restore functioning back to homeostatic levels, with minimal side effects or shortcomings (Abbas et al., 2014). There are five classic signs of inflammation – redness, heat, swelling, pain and loss of function (Lawrence et al., 2002). Each one of these signs is associated with physiological processes associated with an immune response, such as vascular changes, migration and infiltration of immune cells and release of chemical messengers to modulate the inflammatory response.

Depending on the trigger of the inflammation, levels of immunomodulators, individual biological aspects and many other factors, the progress and time scale of inflammation can range from an acute immediate response (e.g. a small cut on the skin) to something that becomes a chronic and uncontrolled pathological condition (e.g. rheumatoid arthritis). It is therefore logical to separate the concepts of immune response based on the associated specifics and time scale, as elaborated in the following section.

1.3.2. Innate & Adaptive Immunity

Immune defense mechanisms consist of native or innate immunity and specific or adaptive immunity. The innate immune defense line begins at epithelial barriers, providing both a physical barrier as well as natural antibiotics, called defensins, secreted by epithelia, blocking the entry of microbes. These defensins are able to contribute to immune defense by creating pores or disrupting the cellular membrane of invaders (Tosi, 2005). If this defense line is breached and microbes enter the circulation or surrounding tissues, they will now be targeted by neutrophils, monocytes, phagocytes, natural killer cells, mast cells, granulocytes as well as plasma proteins such as α- and β-defensins (Warrington et al., 2011). Protection against threatening infections and their rapid elimination is mediated by innate immunity, whereas the highly specialized and effective response is provided by the adaptive immunity. Innate immunity is always present in a healthy individual and is quick in its response, compared to the adaptive immune response; this relies on lymphocyte expansion and differentiation (see Figure 1) in response to an invader and adapts to the presence of pathogens, “remembering” their markers for future protection (Abbas et

al., 2014). Innate immune response also bolsters the adaptive immune response against infectious pathogens.

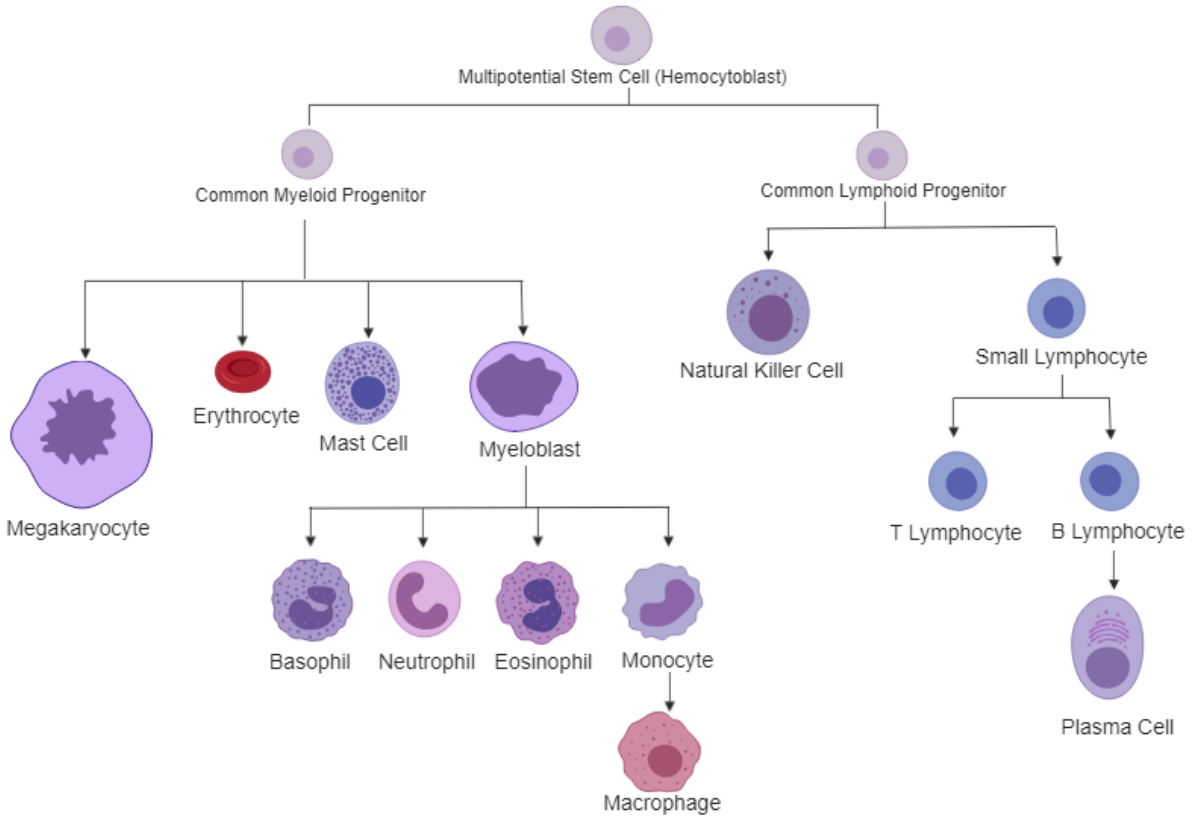

Figure 1. **Formation and Differentiation of Cellular Components of Blood.**

This process is known as hematopoiesis. The process begins with differentiation of multipotent stem cells into blood and immune progenitor cells, giving rise to a large variety of different cell types responsible for different tasks of the circulatory and immune systems.

From an evolutionary stand-point, the innate immunity is much older phylogenetically, with the adaptive immune response coming in later into phylogeny. After encountering a foreign pathogen, the innate immune system is able to respond extremely quickly (within minutes to hours). This quick response can be mounted primarily due to the system's ability to detect pathogen-associated molecular patterns (PAMPs), with the most common gram negative bacterial PAMP being lipopolysaccharide (LPS), an endotoxin that is found on the cellular surface of bacteria and the most common gram positive bacterial PAMP being peptidoglycan, also located on the cellular surface of bacteria. These PAMPs are recognized by pattern recognition receptors (PRRs), which are expressed on the immune cell surface and are actively searching for the molecular patterns that would signify the presence of pathogens. Furthermore, tissue and cell damage, for example during a severe CNS injury, releases molecules from the damaged cells, called alarmins or danger-associated molecular pattern molecules, which are classified as "sterile" inflammatory signaling mediators (Bianchi, 2007; Saïd-Sadier & Ojcius, 2012). PRRs are a rather large family of immune and endothelial receptors and include toll like receptors (TLRs), nucleotide-binding oligomerization domain-like receptors (NODs), C-type lectin receptors and retinoic acid-inducible gene-1-like receptors (RIG-1) (Gordon, 2002; Thompson et al., 2011). Each type of PRRs performs a very important detection function, with its assortment of members in each family.

The most relevant PRR to my thesis is the TLR family, with more than 10 discovered distinct members in both humans and mice (Kawasaki & Kawai, 2014). TLRs, once activated by the trigger molecules, PAMPs activate downstream signaling pathways that promote the innate immune response, with resultant production of inflammatory cytokines, type I interferon (IFN) and other inflammatory mediators (Kawasaki & Kawai, 2014). TLR family of receptors can be

expressed on the cell surface, for extracellular detection of trigger molecules, as well as intracellularly, for cytosolic detection of pathogens (Kawasaki & Kawai, 2014; Takeda et al., 2003). The significance of TLR for my experimental work is that TLR4 acts as a receptor for LPS (Lu et al., 2008; Poltorak et al., 1998). LPS, acting as a PAMP, is an excellent challenge for the immune system and its activation has been linked to the onset of severe septic shock in sepsis patients with gram-negative bacterial infections (Deng et al., 2013).

Structurally, TLR4 is a transmembrane bound receptor, with an extracellular domain responsible for PAMP binding, a series of transmembrane binding domains and an intracellular binding Toll-interleukin 1 (IL-1) receptor (TIR) (Lu et al., 2008; Yanaba et al., 2009). TLR4 has been reported to be expressed on multiple cell types – macrophages, dendritic cells, neutrophils, eosinophils, basophils, T cells, B cells, as well as endothelial and epithelial cells (Akira & Takeda, 2004; Lu et al., 2008; Parker et al., 2005; Yanaba et al., 2009). Upon the binding of LPS to LPS-binding protein (LBP) and a formation of a complex, the TLR4 is able to recognize LPS as a targetable PAMP (Akira & Takeda, 2004; Lu et al., 2008). The activation of TLR4 recruits myeloid differentiation primary-response protein 88 (MyD88), which, via downstream signaling, activates IL-1 receptor-associated kinases-1 (IRAK1), -4 (IRAK4) and TNF-receptor associated factor 6 (TRAF6) (Lu et al., 2008). From here, the pathway bifurcates into two separate directions. The first leading to the production of tumor necrosis factor (TNFα), interleukin (IL) -1β and IL-6 via the removal of nuclear factor kappa-light-chain-enhancer of activated B cells kinase (IKK), allowing phosphorylation of NF-κB inhibitor (Lu et al., 2008). The second direction leading to secretion of pro-inflammatory cytokines TNFα and IL-12 via recruitment of transforming growth factor β-activated kinase (TAK1), consequently leading to activation of mitogen-activated protein kinases (MAPKs), phosphorylation of c-Jun N-terminal kinases

(JNKs), extracellular-signaling-regulated kinases (ERKs), p38 and cAMP response-binding protein (CREB) (Chen et al., 2012; Hoshino et al., 1999; Lu et al., 2008). However, there is also evidence that suggests that TLR4 activation could cause a signaling cascade without the direct involvement of MyD88 via TIR domain of TLR4 (Akira & Takeda, 2004; Lu et al., 2008). This alternative route activates NF-κB, as well as interferon-regulatory factor 3 (IRF3) (Akira & Takeda, 2004; Hoshino et al., 1999).

Those pathogens which managed to bypass the defense systems laid down by the innate immunity or evolved to resist it will face the adaptive immune response. While the innate immune response focuses on recognizing general structures shared by microbes, it is not able to detect specific PAMP via its sensing receptors, the adaptive immune response is able to focus and specialize its response via receptors expressed by lymphocytes to the specific molecules present on microbes, in addition to other non-infectious substances (Abbas et al., 2014). These lymphocytes can target the antigens present on invading cells and generate specific antibodies. The antibodies act as "tags", activating and binding phagocytes, utilizing the innate immune system to shut down the threat. The adaptive immune system includes T cells, B cells and antigen presenting cells (APC) (Bonilla & Oettgen, 2010; Warrington et al., 2011). Compared to the innate immune response, the adaptive immune response takes a lot longer to mount – from days to even weeks, especially if the pathogen that was encountered is completely novel, without any antibodies in memory B cells (Bonilla & Oettgen, 2010). In the case of a novel encounter, APCs and B cells completely internalize the microbe, followed by presentation of microbe's antigens on the surface via histocompatibility complex (MHC) protein (Chaplin, 2010). After the antigen is presented extracellularly, T cells are able to bind to the MHC, recognize the antigens and cause T cell proliferation and subsequent production of even more antibodies (Bonilla &

Oettgen, 2010). MHC can elicit a cellular response from both CD8+ T cells and CD4+ T cells, with MHC class I and class II molecules respectively (Dempsey et al., 2003).

The work in this thesis focuses on the innate immune response, as the main molecular trigger for the immune response in all the conducted experiments is LPS. In addition, the timeline of experiments focused on the early and acute phase of inflammation, immediately after the induction of CNS injury, which did not provide enough time for any presence of an adaptive immune response. Nonetheless, it is important to note that both the innate and adaptive immune response do not work in strict isolation and can complement each other in pathogen detection, elimination and clearance.

1.3.3. Microvascular Dysregulation During Inflammatory Response

Every tissue and organ within our body requires an adequate supply of blood to receive the necessary elements such as oxygen and nutrients, as well as to remove waste and metabolism byproducts, such as CO_2. This is provided by the circulatory system, consisting of the heart (cardiovascular), lungs (pulmonary), arteries, veins, and coronary/portal blood vessels (systemic) (Noordergraaf, 1978; Pittman, 2011). Ultimately, the circulatory system ensures the survival of all cells by maintaining the chemical environment at a composition appropriate for normal function (Pittman, 2011). At the macrocirculation level, the circulatory system provides nourishment, assists in fighting pathogens and disease and maintains body homeostasis (Noordergraaf, 1978). It is at the microcirculation level of circulation that the actual exchange and transfer of oxygen, nutrients and wastes occurs between blood and surrounding tissues. The microcirculation consists of endothelial cells, pericytes, smooth muscles cells, as well as

components in the blood stream such as erythrocytes, leukocytes, platelets and plasma. The microcirculation also plays a critical role in body's immune response, as it provides the delivery network for the immune cells to reach their target. The smallest blood vessels (<100 μm in diameter), such as arterioles, capillaries and venules, together compose the microcirculation (Granger & Senchenkova, 2010; Ince, 2005). Control of blood flow within microcirculation is associated via the vascular tone, which in turn is modulated by a range of mechanisms, such metabolic, myogenic and neurogenic (Ellis et al., 2005). The endothelium regulates the vascular tone via endothelium-derived relaxing factor, identified as nitric oxide, which causes vasodilation and platelet deactivation (Lüscher & Tanner, 1993). In terms of contractility, endothelium-derived contracting factors are generated via the cyclooxygenase pathway and by the endothelial cells, which produce endothelin-1, a potent vasoconstrictor peptide (Lüscher & Tanner, 1993). Through the constrictor and dilator influence exerted via extrinsic and intrinsic factors, blood flow can be further affected beyond the regular control of myogenic precapillary sphincters.

Many pathological conditions cause dysregulation in microcirculation, undermining its ability to maintain homeostatic balance in supplied tissues. During a pro-inflammatory response, the immune system causes an increase in blood flow by making vessels dilated, usually though nitric oxide (NO) and other myogenic mediators, such as ion channels, acting on smooth muscle tissue (Ellis et al., 2005). The other important part of the immune "priming" of the microcirculation is an increase in vascular permeability, allowing more immune mediators and cells to be dispersed into regions of interest (Ince, 2005; Secomb, 2017). In general, vascular permeability can be changed via two separate mechanisms – physical trauma and PAMP's (De Backer et al., 2002). In parallel, inflammatory mediators increase the level of expression of adhesion molecules both

on the endothelium and on the surface of leukocytes, changing their patrolling behaviour by favoring leukocyte-endothelial interactions (Granger & Kubes, 1994). Once "primed" and tethered leukocytes reach the site of inflammation, they go through the process of transendothelial migration and proceed towards invading pathogens and damaged tissues (Lawrence et al., 2002). More on leukocyte recruitment will be covered in the following section.

In more critical disease states or severe trauma, the blood flow can be re-distributed to maintain functional perfusion levels in vital organs, causing near-hypoxic and hypoxic conditions in shunted tissues (Ince, 2005). Another factor that causes disruption in blood flow to tissues is a change in deformability of the red blood cells, which is normally necessary to travel through the small-diameter capillaries and venules. The deformability indicates a reversible change of the shape of erythrocytes in response to a deforming force that is usually a combination of vessel shape and the strength of blood flow (Silva-Herdade et al., 2016). Pro-inflammatory cytokines activate inducible NOS (iNOS) resulting in an increase in NO levels, which in turn increases intracellular Ca^{2+} via Ca^{2+}-ATPase channels (Silva-Herdade et al., 2016). Ultimately, this causes a decrease in blood cell's ability to deform, causing the blood cells to physically block the blood vessels and aggregate, thus causing tissue hypoxia (Sielenkämper et al., 2001). Endothelial dysregulation and damage during an inflammatory assault can cause vascular leakage at many sites, also contributing to severe changes in tissue homeostasis and blood supply. Gap junctions between endothelial cells can also be broken down or damaged by an exacerbated immune response via extravasating leukocytes or neutrophil degranulation processes (Wong et al., 2017). At its worst, the accumulation of these factors can severely alter tissue perfusion, ultimately causing cell death and organ failure (Birnbaum et al., 2003; Ince, 2005). The first symptoms of blood supply disruption can be detected at a microcirculatory level. Within a very short period of

time after trauma or acute inflammatory response, the microcirculation will be disrupted due to a loss of function capillary density and impaired oxygen delivery, causing a rapid onset of tissue hypoxia (Ellis et al., 2005).

There has been a consistent growth in microcirculation research and imaging over the past few decades, with now more than 2000 publications per year (Lal & Leahy, 2016). Earliest techniques that required a degree of invasiveness have been replaced by modern high-speed, high-resolution noninvasive techniques that are able to provide clinically relevant information without any disturbance (Lal & Leahy, 2016). Ranging from a simple an inexpensive video capillaroscopy to the newly emerging hyperspectral imaging (HIS), it is thus becoming more feasible to use microcirculation as a diagnostic and monitoring parameter in many pathophysiological conditions (Lal & Leahy, 2016).

1.3.4. Microcirculation in the Brain following CNS Injury

The brain consumes more energy than any other organ in the body and requires an uninterrupted supply of glucose and oxygen delivered through cerebral vasculature. As a result of this need, the brain's primary arterial supply is provided via major internal carotid and vertebral arteries, while the brain itself is extensively covered by a network of arteries and veins, which are called pial blood vessels (Duvernoy et al., 1981). Anatomically, these pial arteries tend to branch off the pial network at right angles straight into brain tissue, similar to veins that run parallel to these arteries, later joining the pial veins (Duvernoy et al., 1981). Similar to other regions in human body, these penetrating arteries branch out into arterioles and into even larger networks of capillaries, supplying the neural tissue very extensively (Duvernoy et al., 1981). Cerebral

microcirculation, which utilizes microvessels consisting mainly of endothelium and smooth muscle layer, is uniquely adapted to fit the specific priority for the regulation of blood flow and permeability of blood vessels within the brain (Rafols, 2015).

The function of blood-brain barrier (BBB) involves restricting the passage of selective molecules and cells through capillaries and was originally thought to depend solely on the physical integrity of the endothelial tight junctions, as well as absence of endothelial transcellular pores (Rafols, 2015). This concept has since evolved into an idea of a "neurovascular unit", which implies interactions between cerebral microvasculature and their functionally-associated neurons (glia), providing a controlled response under normal conditions, but also during CNS injury, such as TBI (Lo et al., 2004). This unit includes not only the transport and diffusion properties of endothelial cells but also those of perivascular astroglial cells, and filtering properties of the basal lamina (Rafols, 2015).

Experimental models of CNS trauma have revealed morphological changes in brain microvasculature, as well as decreases in cerebral blood flow that are associated with neuronal injury and a reduction in cognition (Rafols et al., 2007; Yanagisawa et al., 1988). Major pathology after TBI is rooted in alterations in cerebral blood flow and within microcirculation that are initiated even within minutes after the onset of the traumatic event (Rafols, 2015). It has been reported that in cases of closed-head injuries, as well as after direct brain injury, there is a state of continuous hypoperfusion, which was determined to be independent of brain swelling and has been observed to last from hours to days after the original CNS injury (J. A. Rafols et al., 2007; Steiner et al., 2004). In experimental stroke, the analysis of penumbra cells and neighbouring blood vessels also reveals a series of pathologies, namely, structural changes in

nerve cells, microvasculature, metabolic changes due to edema formation and onset of hypoperfusion, coupled with Ca^{2+} ion induced constriction of endothelial cells, vascular smooth muscle cells and pericytes. In patients with aneurysm surgery or decompressive craniectomy after stroke, researchers also found an increase in arteriolar contractility and a significant blood flow reduction with a decrease in vascular density within the microcirculation.

The microcirculation in postcapillary venules of the brain also displays another very important and prominent pathology – accumulation of leukocytes during early reperfusion after CNS injury (Ding et al., 2002; Ishikawa et al., 1999; Ritter et al., 2000). Ritter et al. (2000) report a significant increase in leukocyte rolling and adhesion in venules and a significant decrease in blood flow in the microcirculation of the brain shortly after reperfusion. It is thought that brain injury triggers expression of a range of cytokines, which attract leukocytes into ischemic sites of the brain, followed by intercellular adhesion molecule (ICAM)-mediated adhesion to the luminal walls of pial microvasculature (Rafols, 2015). This process is then followed by leukocyte migration through the vessel wall into the brain parenchyma, as shown in primate and rodent models (Okada et al., 1994; Wang et al., 1994). These immune-microvascular events are considered to be responsible for the acute inflammatory response that follows after the onset of CNS injury, such as stroke (Rafols, 2015). The contribution of dysregulated microcirculation to the pathology after CNS injury is also demonstrated by a study that infused saline into the ischemic territory of the brain prior to reperfusion, attempting to prevent leukocyte aggregation and vascular plugging, which successfully ameliorated both the inflammatory response and the infarct volume (Ding et al., 2002). In summary, brain microcirculation is a crucial component in the pathophysiological consequences after CNS injury and should be considered not only as a

therapeutic target for improvement but also as a monitoring parameter for medical research and diagnostics.

1.3.5. Leukocyte Recruitment, Tethering, Rolling & Adhesion Mechanisms

As mentioned previously, recruitment of leukocytes is one of the main pillars of the inflammatory response cascade and is essential in elimination of bacterial and non-bacterial pathogens, as well as removal of damaged and dead tissue (Leick et al., 2014). The term "leukocyte" includes all the white blood cells – mononuclear, polymorphonuclear cells and granulocytes, with the most abundant of circulating leukocytes in mammals (approximately 40-70%) being neutrophils (Abbas et al., 2014). Through signaling immune mediators, cytokines and chemokines, leukocytes are mobilized and brought to the site of pathogen presence or dead tissue (Warrington et al., 2011).

Cytokines are specialized proteins that carry out their tasks via paracrine or autocrine signaling to launch or modulate an immune response (Turner et al., 2014). Cytokines are the main drivers of immune modulation and are involved in both acute and chronic inflammation via a dynamic and complex system of interactions, that sometimes can contradict, as the same modulator can switch its role, depending on the level secreted and the type of receptor it binds to (Turner et al., 2014). Cytokines are generated by many cell types – e.g. leukocytes, keratinocytes, osteoblasts and synovial cells (Borish & Steinke, 2003; Turner et al., 2014). Similarly, a single cytokine molecule can bind to multiple receptors, allowing cytokines to have flexibility in activating a particular transduction pathway, ultimately resulting in quite different downstream (Turner et al., 2014).

Chemokines are molecules that are classified as the largest subset of cytokines and are responsible for positioning and migration of leukocytes across the endothelium, in addition to development and differentiation of leukocytes (Borish & Steinke, 2003; Griffith et al., 2014). Chemokines make up a complex system of approximately 50 endogenous chemokine ligands and 20 GPCRs, all working in tandem to generate primary and secondary adaptive and humoral immune responses (Griffith et al., 2014; Lodowski & Palczewski, 2009). There are four families of chemokines – C-X-C, C-C, C, and CX3C (C – cysteine residue, X-amino acid). In terms of their binding targets, C-X-C focuses on neutrophils, whereas C-C focuses on monocyte, dendritic and T-cells interactions (Borish & Steinke, 2003). Most of the cellular receptors that act as binding sites for chemokines are classified as GPCR (Lodowski & Palczewski, 2009). Endothelium bound chemokines CXCL1, CXCL2 and CXCL8 bind to neutrophils to arrest their movement and alter leukocyte-endothelial interactions from rolling to adhesion (Griffith et al., 2014).

The original description used a two-step model to describe leukocyte-endothelial cell interaction in inflammation, consisting of leukocyte rolling via a cell adhesion molecule, called L-selectin or CD62L, followed by firm adhesion via β2 integrins (von Andrian et al., 1991). Integral molecules were discovered and leukocyte transmigration behaviour was extensively studied through the use of function blocking monoclonal antibodies to adhesion molecules and visualization in rabbit postcapillary venules via intravital microscopy (Luscinskas & Gimbrone, 1996). One of the largest shifts in this field was caused when it was discovered that the administration of LPS, TNFα or IL-1, caused the non-adhesive and non-thrombogenic endothelium to become activated and “tuned” it to be responsive to interactions with circulating leukocytes. This was later revealed to be NF-κB pathway dependent and casually triggered by

proinflammatory cytokines or bacterial endotoxins (Bevilacqua & Gimbrone, 1987; Collins et al., 1995).

Leukocytes, in general, follow a multi-step adhesion cascade in vasculature – free flowing leukocytes, initial chemical attraction to the endothelium, slowing down to a low-velocity rolling (step 1), progressing to an arrest of rolling movement and stabilizing adhesion (step 2), followed by leukocyte flattening (step 3), then crawling on the vascular endothelium, and going through transendothelial cell migration (TEM) between (paracellular route) or through (transcellular) the vascular endothelium (step 4), finally completing the transmigration out of postcapillary venules via elongation (step 5) (Kolaczkowska & Kubes, 2013) (Figure 2). In order for a free-flowing leukocyte to be tethered in step 1, it must interact with a selectin, a type I transmembrane glycoprotein, which will initiate the process of adherence. Selectins are expressed both on leukocytes and endothelial cells, with L-selectins and P-selectin glycoprotein ligand 1 (PSGL-1) expressed on the former and E-selectins being expressed on the latter (Granger & Senchenkova, 2010; Leick et al., 2014). Interestingly, the expression levels of selectins varies from tissue to tissue, with levels of P-selectin being much higher in the microvasculature of the gut compared to the vessels of the skin, despite both being exposed to a large number of potential pathogens (Granger & Senchenkova, 2010). P-selectins are normally stored in specialized vesicles or secretory granules and upon activation, are quickly released into the bi-lipid membrane to present the proteins extracellularly (Kubes & Ward, 2006). These granules are called α-granules if they are located in platelets and Weibel-Palade bodies if they are located in endothelium (Granger & Senchenkova, 2010). In comparison to P-selectin, E-selectin has to be expressed via transcriptional activation, as it is not stored in granules and not available on-demand (Kubes &

Ward, 2006). The transcriptional signals for expression of both selectins are the following cytokines: TNFα, IL-1, IL-4 and IL-13 (Granger & Senchenkova, 2010).

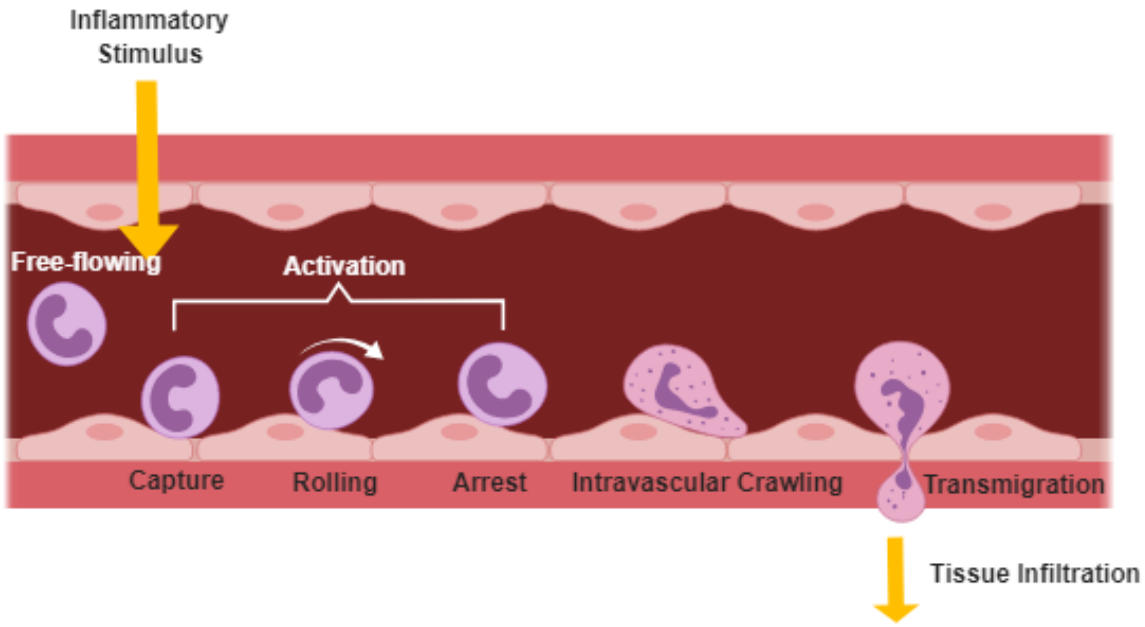

Figure 2. **Leukocyte Activation and Extravasation Schematic.**

A schematic showing basic leukocyte extravasation - movement of leukocyte out of the circulatory system towards the injury or infection site. The extravasation is a cascade process that begins with free-flowing leukocytes in the bloodstream becoming exposed to an inflammatory trigger/stimulus, slowing it down and leading to the first step of activation, the capturing step. In all leukocytes, rapid arrest can be triggered by chemokines, but myeloid cells can also arrest through a chemokine-independent, selectin-dependent pathway. The leukocyte continues to roll slowly until it becomes arrested via cytoskeletal protein and integrin interaction. After the arrest, leukocytes undergoe further flattening and strengthening through integrin clustering and tyrosine phosphorylation signalling. Fully adherent leukocytes begin transmigration through the endothelium via mechanisms that involve PECAM1/JAM-A&B, ICAM1,2 and VCAM1. Transmigration may be paracellular or transcellular, depending on leukocyte type, as well as the type of the inflammatory stimulus and the type of vasculature. The leukocyte then moves towards the target tissue and performs its programmed function, according to its phenotype.

The other important factor that can have a significant impact on leukocyte rolling and adherence is the flow of blood itself, since the shear forces and collisions with other blood cells from drastic changes in hemodynamic pressure can alter the ability of leukocytes to tether and carry them away from the site of chemoattraction (Moazzam et al., 1997). This is one of the main reasons why one rarely sees leukocyte tethering within arterioles or blood vessels with a high rate of blood flow, another significant reason being lower expression levels of selectins within the arteriole endothelium. It is the combination of weaker shear forces and higher level of selectin expression on the endothelium that makes postcapillary venules the main site of leukocyte-endothelial interactions (Granger & Senchenkova, 2010).

In addition to selectins, integrins are also necessary for the process of leukocyte adhesion. Integrins are a family of αβ heterodimeric adhesion receptors and are responsible for transmitting the information about the environmental status into cells via signal transduction pathways (Barczyk et al., 2010). There are two important integrin families - β1 and β2. The β2 integrin family is uniquely expressed on leukocytes and are involved in leukocyte arrest and migration through endothelium (Ley et al., 2007). Integrins are also able to facilitate leukocyte-endothelial interactions by changing their binding affinity via conformational changes after being stimulated by chemokines and cytokines (Barczyk et al., 2010). Integrins expressed on leukocytes bind to a family of Immunoglobulin-like adhesion molecules expressed on endothelium (Granger & Senchenkova, 2010). These molecules include intracellular adhesion molecule-1 (ICAM-1), ICAM -2, vascular cell adhesion molecule-1 (VCAM-1), as well as receptor for advanced glycation end products (RAGE) (Leick et al., 2014).

Endothelium-bound integrins interact with special sites located on leukocytes that greatly assist in leukocyte adhesion. Neutrophils and lymphocytes express lymphocyte function-associated antigen-1 (LFA-1), which interacts with ICAM-1, whereas very late antigen-4 (VLA-4), a β1 integrin, is mostly expressed on monocytes and binds to RAGE (Barreiro et al., 2010; Granger & Senchenkova, 2010; Makino et al., 2007). In inflammation, E-selectin, ICAM-1, and VCAM-1 can remain in the circulation as soluble molecules after undergoing proteolytic cleavage (Leick et al., 2014). Measuring levels of soluble or shed integrins, such as sP-selectin or sICAM-1 can be used to evaluate the strength of leukocyte-endothelial activation and quantify the severity of the immune response (Evans et al., 2009).

1.4. CNS Injury & Inflammation

For a very long time, the CNS was considered to be isolated from immune consequences or regarded as "immune privileged" – meaning it was neither vulnerable to immune activation nor contributing to systemic inflammation (Lucas et al., 2009). This concept has been revised rather extensively in the past two decades. Of course, the CNS is different from other organs and tissues in how it responds to pathogens and other immune challenges. One of the contributing factors to the differences is the extra layer of protection provided by the BBB. While leukocyte recruitment and the activation of innate immune systems can be very rapid and robust in peripheral tissues, it is delayed and rather modest in the brain (Hinson et al., 2015). Experimental rodent models demonstrated that administration of LPS induces a rapid neutrophil invasion in the skin, but a delayed and limited response in the rat brain (Matyszak, 1998; Perry et al., 1995). Nonetheless, the CNS still exhibits major features of inflammation, such as edema, MHC

expression, systemic acute phase response and acute phase protein synthesis, complement activation, synthesis of inflammatory mediators, expression of adhesion molecules and infiltration of immune cells (McNally et al., 2008). In addition, while leukocyte recruitment is rather slow, the resident immune cells of the brain, microglia, are very rapid in response and release inflammatory mediators almost immediately, within minutes to hours (Hinson et al., 2015). Despite the protection provided by the BBB, during brain injury or neurodegenerative and neuroinflammatory disorders, the BBB permeability can be severely dysregulated, compromising the brain's protection and exposing it to systemic levels of circulating inflammatory cells and mediators (Petty & Lo, 2002). Moreover, there is now a good amount of evidence suggesting that inflammation within the CNS contributes to many acute and chronic neurodegenerative disorders and even psychiatric diseases (Lucas et al., 2009; Lukens et al., 2012).

The CNS and immune system are more closely connected than originally thought, with many aspects of systemic inflammation being regulated by the CNS. The very first connection was made when IL-1 was discovered to be an important endogenous pyrogen (Lukens et al., 2012). IL-1 is expressed at low levels in the brain and is quickly upregulated in response to local or peripheral immune activity (Rothwell & Luheshi, 2000). IL-1 has also been shown to mediate fever, slow-wave sleep, appetite suppression and neuroendocrine response, as well as respond to neuroinflammation and cell death in neurodegenerative conditions, such as stroke and TBI (Rothwell & Luheshi, 2000). On a cellular level, IL-1 has an effect on glial, endothelial and neuronal cell function (Rothwell & Luheshi, 2000).

While there is limited understanding behind the pathways that are utilized for the afferent signals from inflamed, injured or infected tissue to the CNS, there is evidence that suggests circulating

IL-6 and other inflammatory mediators, as well as signals via the vagus nerve relay plenty of information to the brain and allow it to regulate many aspects of systemic inflammation (Johnson et al., 2016). Today, it is fully accepted that the brain has the ability to coordinate, regulate and shut down the host defense response and since the connection between the central nervous and immune systems is bidirectional, this may provide the explanation for various behavioural responses to illnesses, commonly presented as fatigue or even depression (Lucas et al., 2009). Vice versa, this may also be the link that provides the explanation how the psychological status of the host could influence resistance or susceptibility to disease states (Lucas et al., 2009; Rothwell & Luheshi, 2000).

Neurons, microglia, astrocytes and oligodendrocytes can produce a variety of inflammatory mediators. And although the level of cytokine and chemokine receptor expression is lower in CNS than in peripheral tissue, it is nonetheless expressed constitutively throughout the CNS, suggesting contributions to the normal physiological function of the CNS (Stoll et al., 2000). TNF-α is another mediator that is central to the neuronal (and peripheral) inflammatory response and has been linked to many neurological conditions, such as Parkinson's disease, multiple sclerosis and others (Leal et al., 2013; Stoll et al., 2000). It is known that TNF-α has two distinct signaling pathways mediated by receptors p55 and p75 (Ferrero et al., 2001). This could be the reason why TNFα has been reported to have both neuroprotective and deleterious roles within CNS, as both receptor isoforms have been detected in the brain (Golan et al., 2004). Another cytokine that also has been reported to have distinct roles is IL-6; signaling through its specific receptor, IL-6R activation leads to an increased production of inflammatory cytokines under pathologic conditions (Van Wagoner & Benveniste, 1999). Under normal physiological conditions, IL-6 levels are reported to be low and appear to be implicated in gene activation (Van

Wagoner & Benveniste, 1999). The complexity of IL-6 modulation lies in the pure number of molecules and pathways that can affect IL-6 levels, for example – IL-1, TNFα, transforming growth factor-β, prostaglandins, β-amyloid, interferon- γ (IFNγ) and IL-4 (Lucas et al., 2009). This overlapping modulation is one of the reasons why following CNS injury, the initial upregulation of cytokines leads to an amplified cascade of secondary cytokine signaling and activation (Wang & Shuaib, 2002). As an example, TNFα is able to stimulate both IL-1 and IL-6 and IL-1 can stimulate both IL-6 and TNFα. This scenario becomes even more complex when the resident CNS immune cells are also factored in the, with their own specific pathways and dynamic signaling responses.

From experimental models we learned that administration of recombinant IL-1ra in rats or mice can reduce ischemic damage by nearly 50%, with IL-1a and IL-1b knock outs showing a reduction of nearly 70% in lesion size (Denes et al., 2011; Mousa & Bakhiet, 2013). Blocking endogenous IL-1 activity with monotherapy also inhibits experimental stroke damage in rats and results in rapid and sustained reduction in disease severity in a spectrum of neurological diseases (Dinarello et al., 2012). In terms of TNFα, we learned that direct administration to the CNS causes an increase in injury size in experimental brain ischemia (Lucas et al., 2009). TNFα inhibitors cause a decrease in injury size, however, pretreatment with TNFα prior to the induction of CNS injury also have shown a decrease in injury size, suggesting a neuroprotective role and time-dependency (Ginis et al., 2002). A later study in rats showed that inhibiting TNFα-converting enzyme (TACE), which is responsible for maturation of TNFα, protected the brain from focal ischemic injury (Wang et al., 2004). In summary, TACE poses to be an attractive target for therapeutic intervention and can be a valuable alternative for treating certain cases of stroke (Lovering & Zhang, 2005). Another interesting target for neuroprotective intervention is

IL-6, as it has been reported to improve CNS wound healing after traumatic injury (Lucas et al., 2009).

It is important to understand that while a lot of immune response elements may seem detrimental to CNS function, immune activity after CNS injury is still poorly understood and, depending on time of observation and severity of the injury may be highly beneficial. For example, formation of glial scar after CNS injury was originally hypothesized to be a negative event, however if this process is prevented, then the neuronal loss at the site is increased, repair of the BBB is delayed and axonal remyelination is dramatically slowed down (Faulkner et al., 2004). This phenomenon can be partly explained by the fact that astrocytes produce neurotrophic factors such as nerve growth factor (NGF) and brain-derived growth factor (BDNF) that are produced at an even greater rate after the injury (Faulkner et al., 2004). Another phenomenon that is crucial in understanding immune-mediated neuropathophysiology after CNS injury is that cytokines may have dual roles, with detrimental acute effects (immediately after the injury), but beneficial effects in the longer term (days and weeks after injury) (Lucas et al., 2009). For example, while the exact pathophysiology is not fully understood, it is known that the initial pro-inflammatory secretion of TNFα or IL-6 is a major contributor to the exacerbation of CNS injury, while the long-term effect of these cytokines may be essential in starting the "clean up" and repair processes within the brain.

1.4.1. CNS Injury-Induced Immunodeficiency

1.4.1.1. Epidemiology of Post CNS Injury Immunodeficiency

As previously discussed, acute traumatic and ischemic events in the CNS result in activation of resident microglial cells. While there is no complete consensus on the overall effect of activated microglia for neuronal survival, it is suggested that any benefit may be overshadowed by the exacerbation of the original CNS damage (Hailer, 2008), there is plenty of evidence suggesting that the immune system is heavily involved in the repair processes following an acute CNS injury. When the natural homeostasis between the immune and nervous systems is disrupted, both systems undergo a series of changes and, depending on the severity of the "homeostatic upset", can induce severe central and peripheral consequences (Shi et al., 2018).

Clinically, infectious complications, such as pneumonia, urinary tract infections and infections of other organ systems are rather common in patients with stroke with an incidence of approximately 30% (Gong et al., 2016; Westendorp et al., 2011; Zheng et al., 2017). The prognosis of patients with stroke is greatly dependent on the occurrence of medical complications, with up to 85% of stroke patients experiencing complicating events during acute care (Langhorne et al., 2000). The most frequently occurring medical complication of severe stroke are infections (Iadecola & Anrather, 2011). The incidence of fatal infections is linked to greater stroke severity and increased age (Langhorne et al., 2000). Another review reports that post-stroke infection is associated with approximately 20% of deaths and is related to significant morbidity in stroke survivors (Shi et al., 2018; Westendorp et al., 2011). Systematic review and meta-analysis of MEDLINE and EMBASE databases revealed that in patients with acute stroke, pneumonia was associated with patient death and the need to prevent infections in patients with CNS injury was stressed (Westendorp et al., 2011).

The clinical impact of TBI resembles that of acute stroke. In general, TBI has a high mortality rate, contributing to a third of all injury-related deaths in the United States (Hazeldine et al., 2015b). In addition, TBI represents a major public health issue and a socioeconomic problem worldwide (Hazeldine et al., 2015b). Hospital-acquired infections (HAIs) are a common occurrence in patients with severe TBI, with lower respiratory tract and surgical site infections being the two of the most common non-neurological complications following severe TBI with an incidence rate of 24–72 and 17–25%, respectively (Cazzadori et al., 1997; Schirmer-Mikalsen et al., 2013). Similarly to stroke epidemiological data, pneumonia was reported as the most frequent extracranial complication (Schirmer-Mikalsen et al., 2013). Most of the studies could not come to a consensus if HAIs in patients with TBI were associated with an increased risk of death, however the studies agreed that HAIs resulted in significant patient morbidity (Hazeldine et al., 2015b). Patients with TBI are particularly susceptible to sepsis, combined with exacerbated inflammatory response, leading the TBI survivor patients to organ dysfunction (Cardozo Júnior & Silva, 2014). TBI patients with HAIs have significantly longer intensive care unit and hospital lengths of stay, resulting in even more complications and worsened outcome (Glance et al., 2011; Rincón-Ferrari et al., 2004; Zygun et al., 2006). In experimental models of TBI, presence of systemic infection has been shown to have a detrimental effect on postinjury motor deficit, cognitive impairment and increased neuronal cell death in the hippocampus, even in mild TBI (Venturi et al., 2009). Among large and recent reviews that analyzed multiple risk factors in TBI patients, it is injury to the CNS that is considered the main factor driving the increased susceptibility of TBI patients to HAIs (Hazeldine et al., 2015b).

Among patients with spinal-cord injuries, infections are among the leading causes of deaths and are associated with impaired wound healing, prolonged hospitalization and poor neurological

recovery (Riegger et al., 2007). In experimental model of SCI, fluorescence-activated cell sorting (FACS) analysis revealed that SCI induced early onset of immune suppression or paralysis, shown by depletion of monocytes, T-lymphocytes, B-lymphocytes, MHC class II and dendritic cells, all within the first week after SCI induction (Riegger et al., 2007). More recent study by Brommer et al. (2016) has demonstrated that SCI directly causes increased risk of bacterial infection in mice as well as in patients, with clinically relevant infection onset in an injury level dependent manner (Brommer et al., 2016). Taken together, it is logical to conclude that any severe injury to CNS causes a series of significant pathological events, setting up the surviving patient for vulnerability to most basic infections and, as a result, worsened outcome.

1.4.2. Pathophysiology of Post CNS Injury Immunodeficiency

Almost immediately during the onset of CNS injury, the immune system mounts a strong inflammatory response in the brain. Most of published literature suggests that inflammation in the brain during the acute phase of stroke promotes the expansion of stroke lesions and worsens neurological deficits (Fu et al., 2015; Urday et al., 2015). The brain, facing the severe injury, and major dysregulation in its normal function, mounts an anti-inflammatory response, in attempt to stop the immune system from further exacerbation of the injury and to restore the homeostatic balance of immune system regulation (Meisel et al., 2005). It is believed that the counteractive systemic immunodepression launched by the brain is the main reason why infections are the leading cause of death in patients with acute CNS-injury.

The damaged brain is thought to promote immune suppression to minimize secondary damage to healthy CNS tissue (Dirnagl et al., 2007; Meisel et al., 2005; Vogelgesang & Dressel, 2011). A

few studies have demonstrated decreased natural killer (NK) cell counts and cytotoxic activity in this particular patient population (Cruse et al., 1992; Miller et al., 1991; Wolach et al., 2001). It is thought that CNS injury causes downregulation of cell-mediated immune response via three major pathways of neuroimmunomodulation – the hypothalamus-pituitary-adrenal (HPA) axis, the sympathetic and parasympathetic nervous systems (Meisel et al., 2005). The central mediators of these pathways include norepinephrine, acetylcholine and glucocorticoid hormones (Chavan et al., 2017; Meisel et al., 2005). These mediators then bind to their receptor targets on the surface of immune cells and cause downregulation of their activity (Shi et al., 2018). This reshaping of peripheral immunity has also been manifested by decreased levels of inflammatory cytokines, dysfunction of monocytes and lymphocytes and significant atrophy of secondary lymphoid organs, such as spleen (Fu et al., 2015; Q. Liu et al., 2017; Meisel et al., 2005). On the level of sympathetic nervous system, nerve terminals release catecholamines for a prolonged time (Zhang et al., 2018), promoting the apoptosis of immune cells, leads to a decrease of peripheral immune cells and general bias towards T helper cell 2 (Th2) immune response (Panina-Bordignon et al., 1997; Sanders et al., 1997). In addition, glucocorticoids are also known to have apoptotic and antiproliferative effects on circulating immune cells (Szabó et al., 1994). Moreover, glucocorticoids have been reported to promote the production of anti-inflammatory cytokines, such as transforming growth factor β (TGF-β) (Hodge et al., 1999), inhibiting proinflammatory cytokine production (Barrat et al., 2002). The cholinergic pathway, which involves acetylcholine as the signalling molecule, is also associated with the resulting pathology after CNS injury, as it inhibits macrophage activity and decrease levels of circulating TNFα, IL-1β and IL-18 (Borovikova et al., 2000). Immunosuppression is also present within the CNS

itself, as neurons are also able to release acetylcholine, glutamate and serotonin, directly modulating neighbouring and infiltrating immune cells (Liu et al., 2017).

This immunosuppressive phenomenon, launched by the brain, has been given the name of CNS injury-induced immunodepression (CIDS) (Meisel et al., 2005), however many studies have chosen other terminology, such as post CNS injury immunodeficiency, post stroke immunosuppression, post spinal cord injury immunosuppression and many others. Lack of a single, unifying term for this syndrome is also reflective of the state of this field – while not ignored, it does not seem to be adequately addressed or discussed at present. To this day, it has not been established whether CIDS plays a neuroprotective role, requiring further research to elucidate its physiological purpose.

1.4.3. Current Treatment Approaches for CIDS

Advances in acute treatment of CNS injury combined with widespread establishment of dedicated stroke units in hospitals has resulted in increased survival numbers and drastically improved patient outcome (Zheng et al., 2017). Despite these advances, little progress has been made in effective management of post CNS injury infections. There have been various attempts (partially successful) to implement strategies to prevent infection after CNS injury, however these attempts have been isolated to individual clinical centres, with heterogenous patient population and have not been established at a level of clinical guidelines. One of such attempts revealed a more favourable outcome for patients with dysphagia after brain injury that were introduced to a standard programme of early behavioural swallowing intervention, including active therapeutic approaches and dietary modification (Carnaby et al., 2006). Prevention of

urinary tract infections in SCI patients with urinary stasis due to neurogenic bladders has also been attempted by either intermittent or complete avoidance of urinary catheterization (Salameh et al., 2015). Perhaps the most promising results were delivered by a Cochrane meta-analysis published in 2012, which concluded that the incidence of infection could be significantly reduced (from 36% to 22%) by utilizing prophylactic antibiotics during the acute phase after CNS injury (Westendorp et al., 2012b). Today, most treatment centers continue to focus on effective and accessible recovery and rehabilitation modalities that can mitigate a wide range of post-brain injury deficits, leading to enhanced quality of life for survivors (Zheng et al., 2017), which suggests that CIDS mitigation falls under the umbrella of current clinical focus.

In experimental models of CNS injury, preventative antibiotic treatment (PAT) has been shown to improve outcome when compared with placebo treatment (Hetze et al., 2013). According to established guidelines, the "gold standard" of treating a post CNS injury infection was to recommend an early antibiotic treatment after diagnosing an infection (Hetze et al., 2013). While both preventative and standard antibiotic treatments showed an improve in survival, only PAT was able to improve functional outcome (Hetze et al., 2013). Since then, several clinical trials have been launched to test the safety and effectiveness of the PAT. While most studies utilize a broad spectrum antibiotic to be able to target infections ranging from pneumonia to urinary tract infection, a few studies also explored the neuroprotective effects of minocycline, sacrificing the bacterial coverage for potentially improved neurological outcome (Amiri-Nikpour et al., 2015; Kohler et al., 2013). While a lengthy meta-analysis of literature concluded that PAT was able to successfully reduce post CNS injury infections, it also highlighted that PAT failed to improve functional outcomes or mortality (Westendorp et al., 2012b). Another major blow to this approach was delivered by the "Preventive Antibiotics in Stroke Study" (PASS), including a

total of 2550 patients from 30 hospital sites in Netherlands, revealing that preventative ceftriaxone does not improve functional outcome at 3 months in adults with acute stroke (Westendorp et al., 2015). Finally, yet another PAT phase III trial (STROKE-INF) enrolled 1217 patients from more than 40 stroke units in the UK and arrived to an even worse conclusion – no reduction in frequency of pneumonia within 14 days after the initial CNS injury (Kalra et al., 2015).

PAT is also criticized as it could potentially induce adverse effects in already vulnerable patients - anaphylactic shock, gastrointestinal complications, neurotoxicity, seizures, ototoxicity, as well as nephrotoxicity are only some of the possible effects. Long term, an established antibiotic treatment practice across all patients with CNS injury may lead to colonisation with antibiotic-resistant bacteria. This, in turn, will lead to immunocompromised patients developing infections that are also very difficult to treat. In summary, this prophylactic pharmacological intervention for CIDS is not sufficient and has the major flaw of antibiotic overuse. It also does not address the neurological impairment that results from systemic immunodeficiency, even if the invading pathogens are eliminated with the antibiotics. There is a obvious unmet need for a novel approach that could ideally utilize body's own systems in managing the immune status with minimal adverse effects.

1.5. The Endocannabinoid System

The history of *cannabis* usage by humans can be traced back to multiple civilizations and goes past the written history, with archaeological evidence suggesting the use of the plant that goes back to several thousand years of medical and recreational use (Pisanti & Bifulco, 2018). The

plant was used by humans for a wide range of its properties and the ability to adapt to various habitats – fiber, rope, food, medicine are some of the main categories of its use (Pisanti & Bifulco, 2018). The medical use of cannabis can be considered to be one of the oldest drugs in human history. Without going into a full list of ailments, the cannabis plant was used to treat a large range of conditions, such as fever, pain, sleeping disorders and constipation. Before the discovery of active components of cannabis, the plant was also adapted for medical use within the western hemisphere for its analgesic, antiemetic, antianxiety and anticonvulsant properties (Battista et al., 2012). The other side of cannabis is that it is currently the most widely used illicit drug in the world and has been associated with a variety of mental health issues, especially in adolescents (Degenhardt et al., 2010; Hall & Degenhardt, 2007). Currently, there is a definite trend towards legalization of cannabis, but it is a slow process, with only a few countries in the world having provided full legal access to both medical and recreational cannabis to their citizens.

The modern scientific beginning in the field of cannabinoids can be marked by the isolation of cannabinol (CBN) in 1899 (Wood et al., 1899). Interestingly, this compound was wrongfully assumed to be responsible for the psychoactive effects of cannabis up until the isolation of cannabidiol (CBD) in 1963 (Mechoulam & Shvo, 1963), just a year later, followed by the discovery and extraction of the main active component Δ^9-tetrahydrocannabinol (Δ^9-THC) by Gaoni and Mechoulam (Gaoni & Mechoulam, 1964). Since then, the *Cannabis sativa* plant has been discovered to have more than 400 chemical entities, of which more than 60 are cannabinoid compounds (Atakan, 2012).

The second major step in cannabinoid research was the determination and characterization of a cannabinoid receptor, with specific binding sites for THC in the rat brain (Devane et al., 1988) and the eventual cloning of the cannabinoid 1 receptor (CB1R) (Matsuda et al., 1990). Shortly after, the newly discovered receptor with its associated ligands was given the name of "cannabinoid receptor system". This was until the discovery of a second receptor, called the cannabinoid 2 receptor (CB2R) (Munro et al., 1993), along with a discovery of a natural (endogenous) cannabinoid ligand, named "anandamide" (Devane et al., 1992). Within three years, another endogenous compound, called 2-arachidonyl glycerol (2-AG) was discovered (R Mechoulam et al., 1995). Extensive research then showed that THC resembles anandamide for its affinity to CB1R, with a more lower efficacy at CB2R than CB1R *in vitro* (R G Pertwee, 2008). Taking the discovered elements together, we get the endocannabinoid system (ECS), consisting of the bioactive ligands, cannabinoid receptors 1 and 2 and the enzymes and transporters that facilitate the processing of the cannabinoid signaling molecules.

1.5.1. Cannabinoid Ligands

Cannabinoid compounds can be divided into major three categories – endogenous cannabinoids synthesized by our body, such as anandamide and 2-AG; plant-derived phytocannabinoids, such as THC and CBD; and synthetic cannabinoids, such as WIN55,212-2 and CP-55,940. There is another class of cannabinoid molecules – eicosanoid lipids, signalling molecules that are derived from polyunsaturated omega-3 or omega-6 fatty acids and are made by the enzymatic or non-enzymatic oxidation of arachidonic acid (Kasuga et al., 2015). It is important to differentiate between each ligand regarding its specificity (or lack of) for each cannabinoid receptor.

WIN55,212-2 and CP-55,940 are both non-selective CB1R and CB2R agonists, whereas arachidonyl-2-chloroethylamide (ACEA) and [(1R,2R,5R)-2-[2,6-dimethoxy-4-(2-methyloctan-2-yl)phenyl]-7,7- dimethyl-4- 49 bicyclo[3.1.1]hept-3-enyl] methanol (HU308) are highly selective to their corresponding receptor, with ACEA being specific to CB1R and HU308 having a strong affinity for CB2R (Hanus et al., 1999). Other ligands of importance are the antagonists and inverse agonists of CB1R - 1-(2,4-Dichlorophenyl)-5-(4-iodophenyl)-4-methyl-N-4-morpholinyl-1H- pyrazole-3-carboxamide (AM281) and CB2R - 1-[2-(morpholin-4-yl)ethyl]-2-methyl-3-(4-methoxybenzoyl)-6-iodoindole (AM630) (Lambert & Fowler, 2005; R. A. Ross et al., 1999).

The phytocannabinoids, with THC being the most well-known for its psychoactive effects, is a large family of chemical compounds that are found in the cannabis plant. There are many other compounds in the plant, most of which are minimally or not psychoactive at all. Some examples of such phytocannabinoids are CBD, CBN, cannabigerol (CBG) and many others (Izzo et al., 2009).There is currently a significant interest in medical use of CBD over it's potential as a safer and more effective alternative in treating seizures; CBD has less adverse psychotropic effects than THC and may possibly act as a potentiator of traditional antiepileptic medications (Zaheer et al., 2018). In addition, CBD has been reported to have a range of anti-inflammatory, anti-oxidative and anti-necrotic protective properties, along with a safe profile in humans (Bergamaschi et al., 2011). CBD is also particularly interesting in its pharmacological profile, as it is able to bind to a number of non-cannabinoid receptors (Mechoulam et al., 2007).

Endocannabinoids are derived from arachidonic acid (AA) and are synthesized within human cells (De Petrocellis & Di Marzo, 2009). 2-AG and anandamide or arachidonylethanolamide

(AEA) are both examples of endocannabinoids that have been extensively studied. Interestingly, upon discovery, both of these endocannabinoids were considered to be similar and even mutually exchangeable in their regulation of long- and short-term plasticity of neurons, learning, memory, antinociception and anxiety (Luchicchi & Pistis, 2012). However, it is now known that AEA and 2-AG are quite different, with different CB receptor affinity, as well as different synthesis and degradation (Luchicchi & Pistis, 2012). AEA synthesis is accomplished by N-acyl phosphatidylethanolamine phospholipase-D (NAPE-PLD), whereas 2-AG is synthesized via phospholipase C (PLC) and diacylglycerol-lipase (DAGL) interaction (Luchicchi & Pistis, 2012). In terms of levels, 2-AG was found to be more abundant and more potent than AEA, while both demonstrating a preference for CB1R over CB2R (Reggio, 2002).

Synthetic cannabinoids, like their endogenous and plant-derived analogs, also have varying degrees of CB receptor affinity, efficacy and a large variety of other pharmacokinetic and pharmacodynamic differences. The development of synthetic cannabinoids also allowed researchers to perform pharmacologic knockout experiments, where a particular CB receptor is taken out of its physiological role. These experiments investigated the specific involvement of CB1 or CB2 receptors in healthy conditions, as well as during pathophysiologic changes.

The endocannabinoid system also contains the enzymes that are responsible for the degradation of the endocannabinoids. AEA is metabolized by fatty acid amide hydrolase (FAAH) into AA and ethanolamine, whereas 2-AG is metabolized by monoacylglycerol lipase (MAGL) into AA and glycerol (R G Pertwee, 2006)(Figure 3).

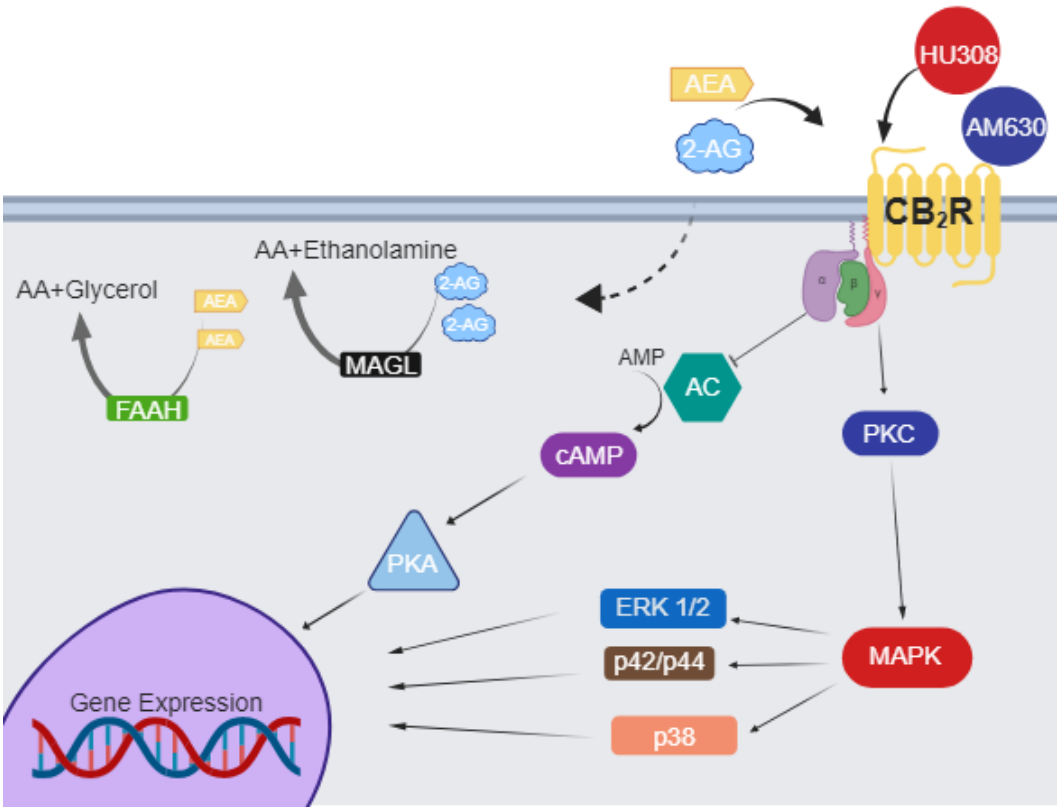

Figure 3. **Simplified Representation of CB2R Pathway.**

Simplified schematic representation of the cannabinoid 2 receptor (CB2R) pathway inside a cell. The pathway begins at the CB2R, which is a classic transmembrane G-protein coupled receptor. CB2R can be activated by a series of endogenous ligands, such as endocannabinoids 2-arachidonoylglycerol (2-AG) or anandamide (AEA) or synthetic cannabinoids HU-308 and AM630. For the purposes of the diagram AEA is shown to bind to CB2R, even though it has lower binding affinity to CB2R than to CB1R. Through the Gi/Go$_\alpha$ subunits, the activity of adenyl cyclase (AC) is inhibited, resulting in a decrease in cAMP and protein kinase A (PKA) activity, ultimately leading to changes in gene expression. Through the G$_{\beta\gamma}$ subunits, CB2R activity mainly works through the highly conserved MAPK/ERK pathway, regulating cellular expression, migration and proliferation.

While FAAH and MAGL are the major enzymes, they are not the only enzymes that metabolize endocannabinoids, with cyclooxygenase-2 (COX-2), 53 lipoxygenase (LOX), cytochrome P450, and serine hydrolases all being potential pathways that can break down the endocannabinoid molecules (Savinainen et al., 2012; Zelasko et al., 2015).

Cannabinoids and endocannabinoids are non-charged lipids that are able to passively traverse the lipid membrane of a cell (Kaczocha et al., 2012), however they are also highly lipophilic molecules, which implies a requirement for a cytosolic protein or chaperone to be able to reach the intracellular target (Huang et al., 2016). These proteins are called the endocannabinoid transporters (eCBTs), with one of the more understood examples being fatty acid binding proteins (FABP) -1,-3,-5 and -7, all of which have the capacity to bind to endocannabinoids and differ in their distribution across the body (Huang et al., 2016).

1.5.2. Cannabinoid Receptors (CB1R & CB2R)

Both CB1R and CB2R belong to Rhodopsin-like G-protein coupled receptor (GPCR) class A family with seven transmembrane domains (Howlett et al., 2002; Matsuda et al., 1990). It is important to note that despite both receptors being cannabinoid, they only share 44% of proteins and about 68% of the transmembrane domain (Pacher et al., 2006).

The CB1R is thought to be responsible for most of the centrally mediated effects of cannabinoids (Compton et al., 1993). In terms of CB1R expression – it is predominantly concentrated in areas of the brain that are responsible for movement control, sensory perception, coordination, learning and memory, emotions, reward centers, hormonal function and even body temperature

(Herkenham et al., 1990). When looking at the pharmacological profile of cannabinoids, it overlaps with receptor localization within the brain, as CB1R can be found in high densities in cerebellum, hippocampus and cerebral cortex, with lower densities being resent in the brain stem (Herkenham et al., 1991; Thomas et al., 1992). On a cellular level, CB1R-mediated inhibition of adenylate cyclase implicates guanine nucleotide-binding protein complex or Gi activity (A. C. Howlett et al., 1986), as well as inhibition of N-type calcium channels (Mackie & Hille, 1992) and an increase in binding of non-hydrolyzable GTPγS (Sim et al., 1996). The original study that revealed the G-protein-coupled structure of CB1R cloned the receptor by screening a G-protein-coupled receptor library (Matsuda et al., 1990). Expression of CB1R extends beyond the CNS – CB1R mRNA has been found in several peripheral tissues – adrenal gland, lung, prostate, heart, uterus, ovary, testis, bone marrows, thymus gland and tonsils (Galiègue et al., 1995a). The other subunit of CB1R, called the Gβγ, is able to activate mitogen activated protein kinases (MAPK), involving extracellular signaling kinase -1 and -2 (ERK1 & 2) c-Jun N-terminal kinase (JNK), as well as p38 MARPK (Bosier et al., 2010; Filomeni et al., 2012; Tanasescu & Constantinescu, 2010).

Activation of CB1R usually results in a signaling cascade via coupled $G\alpha_{i/o}$ G proteins, involving inhibition of adenylate/adenylyl cyclase (AC), in turn reducing the intracellular conversion levels of adenosine monophosphate into cyclic adenosine monophosphate (cAMP) (Orgado et al., 2009). Following the cascade, the altered level of cAMP causes a reduction in activation of protein kinase A (PKA), which phosphorylates a transcription factor, called cAMP response-element binding protein or, as mentioned earlier, CREB (Chanda et al., 2011). CREB, in turn, is able to induce cell proliferation, survival and differentiation (Kim et al., 2001). There are other signalling pathways that are associated with CB1R activation, namely the inhibition of N- and

P/Q-type voltage-gated Ca^{2+} channels (Bosier et al., 2010; R G Pertwee et al., 2010). Resulting changes in calcium and potassium ion currents affects neuronal excitability and leads to a decrease in GABAergic and glutamatergic cellular signalling (Chevaleyre et al., 2006).

A strong CB2R expression profile has been found in spleen and tonsils, as well as other immune tissues (Bouaboula et al., 1996; Munro et al., 1993). Quantitatively, CB2R expression within immune tissue seems to be especially abundant with mRNA expression levels being 10-100 fold higher than CB1R under normal conditions (Galiègue et al., 1995a). Furthermore, the level of CB2R expression within spleen and tonsils is roughly equivalent to the level of CB1R expression within the CNS (Galiègue et al., 1995a). The importance of this comparison comes into play when these levels of receptor expression change under pathologic conditions. A shift in relative and absolute numbers of receptor expression within periphery may potentially have systemic consequences. When looked at immune cell subpopulations within humans, the distribution of CB2R mRNA seems to be the highest in B-cells, followed by natural killer cells, monocytes, polymorphonuclear neutrophil cells, T8 cells and T4 cells (Galiègue et al., 1995a).

Originally, the literature claimed that CB2R was not expressed in the brain and was isolated to immune cells and tissues (Galiègue et al., 1995a), however, through behavioural studies of central effects of CB2R agonists and anatomical localization of CB2R mRNA it has now been recognized that the CB2R may have a functionally relevant role in the CNS, even directly at synapses. (Morgan et al., 2009). Furthermore, it has been shown that microglia, the resident cells in retina, brain and spinal cord that are functionally and morphologically related to macrophages (Dickson et al., 1991; Gehrmann et al., 1995), express CB2R and mediate the action of CB2R within the CNS (Y. Li & Kim, 2017). These discoveries shifted the perspective on the possible

activity and involvement of CB1R and CB2R, as the original view provided a more divided system where each receptor was associated with its own domain, such as the CNS with CB1R and immune cell activity with CB2R. The updated view of cannabinoid receptor expression and localization appears to suggest a more intertwined and dynamic involvement of the ECS at virtually all levels of immune system modulation and control.

Activation of CB2R, just like CB1R, is also associated with a signaling cascade via coupled $G\alpha_{i/o}$ G proteins, inhibition of AC and intracellular cAMP levels, activation of pERK and G protein-coupled inward rectifying K^+-channels (GIRKs), as well as β-arrestin recruitment (Dhopeshwarkar & Mackie, 2014; Felder et al., 1995; a C. Howlett et al., 2002). It is currently not known which signal transduction pathway or pathways are the most relevant nor are all the CB2R-related pathways yet elucidated (Soethoudt et al., 2017). In addition, there appears to be ligand-specific activation bias – under a normalized cell environment, different CB2R ligands are able to preferentially activate different signalling pathways (Basu & Dittel, 2011). Moreover, there are reports of significant differences between rodent and human CB2R orthologues, which complicates the translation of experimental findings from preclinical models to human testing (Soethoudt et al., 2017).

The localization of CB2R to microglia is rather significant, since the function of dormant microglia in a healthy brain is not entirely understood yet and could suggest a role that involves the ECS, even during homeostatic conditions. Under pathological conditions, microglia play an active role as an immunoeffector cell, as they migrate and proliferate during and shortly after the injury and in the resulting inflammation (Benveniste, 1997a; Kreutzberg, 1995; Leong & Ling, 1992). In addition, upon activation, microglia secrete cytokines such as IL-1, IL-6 and TNFα

(Benveniste, 1997b; Reid et al., 1993). Furthermore, it is also known that microglia express MHC class I and II antigens and the CD11/CD18 complex, together with phagocytic and cytolytic functions (Zhou et al., 2014). Since microglia, like other immune cells, go through maturation, differentiation and ultimately activation, all of which is uniquely shaped by gene expression and associated functional capabilities (Adams & Hamilton, 1984; Hamilton et al., 1986), the cannabinoid receptor involvement may not be expressed at similar levels throughout the life cycle of an immune cell, such as microglia or a macrophage. Using an *in vitro* model, where macrophages or microglia are driven from their dormant state to responsive, primed and fully activated, it was shown that CB2R mRNA is not present in dormant cells, becomes present in responsive and primed immune cells and is also present, but at greatly reduced levels, in fully activated immune cells (Carlisle et al., 2002). These findings suggest that CB2R may be upregulated in response to a pathologic stimulus and the role of CB2R may be particularly important in immune cell chemotaxis, phagocytosis and antigen presentation stages. The other important conclusion from the findings by Carlisle et al. is that the CB2R expression "timeline" appears to have a "window" where the immune cells are most receptive to CB2R modulation. This CB2R upregulation "window" is hypothesized to be the optimal time to therapeutically intervene with exogenous cannabinoid ligands or to manipulate the levels of endogenous cannabinoid ligands. Other studies further supported the presence of this window by demonstrating a lack of cannabinoid-related action in fully activated microglia. One study stands out, as it demonstrated that production of inducible nitric oxide, a potent inflammatory mediator, by microglia and macrophages in fully activated stage can be inhibited by CB1R activity (Waksman et al., 1999). This inhibition of nitric oxide production was induced by CP55940, a CB1R agonist, in a fully concentration-dependent manner in a model of interferon gamma

(IFNy)/bacterial lipopolysaccharide (LPS)-inducible nitric oxide production by rat microglial cells (Waksman et al., 1999). Furthermore, pre-treating the microglial cells with CB1R antagonist SR141716A reversed this CP55940-mediated inhibition, suggesting that the nitric oxide inhibition occurs, at the very least partially, through the action of CB1R (Cabral et al., 2001).

1.5.3. CB2R Involvement in Chemotaxis of Immune Cells

Macrophages and microglia in responsive and primed states both go through chemotaxis and antigen presentation, respectively. Chemotaxis is the unique ability of immune cells to migrate, as a response to a stimulus, which is quite different from the more random, stimulus-independent cellular motion (Lauffenburger & Horwitz, 1996). It is also important to differentiate this activity from chemokinesis, where the cells partake in random motion due to a presence of a chemical stimulant (Keller et al., 1978), which is different from chemotaxis, where the motility of the immune cells is aimed towards the highest concentration gradient of the chemical stimulant (T. Jin & Hereld, 2006). Chemotaxis not only initiates the rapid and focused movement towards the chemoattractant, but it also induces and is associated with a wide range of changes in fluxes of ions, integrin activity, superoxide anion production, as well as secretion of lysosomal enzymes (Murdoch & Finn, 2000). Briefly, the term chemoattractants includes a wide range of chemicals, some examples of which include the “classical” bacterial-derived N-formyl peptides, complement fragment peptides C5a and C3a, lipids B4 and platelet-activating factors (Gerard & Gerard, 1994; Goldman & Goetzl, 1982; Schiffmann et al., 1975). Chemokines or cytokines are another group of chemoattractants, selective for leukocytes *in vitro* and cause the accumulation

of inflammatory cells *in vivo* (Baggiolini et al., 1997; Le et al., 2004). Usually, the effects of cytokines are mediated by G-protein-coupled receptors located on target cells, making the case for CB2R involvement (Charo & Ransohoff, 2006; Murdoch & Finn, 2000). Upon binding to the target cell's surface receptor, the chemokine initiates a cascade of signal transduction events within the cell that can cause a change in leukocyte trafficking behaviour, modulate new cell formation and trigger release of more chemokines, effectively regulating host's response to infection (Charo & Ransohoff, 2006). Similarly, there is evidence showing that cannabinoids can influence migratory activity of macrophage and macrophage-like cells, such as microglia. One of such early studies performed by Stefano et al. in 1998 demonstrated that exposing macrophages to anandamide resulted in a transformation from an amoeboid and motile state to that of a rounded and non-motile conformation (Stefano et al., 1998). While the original study proposed an explanation linked to CB1R activity, it was not long until the explanation shifted to the involvement of both CB1R and CB2R, as CP55940, a full agonist at both receptors, caused a decrease in migration *in vitro*, ultimately linking the observed changes primarily to CB2R (Sacerdote et al., 2000). The same group later published a study demonstrating a decrease in chemotactic response in mice to formal-methionyl-leucine-phenylalanine after treatment with cannabidiol (Sacerdote et al., 2005). This finding was reinforced by another drug treatment that was able to block the originally observed decrease in chemotactic response when using a CB2R antagonist SR144528 on macrophages *in vitro* (Sacerdote et al., 2005). Another study by Walter et al. showed that 2-AG triggered migration of microglia *in vitro* and concluded that there was a strong link between macrophage-like cell migration and CB2R activity (Walter et al., 2003). In the same year, a very important study was published, demonstrating that arachidonylcyclopropylamide, a CB1R selective agonist, was able to induce a dose-dependent

increase in migration of BV-2 microglial cell line (A. Franklin & Stella, 2003). However, the support for CB2R involvement also appeared in this study, as the CB1R antagonist SR141716A did not abolish the arachidonylcyclopropylamide-mediated migration, while the CB2R antagonists - SR144528 and cannabinol, as well as two antagonists of cannabinoid orphan receptors GPR18 and GPR55 - O-1918 and CBD, were all able to abolish the change in cell migration (A. Franklin & Stella, 2003). Interestingly, part of that research group went on to demonstrate that 2-AG production in microglia was controlled by P2X7 ionotropic receptors, further implicating and extending the ECS involvement (Witting et al., 2004). Another line of evidence demonstrated that CB2R is associated with THC and CP55940 mediated inhibition of macrophage chemotaxis to RANTES/CCL5 by comparing the effectiveness of CB2R selective ligand O-2137 and CB1R selective ligand ACEA, where the first one showed a robust effect, the latter one did not (Raborn et al., 2008). The same study also treated the cells with THC in CB2R knockout mice and revealed a lack of effect on the chemotaxis of macrophages (Raborn et al., 2008).

1.5.4. CB2R Involvement in Antigen Processing and Presentation

Antigen processing and presentation involves a very complex set of events that need to happen for immune system to work. The activation of helper CD4+ T cells requires physical contact with an antigen-presenting cell. Different from antibodies, the binding does not happen to antigen alone, instead the receptor recognizes the extracellular antigen complex along with the MHC class II molecules on the surface (Schwartz, 1985). These antigen complexes are usually proteins and not carbohydrates or lipids, with the MHC class II molecule complex being a peptide

fragment (Guillet et al., 1987). The protein antigens are also synthesized exogenously to the presenting cells, making this quite a different process when compared to CD8-positive T cells, where the antigen proteins originate endogenously to the presenting cell (Germain, 1986). Antigen presenting cells carry out the following crucial functions – processing and presenting, where processing involves the internalization of the antigen, proteolytic cleavage of the antigen into peptides, formation of the molecular complex and presenting involves the expression of it on the cell surface (Germain, 1986). For example, macrophages are unique in that they are able to internalize particulate antigens by phagocytosis (Unanue & Allen, 1987). Other cells that are also involved in phagocytosis do not have the capacity to have MHC class II molecules and thus do not have a function as antigen-presenting cells (Unanue & Allen, 1987). While the mode of antigen uptake by cells differs, the processing of antigen happens at an organelle level, where the antigens are cleaved. If an antigen-presenting cell is treated with acidotropic agents like chloroquine, monensin and ammonium chloride, which neutralize intracellular pH, then the antigen processing cannot happen (McCoy & Schwartz, 1988). Acid proteases, such as cathepsins are responsible for antigen cleavage, with studies showing that when protease activity is inhibited – the antigen processing is also blocked (van der Drift et al., 1990).

THC was demonstrated to impair the ability of a macrophage to function as an antigen-presenting cells, due to an impairment in its ability to produce IL-2 upon stimulation of soluble protein antigen-specific helper T-cell (McCoy et al., 1999). Treating the macrophage cells with THC resulted in a significant reduction in its ability to respond to the native form of the antigen (McCoy et al., 1999). THC was not able to affect IL-2 secretion when the macrophage cells were presented with a synthetic peptide of the antigen to the T cells, revealing that THC was causing its interference at the level of antigen processing and not presentation (McCoy et al., 1999). It

was also confirmed that macrophages predominantly express CB2R over CB1R mRNA, and THC-induced interference was completely preventable when a CB2R antagonist SR144528 is applied to the cells (McCoy et al., 1999). In summary, there is a strong functional link between CB2R and activity of macrophages at the level of antigen processing.

1.5.5. CB2R Activation as a Neuroprotective and Time-Dependent Approach

Not too long after the discovery of CB2R, the experimental evidence that linked CB2R activity and upregulation with activation of microglia in response to inflammation in CNS began to mount (Maresz et al., 2005). Studies began to treat animals with experimental stroke with CB ligands, such as THC and WIN55212-2 and reported a reduction in cerebral infarction, neuronal loss and a decrease in neurological deficits (Hayakawa et al., 2007; Nagayama et al., 1999). Around the same time, in rats, it was shown that experimental stroke produced an induction of CB1R expression, which was thought to be protective for cortical neurons and aligned well with the function of endogenous signaling pathways (K. L. Jin et al., 2000). This provided the first bit of evidence that experimental stroke could modulate the levels of CB1R expression in the brain. However, this was only the beginning, as consecutive studies that attempted to investigate the involvement of both CB1R and CB2R revealed quite a different picture. One study demonstrated the CB1R mRNA after experimental middle cerebral artery occlusion did not change at 24 hours in neonatal rats (D. Fernández-López et al., 2012) and was reduced in adult rats 5 hours after the onset of injury (Zarruk et al., 2012). The authors went on to claim that the CB agonist WIN55212-2 protects against focal stroke, at least in part, due to the inhibitory effects on microglia (D. Fernández-López et al., 2012). In line with this evidence, administration of

selective CB2R agonist JWH-133 after experimental stroke significantly improved outcome, with this effect being reverse in CB2R knockout mice, as well as in combination with CB2R antagonist administration (Zarruk et al., 2012). This does not entail that CB1R involvement isn't important, since knocking out the CB1R increases the severity of experimental stroke in mice (Parmentier-Batteur et al., 2002). What it does suggest is that both receptors are potentially involved in different aspects of post CNS pathophysiology and that both of CB receptors may have their own "window" for potential therapeutic utility. This notion is evidenced by the same study that used N-methyl-D-aspartate (NMDA) to cause brain lesions, which were more severe in CB1R knockout mice, when compared to wild-type, suggesting that the role of CB1R-related neuroprotective lies within excitotoxicity regulation (Parmentier-Batteur et al., 2002). Not all studies were as clear, as some have shown improvements in animals with experimental stroke even when CB1R antagonists SR141716 or LY32013 were administered (Muthian et al., 2004).

In general, a significant number of studies have reported CB2R activation and upregulation. Suppression of microglial activation has also been attributed to the activity of CB2R in both Huntington's disease and more general CNS inflammation (Maresz et al., 2005; Palazuelos et al., 2009). Another study used a selective CB2R agonist O-1966 in a model of traumatic brain injury and reported reduced cerebral edema, microglial cell activation and recovery of acute motor and exploratory deficits in C57BL/6 mice (Elliott et al., 2011). Going on the same tangent, CB2R is also reported to offer protection against dopaminergic injury in an experimental model of Parkinson's disease by also reducing microglial recruitment when the receptor is overexpressed (Ternianov et al., 2012). Intravenous administration of selective CB2R agonists O-3853 and O-1966 in mice with transient middle cerebral artery occlusion resulted in a reduced number of white blood cell rollers and a reduction in leukocyte adhesion along cerebral vascular

endothelium, in addition to reducing infarct size and improving the motor function (M. Zhang et al., 2007). Similar to previous study, administration of JWH-133, a CB2R agonist, also improved infract outcome by reducing brain lesion and the level of neurological impairment, primarily thought to be driven through the inhibitory effect on the activation of different subpopulation of microglia and macrophages in an experimental stroke model (Zarruk et al., 2012). While CB2R's ability to affect the activity of immune cells is without a doubt one of the main ways the receptor can protect the CNS, there are also other ways the CB2R is able to help. One of the other possible neuroprotective mechanisms is by regulating astroglial reactivity, in addition to being expressed on immune infiltrates within the CNS (Garcia-Ovejero et al., 2009). Another possible neuroprotective mechanism involves the suppression of glutamate release by CB2R activation in CNS reperfusion injury rat model (Contartese et al., 2012). Delayed treatment of rats with experimental stroke with daily doses of CB2R agonist AM1241 did not show any behavioural improvement nor reduction in brain lesion size, suggesting that the offered neuroprotective by CB2R is time-dependent (Yu et al., 2015).

1.5.6. ECS and CNS Injury

The ECS plays an important role in immune system modulation, with mounting evidence suggesting upregulation of the ECS during both local and systemic inflammation. In general, CB2R activation has been associated with anti-inflammatory effects and considering the expression profile on macrophages, neutrophils and lymphocytes, the connection between ECS and consequences of CNS injury becomes very tangible (Kendall & Yudowski, 2016; Varga et al., 1998). Over the last decade, ECS has been revealed to be one of the key regulatory systems

in the brain with heavy involvement in pain perception, learning, memory and inflammation (Kano et al., 2009; Marsicano & Lutz, 2006).

Several studies provided evidence that suggests ECS upregulation following CNS injury represents an adaptive mechanism for immune system regulation (Arévalo-Martín et al., 2008; Garcia-Ovejero et al., 2009). It also has been reported that activation of CB2R on cerebral immune cells may limit neuro-inflammation (Pandey et al., 2009). ECS has been suggested a neuroprotective role during TBI and could potentially be involved in repair mechanisms during degeneration (Bilkei-Gorzo, 2012; Pryce et al., 2003). Animal models of TBI revealed that endogenous levels of 2-AG increase after the brain injury (R Mechoulam & Shohami, 2007). It was suggested that ECS provides an "on demand" generation of endocannabinoids shortly after TBI onset, decreasing the edema severity and reducing neuroinflammation (Shohami et al., 2011). Cannabinoids have also been shown to reduce ischemic injury in myocardial infarction and ischemic stroke models (Capettini et al., 2012). On cellular level, it is thought that AEA is able to exert paracrine protective activity and inhibit T lymphocyte proliferation that happens in the ischemic area of the brain, even leading to immune cell apoptosis (Schwarz et al., 1994). Cerebral macrophage-like cells (microglia) express both CB1R and CB2R, which suggests that cannabinoid activity could have a direct effect on cell populations resident in the brain (Sinha et al., 1998). Interestingly, it has been reported that even peripheral nerve injury can cause an upregulation of CB2R expression in areas of CNS, such as the spinal cord (Zhang et al., 2003). One study administered JWH-133, a synthetic selective CB2R agonist, and demonstrated that CB2R activation can reduce microglial activation and downregulation inflammatory gene expression, responsible for production of IL-6, TNFα, monocyte chemoattractant protein [MCP]-

1 and macrophage inflammatory peptide [MIP]-1α (Zarruk et al., 2012). ECS has also been implicated as a retrograde messenger, mediating feedback inhibition and modulating synaptic plasticity (Chevaleyre et al., 2006; A. C. Howlett, 2005), thus potentially outlining one of roles of ECS in post CNS injury neuronal repair and neurogenesis. Putting all of the above together, ECS may be responsible for reduction of excitotoxicity, inhibition of inflammatory cytokine production and augmentation of stem cell migration and differentiation after CNS injury (Kendall & Yudowski, 2016).

1.5.7. CB2R after CNS Injury

While experimental data suggests beneficial CNS actions (Fernández-López et al., 2007), much less is known about the potential effects of CB2R upregulation in the periphery after CNS injury, especially considering systemic immunosuppressive consequences that result after the onset of CNS insult. In terms of pathway involvement, the ECS exerts an immunosuppressive effect on the immune function through inhibition of cAMP/PKA and at a nuclear level, by phosphorylating IκB-α and thus enhancing the transcription of several apoptotic genes regulated by NF-κB, and interfering in cell cycle by induction of G1/S phase arrest (Malfitano et al., 2006). Specifically, immune suppression by peripheral CB2R activation could potentially contribute or be one of the main driving forces behind CIDS and negatively impact outcome after severe CNS injury, therefore making CB2R a potential pharmacological target for CIDS therapy (Lehmann et al., 2014).

1.6. Central Hypothesis

My research investigated the effect of ECS modulation of the immune response following experimental CNS injury by manipulating the ECS via the CB2R pathway. Given the importance and selectivity of this signaling pathway in modulating the immune system, first, I hypothesized that by pharmacologically targeting CB2R with an agonist as an early treatment will provide a neuroprotective effect, thus limiting the extent of brain injury and reducing the compensatory immunosuppressive response of the brain, reducing the severity of CIDS. Second, I hypothesized that by inhibiting CB2R pathway peripherally after the CNS injury and onset of CIDS, I will be able to restore the immune function and improve the host's ability to mount an immune response to a challenge. The hypothesis is graphically represented in Figure 3.

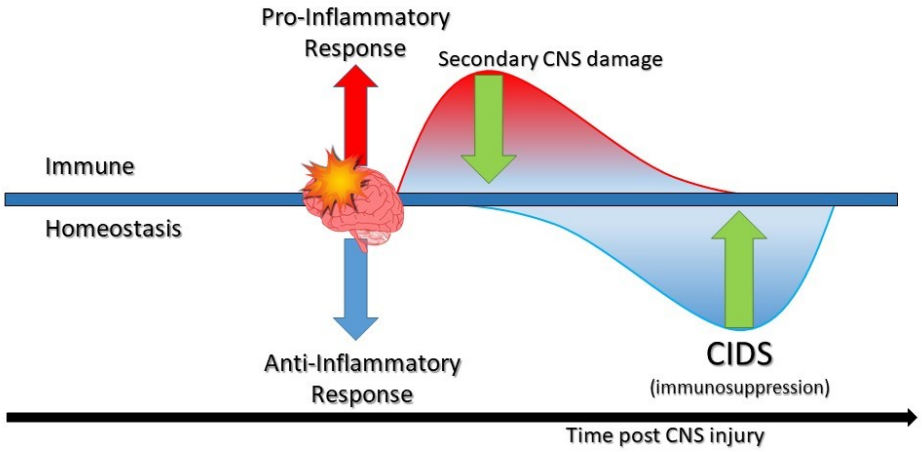

Figure 4. **Immune Dysregulation After CNS Injury.**

Graphical representation of the disruption of the immune homeostasis by CNS injury and the resulting inflammatory dysregulation. Initially, the immune system mounts a pro-inflammatory response to the CNS injury, usually associated with blood-brain-barrier (BBB) breakdown, immune cell infiltration into the brain tissue and further exacerbation of the initial brain injury. As a protective response, the brain promotes a strong compensatory anti-inflammatory response, shutting down the immune activity not just locally within the CNS (to prevent further exacerbation) but also peripherally, ultimately causing systemic immunosuppression. This phenomenon has been termed CNS injury-induced immune deficiency syndrome (CIDS) and is responsible for patients' vulnerability to basic infections and having a negative impact on neurological recovery, as well as patient outcome. Green arrows indicate the two proposed time points where a pharmacological intervention with cannabinoids may be highly beneficial for patient outcome, as it could potentially reduce the extent of secondary CNS injury and reduce the severity of immunosuppression. The time scale is not given a reference frame since the duration can be anywhere from a few hours after the onset of CNS injury to weeks and even months after the onset of CIDS, highly variable between patients and dependent on the severity of the injury, age of the patient, access to primary health care services and other factors.

1.7. Study Objectives

The overarching objective of my research, as mentioned above, was to provide experimental evidence for pharmacological treatment of CIDS via CB2R modulation in *in vivo* models of CNS injury. Specifically, my first objective was to evaluate the effect of early CB2R activation with HU308 on leukocyte-endothelial interaction within intestinal microvasculature and brain injury size after an immunochallenge in an animal model with experimentally induced ischemic CNS injury. My second objective was to inhibit CB2R with a specific antagonist, AM630, after CIDS onset and quantify the leukocyte-endothelial interactions, as well as brain injury size after an immunochallenge in the above-mentioned animal models with experimentally induced ischemic CNS injury. As an extension of the second objective, the importance of correctly timing the manipulation of CB2R signalling was further investigated in pharmacological CB2R blockade and genetic CB2R knockout mice, where leukocyte-endothelial interaction and brain injury size were also quantified after an immunochallenge in an animal model with experimentally induced ischemic CNS injury.

1.8. Experimental Models Overview

1.8.1. CNS Injury Models

To experimentally induce acute CNS injury, I have adapted the hypoxia-ischemia (HI) model of neonatal hypoxic brain damage. Originally developed in rats, the Vannucci HI model (S. J. Vannucci & Hagberg, 2004), brain injury is acquired by combining a permanent unilateral common carotid artery ligation with subsequent exposure to hypoxia. The model reliably

produces persistent motor, sensory, and cognitive impairment. The HI model can induce CNS injury of variable severity, dictated by the duration of exposure to hypoxic condition, after the common carotid artery ligation. The relationship between the two is as follows – the longer the animal is subjected to hypoxia, the larger the insult to the brain tissue. Literature reports that HI for 50 minutes in postnatal day (PND) 5 mice results in a small percentage of animals having a brain injury, whereas 80 minute exposure produced extensive brain infarction in multiple areas (Albertsson et al., 2014). The window that generates an injury large enough to establish severe immune consequences and induce CIDS is rather small, since if the hypoxia of the brain is prolonged, the animal will either not survive the procedure, be too functionally impaired to survive until the immunochallenge or be too weak to withstand the administration of endotoxin long enough to allow observations.

The HI model produced CNS injury reliably, however the injury size was variable – providing the model with a degree of clinical validity but also a major drawback, as consistency in CNS injury size was important in inducing a similar level of immunosuppression. Thus, a second model was utilized that was more focused on avoiding systemic exposure of the animal to hypoxia, that is essential in HI model, as well as providing reperfusion that is seen in classical CNS injury, such as stroke. For the second model, I have utilized an intracranial injection of a naturally-occurring neuropeptide – endothelin-1 (ET-1). Since the early 1990s, ET-1 was used to induce ischemia by applying it directly adjacent to the surface of the MCA after craniotomy. The ET-1 model was then modified to include a stereotaxic injection of ET-1 adjacent to the MCA to produce focal cerebral ischemia (Ansari et al., 2013). Compared to HI, ET-1 model is rather advantageous as it is performed quicker, does not require surgical access to cerebral arteries, allowed me to control artery constriction by altering the dose of ET-1 delivered, as well as

gradual reperfusion rates that more closely mimics the reperfusion in humans. One of the downsides of ET-1 model was the need to perforate the skull of the animal, albeit briefly and requiring only very small diameter holes, enough for a needle to be placed directly into the brain. The other source of variability was the batch of ET-1 used, as it has been reported to affect the size of CNS injury.

1.8.2. Immunochallenge Model

To challenge the impaired immune system after CNS injury, I chose to use an endotoxemia challenge as a model of infection by administering bacterial lipopolysaccharide (LPS) *in vivo*. In a healthy wild-type mouse, introduction of bacterial antigens into the body of the animal, causes a robust and exaggerated pro-inflammatory response mounted by the innate immune system. The resulting inflammatory cascade causes priming of endothelium for leukocyte-endothelial interactions, providing a quantifiable measure when coupled with labelling leukocytes with fluorochromes and observing the interactions via intravital microscopy *in vivo*. LPS has been used for many decades as a trigger of immune response in models of acute sepsis, when in high doses, and models of local inflammation, when used in low dose administration. Since LPS is not a pathogenic living bacterium, the inflammatory cascade and following immunoregulatory changes do not happen the same way they happen in a "real" infection scenario, however this also provides an advantage in experimental setting, since the level of immune activation can be controlled by changing the dose of administered LPS. Administration of LPS causes the endotoxin to induce systemic upregulation of the immune response. It is thus important to have a

reliable *in vivo* readout of immune activity and picking the organ tissue that would adequately represent peripheral immune response.

The main role of intestinal microcirculation is to provide oxygen to the cells of the gut. Intestine is innervated by an extensive microcirculatory network that carries out many functions – from supplying the intestine with glucose and oxygen to an elaborate immune barrier, protecting the host from bacterial pathogens naturally contained within the gut. Injury to the brain has wide systemic consequences and leads to multiple physiologic complications, including intestinal dysfunction and bacterial translocation (Bansal et al., 2009). Impairment of the barrier, combined with other central and peripheral immune consequences after CNS injury, can lead to infection and negatively impact the patient outcome. Interestingly, this physiological impairment of intestine after brain injury is not exclusive to humans and other mammals, as a similar breakdown of intestinal epithelial barrier has also been reported in flies (Katzenberger et al., 2015). Clinically, patients with TBI frequently develop gastrointestinal dysfunction that leads to ulceration, inflammation and increased gut permeability (Hang et al., 2003; Kao et al., 1998). These rapid changes have been reported to occur as early as 3 hours following brain injury and last for more than 7 days with marked mucosal atrophy (Hang et al., 2003). Histopathologic changes in the intestine has been detected within 2 hours after injury, peaking at 24 hours after brain trauma (Hang et al., 2003). Based on this multi-directional connection between central nervous and enteric systems, along with their ability to systemically regulate the immune response (Houser & Tansey, 2017), the intestine was picked as a representative peripheral readout of the immune function after CNS injury.

1.8.3. Immunomodulatory Models

For modulation of ECS, I have chosen synthetic and specific ligands, providing a reliable and controlled action upon the CB2R receptor. For my first objective (early CB2R activation), I used HU308, a specific CB2R agonist to directly activate CB2R by directly binding to its orthosteric activation site. For my second objective (late CB2R inhibition), I have used AM630, a potent and selective CB2R inverse agonist, acting on CB2R by blocking its orthosteric activation site and preventing further activity. For my final objective, I have also used AM630 to pharmacologically "remove" the CB2R and investigate the effects in absence of CB2R signaling. Genetic removal of CB2R causes CB2R agonists (endogenous or exogenous) to have no effect on minimizing leukocyte-endothelial cell interaction, since CB2R null mice fail to show complete resolution of inflammation after LPS treatment.

Chapter 2: Materials and Methods

2.1. Animals

All the performed experiments and procedures involving animals were approved by the Dalhousie University Committee on Laboratory Animals and complied with the Canadian Council for Animal Care guidelines (http://www.ccac.ca/). All experiments that use wild type mice utilized healthy adult male C57BL/6 (6-8 weeks old, 20-30g, n = 5-10), which were purchased from Charles River Laboratories International Inc. (Wilmington, MS, USA). After mice arrived at the Carleton Animal Care Facility (CACF) of the Faculty of Medicine at Dalhousie University, Halifax, Nova Scotia, Canada, the mice were housed in climate controlled and ventilated rack cages and allowed to acclimatize for one week, before any procedures or manipulations. For cannabinoid 2 receptor knockout experiments, DeltaGen CB2R-/- mice were purchased from Jackson Laboratories and a colony was established in-house at CACF. All animals used for the CB2R-/- experiments were generated by mating two homozygous CB2R knockout mutant parents and the male mice were used upon reaching 6-8 weeks of age. CB2R-/- mice were also genotyped using the DNA extracted from ear punches using Accustart II Mouse Genotyping Kit (Quanta Bioscience, MD, USA). PCR results matched the expected bands after following manufacturer's instructions. All involved animals were kept on a standard 12 hrs light/dark cycle, with standard room temperature 22°C and humidity 55% – 60%. Animals had access to a standard diet of rodent chow and water *ad libitum*.

2.2. CNS Injury Models

2.2.1. Hypoxia Ischemia

One of the utilized models for induction of brain injury uses an established perinatal hypoxic-ischemic protocol, described and developed by Vannucci & Vannucci (2005). The model was modified to be used in adult mice, as described below.

Animals were anesthetized using isoflurane gas (2–5%) an O_2 flow rate of 2 L/hr using an anesthetic vaporizer (VetEquip, Pleasanton, CA, USA). Once the animals displayed signs of anesthesia (reduced breathing, lack of motor movement), they were transferred onto a heating pad and prepared for surgery by being placed on their back. To maintain proper anesthesia, a nose cone was placed over the head of the mouse, allowing mice to continuously breathe 1-2% isoflurane at an O_2 flow rate of 0.4 – 0.8 L/hr with a steady oxygen flow. The neck area was gently shaved with a razor, as well as cleaned with alcohol and iodine washes to create aseptic conditions for the surgery site. Once prepared, most of the body was covered with drape to ensure adequate heat distribution over the body of the animal and to prevent hypothermia, which is potentially neuroprotective. Using a surgical blade, a 1-cm incision was made on the left side of the neck. The underlying tissue was gently moved aside to expose the sternohyoid and sternomastoid muscles until the right common carotid artery (RCCA) could be reached. Upon isolation, the RCCA was gently placed on top of curved forceps and two 8-0 silk sutures were tied at the top and bottom sections of the vessel, at least 2mm apart. Once the knots were confirmed to be tight and fixated visually, the RCCA was permanently occluded by transecting the mid-point between the two areas tied off with silk sutures. The surgical site was then

inspected to ensure that no bleeding occurred after RCCA ligation. The wound was then closed with a 5-0 suture with a topical application of Lidocaine gel (2%) directly on top of the wound edges. Ketoprofen (1 mg/mL) was injected subcutaneously at the start of surgery to provide postoperative analgesia. In parallel, isoflurane gas supply was turned off, supplying the animal with pure oxygen. As soon as first signs of normal breathing and slight movement were observed, the animal was transferred to a pre-heated post-surgery cage with easily-accessible food and water. The animals were allowed to recover for two hours and were constantly under observation to ensure minimal discomfort and quick response to any complications at the surgical site.

After recovery, the animals were transferred into an acrylic glass hypoxia chamber, floating in a heated water bath to ensure adequate heating for the animal's body temperature to remain at 37 ± 0.5°C (98.6°F). Once the animal was secured in the chamber with two rubber stopping caps, the chamber's environment was changed to a low-oxygen atmosphere (7.5% O_2 balanced with 92.5% N_2). The duration of hypoxia was chosen to be 50 minutes based on pilot experiments. After the hypoxia, the animals were transferred back into their heated recovery cage. During the recovery, the animals were observed for behavioral and symptomatic changes and given injections of saline every six hours to rehydrate.

2.2.2. Endothelin-1

Animals were anesthetized and maintained with isoflurane gas (2-5%) plus oxygen and air (ratio: 0.2/0.8 L/min). Temperature was maintained at 37°C throughout the surgery using a self-regulating heating blanket. The animals were placed in a stereotactic frame (Model 900, Kopf,

USA) and connected to a facemask delivering a steady flow of maintenance isoflurane gas. The skin directly overlying the intersection between bregma and lambdoid sutures was shaved, and isopropyl alcohol and 2% betadine applied as antiseptic agents. Using a surgical blade, a vertical incision ~1 cm in length was made, beginning above the bregma and extending anteriorly to the lambdoid suture. The skin was retracted, and two holes were drilled in the skull, one 2.3 mm posterior and 1.0 mm left of bregma, the other 2.3 mm posterior and 1.0 mm right of bregma. The stereotaxic coordinates were determined from a Paxinos/Franklin mouse atlas (Franklin & Paxinos, 2008) and set relative to bregma at (i) 0.0 anterior–posterior (AP), +1.50 medial–lateral (ML), −2 dorsal–ventral (DV) and (ii) 0.0 AP, +1.75 ML, −2 DV. Using a microinjection unit (Model 5000, Kopf), an intracerebral injection of vasoconstricting peptide endothelin-1 (ET-1; Sigma-Aldrich, ON, Canada) dissolved in sterile saline (500pmol/µl) was performed. A 2 µL Hamilton Neuros® 7001 syringe (Hamilton Company, NV, USA) was placed into the microinjection unit to deliver the desired volume (1 µl, 2 µl, 2 x 2 µl) of ET-1 (2µg/µl) over a 10-minute period. To prevent backflow, the needle was kept in place and ET-1 was permitted to diffuse into the brain tissue for 30 seconds before the needle was gradually retracted. The incision was then sutured with 5-0 prolene and lidocaine gel was applied topically to the incision edges. After the surgery, the animal was transferred to a heated recovery cage and allowed to recover with access to food and water *ad libitum*. The animal was continuously monitored for any signs of neurological impairment up until the intravital microscopy step.

2.3. Anesthesia for Intravital Microscopy

Prior to the start of intravital microscopy every animal's body weight was measured using a commercially available weighing scale and sodium pentobarbital (90 mg/kg, 54 mg/mL; Ceva Sante Animale, Montreal, Quebec, Canada) was administered by intraperitoneal (I.P.) injection at a 50% dilution with 0.9% sodium chloride (Hospira, Montreal, Quebec, Canada). Mice were properly anesthetized prior to any procedure and the depth of anesthesia was regularly monitored via paw withdrawal reflex. An additional 0.1mL of 90% diluted sodium pentobarbital solution (5.4 mg/mL) was administered intravenously (I.V.) to maintain a sufficient depth of anesthesia throughout the procedure, based on the visual assessment of breathing rate and of the paw withdrawal reflex. In animals with severe neurological impairment, the anesthetic was administered more slowly and with an additional subcutaneous saline injection to ensure appropriate hydration.

2.3.1. Endotoxemia

Once the appropriate anesthesia depth was reached, the animals were placed on a heating pad in a supine position and their body temperature was maintained at 37 ± 0.5°C (98.6°F). Rectal body temperature was monitored continuously and recorded every 15 minutes for the duration of the experiment. Animals breathed room air spontaneously, but oxygen was provided if breathing was impaired/laboured. Mucous and saliva buildup was also extracted from the throat using a short 18G cannula connected to a 10 ml syringe (Becton Dickinson and Company, NJ, USA) as a suction device to prevent obstruction of the trachea. The animals were administered a slow (over ~5 minutes) intraperitoneal injection of lipopolysaccharide endotoxin (LPS, 5 mg/kg; Sigma

Aldrich, St. Louis, MO, USA) to induce endotoxemia. Endotoxemia was carried out over 2 hours until intravital microscopy (IVM).

2.3.2. Fluorochromes

Intravital staining was done thirty minutes prior to the start of the IVM by administering a bolus injection of 0.05% Rhodamine-6G (1.5 mL/kg) and 5% fluorescein isothiocyanate-bovine serum albumin (FITC-BSA) (1 mL/kg, Sigma-Aldrich, ON, Canada) fluorochromes via tail vein injection. FITC-labeled BSA was. Fluorescence excitation was generated by mercury arc lamp (150W), and excitation filters to block the emitted light for Rhodamine-6G (excitation 515-560 nm, emission 590 nm) and FITC (450-490 nm, emission 520 nm). Rhodamine-6G labels mitochondria in leukocytes within injected vessels, producing a visual mark on the immune cells. FITC-labeled BSA complex allows the visualization of blood flow through the vasculature by enhancing blood contrast.

2.3.3. Laparotomy and IVM setup

Fifteen minutes before IVM, the laparotomy was performed after ensuring the animal's anesthetic depth was properly sufficient. A midline skin incision was made on the animal's abdomen using a scalpel to expose the abdominal muscle layer. Using fine tissue scissors, the muscle layer was cut along the *linea alba* to expose the abdominal cavity and prevent bleeding. Using saline soaked cotton tipped applicators the caecum was located, and a portion of the terminal ileum was exteriorized onto a heated platform of a specially designed apparatus that was

fixed to the heating pad. The animal was placed on its side to minimize the tension on the intestine and saline was perfused over the platform with intestine on it to keep in physiological conditions (Figure 5). The perfusion apparatus enabled continuous thermostat-controlled (37°C/ 98° F) saline to be perfused over the exposed intestinal section to reflect normal physiological conditions of moisture and temperature. The saline was pumped at a rate of 5-10 mL/hr and a glass slide construct was placed just slightly above the intestine, not to cause any pressure but allow microscopy via contact with perfused saline. The heating pad with the intravital stage containing the animal and intestine on the platform was placed under the microscope for observation.

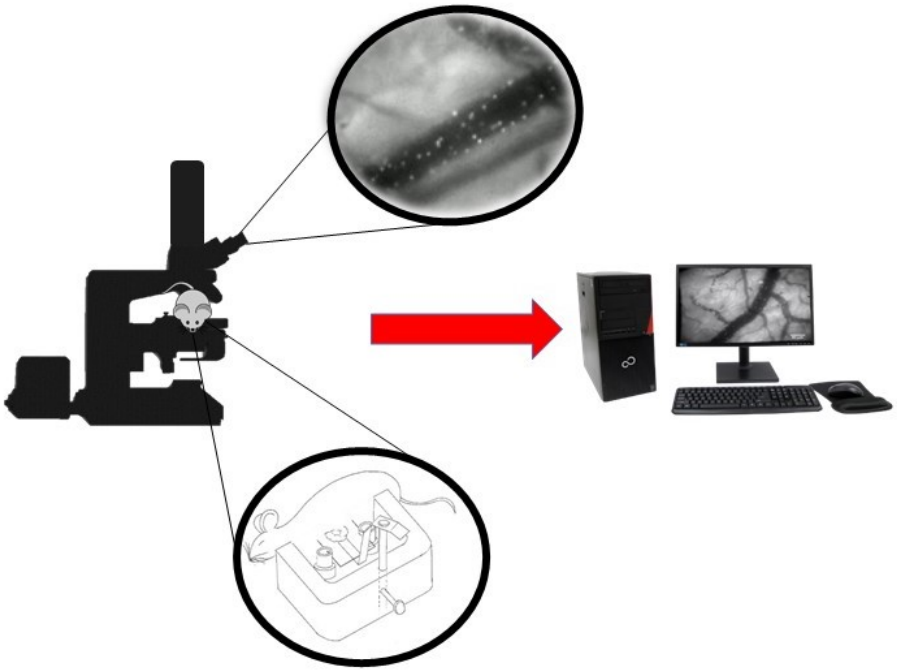

Figure 5. **Simplified Graphical Representation of Intravital Microscopy Workflow.**

Simplified representation of the intravital microscopy suite and the associated workflow. The anesthetized animal goes through the surgical procedures to expose a piece of small intestine that is then placed onto a special stage that is heated and perfused with saline to keep the externalized piece of intestine in physiological environment. The animal is injected with fluorescent dyes

(rhodamine 6G and FITC) to help visualize individual leukocytes, as well as microvascular perfusion. The heating pad construct is then placed under the microscope and video segments (30s) are recorded for future offline analysis.

2.3.4. Microscopy

An epifluorescent microscope was used (Leica DMLM, Wetzlar, Germany) to observe intestinal leukocyte activation as well as capillary perfusion. An attached mercury-arc light source (LEG EBQ 100, Jena, Germany) was used to illuminate the observed area and different excitation filters were utilized to specifically excite the different fluorochromes with corresponding wavelengths. A 460-490 nm band pass excitation filter, which allows blue light to pass through but blocks all other wavelengths, was used to excite FITC and allowed observation of the capillary perfusion. A 530-550 nm band pass excitation filter, which allows only green light to pass, was used to excite Rhodamine-6G and allowed observation of leukocytes. A water immersion lens (Leica N PLAN L 20X/0.40) was used to make a liquid contact between the lens and glass slide over the section of intestine for observation. A black and white DAGE CCD video camera (DAGE MTI Inc., Michigan City, IN), C-mounted on the microscope was used to observe and record video directly onto a computer through an analog-to-digital video converter (DFG/USB2PRO, The Imaging Source, Germany) and image capturing software (IC capture, The Imaging Source, Germany).

1.3.4.1. Leukocyte Activity Recording

Epifluorescent microscope was used to focus on the submucosal venules via the green excitation filter. Six visual fields containing non-branching, submucosal collecting venules (V1) and postcapillary venules (V3) containing a length of at least 300 µm were observed and recorded for 30 seconds each in every animal. Collecting venules (V1) were classified as vessels with a measured diameter of approximately 50-100 µm and accompanied by an adjacent arteriole. Post

capillary venules (V3) were classified as vessels under 50μm in measured diameter. Leukocytes that were adherent to the same spot of endothelia for the duration of the recorded video (30 second) were classified as adherent leukocytes.

1.3.4.2. Functional Capillary Density

Epifluorescent microscope was used to focus on the muscular layers of the small intestine via the blue excitation filter. Since both longitudinal and circular muscle layers in the mouse intestine are very thin, capillaries of both layers are visualized simultaneously. Six randomly selected visual fields focused on intestinal muscle layers were recorded for 30 seconds each. In order to observe the capillary perfusion of the villi in the mucosal layer, the observed section of small intestine was cauterized longitudinally on the anti-mesenteric side using a microcautery blade (Medtronic, FL, USA). Fine tissue scissors were then used to cut the intestinal wall open and gently moved apart to expose the lumen, followed by warm 0.9% saline wash to flush out the luminal contents. Cotton tipped applicators, soaked with warm saline, were then used to gently manipulate the intestine to maximize the surface of the lumen to allow the glass slide to be placed gently above the observation area, only allowing the saline to make the seal and avoiding any additional pressure. The microscope was used to focus on the mucosal villi and six randomly selected areas were recorded, with each field containing at least three clearly visible villi for an offline analysis at a later time point.

2.3.5. Pia Mater Fluorescence Intravital Microscopy

After the desired anesthesia depth was achieved, the animal was stabilized in a stereotactic frame. Animals were kept on a heating blanket with a feedback rectal probe/heating system to maintain body temperature at 37°C. A midline incision of the scalp was made; any bleeding was stopped with gauze pads and pressure. Using a low speed dental drill, a cranial window of 1.5x1.5mm was made at the intersection between bregma and lambdoid sutures. The drill site was flushed and cooled with saline to prevent unnecessary shearing, stress and overheating. Next, the thin dura mater layer was punctured using a 30-gauge needle and a cut-out removed using micro scissors and fine point scissors. The site was immediately flooded with warm saline. Once the imaging site was prepared, a 5% fluorescein isothiocyanate (FITC)-albumin (Sigma-Aldrich, ON, Canada) solution and 0.05% Rhodamine 6G (Sigma-Aldrich) solution were administered via single bolus injection by tail vein. Upon positioning the animal on the microscope stage, a glass cover slip was gently fixated on top of the cranial window, forming a good contact with saline under the slip and ensuring lack of any pressure onto the exposed vessels.

Five small pial venous vessels (diameter < 100 μm) and five capillaries with adequate focus were randomly selected across the field of view, each with a duration of 30 seconds to visualize and quantify leukocyte-endothelium interaction and functional perfusion density.

2.4. Blood & Tissue Collection

Following completion of intravital microscopy, the animal was euthanized by cardiac puncture where blood was drawn into a heparinized syringe. Three microliters of heparin (Pharmaceutical Partners of Canada Inc., Richmond Hill, ON, Canada) was placed into a 30-gauge needle to prevent blood coagulation. On average 0.5mL of blood was obtained, which was then placed in a 1 mL Eppendorf tube and centrifuged at room temperature for 10 minutes at 10,000 x g. The plasma was then isolated and aliquoted into 0.5 mL microtubes, followed by storage at -80°C. Immediately after cardiac puncture, tissue samples of the small intestine and spleen were also taken. A section of the terminal ileum was isolated, longitudinally cut open, and the luminal contents flushed with saline. The tissue section was then placed into a cryogenic tube and frozen in liquid nitrogen. Spleen was also isolated from connective tissue and surgically removed, followed by immediate snap-freeze in liquid nitrogen. Both tissue samples were placed at -80°C for long term storage.

2.5. Neutrophil Isolation & Count

Mouse bone marrow polymorphonuclear neutrophils (PMNs) were isolated from femurs and tibias of 6-8 weeks old, male C57BL/6 mice. Bone marrows were flushed using a 26-gauge needle and 3 cc syringe filled with 1X HBSS (1 mM EDTA, 10 mM HEPES, 2% FBS). Bone marrow cells were centrifuged at 300 x g for 10 minutes at 4°C, and resuspended in 1X HBSS (1 mM EDTA, 10 mM HEPES, 2% FBS). PMNs were then isolated from single cell suspensions of bone marrow by negative selection via using EasySep™ Mouse Neutrophil Enrichment Kit and manual EasySep™ magnet (Stemcell Technologies, Vancouver, BC, Canada). All the steps were

following the manufacturer's instructions. Once the neutrophil cells were isolated and washed, the total number of cells and the purity were assessed on a compound microscope.

2.6. Video Analysis

All intravital records were analyzed in a blinded fashion via offline ImageJ software (NIH, US). Leukocytes that interacted with but did not firmly adhere to the endothelia were defined as rolling leukocytes. Rolling flow parameter was defined as the number of nonadherent, rolling leukocytes passing through an observer-chosen virtual line within a 30 second window of the recording. The number of rolling leukocytes were counted for 30 seconds and used to estimate the number of rolling leukocytes per minute.

Leukocytes that remained adherent to the same position on the endothelia for the duration of the recording (30 seconds) were defined as adherent leukocytes. A predetermined area of vessel was measured and the number of adherent leukocytes within that area was counted. These two values were then used to calculate the number of adherent leukocytes on the cylindrical surface of the luminal side of the recorded vessel.

In order to quantify vascular perfusion, functional capillary density (FCD) parameter was analyzed. FCD was defined as the total length of capillaries with observable erythrocyte perfusion in relation to a predetermined rectangular field in the recorded video segment, expressed in $\mu m/\mu m^2$. For the muscular or tissue layers, a rectangular area was selected based on video quality and visibility. The area was then measured and the lengths of all perfused vessels within that area were added to calculate the final FCD value. For the mucosal villi, unique villi in

each video recording were analysed. First, the area of each villus was measured, followed by measuring the length of the perfused capillaries in each villus and added together to obtain a total area and total perfused capillary length, which was then used to calculate the final FCD value, representative of the recorded visual field.

All of the leukocyte activity counts, and vessel length measurements were performed three separate times, followed by taking an average, which was then used for further analysis.

2.7. Assessment of Infarct Volume

Brains of the animals were extracted post-mortem (shortly after IVM). Brains were placed in a 3D printed brain matrix with slots for a surgical blade to be placed in (Figure 6). The matrix was then cooled at -20°C for ~10 minutes, then removed back to room temperature and sliced with a surgical blade (1 mm) after 30 seconds exposure to room temperature. Each brain slice was then put in a separate well of a large well plate. Each well was then filled with 2% 2,3,5-triphenyltetrazolium chloride (TTC) solution and placed in an incubator for 12 minutes at 37°C. The slices were then removed from each well and placed on a transparent sheet, followed by a digital scan. The infarct size was measured using manual tracing and colour threshold methods of 5 serial sections in ImageJ (version 1.47v). Infarct volume was estimated based on the thickness of each slice and infarct sizes on both sides of the section were compared to ensure accuracy of the estimate.

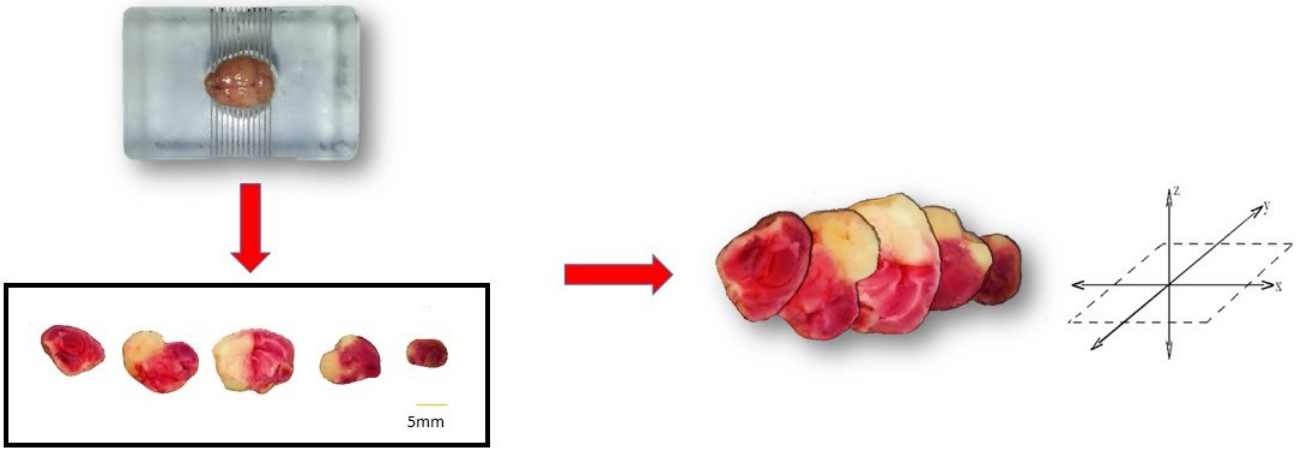

Figure 6. **Brain Infarct Volume Quantification.**

Process of brain infarct volume evaluation and quantification. After post-mortem brain extraction procedure, the brains were placed in a mouse brain matrix, which was then put in a freezer prior to cutting the brain in slices and staining the tissue with metabolic stain tetrazolium chloride (TTC). Brain tissue that stains re/pink d is considered metabolically active, whereas white/yellow tissue colour is considered to be metabolically inactive (dead). The brain slices were then analyzed to quantify the volume of infarct within each brain slice via digital software and final volumes were then reported.

2.8. Behavioural Assessment of Neurological Impairment (Neuroscore)

Neuroscore is described as a non-invasive and *in vivo* assessment of general condition and neurological deficits produced by CNS injury and is expressed as a composite score that was originally developed by Dr. Ulrich Dirnagl (Charité-Universitätsmedizin Berlin, Germany).

Scores ranged from 0 (healthy) to 56 (the worst performance in all categories) and represented the sum of scores for 6 general deficit categories (hair, ears, eyes, posture, spontaneous activity and epileptic behaviour categories) and 7 focal deficits categories (body symmetry, gait, climbing on angled surface, circling behaviour, front limb symmetry, compulsory circling, whisker response to light touch).

In more detail, the 6 general categories were scored as follows:

1. **Hair**

   The mouse is placed on open bench top (OBT), observed with no interference.

   0 – Hair neat and clean.

   1 – Localized piloerection and dirty hair in 2 body parts (typically nose and eyes).

   2 – Piloerection and dirty hair in more than 2 body parts.

2. **Ears**

   The mouse is placed on OBT, observed with no interference, then stimulated by snapping fingers.

   0 – Normal reaction, ears are stretched laterally and behind. They react to noise.

   1 – Stretched laterally but not behind (one or both ears). They react to noise.

   2 – No reaction to noise, stretched laterally but not behind (one or both ears).

3. **Eyes**

The mouse is placed on OBT, observed with no interference.

0 – Eyes are open, clear, quickly follow the surrounding environment/movement.

1 – Eyes are open and characterized by aqueous mucus. They slowly follow the surrounding environment.

2 – Eyes are open and characterized by dark mucus.

3 – Eyes are ellipsoidal in shape and are characterized by dark mucus.

4 – Eyes are closed.

4. **Posture**

The mouse is placed on the palm and swung gently from side to side.

0 – The mouse stands up in the upright position with the back parallel to the palm. During the swing, the mouse stands up rapidly.

1 – The mouse stands humpbacked. During the swing, it flattens the body to gain stability.

2 – The head or part of the trunk lies on the palm.

3 – The mouse lies on one side, barely able to recover into upright position.

4 – The mouse lies in a prone position, not able to recover or stand.

5. **Spontaneous Activity**

The mouse is placed on OBT, without observer interference.

0- The mouse is alert and explores actively.

1- The mouse seems alert, but it is calm and sluggish.

2- The mouse explores intermittently and sluggishly.

3- The mouse is somnolent and numb, very few movements on the spot.

4- No spontaneous movements.

6. **Epileptic behaviour**

a. The mouse is placed on OBT. The worst behaviour is recorded during the whole observation period. This parameter is recorded last after full observation period.

0 – No epileptic behaviour present.

3 – The mouse is reluctant to handling, shows hyperactivity.

6 – The mouse is aggressive, stressed and stares at surrounding environment.

9 – The mouse shows hyperexcitability, chaotic movements and presence of convulsion during handling or shortly after handling (or both).

12 – Generalized seizures associated with wheezing and unconsciousness.

The 7 focal deficit categories were scored as follows:

1. **Body Symmetry**

Mouse is placed on OBT, carefully observing the resting behaviour, describing the nose-tail line.

0 – Normal posture, straight tail.

1 – Slight asymmetry, as body leans on one side with fore and hindlimbs beneath the body, tail is slightly bent.

2 – Moderate asymmetry, as body leans on one side with fore and hindlimbs stretched out, tail is slightly bent.

3 – Prominent asymmetry, as body is bent, one side is on the OBT, tail is bent.

4 – Extreme asymmetry, as body is highly bent, with one side constantly on the OBT, tail is highly bent)

2. **Gait**

Mouse is placed on OBT, allowing fully undisturbed movements.

0- Normal gait, flexible, symmetric and quick.

1- Stiff gait, inflexible. Walks humpbacked, slower than normal.

2- Limping with asymmetric movements.

3- Trembling, drifting, falling.

4- Does not walk spontaneously, when gently pushed with pen, it takes no more than 3 steps.

3. **Climbing**

Mouse is placed on gripping surface 45 degrees to OBT, top of the recovery cage is utilized for this step, as it provides the correct angle and plenty of familiar surface for the mouse. The mouse is then placed in the centre of the surface and observed.

0- Normal, mouse climbs quickly to the top.

1- Climbs with strain, limb weakness apparent.

2- The mouse holds onto the slope, does not slip or climb.

3- The mouse slides down slope, unsuccessful effort to prevent fall.

5- The mouse slides immediately, no effort to prevent fall.

4. **Circling behaviour**

Mouse is placed on OBT, observation of the mouse fully undisturbed.

0- Absent circling behaviour, mouse turns equally on both sides.

1- Mouse takes predominantly one-sided turns.

2- Mouse frequently circles to one side, not constant behaviour.

3- The mouse circles constantly to one side.

3- The mouse circles with pivoting, swaying or no movement.

5. Forelimb symmetry

Mouse is suspended by the tail. Movements and position of forelimbs are observed.

0- Normal symmetry. Both forelimbs are extended towards the bench and move actively.

1- Light asymmetry. Contralateral limb does not extend entirely.

2- Marked asymmetry. Contralateral forelimb bends towards the trunk. The body slightly bends on ipsilateral side.

3- Prominent asymmetry. Contralateral forelimb adheres to the trunk.

4- Slight asymmetry in body/limb movement.

6. Compulsory circling

The forelimbs are placed on bench. Hindlimbs are suspended by the tail. This position reveals the presence of the contralateral limb palsy.

0- Absent circling. Normal extension of both forelimbs.

1- Tendency to turn to one side. The mouse extends both forelimbs but starts to turn preferably to one side.

2- Mouse circles to one side. Tends to turn towards one side with a slower movement compared to healthy mice.

3- Mouse pivots to one side sluggishly. The mouse turns towards one side failing to perform a complete circle

4- The mouse does not advance. The front part of the trunk lies on the bench. Slow and brief movements.

7. Whisker Response

Mouse is placed on the bench. Using a pen, the whiskers and the tip of the ears (from behind) is gently touched. The test is first done on the side with a lesion, then on the contralateral side.

0- Normal symmetrical response. The mouse turns the head towards the stimulated area and withdraws form the stimulus.

1- Light asymmetry, the mouse withdraws slowly when stimulated on the ischemic side. Normal response on the contralateral side.

2- Prominent asymmetry. No response when stimulated on the ischemic side. Normal response on the contralateral side.

3- Absent response ipsilaterally, slow response when stimulated on the contralateral side.

4- Absent response ipsilaterally, no response when stimulated on the contralateral side.

Experimenter did not have any knowledge of the experimental group for behavioural analysis.

Behavioural scores for each category were added and used for further analysis and classification of animals' neurological deficits.

2.9. Experimental Timeline

The experimental timeline is broken down into major steps – (1) induction of CNS injury and (2) immune challenge *(endotoxemia)*. The first step starts with a CNS injury induction surgery (ET-1 or HI), followed by monitoring and recovery for 24 hours after a successful surgery. After surgical recovery, behavioural parameters are assessed to ensure the animal can obtain water and food. In cases of severe impairment, the animals are euthanized. At 21-hour mark, the animals are scored behaviourally and are prepared for transfer to the intravital suite. After anesthesia with pentobarbital, the animals received the cannabinoid treatment, 15 minutes prior to induction of endotoxemia, at approximately 22 hours. Intravital microscopy recordings took place at 24-hour mark, followed by tissue and blood collection at 26 hours. Final step in timeline involved the extraction of the whole brain, followed by metabolic stain of the individual brain slices. Total experimental timeline thus took approximately 27 hours.

CNS Injury Timeline – HI Model

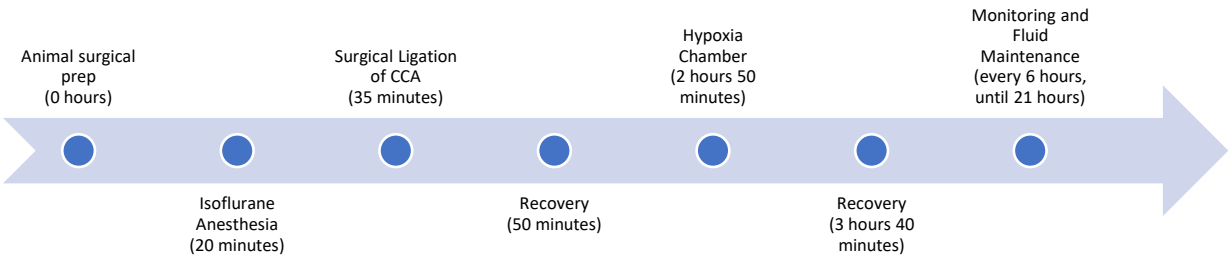

CNS Injury Timeline – ET-1 Model

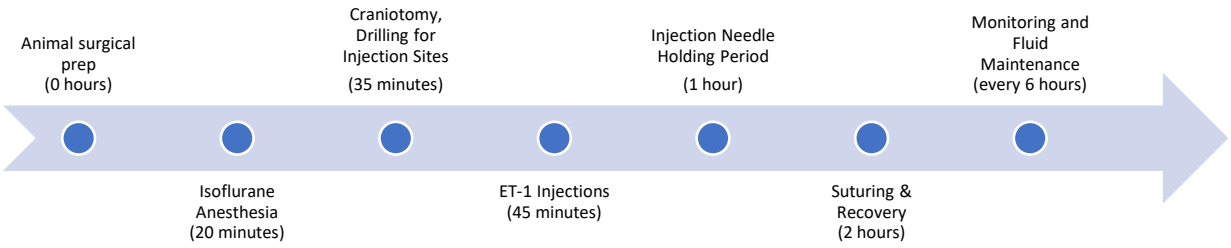

Endotoxemia Timeline- CB2R Antagonist Approach, Intestinal IVM

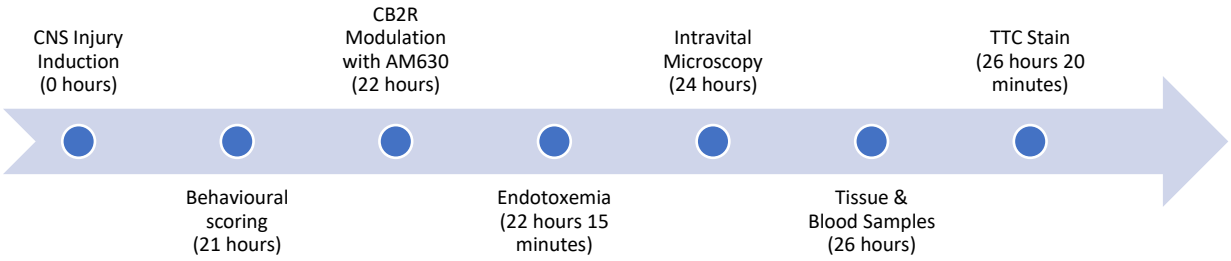

Endotoxemia Timeline- CB2R Agonist Approach, Intestinal IVM

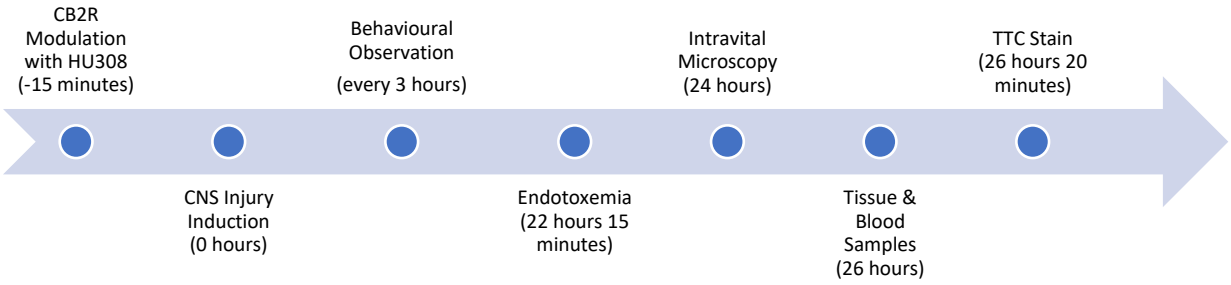

Endotoxemia Timeline- CB2R Agonist Approach, Early Pia Mater IVM

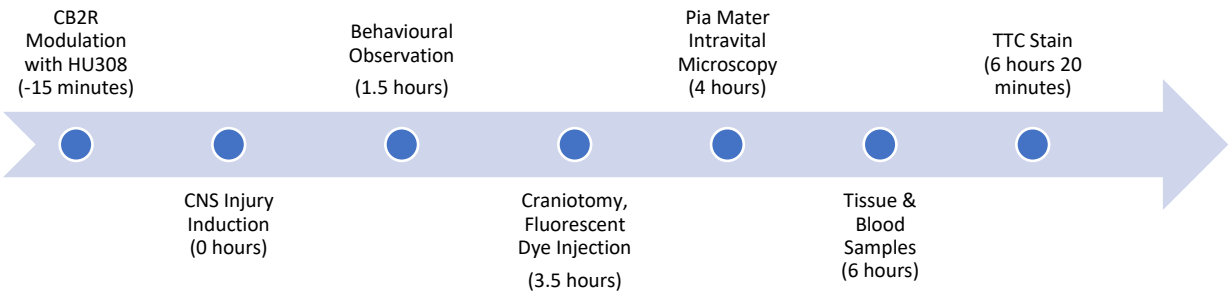

2.10. Plasma Cytokine and Chemokine Analysis

Levels of cytokines, chemokines and adhesion molecules were analysed in plasma samples using a custom made 12-plex assay obtained from R&D systems (Minneapolis, MN, USA). The mouse magnetic luminex assay kit targeted the following analytes IFN-γ, TNF-α, IL-1β, IL-2, IL-4, IL-6, IL-10, IL-12 p70, IL-17A, P-selectin and ICAM-1. The kit was generated based on the Luminex® technology and was measured using a Luminex Technology Bio-Rad 200 Analyzer and BioPlex Manager software (Bio-Rad, Mississauga, ON, Canada). The analysis instruments were calibrated and validated once every 30 days, with sample preparation taking place only when the validation was successful. Preparation of the plasma samples was done following the manufacturer's instructions. All samples were run in technical duplicates and prepared in four-fold dilutions using the supplied R&D systems sample diluent. A 7-point standard curve was generated for each analyte being tested. Before each experimental run, the Luminex systems were primed following manufacturer's instructions and the wash station was prepared using manufacturer's recommended parameters with provided buffers.

For each kit, 50µl of the detection antibody magnetic beads for each analyte was added to each well of the flat bottom 96-well plate. Standards were prepared according to the manufacturer guidelines in three-fold serial dilutions and added to the plate along with the samples. After immobilized antibodies bound to the analytes of interest, the plate was then placed in a Bio-Plex Pro magnetic wash station and washed with the provided R&D buffer solution to remove any unbound substances. Next, 50 µL of the microparticle cocktail was then added to each well of the microplate and incubated in the dark on a horizontal orbital microplate shaker (0.12" orbit) set at 800 ± 50 rpm for 2 hours. After, 50 µL of diluted Biotin-Antibody cocktail was added to each well of the microplate and incubated in the dark for 1 hour, under the same horizontal shaker settings as above. Finally, 50 µL of diluted Streptavidin-PE was added to each well of the microplate and incubated in the dark for 30 minutes, under the same horizontal shaker settings as above. Another cycle of three washes with the R&D Wash Buffer was carried out, followed by adding 100 µL of R&D Wash Buffer to each well and incubated at room temperature for 2 minutes at 800 rpm. The plates were then read within 90 minutes using Bio-Rad 200 luminometer. Raw data was compiled and analysed with Bio-Plex manager software.

2.11. CB2R Pharmacological Modulation

For experiments involving CB2R inhibition, I have used a selective synthetic CB2R inverse agonist AM630 (6-Iodopravadoline; Tocris Bioscience, Ellisville, MO, USA) with a Ki of 32.1 nM at CB2R and 165- times selectivity for CB2 receptor over CB1R. Since AM630 possesses highly lipophilic properties of cannabinoid molecules, AM630 was dissolved in 30% dimethyl sulfoxide (DMSO) vehicle solution. Multiple DMSO dilution have been tried, with 30% being

the first stable dilution at room temperature for a solution to be made. After conducting dose-response experiments (not shown), the effective AM630 dose was determined to be 2.5 mg/kg. The drug was administered via a slow tail-vein injection using a 1 mL human insulin syringe with fixed-needle tip.

For experiments involving CB2R activation, I have used a selective synthetic CB2R agonist HU308 ([(1R,2R,5R)-2-[2,6-dimethoxy-4-(2-methyloctan-2-yl)phenyl]-7,7-dimethyl-4-bicyclo[3.1.1]hept-3-enyl]methanol; Tocris Bioscience, Ellisville, MO, USA) with a Ki value of 22.7 nM for the CB2R. HU308 was shown to be effective at a 2.5 mg/kg dose, after a pilot dose-response experiment (not shown). Prior to administration, HU308 was dissolved in 10% DMSO vehicle solution and delivered via a slow tail-vein injection using a 50cc human insulin syringe with fixed-needle tip.

2.12. Quantitative Two-Step Reverse Transcriptase Polymerase Chain Reaction

2.12.1. RNA Isolation

First, whole spleen and small intestinal samples were efficiently disrupted and mechanically homogenized using a rotor-stator homogenizer in a round-bottom tube. Briefly, RNA was harvested using an RNeasy Mini Kit purchased from Qiagen (Valencia, CA). Cells were lysed in the 6-well plate in which they were seeded and treated, using 350 µl Buffer RLT. The solution was then transferred into a 1.5 ml Eppendorf tube and mixed with equal volume of 70% ethanol, followed by a transfer to a RNeasy Mini spin column placed in a 2 ml collection tube and centrifuged at 8000 x g for 15 s. The flow-through was then discarded and 350µl of Buffer RW1

was added to the column and centrifuged at 8000 x g for 15 s. The flow-through was discarded and 80 µl of DNase diluted in Buffer RDD was added to each column and left at room temperature for 15 min. The column was again washed with 350 µl of Buffer RW1 and centrifuged at 8000 x g for 15 s. The flow-through was discarded and 500 µl Buffer RPE was added to the spin column and centrifuged at 8000 x g for 15 s. The flow-through was discarded and 500 µl Buffer RPE was added to the column and centrifuged at 8000 x g for 2 min. The flow-through was discarded one final time and 35 µl of RNase-free water was used to elute the RNA. The purity and concentration of each RNA sample was determined using a NanoVue Plus Spectrophotometer (GE Healthcare Life Sciences; Piscataway Township, NJ). The purity of the sample was based on the A280/A260 ratio with the value between 1.7-2.0 counted as acceptable for proceeding. Isolated RNA samples were stored at -80°C.

2.12.2.cDNA Synthesis

Approximately 500 ng RNA, isolated as described above, was then reverse transcribed using an iScript™ cDNA synthesis kit (Bio-Rad Laboratories; Hercules, CA) according to the manufacturer's instructions. The iScript reaction mix (2 µl) and iScript reverse transcriptase (0.5 µl) was added to RNA template and nuclease-free water to a final volume of 10 µl and final concentration of RNA template 50 ng/µl. The reaction was incubated in a Bio-Rad T100™ Thermocycler using the recommended reaction protocol: 5 min at 25°C, 30 min at 42°C, and 5 min at 85°C. Once synthesized, the cDNA was stored at -20°C.

2.12.3.qRT-PCR

Quantitative real-time polymerase chain reactions were conducted using the SsoFast EvaGreenTM Supermix® (Bio-Rad Laboratories, Hercules, CA). The cDNA samples were diluted 1:4 in pyrogen-free water. PrimePCR™ SYBR® Green Assay: Cnr2, Mouse (Exonic, 4:135918919-135919031; Bio-Rad Laboratories, Hercules, CA) was used to make 100 nM primer master mixes from 10 µl of both the CB2R forward and reverse primers added to 80 µl of water. A 1 µl sample of diluted cDNA was then added to a master mix solution containing 5 µl EvaGreen Supermix, 3 µl pyrogen-free water, and 1 µl primer mix in a final volume of 10 µl. Negative controls did not contain any cDNA. Reactions were conducted in triplicate using a Stratagene Mx3005p qPCR system (Agilent Technologies, Santa Clara, CA) and a Rotor-Gene 6000 qPCR machine (Qiagen, Valencia, CA). Cycling conditions consisted of a 30 second activation step at 95°C, followed by 40 amplification cycles for 5 seconds at 95°C and 30 seconds at an annealing temperature specific to the primer. To confirm that the PCR reaction had produced the specific and intended products, a melt curve analysis was conducted using MxPro qPCR Software (Agilent Technologies, Santa Clara, CA) cycle threshold (CT) values, indicating the number of cycles it takes for the fluorescent signal to surpass the background fluorescence (Mestdagh et al., 2009). The relative amounts of amplicons were determined by normalizing the CT values of the target cnr2 gene to the endogenous β-actin control (forward primer 'AAGGCCAACCGTGAAAAGAT' and reverse primer 'GTGGTACGACCAGAGGCATAC'). These values were then normalized to the untreated control values, giving the expression fold values.

2.13. Assessment of Splenic Weight

To indirectly assess the splenic response during CNS injury the whole spleen was surgically extracted after animals with CNS injury completed the intravital microscopy protocol and the blood was drawn via cardiac puncture. The spleen was immediately placed onto a tared plastic weighing cup on a scale and weighed two times. The average of the two numbers was recorded as the splenic weight. Groups that had their spleens weighed were the Control, CNS injury + LPS and CB2R agonist treatment + CNS injury + LPS groups.

2.14. Statistical Analysis

All data presented in the results are expressed as means ± standard deviation (SD). All animals were coded and analysed in a non-biased fashion. Statistical analyses of the results were performed using the software GraphPad Prism 6.0 (GraphPad Software Inc, La Jolla, CA, USA). The Kolmogorov-Smirnov test was used to confirm normality of the data. In the intravital microscopy data, differences between groups were analyzed using one-way analysis of variance (ANOVA), followed by the Newman-Keuls test for group wise comparisons. Unless otherwise stated, data which compared two groups were compared by a two-tailed t-test. Data sets with three or more groups testing one measurable variable were tested by a one-way ANOVA. The significance level was considered at $p < 0.05$. In the cytokine and qRT-PCR data, *post-hoc* measures included Tukey's test. Pearson's r was used to investigate the strength of the relationship between two quantitative and continuous variables. Unless otherwise stated, differences between groups were considered statistically significant at $p < 0.05$.

2.15. Experimental Groups

The experimental work shown in this dissertation is a culmination of multiple approaches and CNS injury models, each focusing on a particular aspect of CNS injury induction, as well as addressing the individual treatment specifics. To help the reader be clear about which models were used with which objective, as well as the brief reasoning behind this – I will attempt to describe the work and the decision making behind steps taken by bundling the experimental groups per objective.

The endothelin-1 (ET-1) model was first used to investigate the early cannabinoid treatment approach in *objective 1* and was great at showing peripheral immune consequences after CNS injury. After obtaining the data, it was decided that a local (brain) readout of immune activation was needed, which would be quite difficult to accomplish, since the endothelin-1 model required surgical manipulation of the skull and direct access to the brain. A different model was thus implemented, adult hypoxia-ischemia (HI) model was effective at inducing acute CNS injury without direct surgical manipulation of the brain.

Objective 2 was focused on addressing the peripheral immune consequences directly and was thus investigated with both ET-1 and HI models to ensure that the findings remained reproducible between the two models. Pilot findings did not show the need for a separate brain readout. Upon completing the data sets, it was decided to extend the experiments to genetic knockouts to underline the importance of treatment timing and the danger of inhibiting the target receptors too early. ET-1 was the model that was the most consistent in inducing the CNS injury and produced the least amount of mortality, therefore it was selected for the genetic knockout

experiments. Further details on the limitations of the selected models will be discussed in chapter 4. Animal group numbers are reported in each table below.

Objective 1 Group List:

Group 1 was subjected to ET-1 sham surgery, administered saline i.p., DMSO 10% i.v. as a vehicle control.

Group 2 was subjected to ET-1 sham surgery, administered LPS 5 mg/kg i.p., DMSO 10% i.v. as a vehicle control.

Group 3 was subjected to ET-1 surgery, administered saline i.p., DMSO 10% i.v. as a vehicle control.

Group 4 was subjected to ET-1 surgery, administered LPS 5 mg/kg i.p., DMSO 10% i.v. as a vehicle control.

Group 5 was subjected to ET-1 surgery, administered LPS 5 mg/kg i.p., HU308 2.5 mg/kg in 10% DMSO i.v., CB2R treatment delivered 15 minutes before ET-1 surgery.

Group 6 was subjected to HI sham, administered saline i.p., followed by intravital microscopy of the pia mater 4 hours after HI sham surgery.

Group 7 was subjected to HI surgery, administered saline i.p., DMSO10% followed by intravital microscopy of the pia mater 4 hours after HI surgery.

Group 8 was subjected to HI surgery, administered saline i.p., HU308 2.5 mg/kg i.v. in 10% DMSO 15 minutes before HI surgery, followed by intravital microscopy of the pia mater 4 hours after HI surgery.

Group Name	Model	Specifics
Group 1 – Con/ET-1 Sham n=8	ET-1 Sham	Saline i.p.
Group 2 – LPS n=8	HI Sham, Endotoxemia	LPS 5 mg/kg, i.p., DMSO 10% i.v.
Group 3 – ET-1 n=5	ET-1	Saline i.p., DMSO 10% i.v.
Group 4 – ET-1+LPS n=5	ET-1, Endotoxemia	LPS 5 mg/kg, i.p., DMSO 10% i.v.
Group 5 – ET-1+LPS+HU308 n=5	ET-1, Endotoxemia	HU308 2.5 mg/kg, i.v. LPS 5 mg/kg, i.p.
Group 6 – HI-Sham/Con n=5	HI Sham	Saline i.p.
Group 7 – HI n=6	HI	Saline i.p., DMSO 10% i.v.
Group 8 – CNS Injury+HU308 n=4	HI	Saline i.p., HU308 2.5 mg/kg i.v.

Table 1. CB2 Agonist Approach Group List

Objective 2 Group List:

Group 9 was subjected to ET-1 sham surgery, administered saline i.p., DMSO 30% i.v. as a vehicle control.

Group 10 was subjected to ET-1 sham surgery, administered LPS 5 mg/kg i.p., DMSO 30% i.v. as a vehicle control.

Group 11 was subjected to ET-1 surgery, administered saline i.p., DMSO 30% i.v. as a vehicle control.

Group 12 was subjected to ET-1 surgery, administered LPS 5 mg/kg i.p., DMSO 30% i.v. as a vehicle control.

Group 13 was subjected to ET-1 surgery, administered LPS 5 mg/kg i.p., AM630 2.5 mg/kg in 30% DMSO i.v., CB2R treatment delivered 15 minutes before endotoxemia.

Group 14 was subjected to HI sham surgery, administered saline i.p., DMSO 30% i.v. as a vehicle control.

Group 15 was subjected to HI sham surgery, administered LPS 5 mg/kg i.p., DMSO 30% i.v. as a vehicle control.

Group 16 was subjected to HI surgery, administered saline i.p., DMSO 30% i.v. as a vehicle control.

Group 17 was subjected to HI surgery, administered LPS 5 mg/kg i.p., DMSO 30% i.v. as a vehicle control.

Group 18 was subjected to HI surgery, administered LPS 5 mg/kg i.p., AM630 2.5 mg/kg in 30% DMSO i.v., CB2R treatment delivered 15 minutes before endotoxemia.

Group 19 was subjected to ET-1 sham surgery, administered saline i.p. Animals have a genetically knocked out CB2R.

Group 20 was subjected to ET-1 sham surgery, administered LPS 5 mg/kg i.p. Animals have a genetically knocked out CB2R.

Group 21 was subjected to ET-1 surgery, administered saline i.p. Animals have a genetically knocked out CB2R.

Group 22 was subjected to ET-1 surgery, administered LPS 5 mg/kg i.p. Animals have a genetically knocked out CB2R.

Group 23 was subjected to ET-1 surgery, administered LPS 5 mg/kg i.p., AM630 2.5 mg/kg in 30% DMSO i.v., CB2R treatment delivered 15 minutes before ET-1 surgery to pharmacologically block CB2R activity and compare to mice with a genetic CB2R knock out.

Group Name	Model	Specifics
Group 9 – CON/ET-1 Sham n=8	ET-1 Sham	Saline i.p.
Group 10 – LPS n=8	ET-1 Sham, Endotoxemia	LPS 5 mg/kg, i.p., DMSO 30% i.v.
Group 11 – ET-1 n=4	ET-1	Saline i.p., DMSO 30% i.v.
Group 12 – ET-1+LPS n=4	ET-1, Endotoxemia	LPS 5 mg/kg, i.p., DMSO 30%
Group 13 – ET-1+LPS+AM630 n=5	ET-1, Endotoxemia	LPS 5mg/kg i.p., AM630 2.5 mg/kg i.v.
Group 14 – HI Sham / CON n=8	HI Sham	Saline i.p.
Group 15 – LPS n=8	HI Sham, Endotoxemia	LPS 5 mg/kg i.p., DMSO 30%
Group 16 – HI n=6	HI	DMSO 30% i.v., saline i.p.
Group 17 – HI+LPS n=6	HI, Endotoxemia	DMSO 30% i.v. LPS 5 mg/kg, i.p.
Group 18 – HI+LPS+AM630 n=6	HI, Endotoxemia	LPS 5 mg/kg, i.p. AM630 2.5 mg/kg, i.v.

Group 19 – Control (CB2KO) n=3	ET-1 Sham	Saline i.p.
Group 20 – LPS (CB2KO) n=4	ET-1 Sham, Endotoxemia	LPS 5 mg/kg, i.p.
Group 21 – ET-1 (CB2KO) n=5	ET-1	Saline i.p.
Group 22 – ET-1+LPS (CB2KO) n=5	ET-1, Endotoxemia	LPS 5 mg/kg, i.p.
Group 23 – AM630+ET-1+LPS n=5	ET-1, Endotoxemia Pharmacological CB2R k.o.	AM630 2.5 mg/kg, i.v.

Table 2. CB2 Antagonist Approach Group List.

Chapter 3: Results

3.1. Early CB2R Activation in CNS injury

3.1.1. Infarct Size

HI Model

Brain infarct size was measured in animals with HI-induced CNS injury *post-mortem* following whole brain extraction procedure (Figure 7). Healthy control animals with HI sham procedure did not show any presence of cellular death in the brain tissue. In animals with HI-induced CNS injury, a significant ($p < 0.05$) cerebral infarction was observed. Early activation of CB2R with HU308 (2.5 mg/kg) in animals with CNS injury and endotoxemia significantly reduced the size of brain injury when compared to animals without cannabinoid treatment. Both experimental groups with HI-induced CNS injury showed a significantly ($p < 0.05$) higher level of brain injury compared to healthy control animals.

ET-1 Model

Brain infarct size was also measured in animals with ET-1 induced CNS injury (Figure 8). Healthy animals with sham ET-1 surgeries and injections did not show any significant presence of cellular death in the brain tissue. In animals with induced CNS injury a significant ($p < 0.05$) cerebral infarction was detected. Similar level of brain injury was measured in animals with induced CNS injury and endotoxemia. Early activation of CB2R with HU308 (2.5mg/kg) in animals with CNS injury and endotoxemia significantly ($p < 0.05$) reduced the measured size of

brain injury. All experimental groups with induced CNS injury showed a significantly ($p < 0.05$) higher degree of injury compared to healthy control animals.

3.1.2. Intestinal Intravital Microscopy

Leukocyte Adherence – ET-1 Model

The number of adherent leukocytes in collecting venules (V1) of the mouse intestine has been examined in multiple experimental groups (Figure 9). The number of adherent leukocytes in intestinal venules of healthy control animals with ET-1 sham procedure was minimal. Intraperitoneal administration of LPS has significantly ($p < 0.05$) increased the number of adherent leukocytes in submucosal venules of the small intestine over 30-fold. Animals with ET-1-induced CNS injury showed a similarly low level of adherence as the healthy control animals. Animals with CNS injury demonstrated a significant ($p < 0.05$) reduction in leukocyte adherence after LPS administration when compared to animals without CNS injury. Treatment with HU308 (2.5 mg/kg) prior to CNS injury and LPS administration, resulted in a significant ($p < 0.05$) increase in the number of adhering leukocytes when compared to the group without cannabinoid treatment. The level of adherent leukocytes in animals with CNS injury and endotoxemia was significantly ($p < 0.05$) higher than both the control animals and the animals with CNS injury.

The number of adherent leukocytes in postcapillary venules (V3) of the mouse intestine has been examined in multiple experimental groups (Figure 10). Similar results found in V1 venules were also seen in the postcapillary V3 venules across all groups. The number of adherent leukocytes in the intestinal postcapillary venules of healthy control animals was minimal. Intraperitoneal LPS

administration significantly ($p < 0.05$) increased the number of adherent leukocytes in V3 venules over 60-fold compared to healthy control animals. Animals with ET-1-induced CNS injury and without LPS challenge showed a similarly low number of adherent leukocytes as observed in control group without CNS injury. Animals with CNS injury and endotoxemia showed a significant ($p < 0.05$) reduction in the number of adherent leukocytes when compared to animals with endotoxemia but without induced CNS injury. Administration of HU308 (2.5 mg/kg) prior to CNS injury induction and endotoxemia did not have a significant effect on the number of adhering leukocytes in V3 venules.

Leukocyte Rolling – ET-1 Model

The number of rolling leukocytes in collecting venules (V1) of the mouse intestine has been examined in multiple experimental groups (Figure 11). In healthy control animals, the number of rolling leukocytes was measured to be at an average of approximately 240 cells per minute. The endotoxin challenge caused a significant ($p < 0.05$) reduction in the number of rolling leukocytes compared to V1 venules of control animals. When compared to healthy controls, the animals with CNS injury but without LPS challenge, no change in baseline rolling has been observed. Animal groups with CNS injury and endotoxemia, as well as the group with CNS injury, endotoxemia and CB2R HU308 (2.5 mg/kg) treatment both had a significantly ($p < 0.05$) higher level of rolling when compared to animals with endotoxemia. There was no significant difference between HU308 treated and untreated animals.

The number of rolling leukocytes in postcapillary venules (V3) of the mouse intestine has been examined in multiple experimental groups (Figure 12). In healthy control animals, the number of

rolling leukocytes was measured to be at an average of approximately 110 cells per minute. Experimental group with CNS injury did not have any significant difference in leukocyte rolling compared to the control group. The group with CNS injury and induced endotoxemia showed a significant ($p < 0.05$) reduction in the leukocyte rolling when compared to control animals. Animals with CB2R activated via HU308 (2.5 mg/kg) treatment also showed a significant ($p < 0.05$) decrease in leukocyte rolling when compared to healthy controls. There was no significant difference between HU308 treated and untreated groups.

Functional Capillary Density – ET-1 Model

Microvascular perfusion was evaluated by measuring the functional capillary density (FCD) of muscle capillaries (Figure 13), which is defined as the total length of capillaries with observable erythrocyte perfusion in relation to a selected visual rectangular field. In healthy control animals, the FCD of muscle capillaries was measured to be an average of 220 cm/cm^2. Administration of LPS caused a significant ($p < 0.05$) reduction in FCD of muscle capillaries when compared to the control group. Presence of CNS injury did not have any significant effect on the FCD and kept it at the same level as the control group. Experimental group with CNS injury and endotoxemia showed a significant ($p < 0.05$) reduction in the FCD of muscle capillaries compared to the control group. CB2R activation with HU308 significantly ($p < 0.05$) improved the FCD of muscle capillaries, bringing it to the level of control animals.

Microvascular perfusion was also evaluated by measuring the FCD of mucosal villi (Figure 14), which is defined as the total length of capillaries with observable erythrocyte perfusion within selected mucosal villi in the recorded visual field. In healthy control animals, the FCD was

measured to be an average of 370 cm/cm^2. Administration of LPS caused a significant ($p < 0.05$) reduction in FCD of mucosal villi when compared to the control group. Animals with CNS injury did not demonstrate a significant decrease in the FCD of mucosal villi compared to the control group. Experimental group with CNS injury and endotoxemia showed a significant ($p < 0.05$) reduction in the FCD of mucosal villi compared to control group. There was no observed difference between the group with endotoxemia and the group with CNS injury and endotoxemia, although a trend towards reduction was noted. Animals with CNS injury and endotoxemia also did not show any difference in the FCD of mucosal villi compared to animals with endotoxemia but no CNS injury. CB2R activation with HU308 (2.5 mg/kg) significantly ($p < 0.05$) improved the FCD of mucosal villi, when compared to the CNS injury and endotoxemia group without the cannabinoid treatment. CB2R activation with HU308 increased the mucosal FCD to the level of healthy control group.

3.1.3. Pia Mater Intravital Microscopy

Pia Mater Leukocyte Adherence – HI Model

The number of adherent leukocytes in venules of the mouse pia mater has been examined across multiple experimental groups (Figure 15). The number of adherent leukocytes in pia mater venules of healthy control animals was minimal. Animals with HI-induced CNS injury had a significantly ($p < 0.05$) increased the number of adherent leukocytes in venules of pia mater when compared to the control group. Early activation of CB2R with HU308 (2.5 mg/kg) prior to induction of CNS injury resulted in a significant ($p < 0.05$) decrease in the number of adhering leukocytes, when compared to the group without cannabinoid treatment.

Pia Mater Leukocyte Rolling – HI Model

The number of rolling leukocytes in venules of the mouse pia mater has been examined across multiple experimental groups (Figure 16). The number of rolling leukocytes in pia mater venules of healthy control animals was measured to be approximately an average of 25 cells per minute. Animals with induced CNS injury showed a significantly ($p < 0.05$) lower level of rolling when compared to the healthy control animals. Early activation of CB2R with HU308 (2.5 mg/kg) prior to induction of CNS injury resulted in a significant ($p < 0.05$) decrease in the number of adhering leukocytes, when compared to the group without cannabinoid treatment.

Pia Mater Functional Capillary Density – HI Model

Vascular perfusion was evaluated by measuring the functional capillary density (FCD) of pia mater (Figure 17), which is defined as the total length of capillaries with observable erythrocyte perfusion in relation to a selected visual rectangular field. Between healthy control group, CNS injury group and group with HU308 (2.5 mg/kg) treatment – no significant differences were observed. All experimental groups had an average FCD ranging from 208 to 228 cm/cm^2.

3.1.4. Neuroscore vs Infarct Size in HI Model

Animals with CNS injury induced via hypoxia-ischemia had their neurological and behavioural deficits quantified, followed by a *post-mortem* quantification of brain infarct size. These data points were then paired, plotted and their correlation analyzed (Figure 18). The linear correlation

relationship analysis was calculated to have a Pearson r value equal to 0.8943 with an R square value equal to 0.7998. The strength of relationship between the two variables was calculated to be statistically significant ($p < 0.001$).

3.1.5. Splenic Weight in ET-1 Model

Splenic weight was measured in animals with ET-1 induced CNS injury after *post-mortem* whole spleen extraction procedure across multiple experimental groups (Figure 19). Spleens from healthy control animals weighed in at an average of 107 mg. Animals with induced CNS injury and endotoxemia showed a significant ($p < 0.05$) reduction in splenic weight to an average of 82 mg when compared to controls. Administering HU308 (i.v., 2.5 mg/kg) prior to CNS injury and consequent endotoxemia restores splenic weight back to the level of controls, significantly ($p < 0.05$) different from animals without cannabinoid treatment.

3.1.6. Quantitative RT-PCR

CB2R mRNA expression levels in spleen was assessed by quantitative RT-PCR (Figure 20). While CB2R mRNA expression was detected across all experimental groups, treatment of mice with HU308 (2.5 mg/kg) did not significantly alter the expression levels of CB2R mRNA. Presence of CNS injury or endotoxemia also did not have any statistically significant effect on CB2R mRNA level in spleen.

CB2R mRNA expression levels in intestine was also assessed by quantitative RT-PCR (Figure 21). While CB2R mRNA expression was detected across all experimental groups, treatment of mice with HU308 (2.5 mg/kg) did not significantly alter the expression levels of CB2R mRNA.

Presence of CNS injury or endotoxemia also did not have any statistically significant effect on CB2R mRNA level in intestine. In relative numbers, the group with an activated CB2R before CNS injury showed lower values for CB2R mRNA.

3.2. Late CB2R Inhibition After CNS injury

3.2.1. Infarct Size

HI Model

CNS infarct size was measured in animals with HI- induced CNS injury after *post-mortem* whole brain extraction procedure (Figure 22). Healthy animals with sham surgeries did not show any presence of cellular death in the brain tissue (not shown). In animals with induced CNS injury a significant ($p < 0.05$) cerebral infarction was detected. In animals with induced CNS injury and endotoxemia, the size of cerebral infarction remained comparable to animals with CNS injury but without LPS administration. Inhibition of CB2R in animals with CNS injury and endotoxemia did not change the infarct volume. All experimental groups with induced CNS injury, regardless of endotoxemia (not shown), vehicle used, or presence of treatment showed the same level of injury without any statistically significant differences.

ET-1 Model

CNS infarct size was measured in animals with ET-1 induced CNS injury after *post-mortem* whole brain extraction procedure (Figure 23). Healthy animals with sham surgeries did not show any presence of cellular death in the brain tissue (not shown). In animals with induced CNS

injury a significant ($p < 0.05$) cerebral infarction was detected. In animals with induced CNS injury and endotoxemia, the size of cerebral infarction remained comparable to animals with CNS injury but without LPS administration. Inhibition of CB2R in animals with CNS injury and endotoxemia did not change the infarct volume. All experimental groups with induced CNS injury, regardless of endotoxemia (not shown), vehicle used, or presence of treatment showed the same level of injury without any statistically significant differences.

CB2R K.O.

CNS infarct size was also measured after *post-mortem* whole brain extraction (Figure 24). Healthy animals with sham surgeries did not show any presence of cellular death in the brain tissue at drill sites (not shown). In wild type animals with ET-1-induced CNS injury, a significant ($p < 0.05$) cerebral infarction was detected and measured. Animals with a genetic knock out of CB2R and ET-1-induced CNS injury showed a significant ($p < 0.05$) increase in the size of infarct volume, in comparison to wild type animals who also went through surgical induction of CNS injury. Similarly, animal group with pharmacological inhibition of CB2R with AM630 (2.5 mg/kg) prior to the induction of CNS injury also demonstrated a significant ($p < 0.05$) increase in the size of infarct volume, in comparison to wild type animals who also went through surgical induction of CNS injury. There was no significant difference in infarct volumes between genetic and pharmacological CB2R knock out groups.

3.2.2. Intestinal Intravital Microscopy

Leukocyte Adherence

HI Model

The number of adherent leukocytes in collecting venules (V1) of the mouse intestine has been examined in multiple experimental groups (Figure 25). The number of adherent leukocytes in intestinal venules of healthy control animals with ET-1 sham procedure was minimal. Intraperitoneal administration of LPS has significantly ($p < 0.05$) increased the number of adherent leukocytes in submucosal venules of the intestine over 30-fold. Animals with induced CNS injury showed a similarly low level of adherence as the healthy control animals. Animals with CNS injury demonstrated a significant ($p < 0.05$) reduction in leukocyte adherence after LPS administration. Inhibition of CB2R with AM630 (2.5 mg/kg) prior to LPS administration in animals with CNS injury and induced endotoxemia, resulted in a significant ($p < 0.05$) increase in the number of adhering leukocytes, when compared to the group without cannabinoid treatment. The levels of adherent leukocytes in groups with CNS injury and CNS injury and endotoxemia was not significantly different from each other. The group with CB2R inhibition was significantly ($p < 0.05$) different from every other experimental group.

The number of adherent leukocytes in postcapillary venules (V3) of the mouse intestine has been examined in multiple experimental groups (Figure 26). Similar results found in V1 venules were also seen in the postcapillary V3 venules across all groups. The number of adherent leukocytes in the intestinal postcapillary venules of healthy control animals was minimal. Intraperitoneal LPS administration significantly ($p < 0.05$) increased the number of adherent leukocytes in V3 venules over 60-fold compared to healthy control animals. Animals with induced CNS injury and

without LPS challenge showed a similarly low number of adherent leukocytes as observed in control group without CNS injury. Animals with CNS injury and induced endotoxemia showed a significant ($p < 0.05$) reduction in the number of adherent leukocytes when compared to animals with endotoxemia but without induced CNS injury. The levels of adherent leukocytes in groups with CNS injury and CNS injury and endotoxemia was not significantly different from each other.

ET-1 Model

The number of adherent leukocytes in collecting venules (V1) of the mouse intestine has been examined in multiple experimental groups (Figure 27). The number of adherent leukocytes in intestinal venules of healthy control animals was minimal. Intraperitoneal administration of LPS has significantly ($p < 0.05$) increased the number of adherent leukocytes in submucosal venules of the small intestine over 30-fold. Animals with ET-1-induced CNS injury showed a similarly low level of adherence as the healthy control animals. Animals with CNS injury demonstrated a significant ($p < 0.05$) reduction in leukocyte adherence after LPS administration when compared to animals without CNS injury. Inhibition of CB2R with AM630 (2.5 mg/kg) prior to LPS administration in animals with CNS injury, resulted in a significant ($p < 0.05$) increase in the number of adhering leukocytes when compared to the group without cannabinoid treatment. The levels of adherent leukocytes in groups with CNS injury and CNS injury and endotoxemia was significantly ($p < 0.05$) different from each other.

The number of adherent leukocytes in postcapillary venules (V3) of the mouse intestine has been examined in multiple experimental groups (Figure 28). Similar results found in V1 venules were

also seen in the postcapillary V3 venules across all groups. The number of adherent leukocytes in the intestinal postcapillary venules of healthy control animals was minimal. Intraperitoneal LPS administration significantly ($p < 0.05$) increased the number of adherent leukocytes in V3 venules over 60-fold compared to healthy control animals. Animals with induced CNS injury and without LPS challenge showed a similarly low number of adherent leukocytes as observed in control group without CNS injury. Animals with CNS injury and endotoxemia showed a significant ($p < 0.05$) reduction in the number of adherent leukocytes when compared to animals with endotoxemia but without induced CNS injury. Inhibiting the CB2R with AM630 (2.5 mg/kg) improved the level of leukocyte adherence, numerically close to the level of adherence in experimental group with endotoxemia.

CB2R K.O. ET-1 Model

The number of adherent leukocytes in collecting venules (V1) of the mouse intestine has been examined in multiple experimental groups (Figure 29). Animals in all experimental groups have had their CB2R genetically removed. Control animals had minimal number of adherent leukocytes. Administration of LPS significantly ($p < 0.05$) increased leukocyte adherence, more than 25-fold. CB2R K.O. animals with induced CNS injury did not display any difference in level of leukocyte adherence when compared to control animals. CB2R K.O. animals with induced CNS injury and endotoxemia showed the same level of leukocyte adherence as animals with endotoxemia but without CNS injury.

The number of adherent leukocytes in postcapillary venules (V3) of the mouse intestine has been examined in multiple experimental groups (Figure 30). Animals in all experimental groups have

had their CB2R genetically removed. Similar results found in V1 venules were also seen in the postcapillary V3 venules across all groups. Control animals and animals with induced CNS injury and no endotoxemia both displayed minimal level of leukocyte adherence. Administration of LPS, regardless of presence or absence of CNS injury significantly ($p < 0.05$) increased the number of adherent leukocytes.

Leukocyte Rolling

HI Model

The number of rolling leukocytes in collecting venules (V1) of the mouse intestine has been examined in multiple experimental groups (Figure 31). In healthy control animals, the number of rolling leukocytes was measured to be at an average of approximately 237 cells per minute. The endotoxin challenge caused a significant ($p < 0.05$) reduction in the number of rolling leukocytes compared to V1 venules of control animals. When compared to healthy controls, the animals with CNS injury but without LPS challenge, a significant ($p < 0.05$) reduction in baseline rolling has been observed. Experimental group with CNS injury and LPS challenge showed a significant ($p < 0.05$) decrease in the number of rolling leukocytes. Animals with CNS injury and endotoxemia demonstrated a similar level of leukocyte rolling as the group with endotoxemia but without CNS injury. CB2R inhibition with AM630 (2.5 mg/kg) in animals with CNS injury and induced endotoxemia showed a significant ($p < 0.05$) decrease in leukocyte rolling when compared to control animals and a significant increase in leukocyte rolling when compared to the group with CNS injury and LPS challenge but without the CB2R treatment.

The number of rolling leukocytes in postcapillary venules (V3) of the mouse intestine has been examined in multiple experimental groups (Figure 32). In healthy control animals, the number of rolling leukocytes was measured to be at an average of approximately 112 cells per minute. Experimental group with CNS injury, as well as the group with CNS injury and induced endotoxemia both showed a significant ($p < 0.05$) reduction in the leukocyte rolling when compared to control animals. Animals with the CB2R inhibited via AM630 (2.5 mg/kg) treatment showed a significant ($p < 0.05$) decrease in leukocyte rolling when compared to healthy controls.

ET-1 Model

The number of rolling leukocytes in collecting venules (V1) of the mouse intestine has been examined in multiple experimental groups (Figure 33). In healthy control animals, the number of rolling leukocytes was measured to be at an average of approximately 240 cells per minute. The endotoxin challenge caused a significant ($p < 0.05$) reduction in the number of rolling leukocytes compared to V1 venules of control animals. When compared to healthy controls, the animals with CNS injury but without LPS challenge, no change in baseline rolling has been observed. Animal groups with CNS injury and endotoxemia, as well as the group with CNS injury, endotoxemia and CB2R AM630 (2.5 mg/kg) treatment both had a significantly ($p < 0.05$) higher level of rolling when compared to animals with endotoxemia. There was no significant difference between AM630 treated and untreated groups.

The number of rolling leukocytes in postcapillary venules (V3) of the mouse intestine has been examined in multiple experimental groups (Figure 34). In healthy control animals, the number of

rolling leukocytes was measured to be at an average of approximately 110 cells per minute. Experimental group with endotoxemia, as well as the group with CNS injury and induced endotoxemia both showed a significant ($p < 0.05$) reduction in the leukocyte rolling when compared to control animals. Animals with the CB2R inhibited via AM630 (2.5 mg/kg) treatment also showed a significant ($p < 0.05$) decrease in leukocyte rolling when compared to healthy controls. There was no significant difference between AM630 treated and untreated group.

CB2R K.O. ET-1 Model

The number of rolling leukocytes in collecting venules (V1) of the mouse intestine has been examined in multiple experimental groups (Figure 35). Animals in all experimental groups have had their CB2R genetically removed. The number of rolling leukocytes in the control group was measured to be at an average of approximately 267 cells per minute. Administration of LPS significantly ($p < 0.05$) reduced the number of rolling leukocytes, by approximately 25-fold. Leukocyte rolling was also significantly ($p < 0.05$) reduced in animals with induced CNS injury when compared to control animals. Administration of LPS in animals with CNS injury did not significantly reduce the number of rolling leukocytes, however there is a presence of a negative trend.

The number of rolling leukocytes in postcapillary venules (v3) of the mouse intestine has been examined in multiple experimental groups (Figure 36). Animals in all experimental groups have had their CB2R genetically removed. Similar results found in V1 venules were also seen in the postcapillary V3 venules across all groups. The number of rolling leukocytes in the control group

was measured to be at an average of approximately 85 cells per minute. Administration of LPS significantly ($p < 0.05$) reduced the number of rolling leukocytes, by approximately 25-fold. Leukocyte rolling was also significantly ($p < 0.05$) reduced in animals with induced CNS injury when compared to control animals. Administration of LPS in animals with CNS injury did not significantly reduce the number of rolling leukocytes, however there is a presence of a negative trend.

Functional Capillary Density

HI Model

Microvascular perfusion was evaluated by measuring the functional capillary density (FCD) of muscle capillaries (Figure 37), which is defined as the total length of capillaries with observable erythrocyte perfusion in relation to a selected visual rectangular field. In healthy control animals, the FCD of muscle capillaries was measured to be an average of 224 cm/cm^2. Administration of LPS caused a significant ($p < 0.05$) reduction in FCD of muscle capillaries when compared to the control group. Animal experimental groups with CNS injury, CNS injury and endotoxemia both demonstrated a significant ($p < 0.05$) reduction in FCD of muscle capillaries when compared to the control group. Animals with CNS injury and LPS challenge showed a significant ($p < 0.05$) decrease in the FCD of muscle capillaries compared to animals with endotoxemia. Inhibition of CB2R with AM630 (2.5 mg/kg) did not produce any significant effect on the FCD of muscle capillaries. However, there is a trend of a slight increase in FCD of muscle capillaries in the group with CB2R inhibitor treatment when compared with the untreated group with CNS injury and endotoxemia.

Microvascular perfusion was also evaluated by measuring the FCD of mucosal villi (Figure 38), which is defined as the total length of capillaries with observable erythrocyte perfusion within selected mucosal villi in the recorded visual field. In healthy control animals, the FCD was measured to be an average of 371 cm/cm^2. Administration of LPS caused a significant ($p < 0.05$) reduction in FCD of mucosal villi when compared to the control group. Animals with CNS injury did not demonstrate a significant decrease in the FCD of mucosal villi compared to control group. Experimental group with CNS injury and endotoxemia showed a significant ($p < 0.05$) reduction in the FCD of mucosal villi compared to control group. Animals with CNS injury and endotoxemia showed a decrease in the FCD of mucosal villi compared to animals with endotoxemia but no CNS injury. CB2R inhibition did show a positive trend when compared to the CNS injury and endotoxemia group without the CB2R inhibitor treatment.

ET-1 Model

Vascular perfusion was evaluated by measuring the functional capillary density (FCD) of muscle capillaries (Figure 39), which is defined as the total length of capillaries with observable erythrocyte perfusion in relation to a selected visual rectangular field. In healthy control animals, the FCD of muscle capillaries was measured to be an average of 220 cm/cm^2. Administration of LPS caused a significant ($p < 0.05$) reduction in FCD of muscle capillaries when compared to the control group. Experimental group with CNS injury and endotoxemia showed a significant ($p < 0.05$) reduction in the FCD of muscle capillaries compared to control group. CB2R inhibition did show a positive trend when compared to the CNS injury and endotoxemia group without the CB2R inhibitor treatment.

Vascular perfusion was also evaluated by measuring the FCD of mucosal villi (Figure 40), which is defined as the total length of capillaries with observable erythrocyte perfusion within selected mucosal villi in the recorded visual field. In healthy control animals, the FCD was measured to be an average of 370 cm/cm^2. Administration of LPS caused a significant ($p < 0.05$) reduction in FCD of mucosal villi when compared to the control group. Animals with CNS injury did not demonstrate a significant decrease in the FCD of mucosal villi compared to control group. Experimental group with CNS injury and endotoxemia showed a significant ($p < 0.05$) reduction in the FCD of mucosal villi compared to control group. Animals with CNS injury and endotoxemia also showed a decrease in the FCD of mucosal villi compared to animals with endotoxemia but no CNS injury. CB2R inhibition with AM630 (2.5 mg/kg) did not significantly affect the FCD of mucosal villi, when compared to the CNS injury and endotoxemia group without the CB2R inhibitor treatment. However, the CB2R inhibition increased the mucosal FCD to the level of endotoxemia group.

CB2R K.O. ET-1 Model

Vascular perfusion was evaluated by measuring the functional capillary density (FCD) of muscle capillaries (Figure 41), which is defined as the total length of capillaries with observable erythrocyte perfusion in relation to a selected visual rectangular field. In healthy control animals, the FCD of muscle capillaries was measured to be an average of 193 cm/cm^2. Administration of LPS or induction of CNS injury did not cause any significant changes in FCD of muscle capillaries when compared to the control group. Induction of endotoxemia in animals with CNS injury caused a significant ($p < 0.05$) reduction in the FCD of muscle capillaries.

Vascular perfusion parameter was also evaluated by measuring the FCD of mucosal villi (Figure 42), which is defined as the total length of capillaries with observable erythrocyte perfusion within selected mucosal villi in the recorded visual field. In healthy control animals, the FCD was measured to be an average of 406 cm/cm^2. Administration of LPS caused a significant ($p < 0.05$) reduction in the FCD of mucosal villi. However, presence of CNS injury did not cause significant changes in FCD of mucosal villi. Induction of endotoxemia in animals with CNS injury caused a significant ($p < 0.05$) reduction in the FCD of mucosal villi.

3.2.3. Peripheral Leukocyte Adherence vs. Infarct Size in ET-1 Model

Animals with CNS injury induced via cerebral ET-1 injections had their peripheral leukocyte adherence measured, as well as *post-mortem* quantification of brain infarct size. These data points were then paired, plotted and their correlation analyzed (Figure 43). The linear correlation relationship analysis was calculated to have a Pearson r value equal to -0.8952 with an R square value equal to 0.8014. The strength of relationship between the two variables was calculated to be statistically significant ($p < 0.0001$).

3.2.4. Infarct Volume vs. Neuroscore in Late CB2R Treatment HI Model

Animals with CNS injury induced via hypoxia-ischemia had their neurological and behavioural deficits quantified, followed by a *post-mortem* quantification of brain infarct size. These data points were then paired, plotted and their correlation analyzed (Figure 44). The linear correlation relationship analysis was calculated to have a Pearson r value equal to 0.8683 with an R square

value equal to 0.7540. The strength of relationship between the two variables was calculated to be statistically significant ($p < 0.05$).

3.2.5. Neutrophil Count in ET-1 Model

Animals with CNS injury induced via cerebral ET-1 injections had their bone marrow extracted, neutrophil cells isolated and counted across experimental groups of interest (Figure 45). Healthy control animals without CNS injury showed that the average total neutrophil count was $4.54x10^6$ cells. When the animal was given a CNS injury, the average total neutrophil count in the bone marrow, measured 24 hrs after the injury, was significantly ($p < 0.05$) reduced when compared to control animals. Experimental group with CNS injury and inhibited CB2R with AM630 (2.5 mg/kg) demonstrated an increase in average total neutrophil count to the level of non-significance when compared to the control group. There was also no statistical significance between the treated and untreated groups.

3.2.6. Adhesion Molecule Levels

Plasma samples were collected and the levels of soluble adhesion molecules, P-selectin and ICAM-1, were measured (Figure 46). Control group revealed a minimal level of soluble P-selectin in plasma. Administration of LPS resulted in a significant ($p < 0.05$) increase in the level of soluble P-selectin compared to the control group. Animals with CNS injury showed a trend towards an increase of P-selectin levels; however, it was not statistically significant when compared to heathy controls. In animal group with CNS injury and endotoxemia, the level of P-selectin was not significantly different from the group with endotoxemia but without CNS injury,

although a trend for decrease was observed. Experimental group with CNS injury and endotoxemia, as well as inhibited CB2R with AM630 (2.5. mg/kg) showed a significantly ($p < 0.05$) elevated level of P-selectin when compared to group that was untreated with the cannabinoid drug. The concentration of soluble ICAM-1 was also very low in control animals, with a significant ($p < 0.05$) increase in group with endotoxemia. Administration of LPS in animals with CNS injury did not increase the level of ICAM-1 in plasma and kept it at the same level as the group without endotoxemia. Experimental group with CNS injury and endotoxemia, as well as inhibited CB2R with AM630 (2.5. mg/kg) showed a significantly ($p < 0.05$) elevated level of ICAM-1 when compared to group that was untreated with the cannabinoid drug. The group with AM630 treatment demonstrated a restored concentration of ICAM-1 to the level of endotoxemia group without CNS injury.

3.2.7. Plasma Cytokine Levels

Plasma samples were collected, and the levels of the following cytokines were measured: TNFα, IL-1β, IL-2, IL-4, IL-6, IL-10, IL-12p70, IL-13, IL-17A, and IFN-γ (Figure 47). Administration of LPS significantly ($p < 0.05$) elevated the plasma levels of TNFα, IL-1β, IL-6 and IL-10 compared to control group. Experimental group with induced CNS injury had significantly ($p < 0.05$) elevated levels of IL-17A, IL-12p70, IL-4, and IL-2 compared to control group. Experimental group with CNS injury and induced endotoxemia had significantly ($p < 0.05$) reduced levels of TNFα, IL-1β and IL-6, and significantly ($p < 0.05$) increased level of IL-13 compared to the group with endotoxemia. Group with inhibited CB2R by AM630 (2.5 mg/kg) showed similar cytokine levels across most of the test panel to the group without the

experimental cannabinoid treatment, except more than double the level of TNFα and a significant ($p < 0.05$) reduction in the level of IL-10.

3.3. Figures

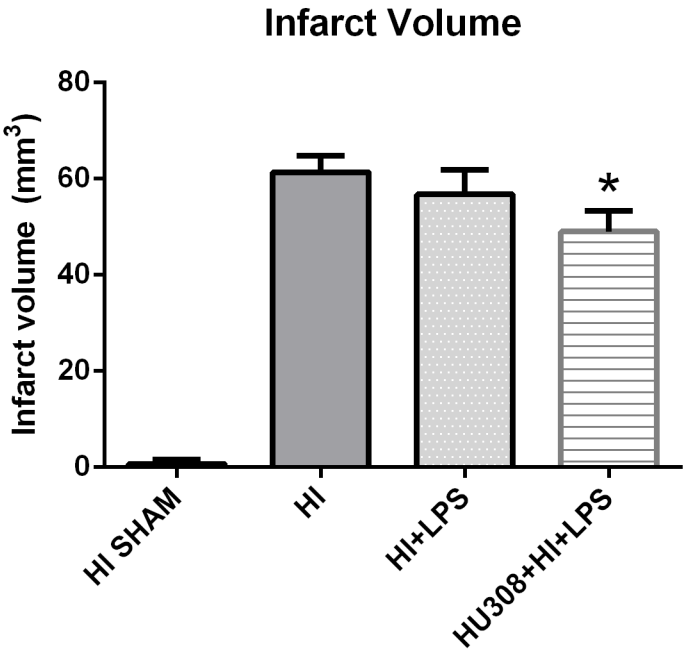

Figure 7. **Brain Infarct Volume in HI Model**

Brain infarct volume quantified as the total volume of tissue stained with tetrazolium chloride (TTC) from each brain slice. HI Sham(n=5); HI(n=6); HU308 (2.5mg/kg i.v.)+ET-1+LPS (n=5). HU308 administered 15 minutes before CNS injury induction, LPS administered at 22 hours. Data presented as mean ± standard deviation. $p < 0.05$ vs HI+LPS.

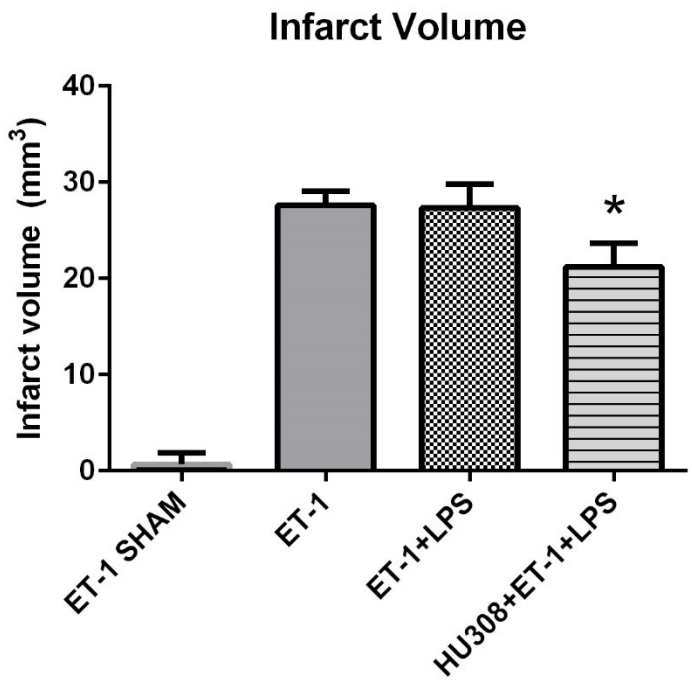

Figure 8. **Brain Infarct Volume in ET-1 Model**

Brain infarct volume quantified as the total volume of tissue stained with tetrazolium chloride (TTC) from each brain slice. ET-1 Sham (n=8); ET-1(n=5); ET-1+LPS (5 mg/kg) (n=5); HU308 (2.5mg/kg i.v.)+ET-1+LPS (n=5). HU308 administered 15 minutes before CNS injury induction, LPS administered at 22 hours. Data presented as mean ± standard deviation. * $p < 0.05$ vs ET-1+LPS.

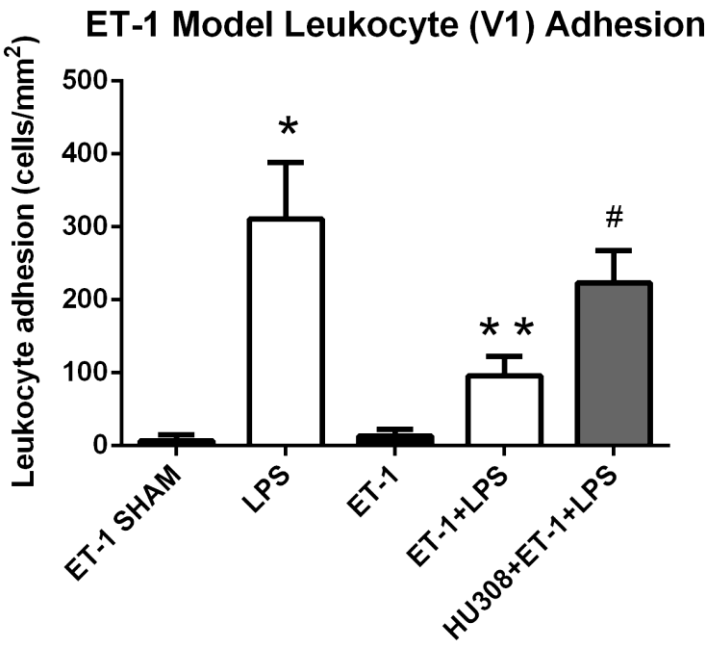

Figure 9. **Leukocyte Adhesion in Intestinal V1 venules, ET-1 Model**

Leukocyte adhesion in collecting venules (V1; >50 um vessel diameter). Control group (ET-1-SHAM, n=8); endotoxemia group LPS (5 mg/kg), (n=8); ET-1(n=5); ET-1+LPS; HU308 (2.5mg/kg i.v.)+ET-1+LPS (n=5). HU308 administered 15 minutes before CNS injury induction, LPS administered at 22 hours, IVM performed at 24 hours. Data presented as mean ± standard deviation. $*$ $p < 0.05$ versus ET-1 SHAM, ** $p < 0.05$ vs LPS, # $p < 0.05$ vs ET-1+LPS.

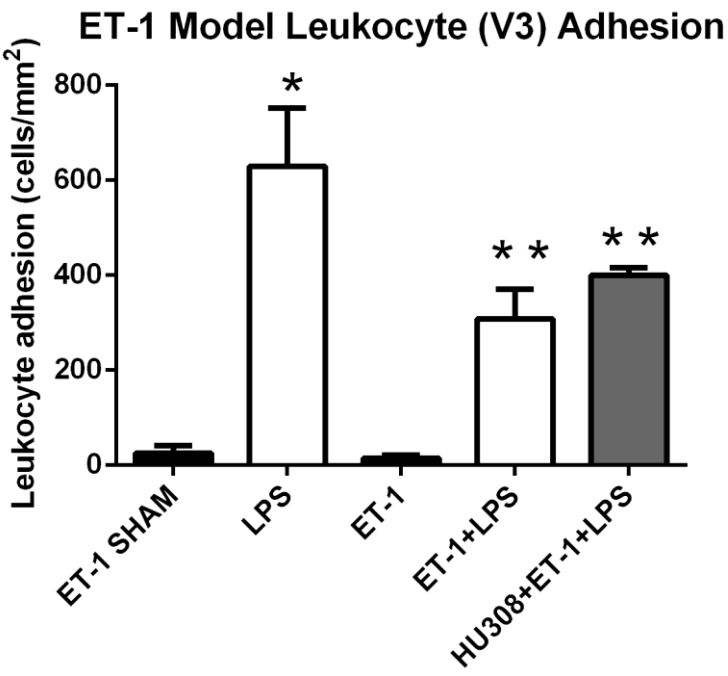

Figure 10. **Leukocyte Adhesion in Intestinal V3 Post Capillary Venules, ET-1 Model**

Leukocyte adhesion in post capillary venules (V3; <50μm vessel diameter). Control group (ET-1-SHAM) (n=8); endotoxemia group LPS (5 mg/kg) (n=8); ET-1 (n=5); ET-1+LPS (n=5); HU308 (2.5mg/kg i.v.)+ET-1+LPS (n=5). HU308 administered 15 minutes before CNS injury induction, LPS administered at 22 hours, IVM performed at 24 hours. Data presented as mean ± standard deviation. $*$ $p < 0.05$ versus ET-1 SHAM, ** $p < 0.05$ vs LPS.

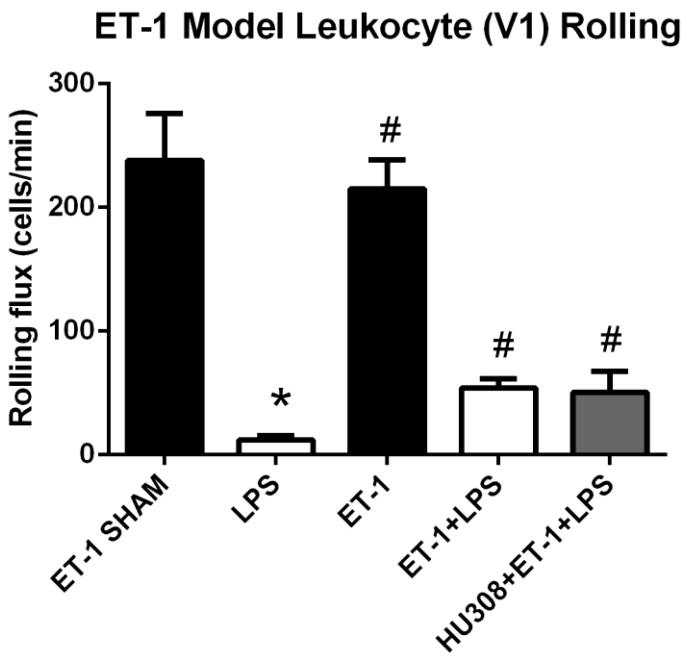

Figure 11. **Leukocyte Rolling in Intestinal V1 Venules, ET-1 Model**

Leukocyte rolling in collecting venules (V1; >50 um vessel diameter). Control group (ET-1-SHAM) (n=8); endotoxemia group LPS (5 mg/kg) (n=8); ET-1(n=5); ET-1+LPS(n=5); HU308 (2.5mg/kg i.v.)+ET-1+LPS (n=5). HU308 administered 15 minutes before CNS injury induction, LPS administered at 22 hours, IVM performed at 24 hours. Data presented as mean ± standard deviation. $*$ $p < 0.05$ versus ET-1 SHAM, # $p < 0.05$ versus LPS.

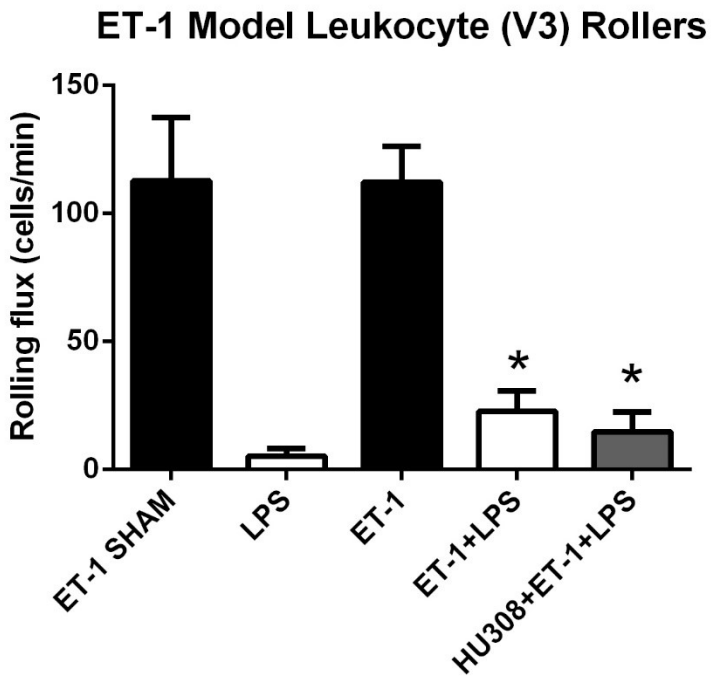

Figure 12. **Leukocyte Rolling in Intestinal Post Capillary V3 Venules, ET-1 Model**

Leukocyte rolling in post capillary venules (V3; <50 um vessel diameter). Control group (ET-1-SHAM) (n=8); endotoxemia group LPS (5 mg/kg) (n=8); ET-1(n=5); ET-1+LPS(n=5); HU308 (2.5mg/kg i.v.)+ET-1+LPS (n=5). HU308 administered 15 minutes before CNS injury induction, LPS administered at 22 hours, IVM performed at 24 hours. Data presented as mean ± standard deviation. ∗ $p < 0.05$ versus ET-1 SHAM.

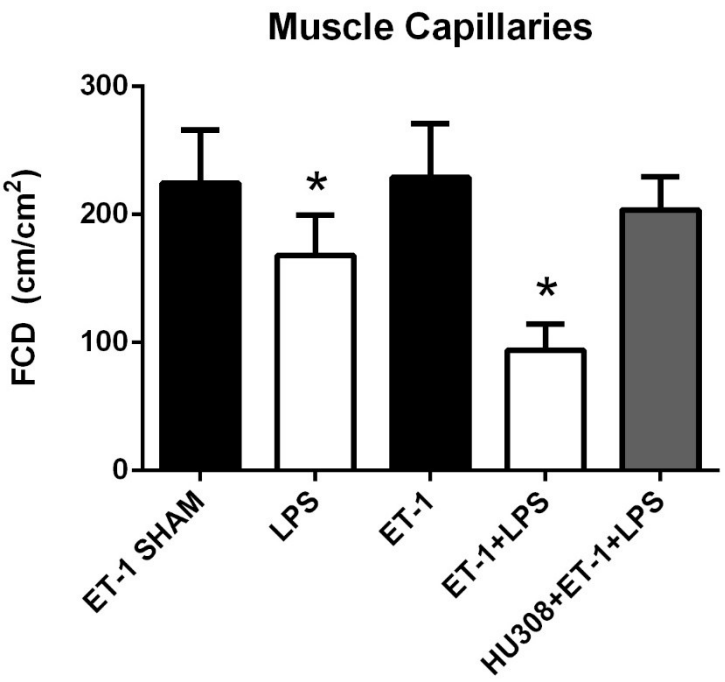

Figure 13. **FCD of Intestinal Muscle Capillaries, ET-1 Model**

Capillary perfusion quantified through functional capillary density (FCD) within the submucosal muscle layers of the intestine. FCD quantified as total length of well perfused capillaries within a predetermined rectangular area of the observed field. Control group (ET-1-SHAM) (n=8); endotoxemia group LPS (5 mg/kg) (n=8); ET-1(n=5); ET-1+LPS(n=5); HU308 (2.5mg/kg i.v.)+ET-1+LPS (n=5). HU308 administered 15 minutes before CNS injury induction, LPS administered at 22 hours, IVM performed at 24 hours. Data presented as mean ± standard deviation. ∗ $p < 0.05$ versus ET-1 SHAM.

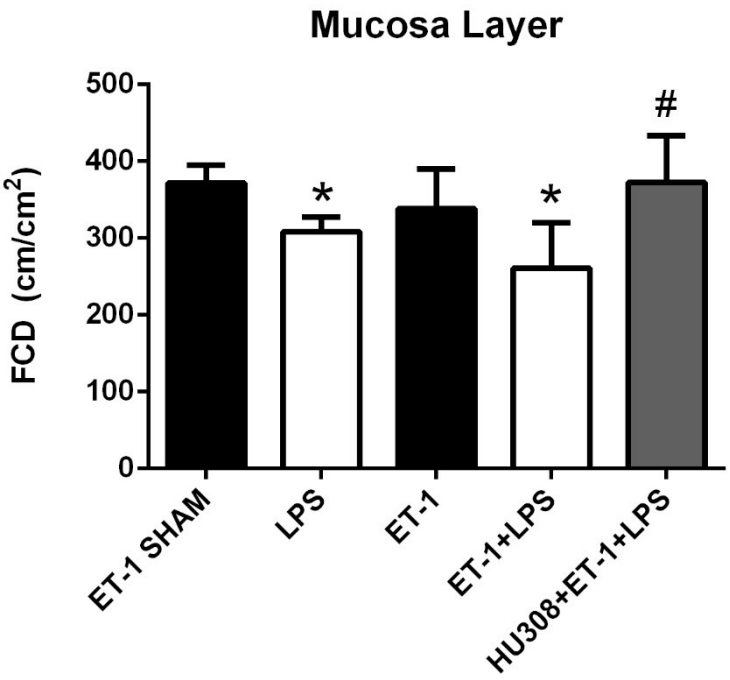

Figure 14. **FCD of Mucosa Layer, ET-1 Model**

Capillary perfusion quantified through functional capillary density (FCD) within the mucosal villi of the intestinal lumen. FCD quantified as total length of well perfused capillaries within a predetermined rectangular area of the observed field. Control group (ET-1-SHAM) (n=8); endotoxemia group LPS (5 mg/kg) (n=8); ET-1(n=5); ET-1+LPS(n=5); HU308 (2.5mg/kg i.v.)+ET-1+LPS (n=5). HU308 administered 15 minutes before CNS injury induction, LPS administered at 22 hours, IVM performed at 24 hours. Data presented as mean ± standard deviation. ∗ $p < 0.05$ versus ET-1 SHAM, # $p < 0.05$ vs ET-1+LPS.

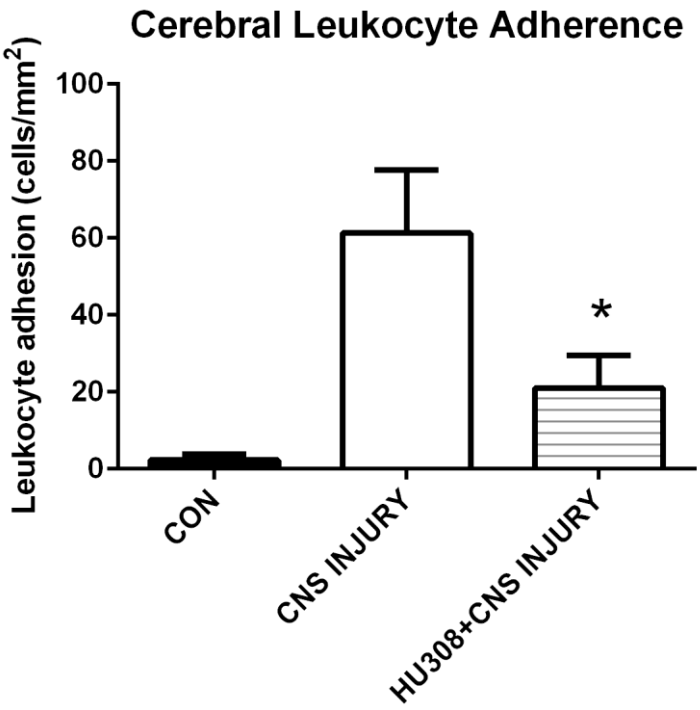

Figure 15. **Leukocyte Adhesion - Pia Mater, HI Model**

The number of adhering leukocytes in venules of the mouse pia mater has been examined across multiple experimental groups. Control (CON) (n=5); HI (CNS INJURY) (n=6); HI + selective CB2R agonist HU308 (2.5 mg/kg i.v.) (CNS INJURY+HU308) (n=4). HU308 administered 15 minutes before CNS injury induction, LPS administered at 2 hours, IVM performed at 4 hours. Data presented as mean ± standard deviation. * $p < 0.05$ vs CNS INJURY.

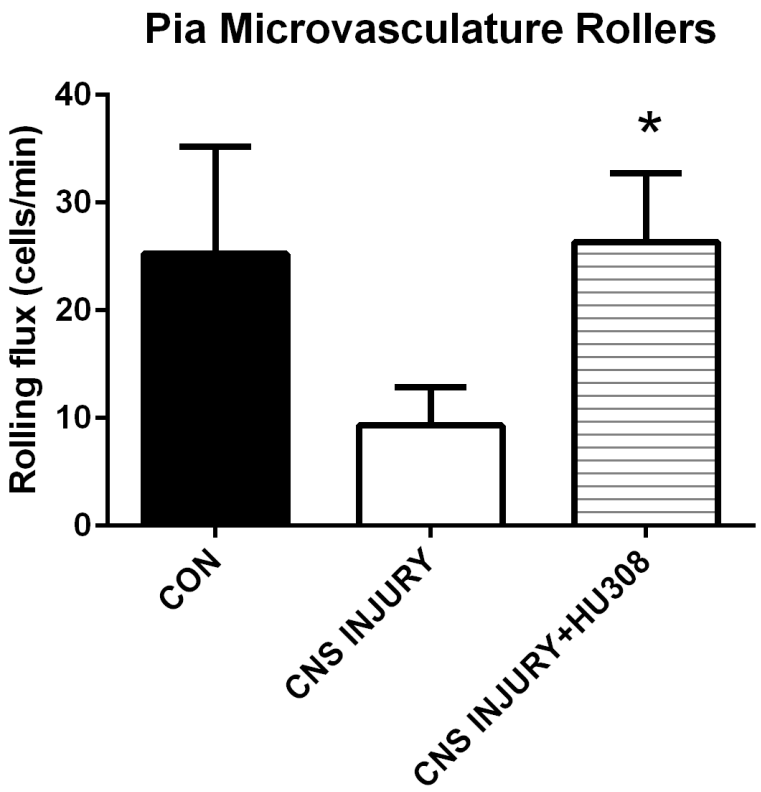

Figure 16**. Leukocyte Rolling - Pia Mater, HI Model**

The number of rolling leukocytes in venules of the mouse pia mater has been examined across multiple experimental groups. Control (CON) (n=5); HI (CNS INJURY) (n=6); HI + selective CB2R agonist HU308 (2.5 mg/kg i.v.) (CNS INJURY+HU308) (n=4). HU308 administered 15 minutes before CNS injury induction, LPS administered at 2 hours, IVM performed at 4 hours. Data presented as mean ± standard deviation. * $p < 0.05$ vs CNS INJURY.

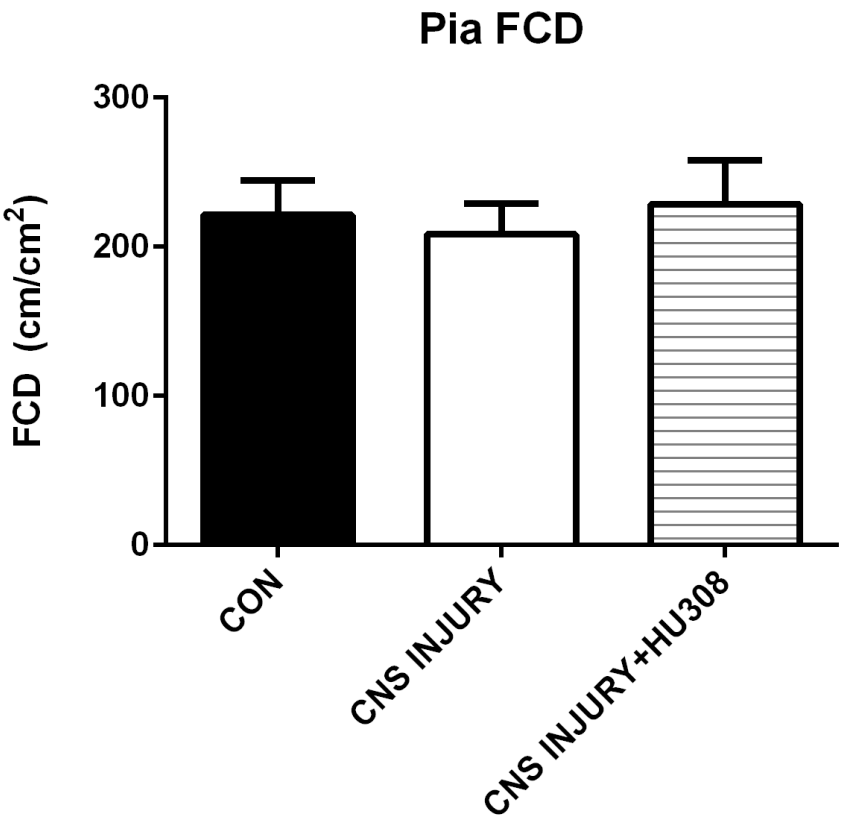

Figure 17. **FCD of Pia Mater Capillaries. HI Model**

Vascular perfusion was evaluated by measuring the FCD of pia mater, which is defined as the total length of capillaries with observable erythrocyte perfusion in relation to a selected visual rectangular field. Control (CON) (n=5); HI (CNS INJURY) (n=6); HI + HU308 (2.5 mg/kg i.v.) (CNS INJURY+HU308) (n=4). HU308 administered 15 minutes before CNS injury induction, LPS administered at 2 hours, IVM performed at 4 hours. Data presented as mean ± standard deviation.

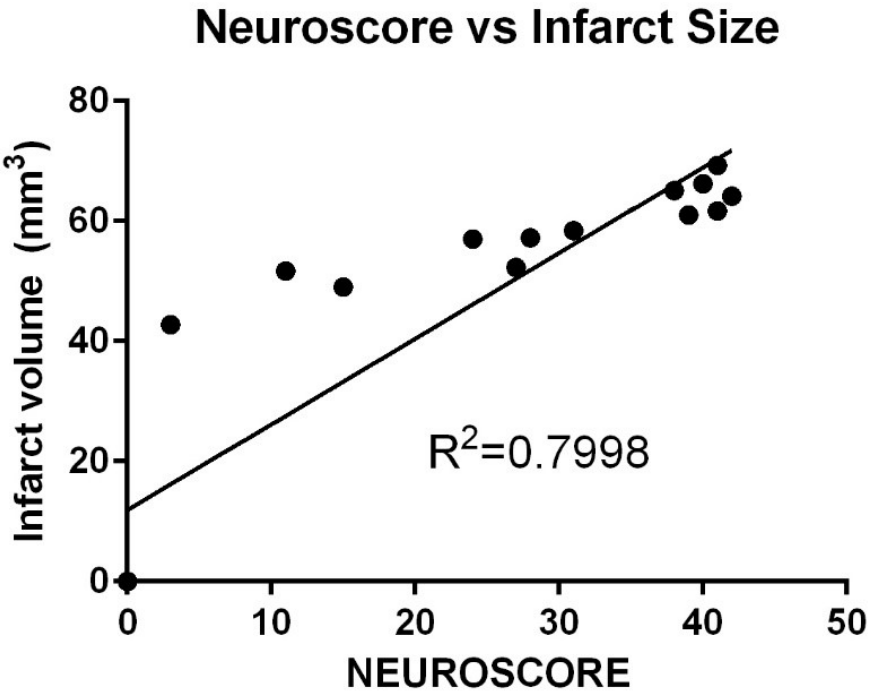

Figure 18. **Brain Infarct volume vs Neuroscore, HI Model**

Animals with CNS injury induced via hypoxia-ischemia had their neurological and behavioural deficits quantified and compared with a *post-mortem* quantification of brain infarct size. The linear correlation relationship between the two variables was calculated to have a Pearson r = 0.8943 with an $R^2 = 0.7998$. The strength of relationship between the two variables was calculated to be statistically significant ($p < 0.001$).

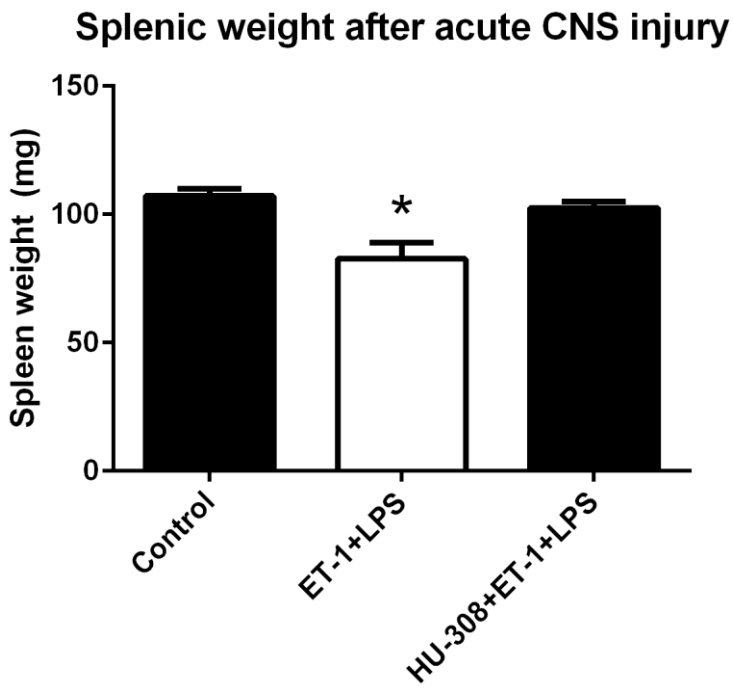

Figure 19. **Splenic weight, ET-1 Model**

Splenic weight was measured in animals with ET-1 induced CNS injury after *post-mortem* whole spleen extraction procedure across multiple experimental groups. Health control (Control) (n=4); ET-1+LPS (5 mg/kg i.p.) (n=5); HU308 (2.5mg/kg i.v.)+ET-1+LPS (5 mg/kg i.p.) (n=4). HU308 administered 15 minutes before CNS injury induction, LPS administered at 22 hours, IVM performed at 24 hours. Data presented as mean ± standard deviation. * $p < 0.05$ vs Control.

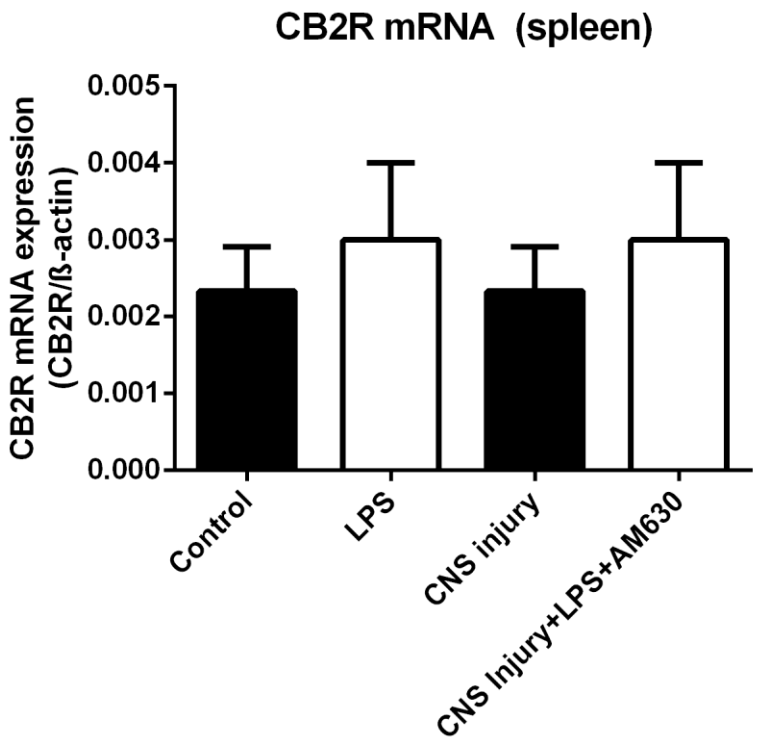

Figure 20. **CB2R mRNA Expression Levels in Spleen**

CB2R mRNA levels from whole spleen tissue quantified via qRT-PCR and normalized to sample matched β-actin mRNA levels. Each experimental group n=4. AM630 administration (2.5mg/kg i.v.) at 22 hours after CNS injury. Data presented as mean ± standard deviation.

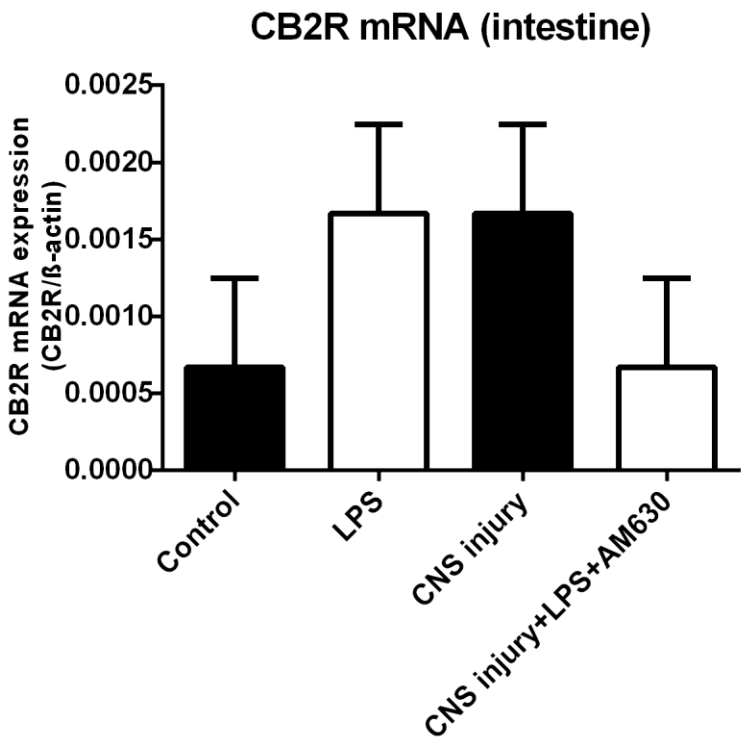

Figure 21. **CB2R mRNA Expression Levels in Intestine**

CB2R mRNA levels from intestinal terminal ileum tissue quantified via qRT-PCR and normalized to sample matched β-actin mRNA levels. Each experimental group n=4. AM630 administration (2.5mg/kg i.v.) at 22 hours after CNS injury. Data presented as mean ± standard deviation.

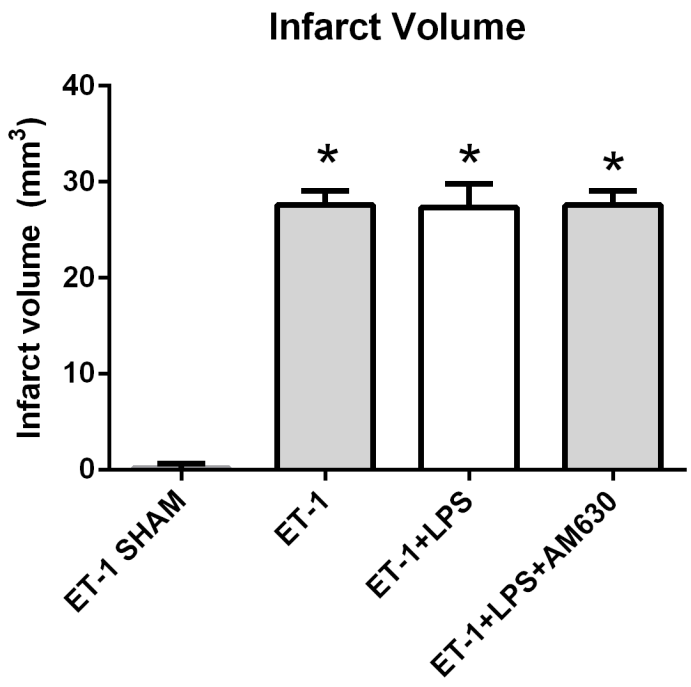

Figure 22. **Brain Infarct Volume in ET-1 Model**

Brain infarct volume quantified as the total volume of tissue stained with tetrazolium chloride (TTC) from each brain slice. ET-1 Sham (n=8); ET-1(n=4); ET-1+LPS (5 mg/kg) (n=4); ET-1+LPS+AM630 (2.5 mg/kg) (n=5). AM630 administered 15 minutes before LPS administration at 22 hours after CNS injury induction, IVM performed at 24 hours. Data presented as mean ± standard deviation. Every experimental group was statistically significant ($p < 0.05$) versus ET-1 SHAM.

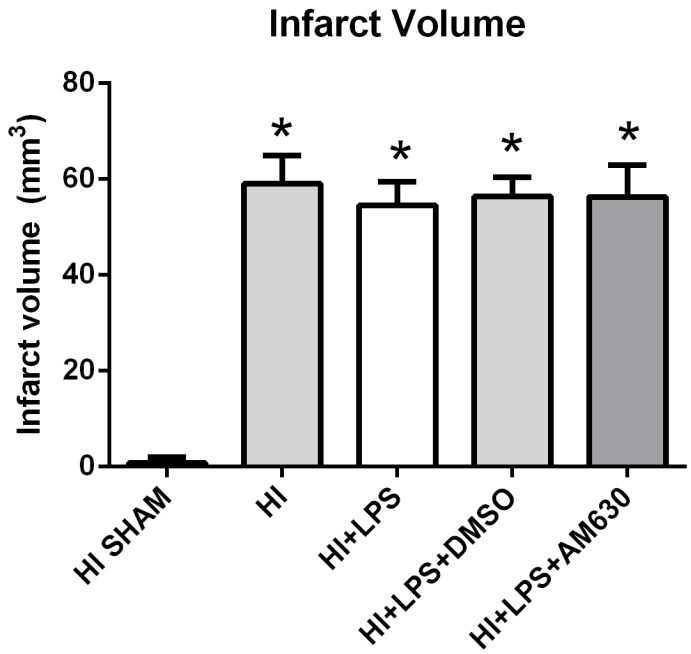

Figure 23. **Brain Infarct Volume in HI Model**

Brain infarct volume quantified as the total volume of tissue stained with tetrazolium chloride (TTC) from each brain slice. HI Sham(n=8); HI(n=6); HI+LPS (5 mg/kg) (n=6); HI+LPS (5 mg/kg) +DMSO(n=6); HI+LPS+AM630 (2.5 mg/kg) (n=6). AM630 administered 15 minutes before LPS administration at 22 hours after CNS injury induction, IVM performed at 24 hours. Data presented as mean ± standard deviation.Every experimental group was statistically significant ($p < 0.05$) versus HI SHAM.

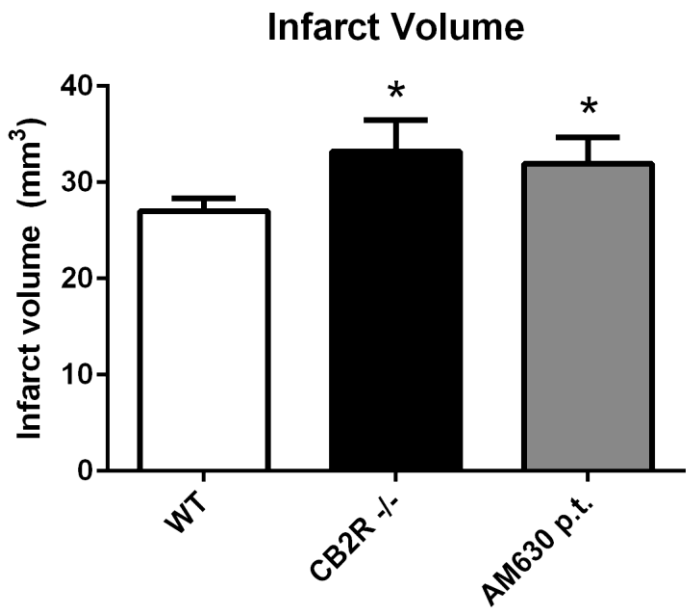

Figure 24. **Brain Infarct Volume of CB2R KO vs WT**

Brain infarct volume quantified as the total volume of tissue stained with tetrazolium chloride (TTC) from each brain slice. WT (wild type) group with ET-1 induced CNS injury (n=8); CB2R -/- group with ET-1 induced CNS injury (n=5), AM630 p.t. (2.5 mg/kg) (n=5). AM630 is a CB2 receptor antagonist, given as a pretreatment 15 minutes before CNS injury induction with ET-1 injection. Brains extracted 24 hours later. Data presented as mean ± standard deviation. * $p < 0.05$ versus WT

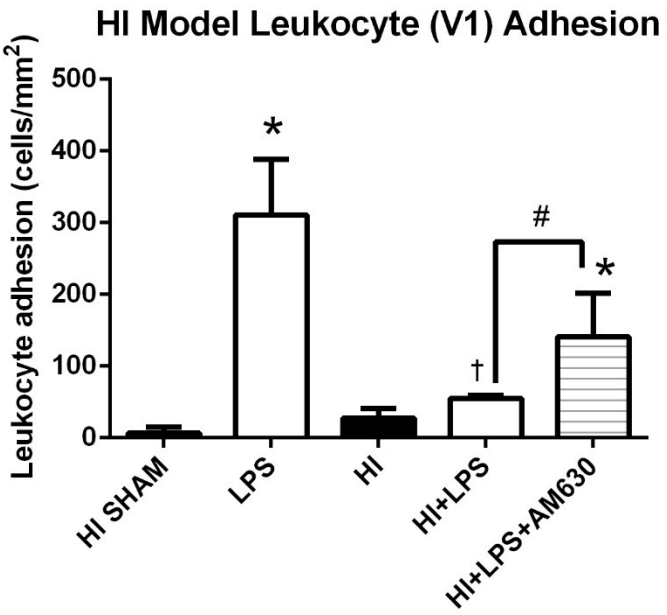

Figure 25. **Intestinal Leukocyte Adhesion in V1 Venules, HI Model**

Leukocyte adhesion in collecting venules (V1; >50 um vessel diameter). HI Sham(n=8); endotoxemia group (LPS) (5 mg/kg) (n=8); HI(n=6); HI + LPS(n=6); HI + LPS + AM630 (2.5 mg/kg) (n=6). AM630 administered 15 minutes before LPS administration at 22 hours after CNS injury induction, IVM performed at 24 hours. Data presented as mean ± standard deviation. *$p < 0.05$ versus HI SHAM. † $p < 0.05$ versus LPS, #$p < 0.05$ versus HI + LPS.

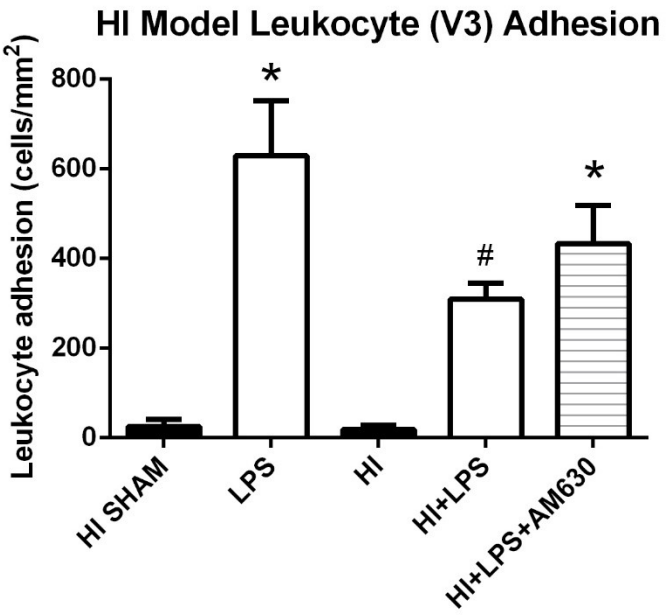

Figure 26. **Leukocyte Adhesion in Intestinal V3 Post Capillary Venules, HI Model**

Leukocyte adhesion in post capillary venules (V3; <50μm vessel diameter). Control group (HI SHAM) (n=8); endotoxemia group (LPS) (5 mg/kg) (n=8); HI (n=6); HI+LPS(n=6); HI+LPS+AM630 (2.5mg/kg) (n=8). AM630 administered 15 minutes before LPS administration at 22 hours after CNS injury induction, IVM performed at 24 hours. Data presented as mean ± standard deviation. ∗ $p < 0.05$ versus HI SHAM. # $p < .0.05$ versus HI+LPS+AM630.

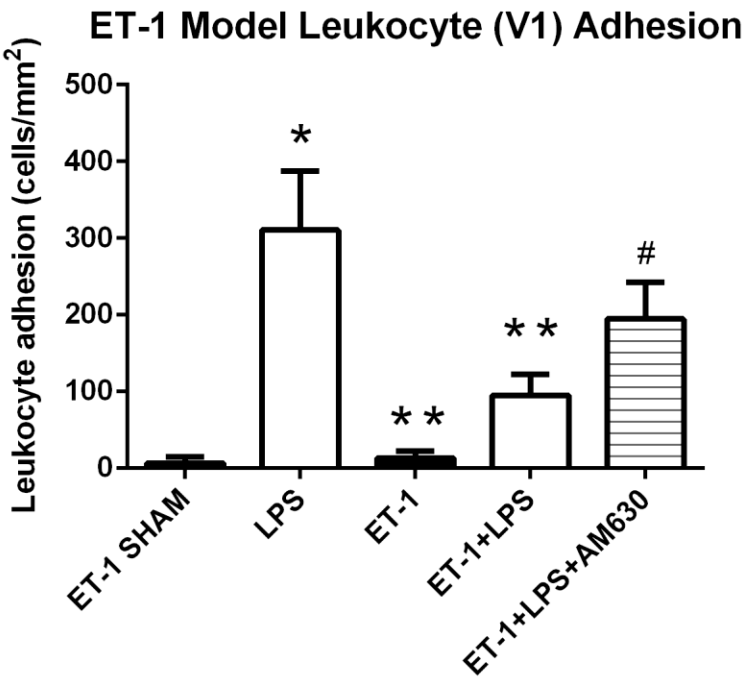

Figure 27. **Leukocyte Adhesion in Intestinal V1 venules, ET-1 Model**

Leukocyte adhesion in collecting venules (V1; >50 um vessel diameter). ET-1 Sham(n=8); endotoxemia group (LPS) (5 mg/kg) (n=8); ET-1(n=4); ET-1 + LPS(n=5); ET-1 + LPS + AM630 (2.5 mg/kg) (n=5). AM630 administered 15 minutes before LPS administration at 22 hours after CNS injury induction, IVM performed at 24 hours. Data presented as mean ± standard deviation. *$p < 0.05$ versus ET-1 SHAM. ** $p < 0.05$ versus LPS, #$p < 0.05$ versus HI + LPS.

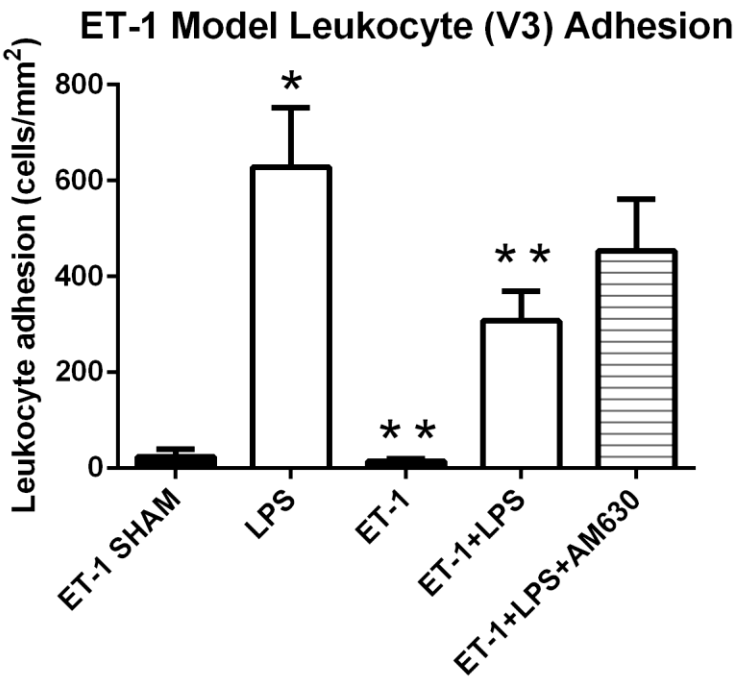

Figure 28. **Leukocyte Adhesion in Intestinal V3 Post Capillary Venules, ET-1 Model**

Leukocyte adhesion in post capillary venules (V3; <50μm vessel diameter). Control group (ET-1 SHAM) (n=8); endotoxemia group (LPS) (5 mg/kg) (n=8); ET-1(n=4); ET-1+LPS(n=5); ET-1+LPS+AM630 (2.5mg/kg) (n=5). AM630 administered 15 minutes before LPS administration at 22 hours after CNS injury induction, IVM performed at 24 hours. Data presented as mean ± standard deviation. ∗ $p < 0.05$ versus ET-1 SHAM. ** $p < .0.05$ versus LPS.

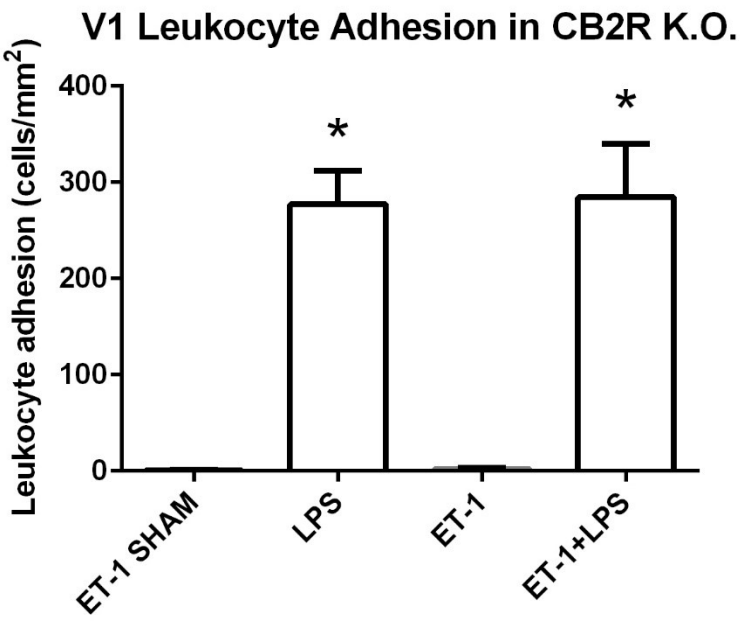

Figure 29. **Leukocyte Adhesion in Intestinal V1 venules, ET-1 Model, CB2R K.O.**

Leukocyte adhesion in collecting venules (V1; >50 um vessel diameter). All animals are CB2R null mice. ET-1 Sham(n=4); endotoxemia group (LPS) (5 mg/kg) (n=4); ET-1(n=5); ET-1 + LPS(n=5); LPS administered at 22 hours after CNS injury induction, IVM performed at 24 hours. Data presented as mean ± standard deviation. *$p < 0.05$ versus ET-1 SHAM.

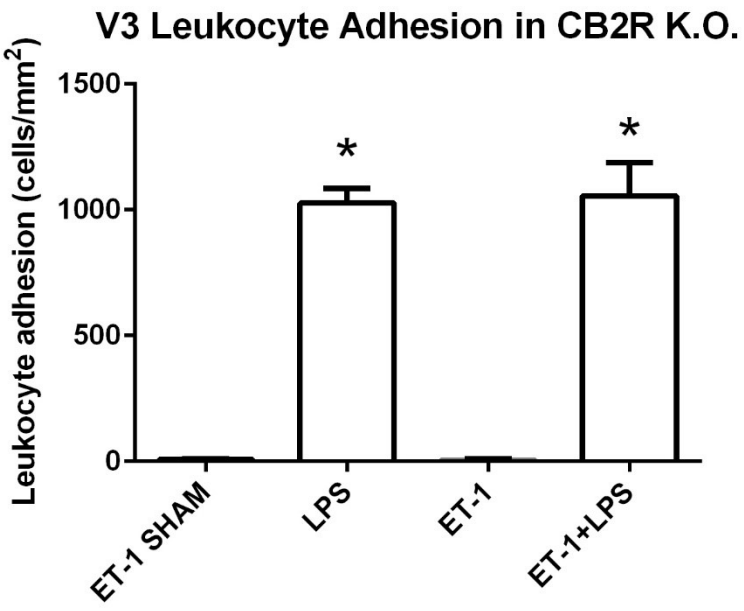

Figure 30. **Leukocyte Adhesion in Intestinal Post Capillary V3 Venules, ET-1 Model, CB2R K.O.**

Leukocyte adhesion in post capillary venules (V3; <50μm vessel diameter). All animals are CB2R null mice. ET-1 Sham(n=4); endotoxemia group (LPS) (5 mg/kg) (n=4); ET-1(n=5); ET-1 + LPS(n=5); LPS administered at 22 hours after CNS injury induction, IVM performed at 24 hours. Data presented as mean ± standard deviation. *$p < 0.05$ versus ET-1 SHAM.

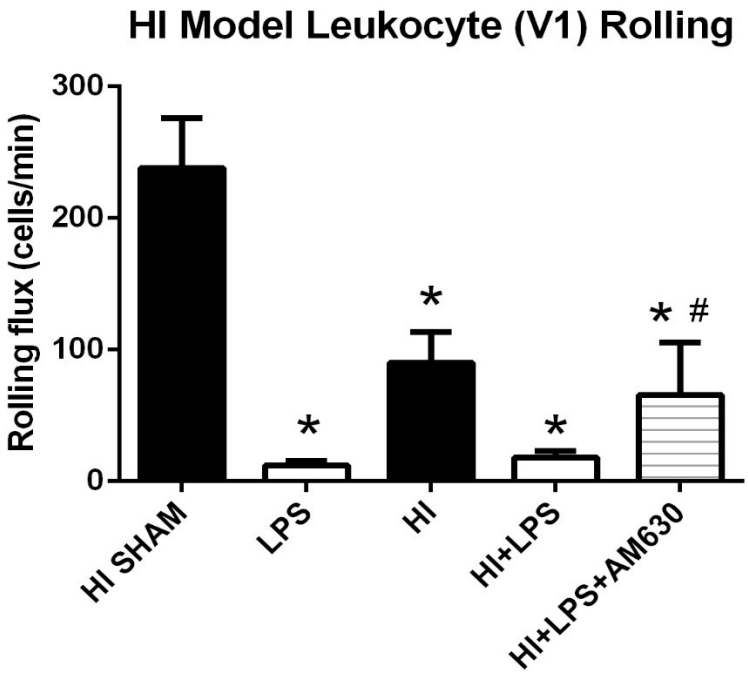

Figure 31. **Leukocyte Rolling in Intestinal V1 Collecting Venules, HI Model**

Leukocyte rolling in collecting venules (V1; >50 um vessel diameter). HI Sham(n=8); endotoxemia group (LPS) (5 mg/kg) (n=8); HI(n=6); HI + LPS(n=6); HI + LPS + AM630 (2.5 mg/kg) (n=6). AM630 administered 15 minutes before LPS administration at 22 hours after CNS injury induction, IVM performed at 24 hours. Data presented as mean ± standard deviation. *$p < 0.05$ versus HI SHAM, #$p < 0.05$ versus HI + LPS.

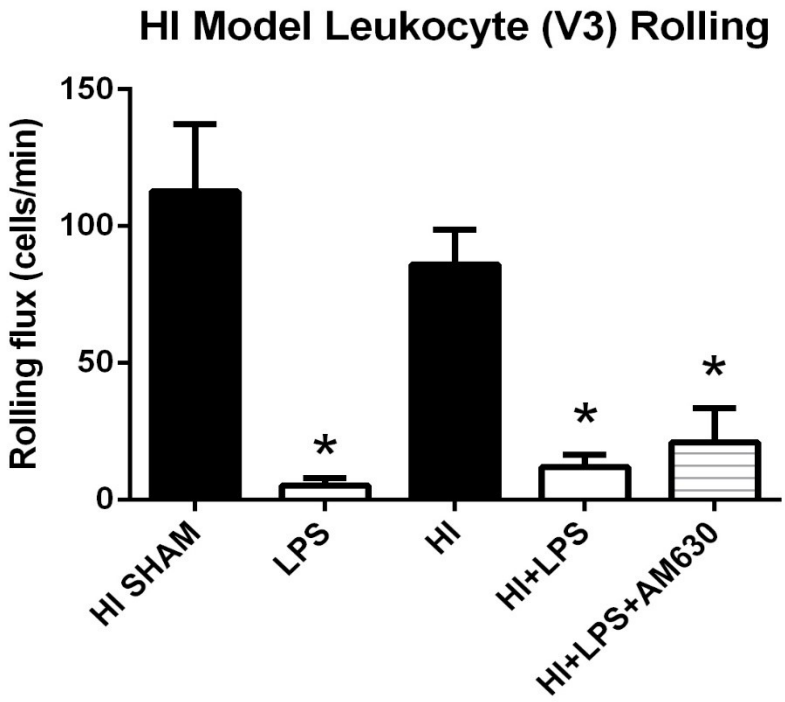

Figure 32. **Leukocyte Rolling in Intestinal Post Capillary V3 Venules, HI Model**

Leukocyte rolling in post capillary venules (V3; <50 um vessel diameter). HI Sham(n=8); endotoxemia group (LPS) (5 mg/kg) (n=8); HI(n=6); HI + LPS(n=6); HI + LPS + AM630 (2.5 mg/kg) (n=6). AM630 administered 15 minutes before LPS administration at 22 hours after CNS injury induction, IVM performed at 24 hours. Data presented as mean ± standard deviation. *p < 0.05 versus HI SHAM, #p < 0.05 versus HI + LPS.

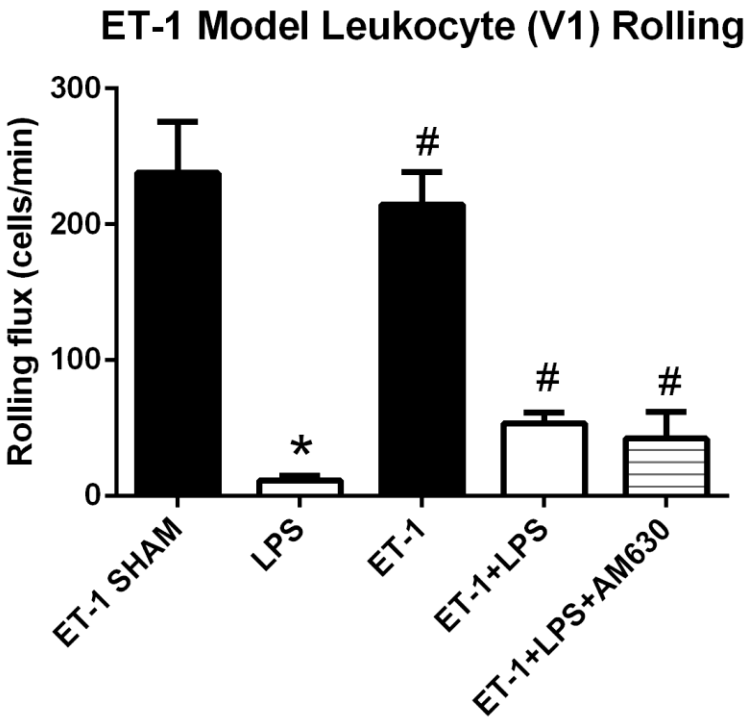

Figure 33. **Leukocyte Rolling in Intestinal V1 Collecting Venules, ET-1 Model**

Leukocyte rolling in collecting venules (V1; >50 um vessel diameter). ET-1 Sham(n=8); endotoxemia group (LPS) (5 mg/kg) (n=8); ET-1(n=4); ET-1 + LPS(n=5); ET-1 + LPS + AM630 (2.5 mg/kg) (n=5). AM630 administered 15 minutes before LPS administration at 22 hours after CNS injury induction, IVM performed at 24 hours. Data presented as mean ± standard deviation. *$p < 0.05$ versus ET-1 SHAM, #$p < 0.05$ versus LPS.

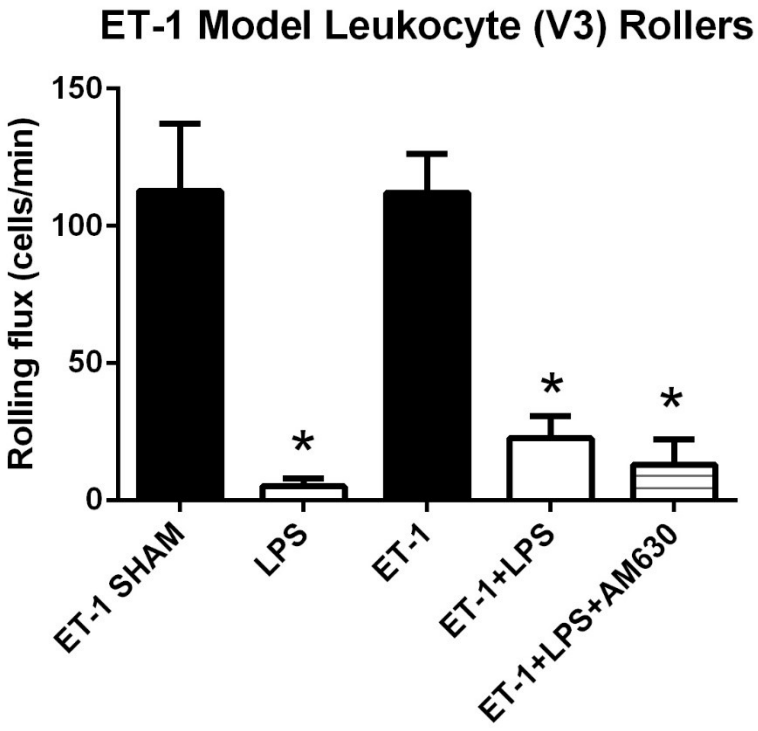

Figure 34. **Leukocyte Rolling in Intestinal Post Capillary V3 Venules, ET-1 Model**

Leukocyte rolling in post capillary venules (V3; <50 um vessel diameter). ET-1 Sham(n=8); endotoxemia group (LPS) (5 mg/kg) (n=8); ET-1(n=4); ET-1 + LPS(n=5); ET-1 + LPS + AM630 (2.5 mg/kg) (n=5). AM630 administered 15 minutes before LPS administration at 22 hours after CNS injury induction, IVM performed at 24 hours. Data presented as mean ± standard deviation. *$p < 0.05$ versus ET-1 SHAM.

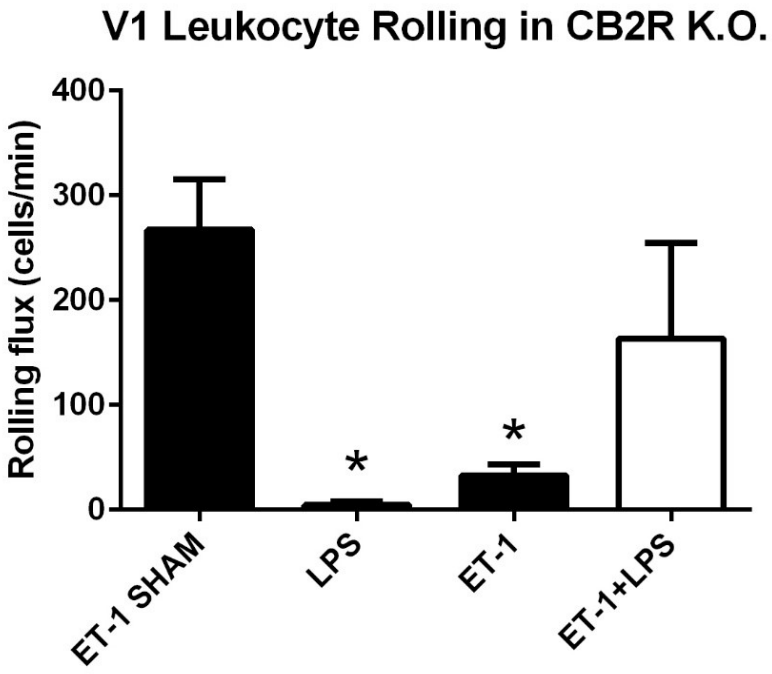

Figure 35. **Leukocyte Rolling in Intestinal V1 Collecting Venules, ET-1 Model, CB2R K.O.**

Leukocyte rolling in collecting venules (V1; >50 um vessel diameter). All animals are CB2R null mice. ET-1 Sham(n=4); endotoxemia group (LPS) (5 mg/kg) (n=4); ET-1(n=5); ET-1 + LPS(n=5); LPS administered at 22 hours after CNS injury induction, IVM performed at 24 hours. Data presented as mean ± standard deviation. *$p < 0.05$ versus ET-1 SHAM.

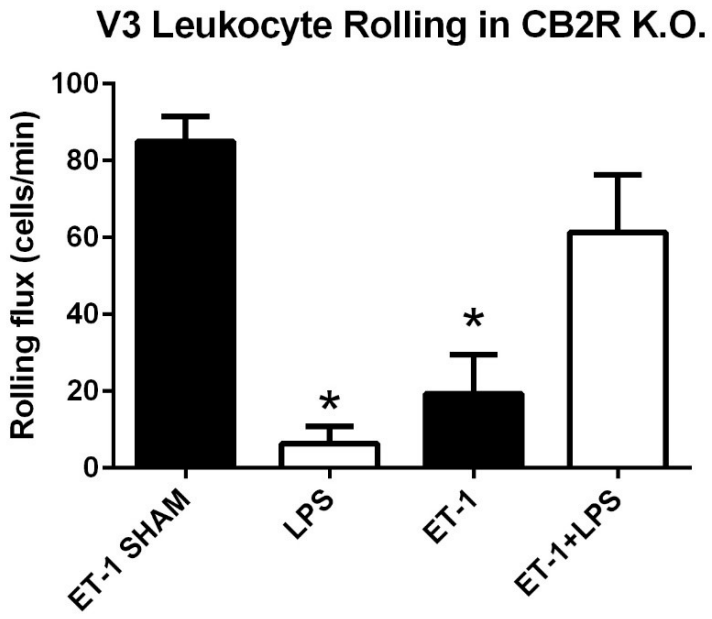

Figure 36. **Leukocyte Rolling in Intestinal Post Capillary V3 Venules, ET-1 Model, CB2R K.O.**

Leukocyte rolling in collecting venules (V1; >50 um vessel diameter). All animals are CB2R null mice. ET-1 Sham(n=4); endotoxemia group (LPS) (5 mg/kg) (n=4); ET-1(n=5); ET-1 + LPS(n=5); LPS administered at 22 hours after CNS injury induction, IVM performed at 24 hours. Data presented as mean ± standard deviation. *$p < 0.05$ versus ET-1 SHAM.

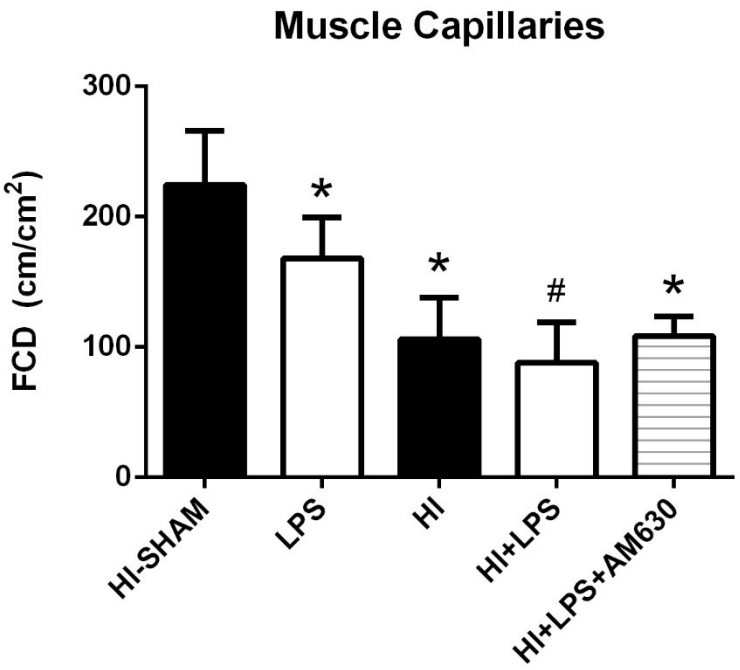

Figure 37. **FCD of Intestinal Muscle Capillaries, HI Model**

Capillary perfusion quantified through functional capillary density (FCD) within the submucosal muscle layers of the intestine. FCD quantified as total length of well perfused capillaries within a predetermined rectangular area of the observed field. Control group (HI-SHAM) (n=8); endotoxemia group LPS (5 mg/kg) (n=8); HI(n=6); HI+LPS(n=6); HI+LPS+AM630 (2.5mg/kg) (n=8). AM630 administered 15 minutes before LPS administration at 22 hours after CNS injury induction, IVM performed at 24 hours. Data presented as mean ± standard deviation. $*$ $p < 0.05$ versus HI-SHAM, # $p < 0.05$ vs LPS.

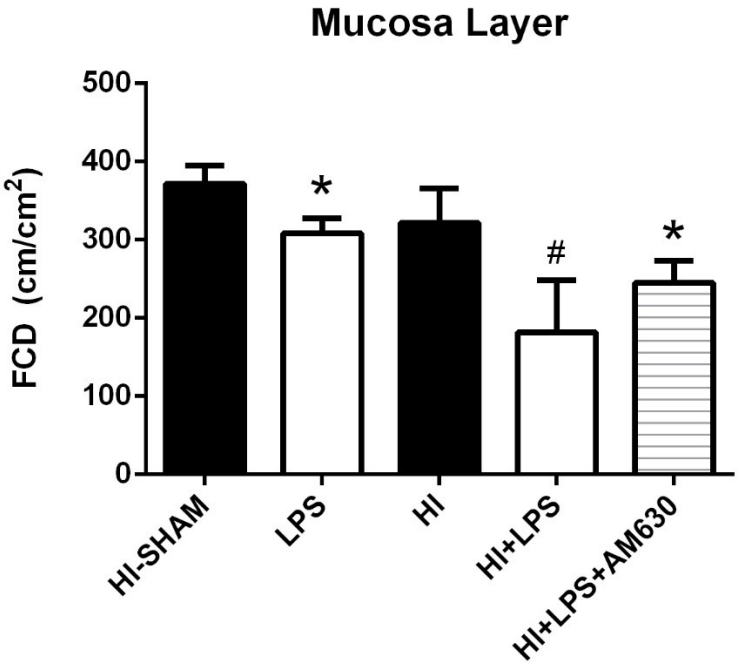

Figure 38. **FCD of Intestinal Mucosa Layer, HI Model**

Capillary perfusion quantified through functional capillary density (FCD) within the mucosal villi of the intestinal lumen. FCD quantified as total length of well perfused capillaries within a predetermined rectangular area of the observed field. Control group (HI-SHAM) (n=8); endotoxemia group LPS (5 mg/kg) (n=8); HI(n=6); HI+LPS(n=6); HI+LPS+AM630 (2.5mg/kg) (n=6). AM630 administered 15 minutes before LPS administration at 22 hours after CNS injury induction, IVM performed at 24 hours. Data presented as mean ± standard deviation. $* p < 0.05$ versus HI-SHAM, $\# p < 0.05$ vs LPS.

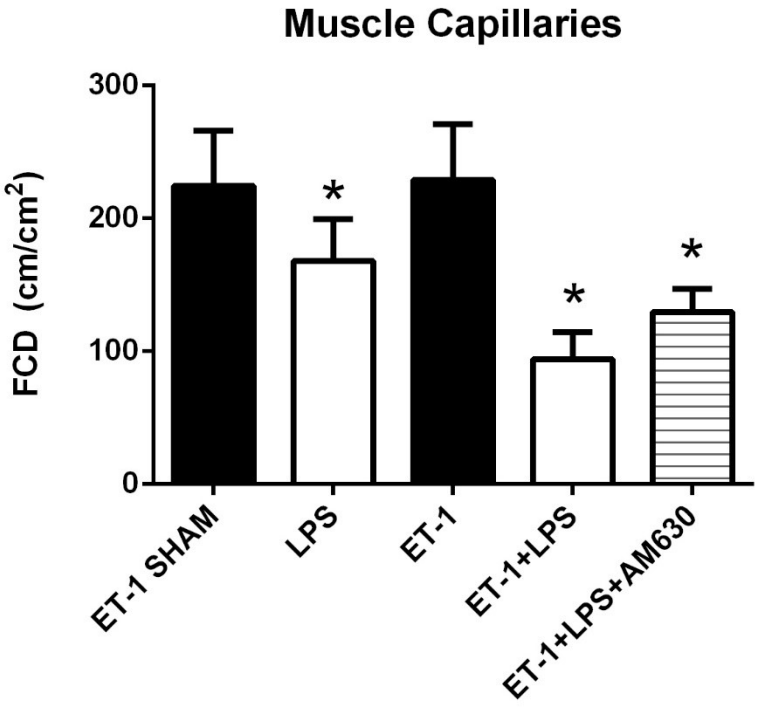

Figure 39. **FCD of Intestinal Muscle Capillaries, ET-1 Model**

Capillary perfusion quantified through functional capillary density (FCD) within the submucosal muscle layers of the intestine. FCD quantified as total length of well perfused capillaries within a predetermined rectangular area of the observed field. Control group (ET-1-SHAM) (n=8); endotoxemia group LPS (5 mg/kg) (n=8); ET-1(n=4); ET-1+LPS(n=4); ET-1+LPS+AM630 (2.5mg/kg) (n=5). AM630 administered 15 minutes before LPS administration at 22 hours after CNS injury induction, IVM performed at 24 hours. Data presented as mean ± standard deviation. $* p < 0.05$ versus ET-1 SHAM.

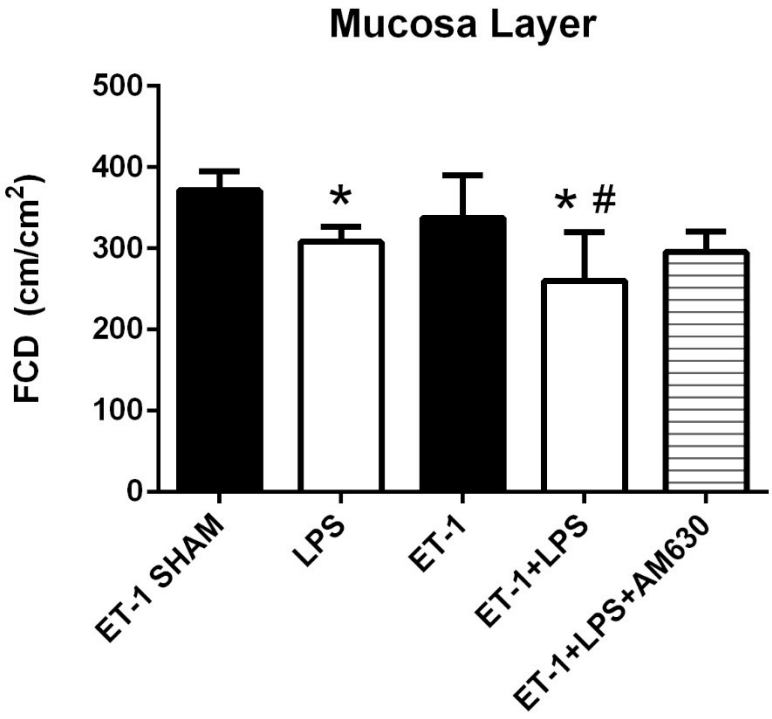

Figure 40. **FCD of Intestinal Mucosa Layer, ET-1 Model**

Capillary perfusion quantified through functional capillary density (FCD) within the mucosal villi of the intestinal lumen. FCD quantified as total length of well perfused capillaries within a predetermined rectangular area of the observed field. Control group (ET-1-SHAM) (n=8); endotoxemia group LPS (5 mg/kg) (n=8); ET-1(n=4); ET-1+LPS(n=4); ET-1+LPS+AM630 (2.5mg/kg) (n=5). AM630 administered 15 minutes before LPS administration at 22 hours after CNS injury induction, IVM performed at 24 hours. Data presented as mean ± standard deviation. $*$ $p < 0.05$ versus ET-1 SHAM, # $p < 0.05$ vs LPS.

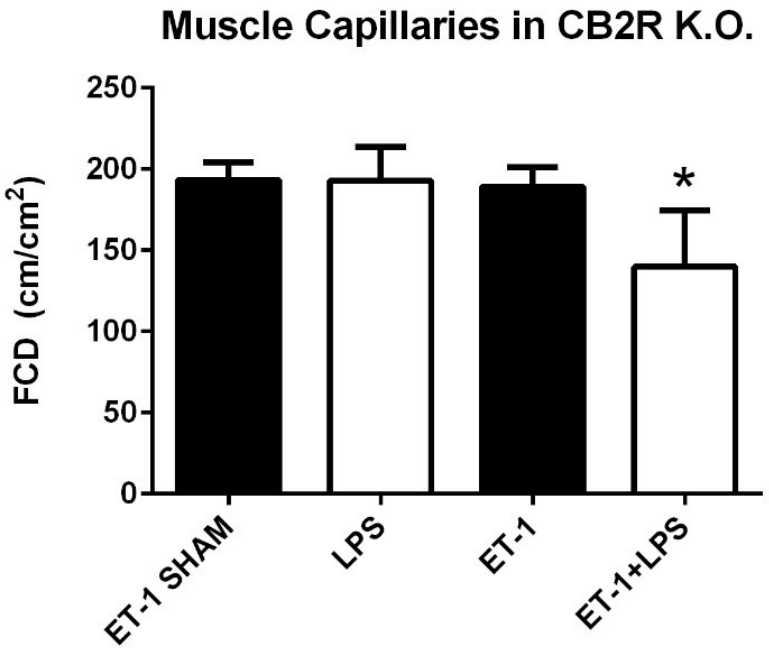

Figure 41. **FCD of Intestinal Muscle Capillaries, ET-1 Model, CB2R K.O.**

Capillary perfusion quantified through functional capillary density (FCD) within the submucosal muscle layers of the intestine. All animals are CB2R null mice. FCD quantified as total length of well perfused capillaries within a predetermined rectangular area of the observed field. Control group (ET-1-SHAM) (n=4); endotoxemia group LPS (5 mg/kg) (n=4); ET-1(n=5); ET-1+LPS(n=5). LPS administered at 22 hours after CNS injury induction, IVM performed at 24 hours. Data presented as mean ± standard deviation. $*$ $p < 0.05$ versus ET-1 SHAM.

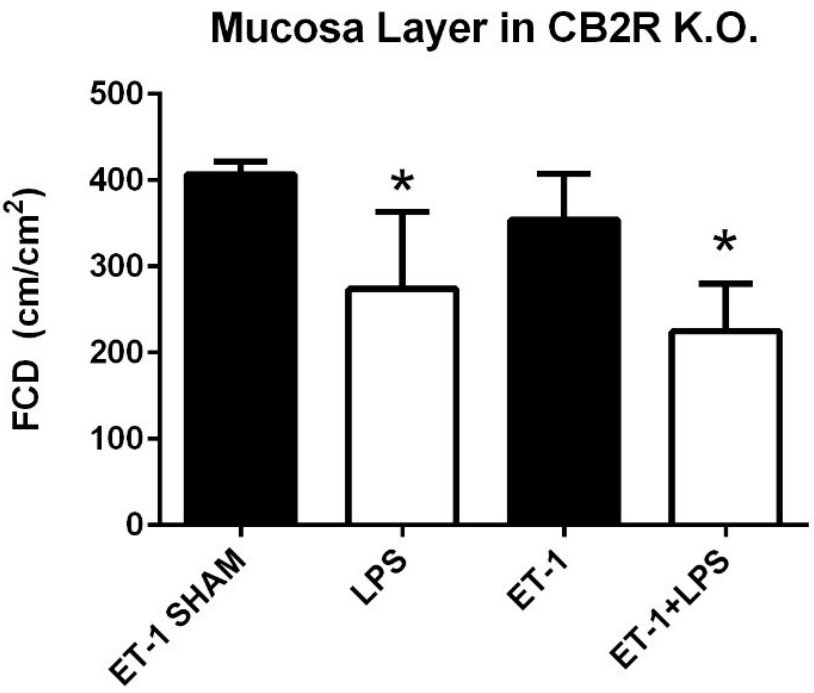

Figure 42. **FCD of Intestinal Muscle Capillaries, ET-1 Model, CB2R K.O.**

Capillary perfusion quantified through functional capillary density (FCD) within the mucosal villi of the intestinal lumen. All animals are CB2R null mice. FCD quantified as total length of well perfused capillaries within a predetermined rectangular area of the observed field. Control group (ET-1-SHAM) (n=4); endotoxemia group LPS (5 mg/kg) (n=4); ET-1(n=5); ET-1+LPS(n=5). LPS administered at 22 hours after CNS injury induction, IVM performed at 24 hours. Data presented as mean ± standard deviation. $*$ $p < 0.05$ versus ET-1 SHAM.

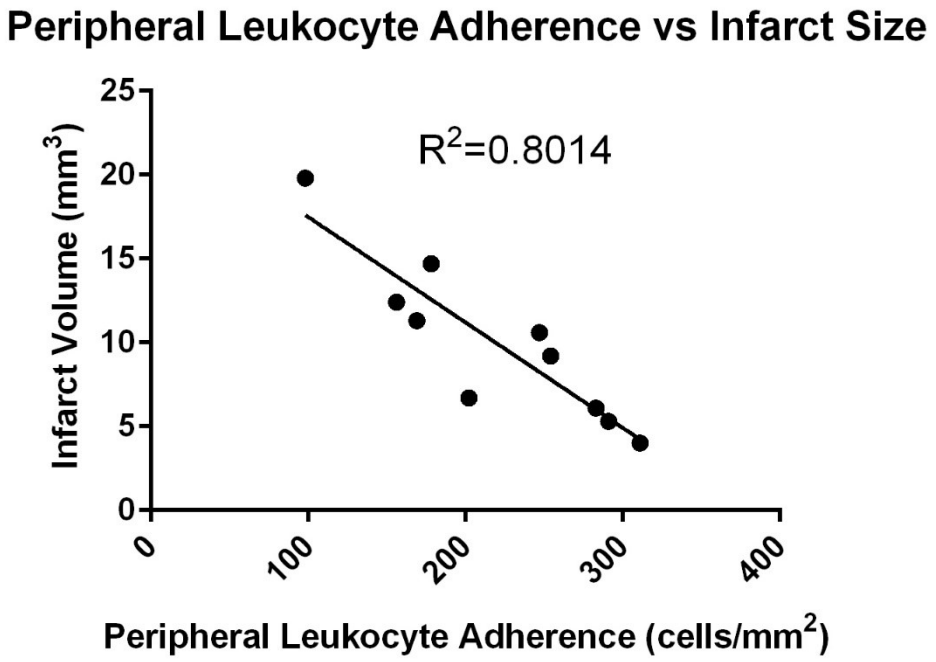

Figure 43. **Correlation Analysis of Peripheral Leukocyte Adherence vs Brain Infarct Size in ET-1 Model.**

Animals with CNS injury induced via cerebral ET-1 injections had their peripheral leukocyte adherence quantified and compared with a *post-mortem* quantification of brain infarct size for correlation. The linear correlation relationship between the two variables was calculated to have a Pearson r = -0.8952 with an $R^2 = 0.8014$. The strength of relationship between the two variables was calculated to be statistically significant ($p < 0.0001$).

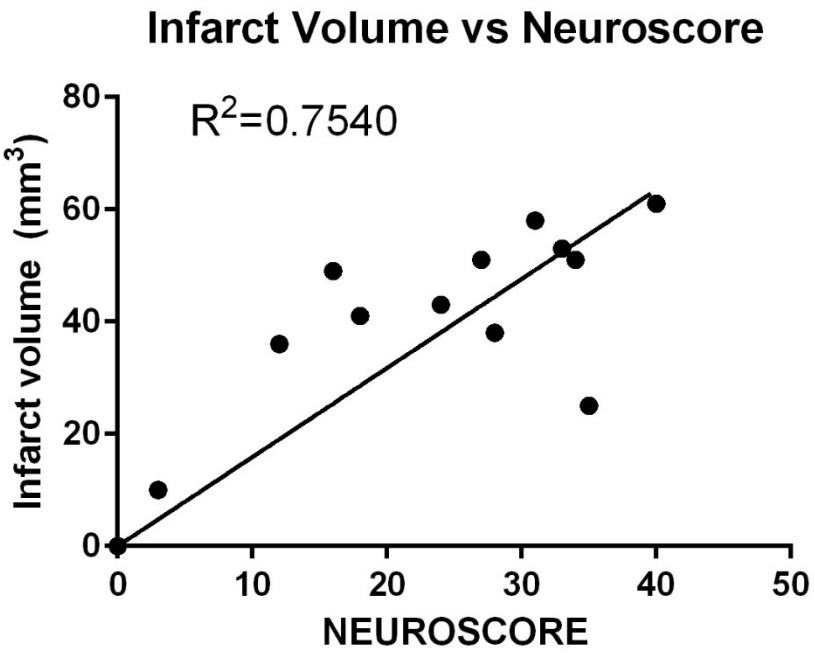

Figure 44. **Correlation Analysis of Brain Infarct volume vs Neuroscore in HI Model.** Animals with CNS injury induced via hypoxia-ischemia had their neurological and behavioural deficits quantified and compared with a *post-mortem* quantification of brain infarct size. The linear correlation relationship between the two variables was calculated to have a Pearson r = 0.8683 with an $R^2 = 0.7540$. The strength of relationship between the two variables was calculated to be statistically significant ($p < 0.001$).

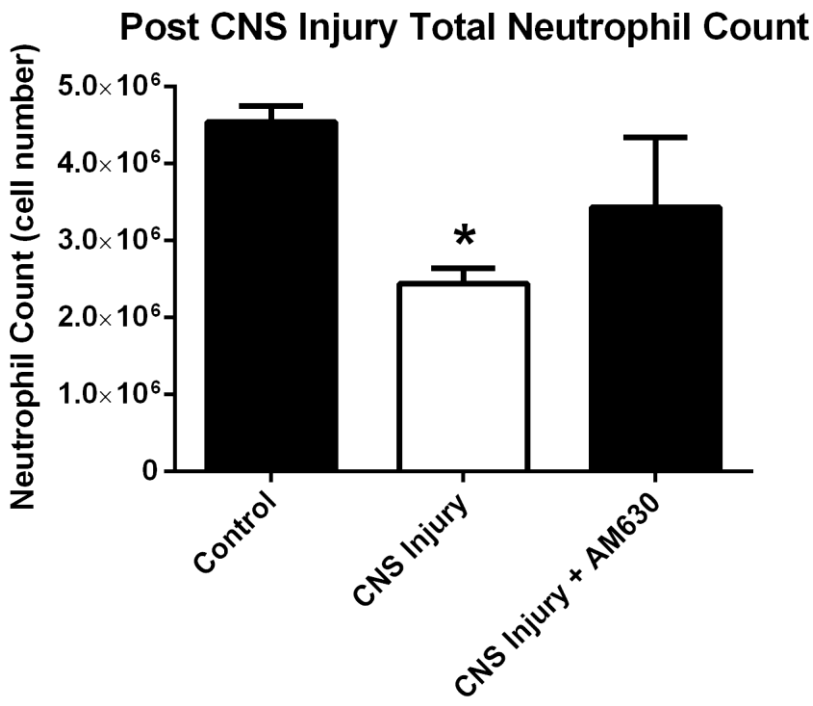

Figure 45. **Neutrophil Count After CNS Injury, ET-1 Model**

Neutrophil cells isolated from bone marrow of animals with CNS injury induced via cerebral ET-1 injections. The cells were counted across experimental groups of interest - healthy control; CNS injury and CNS injury + AM630 (2.5 mg/kg i.v.). AM630 was administered 22 hours after CNS injury induction. All experimental groups have an n=5. Data presented as mean ± standard deviation * $p < 0.05$ vs Control.

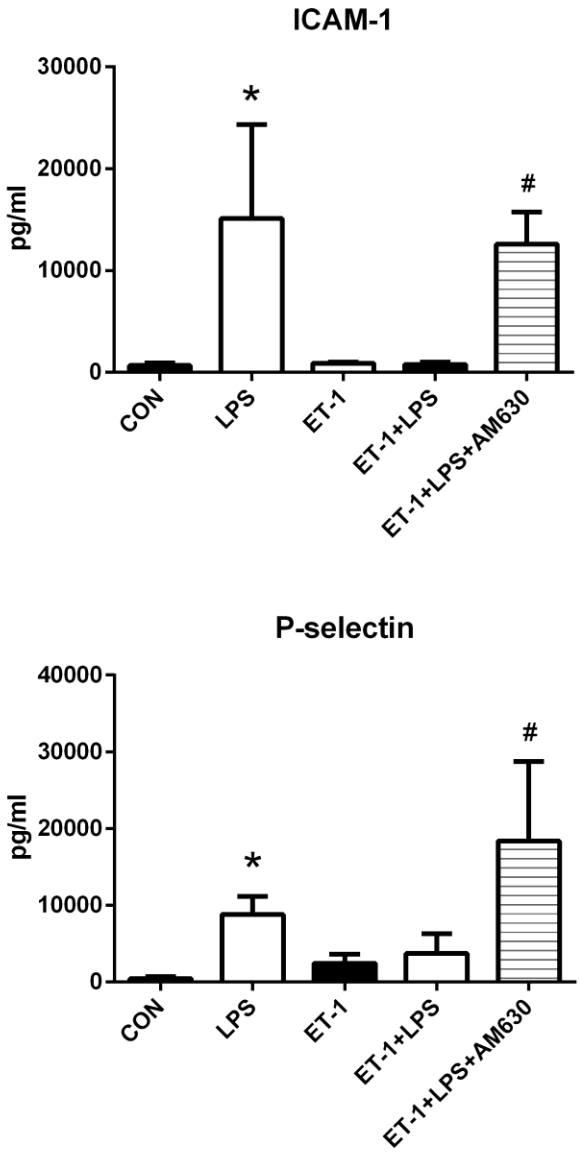

Figure 46. **Blood Plasma Adhesion Molecule Levels, ET-1 Model**

Plasma samples were collected and the levels of soluble adhesion molecules, P-selectin and ICAM-1 (pg/mL) were measured. The following groups were analyzed: control (CON); endotoxemia (LPS) (5mg/kg i.p.); ET-1; ET+LPS (5.mg/kg i.p.) and ET-1+LPS+AM630 (2.5mg/kg i.v.). AM630 was administered 22 hours after CNS injury induction. All selected experimental groups have an n=4, with two technical replicates for each sample. Data presented as mean ± standard deviation * $p < 0.05$ vs CON. # p , 0.05 vs ET-1+LPS.

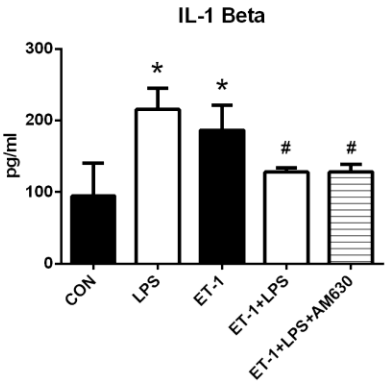
IL-1 Beta
pg/ml
300
200
100
0
*
*
#
#
CON
LPS
ET-1
ET-1+LPS
ET-1+LPS+AM630

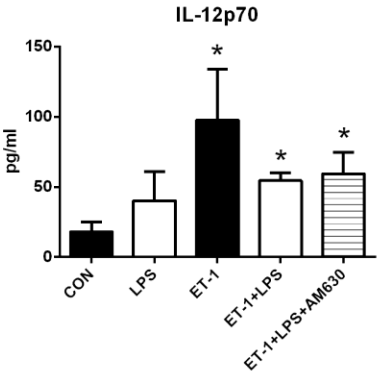
IL-12p70
pg/ml
150
100
50
0
*
*
*
CON
LPS
ET-1
ET-1+LPS
ET-1+LPS+AM630

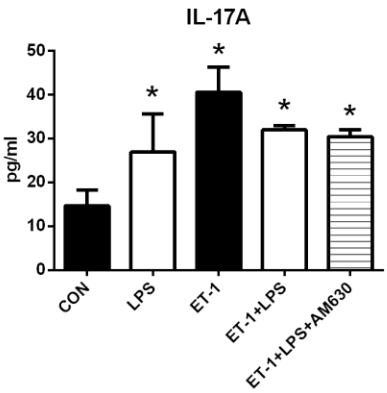
IL-17A
pg/ml
50
40
30
20
10
0
*
*
*
*
CON
LPS
ET-1
ET-1+LPS
ET-1+LPS+AM630

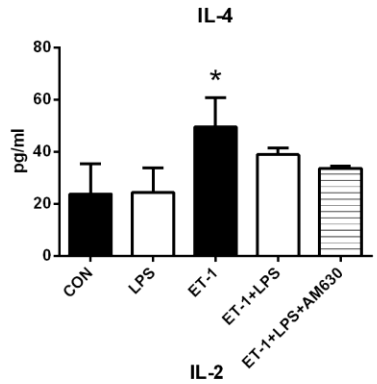
IL-4
pg/ml
80
60
40
20
0
*
CON
LPS
ET-1
ET-1+LPS
ET-1+LPS+AM630

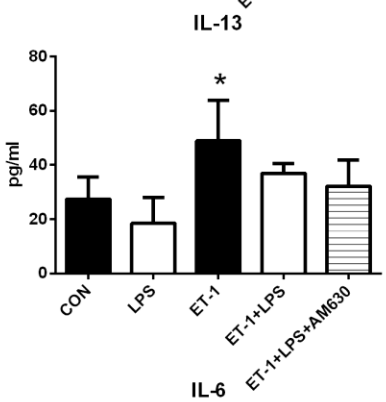
IL-13
pg/ml
80
60
40
20
0
*
CON
LPS
ET-1
ET-1+LPS
ET-1+LPS+AM630

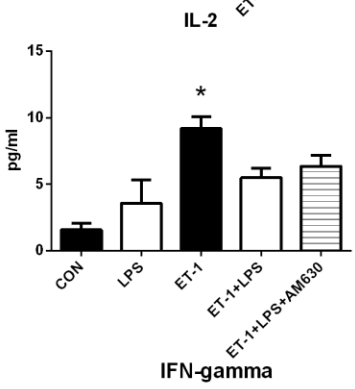
IL-2
pg/ml
15
10
5
0
*
CON
LPS
ET-1
ET-1+LPS
ET-1+LPS+AM630

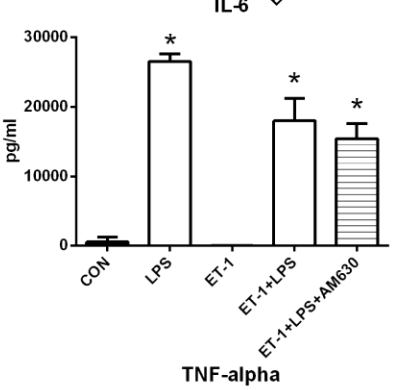
IL-6
pg/ml
30000
20000
10000
0
*
*
*
CON
LPS
ET-1
ET-1+LPS
ET-1+LPS+AM630

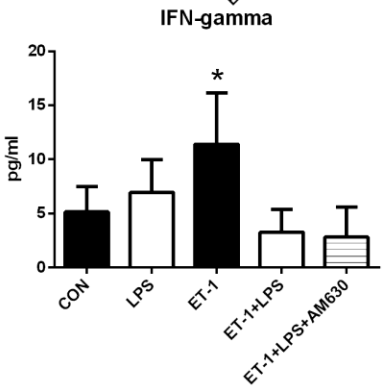
IFN-gamma
pg/ml
20
15
10
5
0
*
CON
LPS
ET-1
ET-1+LPS
ET-1+LPS+AM630

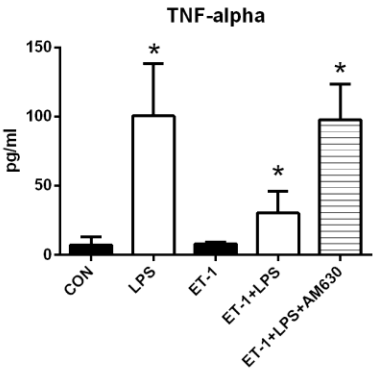
TNF-alpha
pg/ml
150
100
50
0
*
*
*
CON
LPS
ET-1
ET-1+LPS
ET-1+LPS+AM630

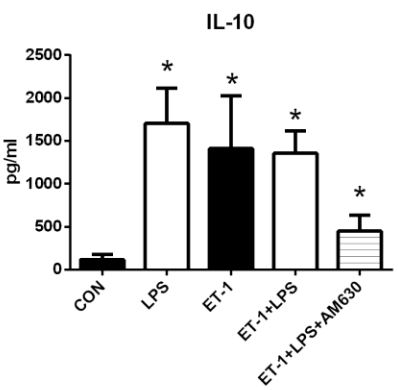
IL-10
pg/ml
2500
2000
1500
1000
500
0
*
*
*
*
CON
LPS
ET-1
ET-1+LPS
ET-1+LPS+AM630

Figure 47. **Blood Plasma Cytokine Concentrations, ET-1 Model**

Plasma samples were collected, and the levels of the following cytokines were measured: TNFα, IL-1β, IL-2, IL-4, IL-6, IL-10, IL-12p70, IL-13, IL-17A, and IFN-γ. The following groups were analyzed: control (CON); endotoxemia (LPS) (5mg/kg i.p.); ET-1; ET+LPS (5.mg/kg i.p.) and ET-1+LPS+AM630 (2.5mg/kg i.v.). All selected experimental groups have an n=4, with two technical replicates for each sample. Data presented as mean ± standard deviation * $p < 0.05$ vs CON. # p , 0.05 vs ET-1+LPS.

Chapter 4: Discussion

4.1. General Results Summary

The research presented in this dissertation focused on preclinical modelling of post CNS injury immunodeficiency. Presented data focused on evaluating the severity of the immunodeficiency in a rodent model and investigating the potential of modulating the endocannabinoid system with synthetic drugs to either prevent the pathological onset of CIDS or improve the immune function to be able to fight off basic pathogens. The results have shown that depending on the timing of treatment, both activation and inhibition of CB2R can be potentially beneficial for the ability of the immune system to fight off an immune challenge, such as an infection. More specifically, intravenous administration of HU308 prior to the onset of CNS injury was able to retain most of the leukocyte-endothelial adhesion parameters and has shown potential as a neuroprotective therapy by reducing the brain injury size. On the other hand, intravenous administration of AM630 after CNS injury and subsequent CIDS is established, provides partial restoration of the leukocyte-endothelial adhesion parameter, without causing any exacerbation in measured brain damage. Bone marrow neutrophil count was significantly reduced in animals with CNS injury, with AM630 administration causing a restoration in the number of neutrophils. The findings obtained from genetic removal of CB2R in mice showed a presence of a strong immune response and a lack of CIDS onset, along with an exacerbation in the size of brain injury, indicating that timing is everything when it comes to therapeutic potential of CB2R modulation. The findings were consistent with the proposed hypothesis that CB2R activation may be beneficial before the onset of acute CNS injury. Further investigation revealed that HU308 administration decreases the number of adhering leukocytes in brain vasculature that occurs shortly after the onset of CNS

injury. In addition, HU308 administration restored mouse splenic weight, suggesting one of the ways the immune system is retained in responsive condition, compared to the atrophied spleen in animals with CIDS. Animals that have been evaluated for their neurological and behavioural deficits after CNS injury have provided composite scores that were then compared to the results obtained via cellular staining. These comparisons revealed that the behavioural "neuroscore" parameter is a good predictor of the brain injury severity and may be utilized as a non-invasive assessment for future studies. Peripheral leukocyte adherence was also compared to the severity of brain injury and determined to have a strong inverse correlation between the two. This finding provided data that supported the idea that the size of the CNS injury influences the severity of the immune system impairment. Soluble adhesion molecule and cytokine levels revealed that the profile is rather dynamic and although it contained some expected changes, such as a reduction in TNFα and IL-6 in animals with CIDS, the larger picture remains to be complicated. Quantitative RT-PCR results revealed that the levels of CB2R mRNA expression remains unchanged throughout the experimental groups. Nonetheless, the mere presence of CB2R mRNA in measured tissues is seen as a positive result, confirming CB2R presence in tissues that were observed in performed experiments.

4.2. Early CB2R Activation in CNS Injury

Rapid death of brain cells after an acute ischemic or traumatic injury is irreversible and practically not preventable, simply because we cannot predict when such event is going to occur. For acute ischemic brain injury, the only pharmacological treatment that is clinically approved by food and drug administration (FDA) and utilized during a brief time window

after the onset of the injury is an intravenous administration of tissue-type plasminogen activator (tPA). This treatment approach has two major flaws: first – it has a potentially small therapeutic window and second – it raises major concerns regarding the risk of intracranial hemorrhage (Barreto, 2011; Sussman & Fitch, 1959). The therapeutic window for i.v. tPA across the world has been approved to a range within 3 to 4.5 hours after the onset of symptoms (Cheng & Kim, 2015). Canadian Alteplase for Stroke Effectiveness Study (CASES) revealed that a successful treatment is possible within the 3-4.5 hour treatment window, advising caution for later time window, due to greater adverse events (Shobha et al., 2011). While there are ongoing studies trying to expand this window, focusing on investigating the efficacy and safety of tPA at various time points, there is still simply not enough time for a lot of patients to get the essential medical intervention. Of course, use of tPA is contraindicated in patients suffering from traumatic or hemorrhagic injury. A more recent intervention involves the procedure of mechanically removing the thrombus from a blood vessel, known as thrombectomy. This surgical procedure became the standard of care for patients with large-vessel occlusion up to 24 hours of the brain injury onset (Albers et al., 2018; Nogueira et al., 2018). It does not take long to conclude that there is definitely a strong need for a therapeutic target to improve post CNS injury outcome.

CNS injury-induced inflammatory processes are a direct result to the cellular death due to the absence of blood supply to the damaged part of the brain. Without a doubt, most of the inflammatory processes have been linked either directly or indirectly to both acute and late stages of post CNS injury pathophysiology. One of such pathophysiological processes is CIDS and the work presented in this dissertation focuses on either preventing the onset of CIDS by reducing the strength and severity of the inflammatory processes or by directly

addressing the immunodeficient state and carefully “reverting” the immune function back to functioning levels.

Promising results have been obtained from the mice treated with HU308. In a schematic description, circulating HU308 prevents the typical consequences of CNS injury by immediately activating the CB2R throughout the acute phase of CNS injury (and the resulting upregulation of CB2R), setting the immune system into a lower-functioning state and yielding a smaller inflammatory response after the ischemic event and thus reducing the extent of compensatory immunosuppressive response. This is further supported by the results obtained via intravital imaging of brain vasculature, within 4 hours after induction of the injury. The findings revealed that HU308 treatment reduced cerebral leukocyte adherence, indicating a lesser presence of activated leukocytes during the first few hours directly after the brain injury. Of course, this view is simplified, as there are many other potential components that may be responsible, at least partially, to the observed neuroprotective effect of HU308. Nonetheless, this anti-inflammatory approach may be an important step in uncovering the delicate interplay between the ECS, CNS, and the immune system.

The role of the spleen in stroke has been noted and studied across many rodent and human studies (Seifert & Offner, 2018; Zierath et al., 2017). In general, the spleen is viewed as a major contributor to the immune response, exacerbating the secondary brain injury. On the preclinical level, splenectomy 2 weeks prior until ischemic or hemorrhagic event resulted in decreased infarct volumes (Seifert & Offner, 2018). Outcomes of studies that focused on the spleen suggested that splenic immune response is a viable target for therapy and could be useful for treating patients with CNS injury (Seifert & Offner, 2018). Interestingly, the

immune response to the brain antigens after CNS injury was not improved by splenectomy, neither was long-term neurological outcome (Zierath et al., 2017). Preclinical models of CNS injury have also reported splenic atrophy, followed by increased regulatory T cell numbers, as well as an increase in the number of circulating macrophages (Ross et al., 2007). Without a doubt, there is enough evidence to suggest that spleen plays an important part in the immune response and has a particular interest to me due to an increased level of CB2Rs expressed within that organ. While experimentally and even clinically, this organ has been considered, and tested, for complete removal either surgically or with irradiation (Ajmo et al., 2008; Ostrowski et al., 2012; Pennypacker & Offner, 2015) – I propose that this organ may also be used to monitor the strength of the immune response in preclinical models. More specifically, the typical presence of splenic atrophy after an acute CNS injury is indicative of the severity of the initial immune response, as well as the presence of immunosuppressive response, resulting in CIDS. Therefore, if an early treatment approach is able to reduce the size of brain injury, decrease the strength of the initial inflammatory response, it should also be able to either reduce or completely avoid splenic atrophy. The obtained results revealed that the splenic mass was restored back to healthy weight in the group that received the cannabinoid agonist intervention. This parameter is a relatively simple readout that provides another data point to evaluate the effectiveness of the treatment approach.

Leukocyte-endothelial interactions have also been examined in comparison to the infarct size. This comparison was done as it is known that the severity of the CNS injury dictates the level of immune impairment. Therefore, if the models that are utilized in this dissertation are able to induce similar pathophysiology to the one observed clinically, then the IVM readout of the immune function should have a strong negative correlation with brain infarct size.

When the data was analyzed, it was determined that peripheral leukocyte adherence goes up in very strong correlation with a decrease in brain infarct size. Thus, this finding can be summarized in one sentence – the larger the brain injury, the weaker the immune response.

4.3. Neuroprotection – Exploring the Potential Mechanisms

Neuroprotective effects of cannabinoids were investigated in various *in vivo* and *in vitro* models. While every model sheds some light at the possible mechanisms behind the reported neuroprotective effects, the mechanisms are not fully elucidated. One relevant study investigated the effect of CBD *in vivo* using a hypoxic-ischemic pig brain injury model (Pazos et al., 2013). Compared to the HI model used in this project, the duration of interrupted of brain blood flow was set to 30 minutes, with a similar reduction in fraction of inspired oxygen, down to approximately 10% (Pazos et al., 2013). While CBD is a ligand that can bind to more than one receptor target and it is not expected to have a high affinity for CB2R, it may be indirectly involved by inhibiting the uptake and breakdown of anandamide, which does bind to CB2R (Pertwee et al., 2010; Pertwee, 2004). As such, the findings of this study may be extrapolated to explain the changes observed in my experiments, since inhibiting the reuptake and breakdown of endogenous CB2R agonists would generally create a similar effect to activating the CB2R with a synthetic agonist, like HU308. CBD was administered 30 minutes after the onset of CNS injury, either alone, in combination with AM630 or a serotonin receptor antagonist. From the cellular perspective, HI brain injury dramatically decreased the number of viable neurons, electroencephalogram background activity, and other various biomarkers associated with the impairment of cellular brain

function (Pazos et al., 2013). It is reasonable to assume that similar changes occurred in the murine HI model, especially considering that the animals used for experiments in this dissertation were exposed to hypoxic conditions even longer, at an even lower oxygen fraction. Similar to this model, HI brain injury was also associated with excitotoxicity via glutamate, oxidative stress and an increase in brain IL-1 levels (Pazos et al., 2013). When compared to the results described in this dissertation, the circulating plasma IL-1 levels go down at 24-hour mark, without any significant change after the cannabinoid intervention. In terms of cannabinoid intervention, the same study continues to report that experimental groups with CBD administration were able to prevent all the pathophysiological changes (Pazos et al., 2013). This is in parallel with my findings that show reduced infarct volume when the CB2R is activated with an early intravenous administration of HU308. Similarly to how the brain injury in animals with CB2R deficiency was exacerbated, the study attempted to elucidate the involvement of CB2R by inhibiting it with AM630 and revealed that the observed neuroprotection was reversed in presence of AM630 (Pazos et al., 2013). Another receptor that appears to be implicated with the neuroprotective effect of CB2R activation is $5HT_{1a}$ receptor, as co-administration of either CB2R antagonist (AM630) or $5HT_{1a}$ receptor antagonist (WAY100635) with CBD was able to reverse the neuroprotective effect, in addition to bioluminescence resonance energy transfer (BRET) studies indicating high affinity for formation of heteromers between $5HT_{1a}$ and CB2 receptors (Pazos et al., 2013). Taking this evidence together, it can be proposed that CB2R signaling may exert its neuroprotective properties via multiple pathways, possibly depending on cellular localization and patterns of expression. One of such possible pathways involves CB2/5HT heteromization complexes, presenting yet another pharmacological target.

The development of brain edema after BBB disruption in acute and subacute phases after the injury event is a critical step in post CNS injury pathophysiology, frequently referred to as the most life-threatening secondary injury after the primary injury itself (L. Li et al., 2018). This event has been experimentally targeted with a CB2R agonist, JWH133, and examined 24 hours following the injury. Interestingly, JWH133 was able to significantly reduce the edema, improve neurobehavioural scores and even reduce BBB permeability (L. Li et al., 2018). The dose of JWH133 (1.5 mg/kg) used was similar to the utilized dose of HU308 (2.5 mg/kg) in this project. Similar to the findings of my research, Li et al. (2018) also found that activation of CB2R resulted in changes in the levels of pro-inflammatory mediators. Although my results did not show a profound change in the levels of IL-1β or TNFα, this may be due to the fact that my experiments were looking at systemic plasma levels and not local levels in the brain.

CB2R activation has been linked with upregulation in IL-10 levels (Xie et al., 2016), which may be one of the ways CB2 activity is able to indirectly induce protective environment for the brain. To be able to understand the significance of that, it is important to consider the great multitude of ways that IL-10 can potentially contribute to neuroprotection. IL-10 is also known as the cytokine synthesis inhibitory factor (CSIF) and can be considered as the most potent anti-inflammatory cytokine. As suggested by its name, one of the main properties of IL-10 is its ability to inhibit the production of proinflammatory cytokines such as TNFα and IFN-γ by T helper 1 (Th1) cells (Saxena et al., 2014). IL-10 can inhibit production of proinflammatory cytokines, antigen presentation and cell proliferation (D'Andrea, 1993; Ito et al., 1999; Joss et al., 2000; Koppelman et al., 1997) This ability alone heavily implicates the role of IL-10 in the onset of CIDS and possibly its resolution. IL-10 is produced by the

majority of the innate and adaptive immune cells, with these same cell types also serving as its targets, suggesting that IL-10 secretion is highly regulated and potentially compartmentalized (Saxena et al., 2014). Studies which have investigated IL-10's targets demonstrated that IL-10 restrains the immune response to pathogens and microbial flora and prevents their pathologies via inhibitory effects on macrophages and dendritic cells (DCs) (Spits & Malefyt, 1992). IL-10 seems to be particularly involved in modulating brain inflammation and repair processes, as IL-10 is up-regulated in both hemispheres after permanent middle cerebral artery occlusion (MCAO), as well as transient MCAO (Fouda et al., 2013).

Interestingly, the up-regulation of IL-10 in both hemispheres is contrasted with up-regulation of inflammatory cytokines only on the ischemic side (Fouda et al., 2013), suggesting that IL-10 is involved at all levels of post CNS injury. What this suggests is that IL-10 potentially acts not only as an anti-inflammatory cytokine but also as a chemical messenger for brain repair processes, and even neurogenesis. This is further supported by the line of evidence that shows that neurons appear to be the major source of IL-10, as well as the main place for receptor expression, along with the microglia and endothelial cells (Fouda et al., 2013). It is this connection between microglia, IL-10 upregulation and one of the main sites of CB2R action within the brain that it becomes probable that the activity of CB2R within the microglia causes a shift in IL-10 expression. Another line of evidence suggests an interaction between IL-10 and CD4+ T cells within the CNS which cooperatively protects the neurons from cell death following injury (Xin et al., 2011). The specific mechanism of neuroprotection seems to involve T cells in maintaining sufficient, glial-derived IL-10 levels near the damaged cell bodies, mediating neuroprotective pathways both directly and

indirectly (Xin et al., 2011). These observations are further supported by reports of a neuroprotective effect after direct binding of IL-10 to neurons that expressed IL-10R, protecting those cells from chemically-induced apoptosis *in vitro* (Koeberle et al., 2004). A lot of cellular death after CNS injury, especially in the penumbra, happens due to apoptotic cell-to-cell signalling, which outlines the potential explanation for the observed improvement in experimental groups with cannabinoid intervention and the resulting increase in plasma IL-10 levels.

The extent of neuroprotective role of IL-10 does not end here. IL-10 has also been shown to provide neuronal trophic support and induce pro-survival effects in primary neuronal cultures. The strongest line of evidence for this revealed that IL-10 binding to its designated receptor on cell surface activates the Janus-associated kinases and transcription factors (Jak-Stat3) and phosphatidylinositol 3-kinase (PI3K)-AKT (Zhou et al., 2009). Although signaling through both of those pathways can potentially enhance the expression of the anti-apoptotic proteins Bcl-2 and Bcl-xL, it is the PI3K-AKT activating the canonical NF-κB pathway that mediates the neuroprotective effect of IL- 10 (Zhou et al., 2009). The same study revealed that when neurons are subjected to glutamate toxicity – IL-10 administration was able to yield a neuroprotective effect by enhancing nuclear p50 and p65 with consequent prevention of cytochrome c release from mitochondria, as well as caspase 3 cleavage (Zhou et al., 2009), resulting in neuronal cell survival and reduction in the severity of injury. Other lines of evidence that utilized different *in-vitro* models were able to demonstrate that IL-10 protects murine cortical and cerebellar neurons from excitotoxic damage, as well as oxygen glucose deprivation by activating IP-3 kinase and STAT-3 survival pathways (Grilli et al., 2000; Sharma et al., 2011).

While the neuroprotective effects described above are very helpful for the CNS during the subacute and late phases, the onset of brain ischemia is rather rapid, and every moment spent in ischemic condition increases the severity of the injury, summoning the need for a fast-acting transcription-independent neuroprotective mechanism. If the pathophysiology after CNS injury is examined closely during the acute phase, it is evident that one of the primary effects of cerebral ischemia is an overload of intracellular calcium levels, causing cell death. Therefore, a rapid mechanism was hypothesized to be modulating intracellular calcium response (Tukhovskaya et al., 2014). Surprisingly, IL-10 is also the main player in this mechanism. It was convincingly demonstrated that IL-10 is capable of protecting neurons from ischemic death in both *in vivo* and *in vitro* models and that this protective effect was developed within 15 minutes after IL-10 application and was strongly associated with the IL-10-elicited elimination of intracellular calcium response to brain ischemia after MCAO procedure (Tukhovskaya et al., 2014). Mechanism wise, IL-10 neuroprotection is usually associated with activation of Jak-Stat3, PI3K-Akt and NF- κB signalling pathways, however IL-10 is capable of rapid neuroprotective effect via modulation of hypoxia-induced intracellular calcium response (Tukhovskaya et al., 2014). The absence of IL-10 production in mouse brain was shown to make the brain tissue more susceptible to ischemic damage, as a consequence of focal ischemic brain injury – providing even more evidence for the significant neuroprotective role of endogenous IL-10 (Grilli et al., 2000).

Another possible mechanism that is linked to cannabinoids' neuroprotective and anti-inflammatory effects in neuronal and glial cells may be mediated through the activity of endogenous IL-1 receptor antagonist (IL-1ra) (Molina-Holgado et al., 2003). IL-1ra is a naturally secreted anti-inflammatory cytokine that blocks all currently known actions of IL-1

and is thought to be protective against CNS injuries of various origins - ischemic, traumatic, and excitotoxic (Molina-Holgado et al., 2003). Interestingly, experimental evidence obtained from primary cultural glial cells revealed that both CB1R and CB2R modulate the release of IL-1ra, with IL-1ra knock-out mice showing a reduced ability to protect against excitotoxicity and inflammatory insults (Molina-Holgado et al., 2003). This arm of evidence provides the potential explanation how the ECS signalling is involved in naturally protecting the injury from further damage. This also outlines one of the possible ways the CB2R can be targeted to "prime" or activate the ECS mechanisms early enough to increase the level of IL-1ra and protect the brain from exacerbated injury.

One of the early post-CNS injury events results in presynaptic Ca^{2+} accumulation, which leads to the activation of phospholipase-C (PLC) and the production of diacylglycerol (DAG), as well as 2-AG (Di Marzo et al., 1998; Sugiura & Waku, 2000). Multiple studies have identified endogenous cannabinoid 2-AG both in the periphery, as well as the brain itself (R Mechoulam et al., 1995; Sugiura et al., 1995). It was also discovered that the naturally occurring levels of 2-AG are significantly elevated after a CNS injury event (Panikashvili et al., 2001), possibly directly as a result of increased level of postsynaptic Ca^{2+}. In terms of involved pathways, 2-AG has been reported to suppress the formation of ROS and inhibit the production of TNFα by murine macrophages in LPS-treated mice (Gallily et al., 2000). It is known that both ROS and TNFα are one of the main contributors to the resulting pathophysiology after CNS injury (Chan, 2001; Shohami et al., 1999), thus making their modulation a very important target for pharmacological intervention. When administered to mice after CNS injury, synthetic 2-AG was able to reduce infract volume and reduce hippocampal cell death (Panikashvili et al., 2001). Since 2-AG is an endogenous

ligand at both CB1R and CB2R, this neuroprotective mechanism is potentially directly involved in the observed neuroprotective effects of HU308 administration in this project.

One possible alternative neuroprotective mechanism that is associated with cannabinoid activation is related to peroxisome proliferator activated receptor (PPAR). It has been shown that endogenous cannabinoid-like compounds such as N-oleoylethanolamine, anandamide, nalonid ether and virodhamine were found to bind to the purified PPRAα ligand binding domain and increase PPRAα-driven transcriptional activity (Sun et al., 2007). While this neuroprotective mechanism isn't exerted directly through the CB2R-associated pathway, nuclear receptor activation may be triggered due to off-target effect and at least some affinity of the administered ligand towards the CB1R. Off-target signalling could explain some of the long-term neuroprotective effects on transcriptional level, providing support for brain repair in the acute phase shortly after the CNS injury, but also for days and weeks after the injury, when neuronal repair processes become more dominant.

Selective activation of CB2R may also exhibit neuroprotective properties such as a reduction in neuroinflammation and in neurovascular injury via alternative macrophage polarization (Braun et al., 2018). Inflammatory activation may produce both detrimental and reparative functions after CNS injury, suggesting a delicate balance is essential to improve outcome. In general, the exact role of CB2R signalling or the specific pathway that is utilized during and after CNS injury remains unresolved. Some of the experimental findings reported in this dissertation have also been echoed in other adult permanent ligation/hypoxia studies, where CB2R deficient mice developed more extensive brain injury size compared to their wild type counterparts (Kossatz et al., 2016). The same study went further in the post CNS injury

timeline and evaluated behavioural deficits at day 7 after the injury, revealing that mice without functional CB2R lacked any progressive recovery in motor learning, coordination and balance parameters. The possible pathway that is responsible for the increase of lesion size, is suggested to be exacerbation of inflammatory hypoxia-inducible factor 1-alpha (HIF-1α) and mucin-domain containing-3 (TIM-3) expression in mice without CB2R is present in both lesioned and non-lesioned areas of the brain. This involvement further supports the notion that CB2R may be directly involved in neuroprotective mechanisms following CNS injury by modulating inflammatory signalling pathways in astrocytes and microglia within the brain (Kossatz et al., 2016). Another line of evidence suggests that CB2R antagonism is able to reverse the neuroprotective effects of minocycline, specifically at the level of activation and reactivity but not proliferation processes of microglia and also exacerbating the extent of TBI damage (Lopez-Rodriguez et al., 2015). Yet another CB2R pathway that could contribute to the lack of neuroprotection in CB2R K.O. mice is the absence of CB2R-associated cortical activation of the AMP-activated protein kinase (AMPK)/CREB signalling pathway, which is ultimately responsible for brain-derived neurotrophic factor expression (Choi et al., 2013). Another study of axotomized neurons revealed that CB2R protected the neurons by regulating Akt (protein kinase B) and JNK phosphorylation through a PI3K-dependent pathway, without any involvement of ERK1/2 or p38 signaling (Viscomi et al., 2009). It was previously discussed that CB2R activity was able to attenuate microglial accumulation after CNS injury. Another study investigated this further in germinal matrix hemorrhage (GMH) model and revealed that CB2R activity is able to promote an M1 to M2 phenotype transformation in microglia, increasing anti-inflammatory cytokine release through the cAMP/PKA pathway (Tao et al., 2016). In summary, the elucidation of one

pathway that is responsible for the neuroprotective properties of CB2R associated signalling after CNS injury has proven to be rather difficult. Based on the current state of available literature, I propose that multiple pathways may be responsible for the observed neuroprotective effects and the activation of these pathways may also be specific not only to the type of CNS injury but also to the extent, location and the severity of it. To take the discussion into even more speculative direction, it is possible that the type of CB2R-related pathway that becomes activated may also be dependent on the ligand that binds to the receptor(s), as well as the expression profile of the target receptor(s). For example, a promiscuous ligand like CBD may be essential in inducing the neuroprotective processes via both CB1R and CB2R signalling, while contributing to the induction of CIDS. However, the presence of a positive allosteric modulator (PAM) may invoke a different pathway or cascade of pathways, even if the same ligand (i.e. CBD) is present at the CB1 and CB2 receptors, highlighting the importance of understanding ligand-specific pharmacology of the ECS. It is likely that a good cannabinoid candidate for clinical intervention may be specific to the type of CNS injury, as well as to the time point since the injury occurred, in order to avoid disturbing the particular neuroprotective mechanism that has been established, yet still allow peripheral immune activity, thus alleviating CIDS.

4.4. Late CB2R Inhibition as CIDS Therapy

IVM has provided the ability to visualize the impairment of leukocyte-endothelial interactions in collecting and postcapillary venules of the intestinal microcirculation after a single episode of unilateral forebrain hypoxia-ischemia procedure. CNS injury, as expected,

was able to directly induce a change in the immune response that was detectable and quantifiable with the techniques used. This was a very crucial step as it allowed the establishment of an *in vivo* protocol to model CIDS, utilizing an endotoxin to challenge an immune system at a later point after the initial onset of the CNS injury. After a secondary verification of the systemic immunosuppressive effect of an acute CNS injury by measuring circulating cytokine levels, a reduction in cytokine levels, such as TNFα and IL-6, was measured indicating an alteration in the normal function of the immune response. This protocol was then used to evaluate the cannabinoid intervention in its ability to change the impaired immune response after the CNS injury.

Intestinal immune function was evaluated via IVM. This method allows *in vivo* readout of the immune response within the small intestine. In animals with acute CNS injury, a reduction in the baseline rolling flux of leukocytes was observed. In animals with acute CNS injury and endotoxemia, a major reduction in leukocyte-endothelial interaction was also observed. Impaired red blood cell transport and lack of adequate microvascular perfusion causes tissue hypoxia and ischemia (De Backer et al., 2002; Salgado et al., 2010). As a secondary readout of post CNS injury microvascular impairment, functional capillary density was measured and evaluated. LPS administration was found to significantly reduce the FCD in both muscle and mucosal layers of the small intestine. The animals with CNS injury and induced endotoxemia were demonstrated to have the worst microvascular perfusion impairment out of all groups, suggesting a combined effect of endotoxemia and CNS injury (Burkovskiy et al., 2016).

The observed changes are in line with clinical findings, which suggest that extensive brain injury induces leukopenia and decreases lymphocyte counts in spleen, thymus and lymph nodes (Hug et al., 2009). However, not all clinical studies demonstrate this effect across all immune cell types. One particular study compared brain infarct volume as a dichotomous variable to serial T cell counts, with no significant association found all the way from baseline through day 6 (Haeusler et al., 2008). Further investigation of post brain injury reduction of immune cell counts revealed that infarct volume on 24- to 36-hour follow-up CT/MR imaging was strongly associated with reduced lymphocyte counts after adjusting for age and sex, as well as other factors (Hug et al., 2009). This clinically-observed inverse relationship between lymphocyte counts and infarct volume rightfully prompted an investigation of such phenomenon within the preclinical CIDS model, utilized in this research. Since IVM allows direct visualization of leukocyte-endothelial activity *in vivo*, it was decided to check if the leukocyte activity could be shown to be inversely related to brain injury size. It is also important to note that there are at least two major factors which actively contribute to the ability to detect immune impairment with IVM. One of these factors is the timing of observation – since a "too early" observation before the onset of CIDS would most likely not show a full immune impairment, if any at all, making it essential to pick a time point that corresponds to a measurable impairment, similar to clinical observations. The second factor that contributes to the severity of the immune impairment is the size of the CNS injury. Small infarct size could lead to a delayed onset of CIDS or completely avoid it altogether, at least in the scope of the sensitivity of methods used to measure it, such as systemic circulating cytokines. Using obtained IVM data and pairing it with brain infarct volume, the correlation between leukocyte adherence values and infarct size was found to be

quite strong (Pearson r value = -0.8952), suggesting a statistically significant inverse relationship between brain injury size and level of immune function.

In one clinical study, lymphocytopenia was most detected among the NK cell subset (Hug et al., 2009). Similarly, a preclinical study in mice revealed that CNS injury reduced NK cell counts, making them vulnerable to septicemia (Prass et al., 2003). CNS injury induced via cerebral ET-1 injections also produced a cytopenic effect. Neutrophil cells were isolated from the bone marrow 24 hours after the onset of CNS injury and counted. As expected, the neutrophil count was significantly reduced when compared to control animals. Interestingly, inhibition of CB2R with AM630 produced a reversal and increased the number of neutrophils back to the level of control animals.

Treating the animal with CIDS by administering AM630 to inhibit the activity of the CB2R was able to restore the immune response and showed a significant improvement in leukocyte adherence parameters when compared to the untreated group with CIDS. This provided the evidence that CB2R acts as an applied “brake” on immune function and that once removed, the ability of immune system to perform its function, such as fighting off basic infection is restored. While primary readouts revealed promising results, secondary readouts like microvascular perfusion did not show much improvement. Perhaps the microvascular perfusion parameter can be improved with a different regimen of cannabinoid treatment administration and possibly by extending the observation time, the positive trend for mucosal and muscle perfusion parameters can become statistically significant (Burkovskiy et al., 2016). Circulating adhesion molecules P-selectin and ICAM-1, levels of which have been dramatically decreased in animals with CIDS have also re-appeared in circulation at a much

higher level, comparable to an animal with endotoxemia but without CNS injury after AM630 administration.

Treatment with AM630 also reduced the levels of IL-10, which could explain one of the ways the immune function is improved, along with an increase in circulating levels of a strong proinflammatory cytokine TNFα. Clinical observations in patients with severe CNS injury revealed that the level of circulating IL-10 was greatly increased compared to control groups and it was also higher in patients-at-risk when compared to their healthy controls (Chang et al., 2010). It was also shown that increased IL-10 levels are strong and independently predictive indicators of severe neurological impairment in ischemic stroke patients (Chang et al., 2010). The same study also suggested that an increase in the circulating IL-10 level during the acute phase of ischemic stroke was independently predictive of major adverse clinical outcome (Chang et al., 2010). However, with the removal of anti-inflammatory "brakes" on the immune system, the danger of reactivated immune system becomes a significant threat to the vulnerable brain.

On the side of behavioural observations, animals with severe injury yielded large composite scores after behavioural evaluation. The composite score number represents the degree of neurological impairment and was tested in the model to be used as a non-invasive predictor of the brain injury size to classify the animal according to the *post-mortem* metabolic brain staining results. After comparative analysis, "neuroscore" was able to predict the extent of brain injury and should be used in future studies that involve longer term treatments and focus on survival. Neuroscore should be used as a tool to provide an early evaluation of brain injury size to place an animal in a separate class, corresponding to the level of its immune

impairment. Unfortunately, this behavioural score is effective at predicting the severity of the injury when the lesion occurs in areas of the brain that affects motor function, spatial orientation and reaction to external stimuli. When the score was used to evaluate animals with smaller injury size or with brain injury in areas that are not as evident from motor standpoint – the scoring system was not effective in predicting the severity of the injury.

4.5. Immunosuppression and the Danger of Re-activation

In general, the inflammatory response after brain injury can be broken down into three major phases (Iadecola & Anrather, 2011). The acute phase is usually described as the first few hours after the onset of the injury, associated with the dead cell "clean up" by resident microglia and macrophages, as well as infiltration of neutrophils. This phase is then followed by the subacute phase, spanning a few days after the brain injury and is usually associated with the resolution of inflammation and the beginnings of tissue repair and restoration. The final late phase is associated with the formation of glial scar, tissue repair and neurogenesis. Of course, these phases exist to help the understanding of the processes involved shortly after the brain injury. The actual picture is a lot more dynamic, with some neurogenic processes starting a lot earlier than late phase, with evidence suggesting that brain injury may induce neurogenesis in human brain via increased expression of neuronal stem and progenitor cell protein markers (W. Zheng et al., 2013). The pathogenic dynamics and overlap of these phases are what makes it so difficult to pick a relatively safe therapeutic window for targeting the CB2R and bringing the immune system back to its balanced and functional state. Figure 46 represents this delicate balance between inducing neuroprotective effects or

pushing the scale towards inflammation (both on brain and peripheral levels) via targeting the ECS with drugs outside the therapeutic window.

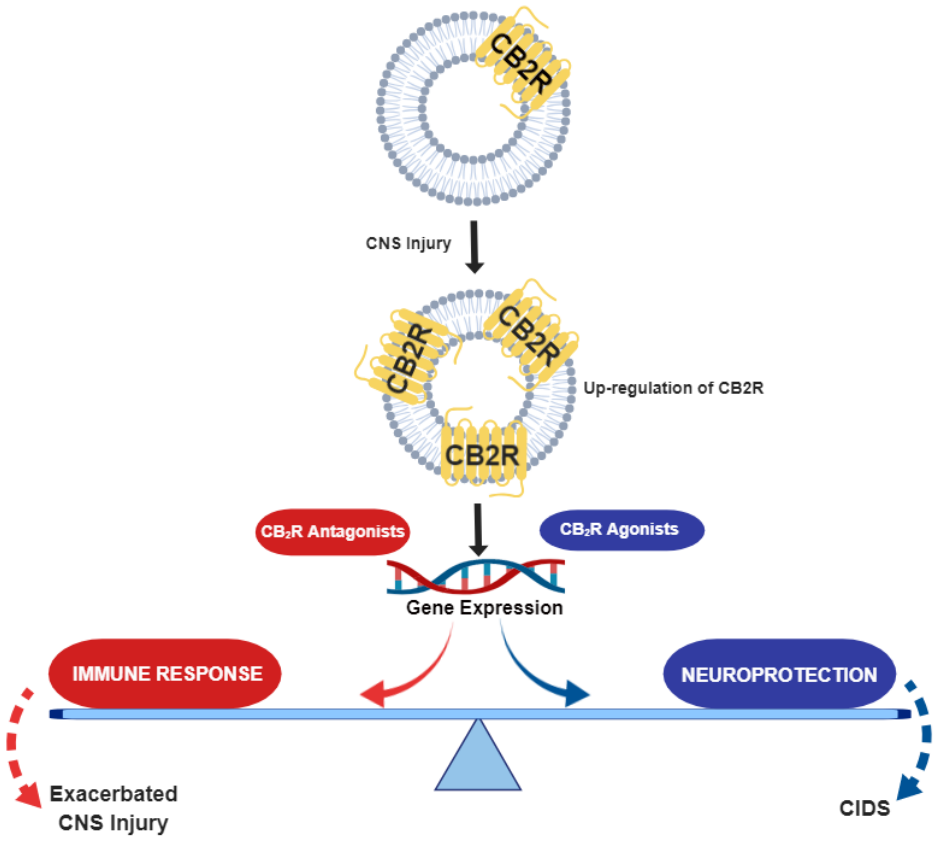

Figure 48. **The Danger of Re-activating the Immune Response.**

The diagram represents the CB2R expression changes triggered by CNS injury, which are then targeted via cannabinoid ligands. The main point is to keep the delicate balance between having an adequate immune function and sufficient amount of neuroprotection via local (CNS) shut down of immune activity. Multiple factors can tip the scales towards having a strong immune response, essentially eliminating CIDS, however this would compromise the brain and exacerbate the extent of CNS injury even more, severely affecting patient outcome. On the other hand, dysregulated immune response, as a natural protective mechanism induced by the damaged brain, compromises the ability of the body to fight off even the basic infection. It is proposed that intervention timing is one the major factors that could keep the scales balanced or at least tilt them in either direction without having a negative effect on outcome. If the CB2R is inhibited too early, it could send the immune system into an uncontrolled state and increase the size of brain injury. If the CB2R is activated too late, it could further contribute to CIDS and potentially amplify its severity.

As previously discussed, systemic immunosuppression after CNS injury is thought to be a defensive measure rolled out by the CNS itself that is meant to minimize secondary damage directly after the injury during the acute phase (Dirnagl et al., 2007; Meisel et al., 2005; Vogelgesang & Dressel, 2011). Inhibition of CB2R activity is equivalent to letting go of the "brakes" applied onto the immune system and allowing immune re-activation to take place. The brain is particularly vulnerable in post CNS injury period, as the injury itself causes a disruption in the BBB, compromising the natural barrier that normally protects the CNS from systemically circulating immune cells. Re-activation of the immune system opens the potential for inflicting further CNS damage, exacerbating neurological deficits, interrupting cellular repair mechanisms and ultimately worsening the outcome. The data obtained from experimental inhibition of CB2R with AM630 administration revealed that this approach did not exacerbate the injury in mice with hypoxia-ischemia brain injury. However, this does not remove the danger potential out of the picture. Exacerbation of brain injury could be caused by a higher degree of immune function reversal, which could be achieved with either a larger dose, a longer observation time or simply in an organism that is individually more sensitive to CB2R inhibition.

While the primary CNS damage was already established by the time AM630 has been introduced into the animal, the secondary wave of CNS damage associated with immune cell infiltration remain possible. While this is a very serious concern, it is rather difficult to assess *in vivo*, as the nature of neurological deficits and the systemic administration of LPS poses a variety of challenges associated with animal well-being and suffering. It is thus logical to switch to a model of CNS injury that is less severe, or perhaps location-specific to avoid severe damage in areas that make further investigation impossible due to animal's inability to feed and drink water. A very good candidate for the next model that can encompass all the important pathophysiological

features of brain ischemia, while allowing the researcher to control the location and the severity of the injury is the model of photothrombotic stroke, which utilizes photosensitive dye (Rose Bengal) that, upon light activation, induces endothelial damage with platelet activation and thrombosis, resulting in local blood flow interruption (Labat-gest & Tomasi, 2013).

The other, potentially dangerous, side effect of CB2R inhibition with AM630 is associated with deactivating the CB2R too early. While the CB2R K.O. is not fully equivalent to pharmacological inhibition of CB2R, the data obtained from CB2R K.O. mice demonstrated that mice with CB2R deficiency show no detectable signs of CIDS after acute CNS injury. If CB2R K.O. are subjected to experimental endotoxemia at the same time as their counterparts with a functioning CB2R, IVM revealed no changes in leukocyte adherence parameters when compared to animals without acute CNS injury. The same trends of results are observed in both collecting and postcapillary venules. While this may be seen as a positive observation, since the immunodeficiency has been either delayed or completely avoided – it is definitely not, as it reveals and emphasizes the neuroprotective importance of the "brake" mechanism applied to the immune system after CNS injury. This is supported by an increase in brain infarct volume in animals with CB2R deficiency. It is proposed that the increase in the volume of brain injury can be attributed to an exacerbated inflammatory response. In a normally functioning system, the CB2R is activated by endogenous ligands, secreted in response to the traumatic event by the resident cells of the brain, which then induce a decrease in immune activity. However, without a functioning CB2R on immune cells, the acute neutrophil and lymphocyte antigen 6 complex, locus C^{hi} monocyte recruitment are both enhanced (Kapellos et al., 2019). The same study by Kapellos et al., (2019) also revealed that the proinflammatory phenotype in CB2R deficient mice is neutrophil-intrinsic, rather than stromal cell-dependent, suggesting enhanced migration-related

transcription profile and increased adhesive phenotype. This role of CB2R in acute neutrophil mobilization to sites of injury and inflammation is what makes this receptor potentially dangerous as a drug target, since it can lead towards a pathophysiological exacerbation of injury. However, with appropriate understanding of CNS injury immune consequences timeline, as well as of CB2R expression – it may be quite possible to use CB2R as a therapeutic drug target for intervention.

In CB2R K.O. experimental group, administration of LPS in animals with CNS injury did not result in a significant reduction in the number of rolling leukocytes, which is usually observed in animals with a functioning CB2R. In animals without genetic removal of CB2R, the response to administered endotoxin results in a dramatic increase in leukocyte adhesion, paired with a decrease in the number of leukocytes exhibiting rolling behaviour. This shift is normal, as the leukocyte pool is limited in number and upon activation, the number of rolling leukocytes would decrease, as the number of leukocytes become activated, attach to vascular endothelium and begin transmigration to the site of injury or infection (Granger & Senchenkova, 2010). Interestingly, the same shift did not happen in animals without a functional CB2R, suggesting that CB2R signaling may have resulted either in an incomplete shift to adherence, or additional leukocytes have been recruited due to the lack of immunoregulatory aspect of CB2R. To further elucidate the mechanism behind this, more research needs to be done in a cell model without functional CB2R present. In addition, the time course of this phenomena needs to be studied closer to investigate if the animal without CB2R simply needs more time to exhibit the same leukocyte behaviour as observed in wild type animals.

4.6. CNS & ECS after CNS Injury

In terms of physiology, the outcome after CNS injury is largely dependent on the delicate balance between the detrimental degenerative and repair mechanisms that are both intrinsic to the brain. Of course, medical interventions, continued care, and assisted recovery all contribute to improvements in physiology, however there are other factors that may add to or subtract from the chances the patient has for a successful recovery. The level of local vasoconstriction during and after the brain injury largely dictates the severity of neurological impairment and ultimately outcome

CB2R mRNA expression was assessed in intestine and spleen by quantitative RT-PCR. It was important to examine intestinal tissue because the performed experiments showed physiological changes in intestinal microcirculation, therefore plotting the course to investigate any possible transcriptional changes which may have occurred in the intestinal tissue. Transcriptional changes in the spleen were also investigated, as the organ is highly involved in the immune response and its modulation. It is known that the spleen and tonsils tend to contain one of the highest level of CB2R expression in the body (Galiègue et al., 1995b), with changes in receptor expression expected to happen in spleen before any other organ. Although the expression changes may be quite dynamic, with quick upregulation happening right after the CNS injury event, there is still a challenge in only taking a snapshot of CB2R expression at one individual time point and potentially missing an upregulatory spike, creating the most opportune window for a cannabinoid intervention. Changes in CB2R transcription levels in splenocytes could potentially play an important role in the later stages, especially when the cells are circulating in the blood after CIDS is reduced or reversed with the cannabinoid treatment. It is thus very important to detect

any transcriptional changes in major immune modulators, as it could be a diagnostic readout of the level of immune impairment during the immunodeficient phase after a CNS injury. CB2R expression on the surface on leukocytes has been shown to change in a time-dependent manner upon LPS administration (Kasten et al., 2010). Literature does not have a consensus on what direction the expression profile of CB2R should go upon the exposure to endotoxin. One study reported that applying LPS to peritoneal macrophages resulted in a decrease of CB2R mRNA expression profile (Carlisle et al., 2002). Another study suggested a time-dependent increase in CB2R mRNA expression profile after LPS application in rat brain and mouse raw 264.7 macrophages (Mukhopadhyay et al., 2006).

4.7. Neuroprotection via ECS and Balanced Immunosuppression

ECS, which until fairly recently, was usually associated with a promise of therapeutic potential that was overshadowed by the psychoactive side effect of THC. Recent advances in medicinal chemistry and identification of active components in the cannabis plant allowed the creation of molecules that have teased out the therapeutic effect away from the psychoactive. In the field of CNS injury, synthesis of camphor-resorcinol derivates, which are classified as novel generation of CB2R selective ligands, was a recent breakthrough (Magid et al., 2019) that brought the idea of a “golden bullet” or “magic pill” for CNS injury pathophysiology closer to reality. These novel ligands display very potent binding and strong agonist properties at CB2R, with very low affinity for the CB1R and very strong anti-inflammatory characteristics (Magid et al., 2019). In experimental model of TBI, these compounds resulted in enhanced neurobehavioural recovery, inhibition of TNFα synthesis, improved synaptogenesis, and partial recovery of the cortical spinal tract (Magid et al., 2019). These results appear very promising, especially considering that

this recent study was the first study that showed neuronal reorganization as a mechanism by which the ECS, via CB2R activity, is able to promote recovery after TBI.

It would be exciting to take the latest CB2R agonist with the strongest anti-inflammatory profile and immediately introduce it to the CIDS model. However, it is important to consider the idea of balanced immunosuppression, not just as a consequence of CNS injury but as a valid, even healthy event that helps the brain protect itself. Would generating a strong or even complete immunosuppression be helpful early on? How much immunosuppression is "enough" to protect the brain, without compromising the immune status of the patient? These questions are very difficult to answer, most likely even impossible, without considering individual patient specifics and becoming familiar with patient's history.

If we examine a study from 2012 that utilized JWH-133, a CB2R agonist, which was able to reduce brain infarct size and alleviate the neurological impairment after permanent MCAO (Zarruk et al., 2012), it is fairly logical to expect that by inhibiting CB2R, these parameters would also be the one that would be compromised among the first. In the end, is treating CIDS more important if the level of neurological impairment is exacerbated and the damage is brought back? The answer, similar to the desired therapy, is somewhere in the middle.

4.8. Clinical Perspective

In general, immunomodulatory approach to treating experimental CNS injury consequences, such as CIDS, is rather difficult to translate and implement into clinical practice. There are many reasons for bench-to-bedside transition failures and it is important to identify not only the

limitations of the research presented in this dissertation, which is discussed in the next section, but also the major contributing factors to the lack of therapeutic options and negative results when transitioning preclinical findings into clinical application.

Perhaps one of the main contributing factors lies in the vast difference between human pathophysiology after CNS injury and that of experimental models. Specific details related to the models used in this research will be discussed below, but in general, a large portion of CNS injury models in scientific literature involves permanent and mechanical occlusion, which induces thromboinflammation and secondary microthrombosis (Drieu et al., 2018). Since it is not known if thromboinflammation is a universal property of human ischemic brain injury, a lot of approaches need to be re-evaluated in models without that, before transitioning into clinical trials (Drieu et al., 2018). One particular study in 2012 concluded that transient mechanical vascular occlusion models should be phased out from preclinical stroke research (Hossmann, 2012). Moreover, due to methodological limitations of preclinical models of CNS injury and the expectation to have a standardized injury, a lot of models utilize complete occlusion and full reperfusion, which is clinically present in only a small fraction of patients and is likely to influence the resulting pathophysiological parameters and treatment windows.

Other factors, such as poor study design, incorrect or irrelevant drug administration times, wrong dosage, lack of standardized methods, underpowered preclinical and clinical trials, all contribute to slow progress and lack of improvement in clinical practice. Some publications question whether the most efficacious drugs are being selected to advance to clinical trials, suggesting that selection bias is slowing down the progress in developing effective treatments (O'Collins et al., 2006). Finally, most of the risk factors associated with CNS injuries, such as stroke –

hypertension, drug and alcohol consumption, atherosclerosis, aging, stress and many others are usually not replicated in animals, which are usually healthy and young.

Relating literature to the findings of this dissertation, there are some evident issues with translating these results to bedside. First, on the level of experimental CNS injury models – the HI injury is induced via permanent occlusion and a global exposure to hypoxic conditions, whereas ET-1 model is closer to a large proportion of clinical cases with ischemic brain injury, with gradual reperfusion and not complete occlusion. HI model has innate variability in the severity and the location of the induced brain injury. Even though the HI model was difficult to standardize between groups, the model variability is certainly resembling the large spectrum of injury sizes and locations among patients, as some animals were barely affected by the surgical occlusion and hypoxia, whereas others died or had to be euthanized during the acute phase of the injury due to meeting multiple predetermined humane endpoints.

Second, the data obtained from intestinal microvasculature demonstrated the strength of the immune response to an endotoxin challenge. While LPS administration is a very effective, established and standardized way to provoke a systemic inflammatory response, it does not resemble the prevalent clinical infection in patients with CIDS, such as UTI or pneumonia. Infections acquired as a consequence of CIDS are predominantly bacterial and thus can either grow unchecked and worsen the overall condition or, if the immune system is adequately performing its task, gradually decrease in its severity. Both scenarios are not possible with LPS administration, since the endotoxin challenge is injected via weight-based dosage and evokes a continuous inflammatory response, resembling that of a septic shock, rather than a UTI or lung infection.

Third, the cannabinoid treatments, due to their highly lipophilic properties, had to be dissolved in DMSO before intravenous administration. While the solvent was effective in delivering the drug to the target, as evidenced by the leukocyte-endothelial data, it cannot be used in humans, especially at such high concentrations. While there are other available solvents and routes of cannabinoid treatment administration, these would first need to be tested and evaluated for efficacy in a preclinical CIDS model, before transitioning to clinical application.

Finally, the data presented in this work is obtained from controlled experiments where each animal went through a predetermined timeline and evaluated in its ability to have an adequate immune response after cannabinoid intervention. Ultimately, before any clinical transition takes place, the cannabinoid treatment approach needs to be evaluated on its effect on outcome. Experiments performed in a prolonged timeline that can be long enough to capture neurological improvements associated with less severe CIDS, reduced inflammation in the brain and more repair-initiated mechanisms. Post CNS injury and CIDS survival is also very important to examine experimentally, as it will provide further insight in the potential of ECS to treat CIDS.

4.9. Limitations

The research presented in this dissertation revealed the potential role of CB2R modulation as a therapeutic target for CIDS. However, there are multiple limitations in various aspects of the utilized approaches that need to be kept in mind when reading this dissertation and to be addressed in future research.

At the beginning of this project, there was no established *in vivo* CIDS model. Logically, the first step was to create the known pathophysiological conditions in an *in vivo* model. Namely, presence of a measurable CNS injury, followed by an inability or a reduced ability to have an

immune response to an invading pathogen. IVM revealed that CNS injury caused an alteration in leukocyte-endothelial interactions in both collecting and postcapillary venules of the intestinal microcirculation. The immune state is affected by the severity of the CNS injury and thus accurate identification of therapeutic window is not only necessary but may be species-specific, as well as ligand-specific. Essentially, it is reasonable to expect that there is a point where CB2R inhibition is the most effective, just like there is a point in the pathophysiological timeline of CIDS where the inhibition may be detrimental both neurologically and survival-wise. Current approach revealed that CB2R expression was not altered, however this needs to be further elucidated at various time points. While the CB2R K.O. model was quite effective in demonstrating the overall importance of CB2R signaling, as well as the timing of administering the cannabinoid treatment, it is also necessary to take the pharmacokinetic and pharmacodynamic profiles of candidate CB2R compounds, as to prevent a similar "knock out" effect via pharmacological inhibition, which could tip the scales the other way and lead to a detrimental outcome. In addition, the selected CB2R K.O. model also carries limitations that are associated with its genetic modification. The limitations that might be relevant to performed experiments with Cnr2 -/- are the following: (1) these mice have increased severity in experimental autoimmune encephalitis, (2) they also have increased microglial activation and exacerbated Huntington disease progression/excitotoxicity. Both of which suggests that there are potentially significant changes in immune function at both local and peripheral levels. As a result, it is strongly suggested to investigate the findings with a pharmacological knock out model in a wild type animal.

Presented research evaluated the effectiveness of CB2R modulation on properties of a limited pool of immune cells, such as neutrophils and molecules, such as IL-10 or IL-6. However, there

is a definite need to investigate the effect of CB2R modulation not only on other cells types, such as monocytes, macrophages and cells of the adaptive immune system, but also on the effect over time, which may be very dynamic and heavily contribute to the final outcomes. These experiments would require cell type characterization and evaluation of drug response at different time points, making it very difficult to contain everything to a single *in vivo* model, yet not having the full complexity of CIDS pathophysiology in an *in vitro* model. There is evidence suggesting that zebrafish may serve as an effective model evaluate the effectiveness of CB2R drugs and see the direct effect of labelled immune cells via transgenic zebrafish lines, allowing visualization and over-time observation of immune cell activity. Not only zebrafish exhibit similar post CNS injury symptoms, they also express both CB1R and CB2R, along with other major endocannabinoid-related genes (L. Ellis, 2018).

Severity of the CNS injury is not only complicated from the standpoint of CIDS onset but also in the level of BBB disruption, affecting the distribution of highly lipophilic cannabinoid drugs across the CNS and potentially contributing to non-CB2R-related off-target side effects. There is evidence suggesting that CB2R activation may reduce BBB damage in intracerebral hemorrhage rat model (L. Li et al., 2018). This evidence opens the door to the notion that the proposed cannabinoid interventions need to be evaluated at multiple points – ability to reduce the initial injury size, the potential to prevent secondary damage and edema and the ability to act as an agent to restore the immune function after CIDS is established.

Proposed approaches for both early activation and late inhibition of CB2R are not founded on obtained clinical cannabinoid use data that would normally be used to suggest dosage and administration guidelines, as this data is simply not available – thus making the process of

finding the best pharmacological ligand, along with the most appropriate dosage should be prioritized for future research. The origin of the CNS injury is also important to be representative of the patient population – traumatic brain injury, spinal cord injury, and neonatal hypoxia are all different not only in the method of injury induction and degree of CIDS severity but also could potentially affect the effectiveness of the cannabinoid intervention. This becomes more complicated, since on the clinical side, there are essentially unlimited possibilities of patient outcomes, with both CNS injury specifics and patients' response to the CNS injury being on a variable continuum, which is quite different from the consistency of a preclinical model, where a certain proportion of pathophysiology may not even be exhibited or over-represented (Enlimomab Acute Stroke Trial Investigators, 2001).

Microvascular perfusion is one of the crucial indicators of general physiological condition of the vasculature. The utilized endotoxemia model was very effective at reducing the capillary perfusion parameters primarily due to following factors: leukocyte plugging of the vessels, stiffness of erythrocytes and leukocytes, endothelial cell swelling, increased blood viscosity, disseminated intravascular coagulation and tissue edema. While the cannabinoid treatment was able to restore some of the measured immune parameters, not a lot of improvement was observed within the vascular perfusion parameter. This could be attributed to the timing of the experimental observation or the fact that systemic LPS administration causes a very strong immunoactivation, without the room for improvement. As such, a less severe immunochallenge would potentially allow more improvement in microvascular perfusion parameters, displaying a better trend. While all possible measures were taken to minimize the exposure of fluorescent dyes to light, another factor that could have affected the measured perfusion parameters would

be the bleaching of the dye used, as it relies on effective excitation by the light source, for both leukocyte tagging and blood perfusion measurements.

Older animals with CNS injury should also be evaluated for both early and late cannabinoid treatment approaches. Patients with CNS injury that are statistically likely to be at risk of fatal infections are likely to be older individuals. In addition to this, increasing evidence has demonstrated significant sex differences in the pathophysiology and outcome after acute CNS injury, thus making the sex aspect of CIDS onset and treatment response an important next step for further investigation. It is important to note that a lot of evidence appears to suggest a multifactorial mechanism by which estrogen and progesterone provide neuroprotection, therefore the type and concentration of the hormones need to be kept in consideration in future models. In addition, there are known sex differences in the ECS of animals, with female rodents being more sensitive than males to effects of cannabinoids, with most of the response differences attributed to activational and organizational effects of the gonadal hormones (Craft et al., 2013). That is not the only known sex difference that is applicable to this field, as stroke remains in the top three causes of death in women, while most of the preclinical work is being conducted in male animals (Spychala et al., 2017). There are also other lines of evidence suggesting variations between sex in microglia, dendritic cells, neutrophils and other lymphocytes, potentially affecting and drawing more differences in sex-associated pathophysiological consequences of CNS injury (Felger et al., 2010; F. Liu & McCullough, 2011). An important distinction is to be made here, as sex differences do not only convey differences on physiological level that are specific to each sex but can also potentially act as a way to provide deeper understanding of pathophysiology of CIDS and even provide a possible treatment approach, utilizing the sex-specific physiological parameters that yield neuroprotective outcomes.

While my dissertation proposes a significant role for the involvement of endogenous IL-10 that was affected either directly or indirectly after the cannabinoid antagonist intervention, it is important to remain critical to the observed results. This project did not examine the time course of circulating IL-10 levels and it did not examine the long-term outcome, so the findings need to be held in perspective when it comes to interpretation of the results, as well as in the proposed significance of increased IL-10 levels in the cannabinoid treatment group. While a good number of pre-clinical studies have shown strong beneficial effects with adopting an anti-inflammatory therapeutic approach in the treatment of ischemic stroke – clinical studies have painted a very different picture with a number of studies reporting no benefit or even worsened outcome in ischemic stroke patients after anti-inflammatory intervention (Fouda et al., 2013). The intricate network of immunoregulatory pathways and mechanisms involved in modulating the action and availability of endogenous immunoregulatory cytokines makes the therapeutic potential specifically targeting a single parameter rather limited and perhaps too simplistic and ineffective to circumnavigate the pathophysiological cascades and consequences after CNS injury. It is therefore highly beneficial that the cannabinoid intervention proposed in this project taps into ECS activity, which in turn may exert its action through a multitude of pathways, involving endogenous ligands and induce the desired immunomodulatory effects.

Finally, one of the limitations is the possibility of experimenter bias. The same person carried out the surgical techniques, provided recovery support, monitored and recorded behavioural parameters, analysed the recorded videos, quantified the results – the experimenter was aware which experimental group was being worked on. Complete double blinded design was not possible with a single experimenter and even though a lot of effort was made to remain objective

and to mask the source of video files before analysis, it was simply not possible to eliminate all potential bias.

4.10. Future Directions

There are multiple directions that need to be extensively pursued in order to create a strong preclinical foundation and basic scientific understanding of all the involved components and systems. As such, studies should focus on elucidation of the major contributing pathways, which could lead to an improvement in selection of an appropriate ligand or a combination of. Intestine as an organ and its environment are not only linked to the activity and physiological function of CNS but can have profound effects through physiological contributions of the microbiota, regulation of intestinal immune barrier and altered activity of nerves in periphery (Houser & Tansey, 2017). There is an emerging body of evidence suggesting that changes in composition of intestinal bacterial populations are associated with a range of neurologic and neurodevelopment disorders (Dinan & Cryan, 2017). Thus, to evaluate and develop future novel therapeutic approaches, as well as to elucidate the pathways associated with the impairment of the gut after CNS injury, it is important to keep in mind the complicated link between intestinal microcirculation and CNS injury in upcoming preclinical research.

It is essential to investigate various time points throughout the onset of CNS injury to the establishment of CIDS to identify the optimal treatment window for the proposed early and late CB2R modulation therapies. The models should be optimized for maximum clinical relevance, not only in the type and severity of CNS injury but also in how the immune system is challenged and evaluated. Moreover, the ligands themselves need to be re-evaluated to ensure that the level

of CB2R activation is sufficient, yet not abnormal, to not to induce any unwanted side-effects through off target CB1R binding or prolonged CB2R activity. Utilizing endogenous enzymes and ligands, as well as enhancing the desired activity of CB2R via positive or negative allosteric modulation would also be an important direction to explore. Finally, it would be very beneficial if CIDS, both as a neuroprotective and a pathophysiological phenomenon, was to be standardized in literature, with a set of diagnostic parameters that can be used to start generating treatment approaches on the preclinical level that could be prepared for clinical use and have an actual impact on patient care and outcome.

4.11. Conclusion

The work in this dissertation established and demonstrated that experimental ischemic CNS injury induced either surgically or chemically via intracerebral ET-1 injection has a detrimental impact on murine immune function, as evidence by impairment in leukocyte-endothelial interactions within intestinal microvasculature. CNS injury also reduces the number of neutrophils in the bone marrow, as well as causes splenic atrophy. Circulating plasma cytokine levels are altered in the established CIDS models and generally indicate an impaired immune response to endotoxin challenge. Intravital microscopy has revealed that CB2R-related modulation of leukocyte activation is involved in the impaired immune response following CNS injury. Pharmacological manipulation of the CB2R produced promising results – early CB2R activation with HU308 reduced brain injury size and ameliorated the immune function at 24-hour time point, whereas late CB2R inhibition with AM630 reduced the severity of immune suppression at 24-hour time point. In conclusion, CB2R modulation presents a viable

pharmacological target for intervention to either prevent CIDS in acute CNS injury by reducing the initial damage to the brain or to directly improve the immune activity in cases where CIDS is already physiologically established. While the obtained data is promising, pathway elucidation is critical and further investigation of the effect of CB2R modulation on long term neurological outcome and survival is necessary before considering transferring any of these findings to bedside.

References

Figures 1, 2, 3, 4, 5 and 48 have been created with the help of BioRender software under 'personal academic use' license. (BioRender 2019, Toronto, ON).

Abbas, A., Lichtman, A., & Pillai, S. (2014). *Basic Immunology: Functions and Disorders of the Immune System* (4th ed.). Elsevier Health Sciences.

Adams, D. O., & Hamilton, T. A. (1984). The Cell Biology of Macrophage Activation. *Annual Review of Immunology*, *2*(1), 283–318.

Ajmo, C. T., Vernon, D. O. L., Collier, L., Hall, A. A., Garbuzova-Davis, S., Willing, A., & Pennypacker, K. R. (2008). The spleen contributes to stroke-induced neurodegeneration. *Journal of Neuroscience Research*, *86*(10), 2227–2234.

Akira, S., & Takeda, K. (2004). Toll-Like Receptor Signalling. *Nature reviews. Immunology*, *4*(July).

Albers, G. W., Marks, M. P., Kemp, S., Christensen, S., Tsai, J. P., Ortega-Gutierrez, S., McTaggart, R. A., Torbey, M. T., Kim-Tenser, M., Leslie-Mazwi, T., Sarraj, A., Kasner, S. E., Ansari, S. A., Yeatts, S. D., Hamilton, S., Mlynash, M., Heit, J. J., Zaharchuk, G., Kim, S., Carrozzella, J., Palesch, Y. Y., Demchuk, A. M., Bammer, R., Lavori, P. W., Broderick, J. P., & Lansberg, M. G. (2018). Thrombectomy for Stroke at 6 to 16 Hours with Selection by Perfusion Imaging. *New England Journal of Medicine*, *378*(8), 708–718.

Albertsson, A.-M., Bi, D., Duan, L., Zhang, X., Leavenworth, J. W., Qiao, L., Zhu, C., Cardell, S., Cantor, H., Hagberg, H., Mallard, C., & Wang, X. (2014). The immune response after hypoxia-ischemia in a mouse model of preterm brain injury. *Journal of Neuroinflammation*, *11*(1), 153.

Amiri-Nikpour, M. R., Nazarbaghi, S., Hamdi-Holasou, M., & Rezaei, Y. (2015). An open-label evaluator-blinded clinical study of minocycline neuroprotection in ischemic stroke: gender-dependent effect. *Acta Neurologica Scandinavica*, *131*(1), 45–50.

Ansari, S., Azari, H., Caldwell, K. J., Regenhardt, R. W., Hedna, V. S., Waters, M. F., Hoh, B. L., & Mecca, A. P. (2013). Endothelin-1 Induced Middle Cerebral Artery Occlusion Model for Ischemic Stroke with Laser Doppler Flowmetry Guidance in Rat. *Journal of Visualized Experiments*, (72).

Arévalo-Martín, a, García-Ovejero, D., Gómez, O., Rubio-Araiz, A., Navarro-Galve, B., Guaza, C., Molina-Holgado, E., & Molina-Holgado, F. (2008). CB2 cannabinoid receptors as an emerging target for demyelinating diseases : from neuroimmune interactions to cell replacement strategies. *British journal of pharmacology*, *153*(2), 216–25.

Atakan, Z. (2012). Cannabis, a complex plant: different compounds and different effects on individuals. *Therapeutic advances in psychopharmacology*, *2*(6), 241–54.

Baggiolini, M., Dewald, B., & Moser, B. (1997). Human Chemokines: An Update. *Annual Review of Immunology*, *15*(1), 675–705.

Bansal, V., Costantini, T., Kroll, L., Peterson, C., Loomis, W., Eliceiri, B., Baird, A., Wolf, P., & Coimbra, R. (2009). Traumatic brain injury and intestinal dysfunction: uncovering the neuro-enteric axis. *Journal of neurotrauma*, *26*(8), 1353–9.

Barczyk, M., Carracedo, S., & Gullberg, D. (2010). Integrins. *Cell and Tissue Research*, *339*(1), 269–280.

Barrat, F. J., Cua, D. J., Boonstra, A., Richards, D. F., Crain, C., Savelkoul, H. F., de Waal-Malefyt, R., Coffman, R. L., Hawrylowicz, C. M., & O'Garra, A. (2002). In vitro generation of interleukin 10-producing regulatory CD4(+) T cells is induced by immunosuppressive drugs and inhibited by T helper type 1 (Th1)- and Th2-inducing cytokines. *The Journal of experimental medicine*, *195*(5), 603–16.

Barreiro, O., Martin, P., Gonzalez-Amaro, R., & Sanchez-Madrid, F. (2010). Molecular cues guiding inflammatory responses. *Cardiovascular Research*, *86*(2), 174–182.

Barreto, A. D. (2011). Intravenous Thrombolytics for Ischemic Stroke. *Neurotherapeutics*, *8*(3), 388–399.

Basu, S., & Dittel, B. N. (2011). Unraveling the complexities of cannabinoid receptor 2 (CB2) immune regulation in health and disease. *Immunologic research*, *51*(1), 26–38.

Battista, N., Di Tommaso, M., Bari, M., & Maccarrone, M. (2012). The endocannabinoid system: an overview. *Frontiers in behavioral neuroscience*, *6*, 9.

Benveniste, E. N. (1997a). Role of macrophages/microglia in multiple sclerosis and experimental allergic encephalomyelitis. *Journal of molecular medicine (Berlin, Germany)*, *75*(3), 165–73.

Benveniste, E. N. (1997b). Cytokines: influence on glial cell gene expression and function. *Chemical immunology*, *69*, 31–75.

Bergamaschi, M. M., Queiroz, R. H. C., Zuardi, A. W., & Crippa, J. A. S. (2011). Safety and side effects of cannabidiol, a Cannabis sativa constituent. *Current drug safety*, *6*(4), 237–49.

Bevilacqua, M., & Gimbrone, M. (1987). Inducible Endothelial Functions in Inflammation and Coagulation. *Seminars in Thrombosis and Hemostasis*, *13*(04), 425–433.

Bianchi, M. E. (2007). DAMPs, PAMPs and alarmins: all we need to know about danger. *Journal of Leukocyte Biology*, *81*(1), 1–5.

Bilkei-Gorzo, A. (2012). The endocannabinoid system in normal and pathological brain ageing. *Philosophical Transactions of the Royal Society B: Biological Sciences*, *367*(1607), 3326–3341.

Birnbaum, J., Lehmann, C., Stauss, H. M., Weber, M., Georgiew, A., Lorenz, B., Pulletz, S., Gründling, M., Pavlovic, D., Wendt, M., & Kox, W. J. (2003). Sympathetic modulation of intestinal microvascular blood flow oscillations in experimental endotoxemia. *Clinical hemorheology and microcirculation*, *28*(4), 209–20.

Bonilla, F. A., & Oettgen, H. C. (2010). Adaptive immunity. *Journal of Allergy and Clinical Immunology*, *125*(2), S33–S40.

Borish, L. C., & Steinke, J. W. (2003). 2. Cytokines and chemokines. *The Journal of allergy and clinical immunology*, *111*(2 Suppl), S460-75.

Borovikova, L. V., Ivanova, S., Zhang, M., Yang, H., Botchkina, G. I., Watkins, L. R., Wang, H., Abumrad, N., Eaton, J. W., & Tracey, K. J. (2000). Vagus nerve stimulation attenuates the systemic inflammatory response to endotoxin. *Nature*, *405*(6785), 458–462.

Bosier, B., Muccioli, G. G., Hermans, E., & Lambert, D. M. (2010). Functionally selective cannabinoid receptor signalling: therapeutic implications and opportunities. *Biochemical pharmacology*, *80*(1), 1–12.

Bouaboula, M., Poinot-Chazel, C., Marchand, J., Canat, X., Bourrié, B., Rinaldi-Carmona, M., Calandra, B., Le Fur, G., & Casellas, P. (1996). Signaling pathway associated with stimulation of CB2 peripheral cannabinoid receptor. Involvement of both mitogen-activated protein kinase and induction of Krox-24 expression. *European journal of biochemistry*, *237*(3), 704–11.

Braun, M., Khan, Z. T., Khan, M. B., Kumar, M., Ward, A., Achyut, B. R., Arbab, A. S., Hess, D. C., Hoda, M. N., Baban, B., Dhandapani, K. M., & Vaibhav, K. (2018). Selective activation of cannabinoid receptor-2 reduces neuroinflammation after traumatic brain injury via alternative macrophage polarization. *Brain, Behavior, and Immunity*, *68*, 224–237.

Brommer, B., Engel, O., Kopp, M. A., Watzlawick, R., Müller, S., Prüss, H., Chen, Y., DeVivo, M. J., Finkenstaedt, F. W., Dirnagl, U., Liebscher, T., Meisel, A., & Schwab, J. M. (2016). Spinal cord injury-induced immune deficiency syndrome enhances infection susceptibility dependent on lesion level. *Brain*, *139*(3), 692–707.

Brown, D. L., Boden-Albala, B., Langa, K. M., Lisabeth, L. D., Fair, M., Smith, M. A., Sacco, R. L., Morgenstern, L. B., Kwiatkowski, T. G., Frankel, M., Brott, T. G., & Walker, M. D. (2006). Projected costs of ischemic stroke in the United States. *Neurology*, *67*(8), 1390–5.

Burkovskiy, I., Zhou, J., & Lehmann, C. (2016). Experimental cannabinoid 2 receptor inhibition in CNS injury-induced immunodeficiency syndrome. *Microcirculation (New York, N.Y. : 1994)*, *23*(4), 283–292.

Cabral, G. A., Harmon, K. N., & Carlisle, S. J. (2001). Cannabinoid-mediated Inhibition of Inducible Nitric Oxide Production by Rat Microglial Cells: Evidence for CB1 Receptor Participation. In *Neuroimmune Circuits, Drugs of Abuse, and Infectious Diseases* (Vol. 493, pp. 207–214). Boston: Kluwer Academic Publishers.

Capettini, L. S. A., Savergnini, S. Q., da Silva, R. F., Stergiopulos, N., Santos, R. A. S., Mach, F., & Montecucco, F. (2012). Update on the Role of Cannabinoid Receptors after Ischemic Stroke. *Mediators of Inflammation*, *2012*, 1–8.

Cardozo Júnior, L. C. M., & Silva, R. R. da. (2014). Sepsis in intensive care unit patients with traumatic brain injury: factors associated with higher mortality. *Revista Brasileira de terapia intensiva*, *26*(2), 148–54.

Carlisle, S. J., Marciano-Cabral, F., Staab, A., Ludwick, C., & Cabral, G. A. (2002). Differential expression of the CB2 cannabinoid receptor by rodent macrophages and macrophage-like cells in relation to cell activation. *International immunopharmacology*, *2*(1), 69–82.

Carnaby, G., Hankey, G. J., & Pizzi, J. (2006). Behavioural intervention for dysphagia in acute stroke: a randomised controlled trial. *The Lancet Neurology*, *5*(1), 31–37.

Cazzadori, A., Di Perri, G., Vento, S., Bonora, S., Fendt, D., Rossi, M., Lanzafame, M., Mirandola, F., & Concia, E. (1997). Aetiology of pneumonia following isolated closed head injury. *Respiratory medicine*, *91*(4), 193–9.

Chan, P. H. (2001). Reactive Oxygen Radicals in Signaling and Damage in the Ischemic Brain. *Journal of Cerebral Blood Flow & Metabolism*, *21*(1), 2–14.

Chanda, D., Kim, D.-K., Li, T., Kim, Y.-H., Koo, S.-H., Lee, C.-H., Chiang, J. Y. L., & Choi, H.-S. (2011). Cannabinoid receptor type 1 (CB1R) signaling regulates hepatic gluconeogenesis via induction of endoplasmic reticulum-bound transcription factor cAMP-responsive element-binding protein H (CREBH) in primary hepatocytes. *The Journal of biological chemistry*, *286*(32), 27971–9.

Chang, L.-T., Yuen, C.-M., Liou, C.-W., Lu, C.-H., Chang, W.-N., Youssef, A. a, & Yip, H.-K. (2010). Link between interleukin-10 level and outcome after ischemic stroke. *Neuroimmunomodulation*, *17*(4), 223–8.

Chaplin, D. D. (2010). Overview of the immune response. *The Journal of allergy and clinical immunology*, *125*(2 Suppl 2), S3-23.

Charo, I. F., & Ransohoff, R. M. (2006). The Many Roles of Chemokines and Chemokine Receptors in Inflammation. *New England Journal of Medicine*, *354*(6), 610–621.

Chavan, S. S., Pavlov, V. A., & Tracey, K. J. (2017). Mechanisms and Therapeutic Relevance of Neuro-immune Communication. *Immunity*, *46*(6), 927–942.

Chen, Y.-J., Hsieh, M.-Y., Chang, M. Y., Chen, H.-C., Jan, M.-S., Maa, M.-C., & Leu, T.-H. (2012). Eps8 protein facilitates phagocytosis by increasing TLR4-MyD88 protein interaction in lipopolysaccharide-stimulated macrophages. *The Journal of biological chemistry*, *287*(22), 18806–19.

Cheng, N. T., & Kim, A. S. (2015). Intravenous Thrombolysis for Acute Ischemic Stroke Within 3 Hours Versus Between 3 and 4.5 Hours of Symptom Onset. *The Neurohospitalist*, *5*(3), 101–9.

Chevaleyre, V., Takahashi, K. A., & Castillo, P. E. (2006). ENDOCANNABINOID-MEDIATED SYNAPTIC PLASTICITY IN THE CNS. *Annual Review of Neuroscience*, *29*(1), 37–76.

Choi, I.-Y., Ju, C., Anthony Jalin, A. M. A., Lee, D. I., Prather, P. L., & Kim, W.-K. (2013). Activation of Cannabinoid CB2 Receptor–Mediated AMPK/CREB Pathway Reduces Cerebral Ischemic Injury. *The American Journal of Pathology*, *182*(3), 928–939.

Collins, T., Read, M. A., Neish, A. S., Whitley, M. Z., Thanos, D., & Maniatis, T. (1995). Transcriptional regulation of endothelial cell adhesion molecules: NF-kappa B and cytokine-inducible enhancers. *FASEB journal : official publication of the Federation of American Societies for Experimental Biology*, *9*(10), 899–909.

Compton, D. R., Rice, K. C., De Costa, B. R., Razdan, R. K., Melvin, L. S., Johnson, M. R., & Martin, B. R. (1993). Cannabinoid structure-activity relationships: correlation of receptor binding and in vivo activities. *The Journal of pharmacology and experimental therapeutics*, *265*(1), 218–26.

Contartese, A., Valoti, M., Corelli, F., Pasquini, S., Mugnaini, C., Pessina, F., Aldinucci, C., Sgaragli, G., & Frosini, M. (2012). A novel CB2 agonist, COR167, potently protects rat brain cortical slices against OGD and reperfusion injury. *Pharmacological Research*, *66*(6), 555–563.

Craft, R. M., Marusich, J. A., & Wiley, J. L. (2013). Sex differences in cannabinoid pharmacology: a reflection of differences in the endocannabinoid system? *Life sciences*, *92*(8–9), 476–81.

Cripps, R. A., Lee, B. B., Wing, P., Weerts, E., Mackay, J., & Brown, D. (2011). A global map for traumatic spinal cord injury epidemiology: towards a living data repository for injury prevention. *Spinal Cord*, *49*(4), 493–501.

Cruse, J. M., Lewis, R. E., Bishop, G. R., Kliesch, W. F., & Gaitan, E. (1992). Neuroendocrine-immune interactions associated with loss and restoration of immune system function in spinal cord injury and stroke patients. *Immunologic research*, *11*(2), 104–16.

D'Andrea, A. (1993). Interleukin 10 (IL-10) inhibits human lymphocyte interferon gamma- production by suppressing natural killer cell stimulatory factor/IL-12 synthesis in accessory cells. *Journal of Experimental Medicine*, *178*(3), 1041–1048.

De Backer, D., Creteur, J., Preiser, J.-C., Dubois, M.-J., & Vincent, J.-L. (2002). Microvascular Blood Flow Is Altered in Patients with Sepsis. *American Journal of Respiratory and Critical Care Medicine*, *166*(1), 98–104.

De Petrocellis, L., & Di Marzo, V. (2009). An introduction to the endocannabinoid system: from the early to the latest concepts. *Best Practice & Research Clinical Endocrinology & Metabolism*, *23*, 1–15.

Degenhardt, L., Coffey, C., Carlin, J. B., Swift, W., Moore, E., & Patton, G. C. (2010). Outcomes of occasional cannabis use in adolescence: 10-year follow-up study in Victoria, Australia. *British Journal of Psychiatry*, *196*(04), 290–295.

Demaerschalk, B. M., Hwang, H.-M., & Leung, G. (2010). US cost burden of ischemic stroke: a systematic literature review. *The American journal of managed care*, *16*(7), 525–33.

Dempsey, P. W., Vaidya, S. A., & Cheng, G. (2003). The Art of War: Innate and adaptive immune responses. *Cellular and Molecular Life Sciences (CMLS)*, *60*(12), 2604–2621.

Denes, A., Pinteaux, E., Rothwell, N. J., & Allan, S. M. (2011). Interleukin-1 and stroke: biomarker, harbinger of damage, and therapeutic target. *Cerebrovascular diseases (Basel, Switzerland)*, *32*(6), 517–27.

Deng, M., Scott, M. J., Loughran, P., Gibson, G., Sodhi, C., Watkins, S., Hackam, D., & Billiar, T. R. (2013). Lipopolysaccharide Clearance, Bacterial Clearance, and Systemic Inflammatory Responses Are Regulated by Cell Type-Specific Functions of TLR4 during Sepsis. *The Journal of Immunology*, *190*(10), 5152–5160.

Devane, W. A., Dysarz, F. A., Johnson, M. R., Melvin, L. S., & Howlett, A. C. (1988). Determination and characterization of a cannabinoid receptor in rat brain. *Molecular pharmacology*, *34*(5), 605–13.

Devane, W. A., Hanus, L., Breuer, A., Pertwee, R. G., Stevenson, L. A., Griffin, G., Gibson, D., Mandelbaum, A., Etinger, A., & Mechoulam, R. (1992). Isolation and structure of a brain constituent that binds to the cannabinoid receptor. *Science (New York, N.Y.)*, *258*(5090), 1946–9.

Dhopeshwarkar, A., & Mackie, K. (2014). CB2 Cannabinoid Receptors as a Therapeutic Target--What Does the Future Hold? *Molecular Pharmacology*, *86*(4), 430–437.

Di Marzo, V., Melck, D., Bisogno, T., & De Petrocellis, L. (1998). Endocannabinoids: endogenous cannabinoid receptor ligands with neuromodulatory action. *Trends in neurosciences*, *21*(12), 521–8.

Dickson, D. W., Mattiace, L. A., Kure, K., Hutchins, K., Lyman, W. D., & Brosnan, C. F. (1991). Microglia in human disease, with an emphasis on acquired immune deficiency syndrome. *Laboratory investigation; a journal of technical methods and pathology*, *64*(2), 135–56.

Dinan, T. G., & Cryan, J. F. (2017). Gut instincts: microbiota as a key regulator of brain development, ageing and neurodegeneration. *The Journal of Physiology*, *595*(2), 489–503.

Dinarello, C. A., Simon, A., & van der Meer, J. W. M. (2012). Treating inflammation by blocking interleukin-1 in a broad spectrum of diseases. *Nature reviews. Drug discovery*, *11*(8), 633–52.

Ding, Y., Li, J., Rafols, J. A., Phillis, J. W., & Diaz, F. G. (2002). Prereperfusion saline infusion into ischemic territory reduces inflammatory injury after transient middle cerebral artery occlusion in rats. *Stroke*, *33*(10), 2492–8.

Dirnagl, U., Klehmet, J., Braun, J. S., Harms, H., Meisel, C., Ziemssen, T., Prass, K., & Meisel, A. (2007). Stroke-induced immunodepression: experimental evidence and clinical relevance. *Stroke; a journal of cerebral circulation*, *38*(2 Suppl), 770–3.

Drieu, A., Levard, D., Vivien, D., & Rubio, M. (2018). Anti-inflammatory treatments for stroke: from bench to bedside. *Therapeutic Advances in Neurological Disorders*, *11*, 175628641878985.

Duvernoy, H. M., Delon, S., & Vannson, J. L. (1981). Cortical blood vessels of the human brain. *Brain research bulletin*, *7*(5), 519–79.

Elliott, M. B., Tuma, R. F., Amenta, P. S., Barbe, M. F., & Jallo, J. I. (2011). Acute Effects of a Selective Cannabinoid-2 Receptor Agonist on Neuroinflammation in a Model of Traumatic Brain Injury. *Journal of Neurotrauma*, *28*(6), 973–981.

Ellis, C. G., Jagger, J., & Sharpe, M. (2005). The microcirculation as a functional system. *Critical Care*, *9*(Suppl 4), S3.

Ellis, L. (2018). Zebrafish as a High-Throughput In Vivo Model for Testing the Bioactivity of Cannabinoids. In *Recent Advances in Cannabinoid Research [Working Title]*. IntechOpen.

Enlimomab Acute Stroke Trial Investigators. (2001). Use of anti-ICAM-1 therapy in ischemic stroke: results of the Enlimomab Acute Stroke Trial. *Neurology*, *57*(8), 1428–34.

Evans, R., Patzak, I., Svensson, L., De Filippo, K., Jones, K., McDowall, A., & Hogg, N. (2009). Integrins in immunity. *Journal of cell science*, *122*(Pt 2), 215–25.

Faulkner, J. R., Herrmann, J. E., Woo, M. J., Tansey, K. E., Doan, N. B., & Sofroniew, M. V. (2004). Reactive Astrocytes Protect Tissue and Preserve Function after Spinal Cord Injury. *Journal of Neuroscience*, *24*(9), 2143–2155.

Feigin, V. L., Krishnamurthi, R. V., Parmar, P., Norrving, B., Mensah, G. A., Bennett, D. A., Barker-Collo, S., Moran, A. E., Sacco, R. L., Truelsen, T., Davis, S., Pandian, J. D., Naghavi, M., Forouzanfar, M. H., Nguyen, G., Johnson, C. O., Vos, T., Meretoja, A., Murray, C. J. L., Roth, G. A., GBD 2013 Writing Group, & GBD 2013 Stroke Panel Experts Group. (2015). Update on the Global Burden of Ischemic and Hemorrhagic Stroke in 1990-2013: The GBD 2013 Study. *Neuroepidemiology*, *45*(3), 161–176.

Felder, C. C., Joyce, K. E., Briley, E. M., Mansouri, J., Mackie, K., Blond, O., Lai, Y., Ma, A. L., & Mitchell, R. L. (1995). Comparison of the pharmacology and signal transduction of the human cannabinoid CB1 and CB2 receptors. *Molecular pharmacology*, *48*(3), 443–50.

Felger, J. C., Abe, T., Kaunzner, U. W., Gottfried-Blackmore, A., Gal-Toth, J., McEwen, B. S., Iadecola, C., & Bulloch, K. (2010). Brain dendritic cells in ischemic stroke: Time course, activation state, and origin. *Brain, Behavior, and Immunity*, *24*(5), 724–737.

Fernández-López, D., Faustino, J., Derugin, N., Wendland, M., Lizasoain, I., Moro, M. A., & Vexler, Z. S. (2012). Reduced infarct size and accumulation of microglia in rats treated with WIN 55,212-2 after neonatal stroke. *Neuroscience*, *207*, 307–315.

Fernández-López, David, Pazos, M. R., Tolón, R. M., Moro, M. A., Romero, J., Lizasoain, I., & Martínez-Orgado, J. (2007). The cannabinoid agonist WIN55212 reduces brain damage in an in vivo model of hypoxic-ischemic encephalopathy in newborn rats. *Pediatric research*, *62*(3), 255–60.

Ferrero, E., Zocchi, M. R., Magni, E., Panzeri, M. C., Curnis, F., Rugarli, C., Ferrero, M. E., & Corti, A. (2001). Roles of tumor necrosis factor p55 and p75 receptors in TNF-α-induced vascular permeability. *American Journal of Physiology-Cell Physiology*, *281*(4), C1173–C1179.

Filomeni, G., Piccirillo, S., Rotilio, G., & Ciriolo, M. R. (2012). p38MAPK and ERK1/2 dictate cell death/survival response to different pro-oxidant stimuli via p53 and Nrf2 in neuroblastoma cells SH-SY5Y. *Biochemical Pharmacology*, *83*(10), 1349–1357.

Fouda, A. Y., Kozak, A., Alhusban, A., Switzer, J. a, & Fagan, S. C. (2013). Anti-inflammatory IL-10 is upregulated in both hemispheres after experimental ischemic stroke: Hypertension blunts the response. *Experimental & translational stroke medicine*, *5*(1), 12.

Franklin, A., & Stella, N. (2003). Arachidonylcyclopropylamide increases microglial cell migration through cannabinoid CB2 and abnormal-cannabidiol-sensitive receptors. *European journal of pharmacology*, *474*(2–3), 195–8.

Franklin, K. B. J., & Paxinos, G. (2008). *The mouse brain in stereotaxic coordinates*. Boston.

Fu, Y., Liu, Q., Anrather, J., & Shi, F.-D. (2015). Immune interventions in stroke. *Nature Reviews Neurology*, *11*(9), 524–535.

Furlan, J. C., Noonan, V., Singh, A., & Fehlings, M. G. (2011). Assessment of Impairment in Patients with Acute Traumatic Spinal Cord Injury: A Systematic Review of the Literature. *Journal of Neurotrauma*, *28*(8), 1445–1477.

Galiègue, S., Mary, S., Marchand, J., Dussossoy, D., Carrière, D., Carayon, P., Bouaboula, M., Shire, D., Le Fur, G., & Casellas, P. (1995a). Expression of central and peripheral cannabinoid receptors in human immune tissues and leukocyte subpopulations. *European journal of biochemistry / FEBS*, *232*(1), 54–61.

Galiègue, S., Mary, S., Marchand, J., Dussossoy, D., Carrière, D., Carayon, P., Bouaboula, M., Shire, D., Le Fur, G., & Casellas, P. (1995b). Expression of central and peripheral cannabinoid receptors in human immune tissues and leukocyte subpopulations. *European journal of biochemistry*, *232*(1), 54–61.

Gallily, R., Breuer, A., & Mechoulam, R. (2000). 2-Arachidonylglycerol, an endogenous cannabinoid, inhibits tumor necrosis factor-alpha production in murine macrophages, and in mice. *European journal of pharmacology*, *406*(1), R5-7.

Gaoni, Y., & Mechoulam, R. (1964). Isolation, Structure, and Partial Synthesis of an Active Constituent of Hashish. *Journal of the American Chemical Society*, *86*(8), 1646–1647.

Garcia-Ovejero, D., Arevalo-Martin, A., Petrosino, S., Docagne, F., Hagen, C., Bisogno, T., Watanabe, M., Guaza, C., Di Marzo, V., & Molina-Holgado, E. (2009). The endocannabinoid system is modulated in response to spinal cord injury in rats. *Neurobiology of disease*, *33*(1), 57–71.

Gehrmann, J., Matsumoto, Y., & Kreutzberg, G. W. (1995). Microglia: intrinsic immuneffector cell of the brain. *Brain research. Brain research reviews*, *20*(3), 269–87.

Gerard, C., & Gerard, N. P. (1994). C5A Anaphylatoxin and Its Seven Transmembrane-Segment Receptor. *Annual Review of Immunology*, *12*(1), 775–808.

Germain, R. N. (1986). Immunology: The ins and outs of antigen processing and presentations. *Nature*, *322*(6081), 687–688.

Ginis, I., Jaiswal, R., Klimanis, D., Liu, J., Greenspon, J., & Hallenbeck, J. M. (2002). TNF-α–Induced Tolerance to Ischemic Injury Involves Differential Control of NF-κB Transactivation: The Role of NF-κB Association with p300 Adaptor. *Journal of Cerebral Blood Flow & Metabolism*, *22*(2), 142–152.

Glance, L. G., Stone, P. W., Mukamel, D. B., & Dick, A. W. (2011). Increases in Mortality, Length of Stay, and Cost Associated With Hospital-Acquired Infections in Trauma Patients. *Archives of Surgery*, *146*(7), 794.

Golan, H., Levav, T., Mendelsohn, A., & Huleihel, M. (2004). Involvement of Tumor Necrosis Factor Alpha in Hippocampal Development and Function. *Cerebral Cortex*, *14*(1), 97–105.

Goldman, D. W., & Goetzl, E. J. (1982). Specific binding of leukotriene B4 to receptors on human polymorphonuclear leukocytes. *Journal of immunology (Baltimore, Md. : 1950)*, *129*(4), 1600–4.

Gong, S., Zhou, Z., Zhou, M., Lei, Z., Guo, J., Chen, N., & He, L. (2016). Validation of risk scoring models for predicting stroke-associated pneumonia in patients with ischaemic stroke. *BMJ*, *1*(3), 122–126.

Gordon, S. (2002). Pattern Recognition Receptors: Doubling Up for the Innate Immune Response. *Cell*, *111*(7), 927–930.

Granger, D., & Kubes, P. (1994). The microcirculation and inflammation: modulation of leukocyte-endothelial cell adhesion. *J. Leukoc. Biol.*, *55*(5), 662–675.

Granger, & Senchenkova, E. (2010). *Inflammation and the Microcirculation*. *San Rafael (CA): Morgan & Claypool Life Sciences*.

Griffith, J. W., Sokol, C. L., & Luster, A. D. (2014). Chemokines and Chemokine Receptors: Positioning Cells for Host Defense and Immunity. *Annual Review of Immunology*, *32*(1), 659–702.

Grilli, M., Barbieri, I., & Basudev, H. (2000). Interleukin-10 modulates neuronal threshold of vulnerability to ischaemic damage. *European Journal of …*, *12*(March), 2265–2272.

Guillet, J. G., Lai, M. Z., Briner, T. J., Buus, S., Sette, A., Grey, H. M., Smith, J. A., & Gefter, M. L. (1987). Immunological self, nonself discrimination. *Science (New York, N.Y.)*, *235*(4791), 865–70.

Haeusler, K. G., Schmidt, W. U. H., Föhring, F., Meisel, C., Helms, T., Jungehulsing, G. J., Nolte, C. H., Schmolke, K., Wegner, B., Meisel, A., Dirnagl, U., Villringer, A., & Volk, H.-D. (2008). Cellular Immunodepression Preceding Infectious Complications after Acute Ischemic Stroke in Humans. *Cerebrovascular Diseases*, *25*(1–2), 50–58.

Hailer, N. P. (2008). Immunosuppression after traumatic or ischemic CNS damage: It is neuroprotective and illuminates the role of microglial cells. *Progress in Neurobiology*, *84*(3), 211–233.

Hall, W., & Degenhardt, L. (2007). Prevalence and correlates of cannabis use in developed and developing countries. *Current Opinion in Psychiatry*, *20*(4), 393–397.

Hamilton, T. A., Jansen, M. M., Somers, S. D., & Adams, D. O. (1986). Effects of bacterial lipopolysaccharide on protein synthesis in murine peritoneal macrophages: Relationship to activation for macrophage tumoricidal function. *Journal of Cellular Physiology*, *128*(1), 9–17.

Hang, C.-H., Shi, J.-X., Li, J.-S., Wu, W., & Yin, H.-X. (2003). Alterations of intestinal mucosa structure and barrier function following traumatic brain injury in rats. *World journal of gastroenterology*, *9*(12), 2776–81.

Hanus, L., Breuer, A., Tchilibon, S., Shiloah, S., Goldenberg, D., Horowitz, M., Pertwee, R. G., Ross, R. A., Mechoulam, R., & Fride, E. (1999). HU-308: a specific agonist for CB(2), a peripheral cannabinoid receptor. *Proceedings of the National Academy of Sciences of the United States of America*, *96*(25), 14228–33.

Hayakawa, K., Mishima, K., Nozako, M., Hazekawa, M., Ogata, A., Fujioka, M., Harada, K., Mishima, S., Orito, K., Egashira, N., Iwasaki, K., & Fujiwara, M. (2007). Δ9-tetrahydrocannabinol (Δ9-THC) prevents cerebral infarction via hypothalamic-independent hypothermia. *Life Sciences*, *80*(16), 1466–1471.

Hazeldine, J., Lord, J. M., & Belli, A. (2015a). Traumatic Brain Injury and Peripheral Immune Suppression: Primer and Prospectus. *Frontiers in neurology*, *6*, 235.

Hazeldine, J., Lord, J. M., & Belli, A. (2015b). Traumatic Brain Injury and Peripheral Immune Suppression: Primer and Prospectus. *Frontiers in neurology*, *6*, 235.

Herkenham, M., Lynn, a B., Johnson, M. R., Melvin, L. S., de Costa, B. R., & Rice, K. C. (1991). Characterization and localization of cannabinoid receptors in rat brain: a quantitative in vitro autoradiographic study. *The Journal of neuroscience : the official journal of the Society for Neuroscience*, *11*(2), 563–83.

Herkenham, M., Lynn, A. B., Little, M. D., Johnson, M. R., Melvin, L. S., de Costa, B. R., & Rice, K. C. (1990). Cannabinoid receptor localization in brain. *Proceedings of the National Academy of Sciences*, *87*(5).

Hetze, S., Engel, O., Römer, C., Mueller, S., Dirnagl, U., Meisel, C., & Meisel, A. (2013). Superiority of Preventive Antibiotic Treatment Compared with Standard Treatment of Poststroke Pneumonia in Experimental Stroke: A Bed to Bench Approach. *Journal of Cerebral Blood Flow & Metabolism*, *33*(6), 846–854.

Hinson, H. E., Rowell, S., & Schreiber, M. (2015). Clinical evidence of inflammation driving secondary brain injury: a systematic review. *The journal of trauma and acute care surgery*, *78*(1), 184–91.

Hodge, S., Hodge, G., Flower, R., & Han, P. (1999). Methyl-prednisolone up-regulates monocyte interleukin-10 production in stimulated whole blood. *Scandinavian journal of immunology*, *49*(5), 548–53.

Hoshino, K., Takeuchi, O., Kawai, T., Sanjo, H., Ogawa, T., Takeda, Y., Takeda, K., & Akira, S. (1999). Cutting edge: Toll-like receptor 4 (TLR4)-deficient mice are hyporesponsive to lipopolysaccharide: evidence for TLR4 as the Lps gene product. *Journal of immunology (Baltimore, Md. : 1950)*, *162*(7), 3749–52.

Hossmann, K.-A. (2012). The Two Pathophysiologies of Focal Brain Ischemia: Implications for Translational Stroke Research. *Journal of Cerebral Blood Flow & Metabolism*, *32*(7), 1310–1316.

Houser, M. C., & Tansey, M. G. (2017). The gut-brain axis: is intestinal inflammation a silent driver of Parkinson's disease pathogenesis? *npj Parkinson's Disease*, *3*(1), 3.

Howlett, a C., Barth, F., Bonner, T. I., Cabral, G., Casellas, P., Devane, W. a, Felder, C. C., Herkenham, M., Mackie, K., Martin, B. R., Mechoulam, R., & Pertwee, R. G. (2002). International Union of Pharmacology. XXVII. Classification of cannabinoid receptors. *Pharmacological reviews*, *54*(2), 161–202.

Howlett, A. C. (2005). Cannabinoid receptor signaling. *Handbook of experimental pharmacology*, (168), 53–79.

Howlett, A. C., Qualy, J. M., & Khachatrian, L. L. (1986). Involvement of Gi in the inhibition of adenylate cyclase by cannabimimetic drugs. *Molecular pharmacology*, *29*(3), 307–13.

Huang, H., McIntosh, A. L., Martin, G. G., Landrock, D., Chung, S., Landrock, K. K., Dangott, L. J., Li, S., Kier, A. B., & Schroeder, F. (2016). FABP1: A Novel Hepatic Endocannabinoid and Cannabinoid Binding Protein. *Biochemistry*, *55*(37), 5243–5255.

Hug, A., Dalpke, A., Wieczorek, N., Giese, T., Lorenz, A., Auffarth, G., Liesz, A., & Veltkamp, R. (2009). Infarct volume is a major determiner of post-stroke immune cell function and susceptibility to infection. *Stroke; a journal of cerebral circulation*, *40*(10), 3226–32.

Iadecola, C., & Anrather, J. (2011). The immunology of stroke: from mechanisms to translation. *Nature medicine*, *17*(7), 796–808.

Ince, C. (2005). The microcirculation is the motor of sepsis. *Crit Care*, *9*(Suppl 4), S13-9.

Ishikawa, M., Sekizuka, E., Sato, S., Yamaguchi, N., Inamasu, J., Bertalanffy, H., & Kawase, T. (1999). Effects of Moderate Hypothermia on Leukocyte- Endothelium Interaction in the Rat Pial Microvasculature After Transient Middle Cerebral Artery Occlusion. *Stroke*, *30*(8), 1679–1686.

Ito, S., Ansari, P., Sakatsume, M., Dickensheets, H., Vazquez, N., Donnelly, R. P., Larner, A. C., & Finbloom, D. S. (1999). Interleukin-10 inhibits expression of both interferon alpha- and interferon gamma- induced genes by suppressing tyrosine phosphorylation of STAT1. *Blood*, *93*(5), 1456–63.

Izzo, A. A., Borrelli, F., Capasso, R., Di Marzo, V., & Mechoulam, R. (2009). Non-psychotropic plant cannabinoids: new therapeutic opportunities from an ancient herb. *Trends in pharmacological sciences*, *30*(10), 515–27.

Jin, K. L., Mao, X. O., Goldsmith, P. C., & Greenberg, D. A. (2000). CB1 cannabinoid receptor induction in experimental stroke. *Annals of neurology*, *48*(2), 257–61.

Jin, T., & Hereld, D. (2006). Moving toward understanding eukaryotic chemotaxis. *European Journal of Cell Biology*, *85*(9–10), 905–913.

Johnson, R. L., Murray, S. T., Camacho, D. K., & Wilson, C. G. (2016). Vagal nerve stimulation attenuates IL-6 and TNFα expression in respiratory regions of the developing rat brainstem. *Respiratory Physiology & Neurobiology*, *229*, 1–4.

Joss, A., Akdis, M., Faith, A., Blaser, K., & Akdis, C. A. (2000). IL-10 directly acts on T cells by specifically altering the CD28 co-stimulation pathway. *European journal of immunology*, *30*(6), 1683–90.

Kaczocha, M., Lin, Q., Nelson, L. D., McKinney, M. K., Cravatt, B. F., London, E., & Deutsch, D. G. (2012). Anandamide externally added to lipid vesicles containing trapped fatty acid amide hydrolase (FAAH) is readily hydrolyzed in a sterol-modulated fashion. *ACS chemical neuroscience*, *3*(5), 364–8.

Kalra, L., Irshad, S., Hodsoll, J., Simpson, M., Gulliford, M., Smithard, D., Patel, A., Rebollo-Mesa, I., & STROKE-INF Investigators. (2015). Prophylactic antibiotics after acute stroke for reducing pneumonia in patients with dysphagia (STROKE-INF): a prospective, cluster-randomised, open-label, masked endpoint, controlled clinical trial. *The Lancet*, *386*(10006), 1835–1844.

Kano, M., Ohno-Shosaku, T., Hashimotodani, Y., Uchigashima, M., & Watanabe, M. (2009). Endocannabinoid-Mediated Control of Synaptic Transmission. *Physiological Reviews*, *89*(1), 309–380.

Kao, C.-H., ChangLai, S.-P., Chieng, P.-U., & Yen, T.-C. (1998). Gastric emptying in head-injured patients. *The American Journal of Gastroenterology*, *93*(7), 1108–1112.

Kapellos, T. S., Taylor, L., Feuerborn, A., Valaris, S., Hussain, M. T., Rainger, G. E., Greaves, D. R., & Iqbal, A. J. (2019). Cannabinoid receptor 2 deficiency exacerbates inflammation and neutrophil recruitment. *The FASEB Journal*, fj.201802524R.

Kasuga, K., Suga, T., & Mano, N. (2015). Bioanalytical insights into mediator lipidomics. *Journal of Pharmaceutical and Biomedical Analysis*, *113*, 151–162.

Katzenberger, R. J., Ganetzky, B., & Wassarman, D. A. (2015). The gut reaction to traumatic brain injury. *Fly*, *9*(2), 68.

Kawasaki, T., & Kawai, T. (2014). Toll-like receptor signaling pathways. *Frontiers in immunology*, *5*, 461.

Keller, H. U., Wissler, J. H., Hess, M. W., & Cottier, H. (1978). Distinct chemokinetic and chemotactic responses in neutrophil granulocytes. *European Journal of Immunology*, *8*(1), 1–7.

Kendall, D. A., & Yudowski, G. A. (2016). Cannabinoid Receptors in the Central Nervous System: Their Signaling and Roles in Disease. *Frontiers in cellular neuroscience*, *10*, 294.

Kim, J., Amano, O., Wakayama, T., Takahagi, H., & Iseki, S. (2001). The role of cyclic AMP response element-binding protein in testosterone-induced differentiation of granular convoluted tubule cells in the rat submandibular gland. *Archives of oral biology*, *46*(6), 495–507.

Koeberle, P. D., Gauldie, J., & Ball, A. K. (2004). Effects of adenoviral-mediated gene transfer of interleukin-10, interleukin-4, and transforming growth factor-beta on the survival of axotomized retinal ganglion cells. *Neuroscience*, *125*(4), 903–20.

Kohler, E., Prentice, D. A., Bates, T. R., Hankey, G. J., Claxton, A., van Heerden, J., & Blacker, D. (2013). Intravenous Minocycline in Acute Stroke. *Stroke*, *44*(9), 2493–2499.

Kolaczkowska, E., & Kubes, P. (2013). Neutrophil recruitment and function in health and inflammation. *Nature Reviews Immunology*, *13*(3), 159–175.

Koppelman, B., Neefjes, J. J., de Vries, J. E., & de Waal Malefyt, R. (1997). Interleukin-10 Down-Regulates MHC Class II αβ Peptide Complexes at the Plasma Membrane of Monocytes by Affecting Arrival and Recycling. *Immunity*, *7*(6), 861–871.

Kossatz, E., Maldonado, R., & Robledo, P. (2016). CB2 cannabinoid receptors modulate HIF-1α and TIM-3 expression in a hypoxia-ischemia mouse model. *European Neuropsychopharmacology*, *26*(12), 1972–1988.

Kreutzberg, G. W. (1995). Microglia, the first line of defence in brain pathologies. *Arzneimittel-Forschung*, *45*(3A), 357–60.

Krueger, H., Noonan, V. K., Trenaman, L. M., Joshi, P., & Rivers, C. S. (2013). The economic burden of traumatic spinal cord injury in Canada. *Chronic diseases and injuries in Canada*, *33*(3), 113–22.

Kubes, P., & Ward, P. A. (2006). Leukocyte Recruitment and the Acute Inflammatory Response. *Brain Pathology*, *10*(1), 127–135.

Labat-gest, V., & Tomasi, S. (2013). Photothrombotic Ischemia: A Minimally Invasive and Reproducible Photochemical Cortical Lesion Model for Mouse Stroke Studies. *Journal of Visualized Experiments*, (76).

Lal, C., & Leahy, M. J. (2016). An Updated Review of Methods and Advancements in Microvascular Blood Flow Imaging. *Microcirculation*, *23*(5), 345–363.

Lambert, D. M., & Fowler, C. J. (2005). The endocannabinoid system: drug targets, lead compounds, and potential therapeutic applications. *Journal of medicinal chemistry*, *48*(16), 5059–87.

Langhorne, P., Stott, D. J., Robertson, L., MacDonald, J., Jones, L., McAlpine, C., Dick, F., Taylor, G. S., & Murray, G. (2000). Medical Complications After Stroke : A Multicenter Study. *Stroke*, *31*(6), 1223–1229.

Lauffenburger, D. A., & Horwitz, A. F. (1996). Cell migration: a physically integrated molecular process. *Cell*, *84*(3), 359–69.

Lawrence, T., Willoughby, D. A., & Gilroy, D. W. (2002). Anti-inflammatory lipid mediators and insights into the resolution of inflammation. *Nature Reviews Immunology*, *2*(10), 787–795.

Le, Y., Zhou, Y., Iribarren, P., & Wang, J. (2004). Chemokines and chemokine receptors: their manifold roles in homeostasis and disease. *Cellular & molecular immunology*, *1*(2), 95–104.

Leal, M. C., Casabona, J. C., Puntel, M., & Pitossi, F. J. (2013). Interleukin-1β and tumor necrosis factor-α: reliable targets for protective therapies in Parkinson's Disease? *Frontiers in cellular neuroscience*, *7*, 53.

Lehmann, C., Burkovskiy, I., Kuethe, J., Zhou, J., Caldwell, C., & Kelly, M. E. M. (2014). Inhibition of the cannabinoid 2 receptor in CNS-injury induced immunodeficiency syndrome. *Medical Hypotheses*, *82*(6).

Leick, M., Azcutia, V., Newton, G., & Luscinskas, F. W. (2014). Leukocyte recruitment in inflammation: basic concepts and new mechanistic insights based on new models and microscopic imaging technologies. *Cell and tissue research*, *355*(3), 647–56.

Leong, S.-K., & Ling, E.-A. (1992). Amoeboid and ramified microglia: Their interrelationship and response to brain injury. *Glia*, *6*(1), 39–47.

Ley, K., Laudanna, C., Cybulsky, M. I., & Nourshargh, S. (2007). Getting to the site of inflammation: the leukocyte adhesion cascade updated. *Nature Reviews Immunology*, *7*(9), 678–689.

Li, L., Yun, D., Zhang, Y., Tao, Y., Tan, Q., Qiao, F., Luo, B., Liu, Y., Fan, R., Xian, J., & Yu, A. (2018). A cannabinoid receptor 2 agonist reduces blood–brain barrier damage via induction of MKP-1 after intracerebral hemorrhage in rats. *Brain Research*, *1697*, 113–123.

Li, Y., & Kim, J. (2017). Distinct roles of neuronal and microglial CB2 cannabinoid receptors in the mouse hippocampus. *Neuroscience*, *363*, 11–25.

Liu, F., & McCullough, L. D. (2011). Middle cerebral artery occlusion model in rodents: methods and potential pitfalls. *Journal of biomedicine & biotechnology*, *2011*, 464701.

Liu, Q., Jin, W.-N., Liu, Y., Shi, K., Sun, H., Zhang, F., Zhang, C., Gonzales, R. J., Sheth, K. N., La Cava, A., & Shi, F.-D. (2017). Brain Ischemia Suppresses Immunity in the Periphery and Brain via Different Neurogenic Innervations. *Immunity*, *46*(3), 474–487.

Lo, E. H., Broderick, J. P., & Moskowitz, M. A. (2004). tPA and Proteolysis in the Neurovascular Unit. *Stroke*, *35*(2), 354–356.

Lodowski, D. T., & Palczewski, K. (2009). Chemokine receptors and other G protein-coupled receptors. *Current opinion in HIV and AIDS*, *4*(2), 88–95.

Lopez-Rodriguez, A. B., Siopi, E., Finn, D. P., Marchand-Leroux, C., Garcia-Segura, L. M., Jafarian-Tehrani, M., & Viveros, M.-P. (2015). CB1 and CB2 Cannabinoid Receptor Antagonists Prevent Minocycline-Induced Neuroprotection Following Traumatic Brain Injury in Mice. *Cerebral Cortex*, *25*(1), 35–45.

Lovering, F., & Zhang, Y. (2005). Therapeutic potential of TACE inhibitors in stroke. *Current drug targets. CNS and neurological disorders*, *4*(2), 161–8.

Lu, Y.-C., Yeh, W.-C., & Ohashi, P. S. (2008). LPS/TLR4 signal transduction pathway. *Cytokine*, *42*(2), 145–151.

Lucas, S.-M., Rothwell, N. J., & Gibson, R. M. (2009). The role of inflammation in CNS injury and disease. *British Journal of Pharmacology*, *147*(S1), S232–S240.

Luchicchi, A., & Pistis, M. (2012). Anandamide and 2-arachidonoylglycerol: Pharmacological properties, functional features, and emerging specificities of the two major endocannabinoids. *Molecular Neurobiology*, *46*(2), 374–392.

Lukens, J. R., Gross, J. M., & Kanneganti, T.-D. (2012). IL-1 family cytokines trigger sterile inflammatory disease. *Frontiers in Immunology*, *3*, 315.

Lüscher, T. F., & Tanner, F. C. (1993). Endothelial Regulation of Vascular Tone and Growth. *American Journal of Hypertension*, *6*(7_Pt_2), 283S-293S.

Luscinskas, Ph.D, F. W., & Gimbrone, M. A. (1996). ENDOTHELIAL-DEPENDENT MECHANISMS IN CHRONIC INFLAMMATORY LEUKOCYTE RECRUITMENT. *Annual Review of Medicine*, *47*(1), 413–421.

Mackie, K., & Hille, B. (1992). Cannabinoids inhibit N-type calcium channels in neuroblastoma-glioma cells. *Proceedings of the National Academy of Sciences of the United States of America*, *89*(9), 3825–9.

Magid, L., Heymann, S., Elgali, M., Avram, L., Cohen, Y., Liraz-Zaltsman, S., Mechoulam, R., & Shohami, E. (2019). Role of CB 2 Receptor in the Recovery of Mice after Traumatic Brain Injury. *Journal of Neurotrauma*, neu.2018.6063.

Makino, A., Shin, H. Y., Komai, Y., Fukuda, S., Coughlin, M., Sugihara-Seki, M., & Schmid-Schönbein, G. W. (2007). Mechanotransduction in leukocyte activation: a review. *Biorheology*, *44*(4), 221–49.

Malfitano, A. M., Matarese, G., Pisanti, S., Grimaldi, C., Laezza, C., Bisogno, T., Di Marzo, V., Lechler, R. I., & Bifulco, M. (2006). Arvanil inhibits T lymphocyte activation and ameliorates autoimmune encephalomyelitis. *Journal of Neuroimmunology*, *171*(1–2), 110–119.

Maresz, K., Carrier, E. J., Ponomarev, E. D., Hillard, C. J., & Dittel, B. N. (2005). Modulation of the cannabinoid CB2 receptor in microglial cells in response to inflammatory stimuli. *Journal of Neurochemistry*, *95*(2), 437–445.

Marsicano, G., & Lutz, B. (2006). Neuromodulatory functions of the endocannabinoid system. *Journal of endocrinological investigation*, *29*(3 Suppl), 27–46.

Matsuda, L. A., Lolait, S. J., Brownstein, M. J., Young, A. C., & Bonner, T. I. (1990). Structure of a cannabinoid receptor and functional expression of the cloned cDNA. *Nature*, *346*(6284), 561–564.

Matyszak, M. K. (1998). Inflammation in the CNS: balance between immunological privilege and immune responses. *Progress in neurobiology*, *56*(1), 19–35.

McCoy, K. L., Matveyeva, M., Carlisle, S. J., & Cabral, G. A. (1999). Cannabinoid inhibition of the processing of intact lysozyme by macrophages: evidence for CB2 receptor participation. *The Journal of pharmacology and experimental therapeutics*, *289*(3), 1620–5.

McCoy, K. L., & Schwartz, R. H. (1988). The role of intracellular acidification in antigen processing. *Immunological reviews*, *106*, 129–47.

McNally, L., Bhagwagar, Z., & Hannestad, J. (2008). Inflammation, Glutamate, and Glia in Depression: A Literature Review. *CNS Spectrums*, *13*(06), 501–510.

Mechoulam, R, Ben-Shabat, S., Hanus, L., Ligumsky, M., Kaminski, N. E., Schatz, A. R., Gopher, A., Almog, S., Martin, B. R., & Compton, D. R. (1995). Identification of an endogenous 2-monoglyceride, present in canine gut, that binds to cannabinoid receptors. *Biochemical pharmacology*, *50*(1), 83–90.

Mechoulam, R, & Shohami, E. (2007). Endocannabinoids and traumatic brain injury. *Molecular neurobiology*, *36*(1), 68–74.

Mechoulam, R, & Shvo, Y. (1963). Hashish. I. The structure of cannabidiol. *Tetrahedron*, *19*(12), 2073–8.

Mechoulam, Raphael, Peters, M., Murillo-Rodriguez, E., & Hanuš, L. O. (2007). Cannabidiol – Recent Advances. *Chemistry & Biodiversity*, *4*(8), 1678–1692.

Meisel, C., Schwab, J. M., Prass, K., Meisel, A., & Dirnagl, U. (2005). Central nervous system injury-induced immune deficiency syndrome. *Nature reviews. Neuroscience*, *6*(10), 775–86.

Menon, D. K., Schwab, K., Wright, D. W., Maas, A. I., & Demographics and Clinical Assessment Working Group of the International and Interagency Initiative toward Common Data Elements for Research on Traumatic Brain Injury and Psychological Health. (2010). Position Statement: Definition of Traumatic Brain Injury. *Archives of Physical Medicine and Rehabilitation*, *91*(11), 1637–1640.

Miller, C. H., Quattrocchi, K. B., Frank, E. H., Issel, B. W., & Wagner, F. C. (1991). Humoral and cellular immunity following severe head injury: review and current investigations. *Neurological research*, *13*(2), 117–24.

Moazzam, F., DeLano, F. A., Zweifach, B. W., & Schmid-Schönbein, G. W. (1997). The leukocyte response to fluid stress. *Proceedings of the National Academy of Sciences of the United States of America*, *94*(10), 5338–43.

Molina-Holgado, F., Pinteaux, E., Moore, J. D., Molina-Holgado, E., Guaza, C., Gibson, R. M., & Rothwell, N. J. (2003). Endogenous interleukin-1 receptor antagonist mediates anti-inflammatory and neuroprotective actions of cannabinoids in neurons and glia. *The Journal of neuroscience : the official journal of the Society for Neuroscience*, *23*(16), 6470–4.

Morgan, N. H., Stanford, I. M., & Woodhall, G. L. (2009). Functional CB2 type cannabinoid receptors at CNS synapses. *Neuropharmacology*, *57*(4), 356–368.

Mousa, A., & Bakhiet, M. (2013). Role of cytokine signaling during nervous system development. *International journal of molecular sciences*, *14*(7), 13931–57.

Mukhopadhyay, S., Das, S., Williams, E. A., Moore, D., Jones, J. D., Zahm, D. S., Ndengele, M. M., Lechner, A. J., & Howlett, A. C. (2006). Lipopolysaccharide and cyclic AMP regulation of CB2 cannabinoid receptor levels in rat brain and mouse RAW 264.7 macrophages. *Journal of Neuroimmunology*, *181*(1–2), 82–92.

Munro, S., Thomas, K. L., & Abu-Shaar, M. (1993). Molecular characterization of a peripheral receptor for cannabinoids. *Nature*, *365*(6441), 61–65.

Murdoch, C., & Finn, A. (2000). Chemokine receptors and their role in inflammation and infectious diseases. *Blood*, *95*(10), 3032–43.

Muthian, S., Rademacher, D. J., Roelke, C. T., Gross, G. J., & Hillard, C. J. (2004). Anandamide content is increased and CB1 cannabinoid receptor blockade is protective during transient, focal cerebral ischemia. *Neuroscience*, *129*(3), 743–750.

Nagayama, T., Sinor, A. D., Simon, R. P., Chen, J., Graham, S. H., Jin, K., & Greenberg, D. A. (1999). Cannabinoids and neuroprotection in global and focal cerebral ischemia and in neuronal cultures. *The Journal of neuroscience : the official journal of the Society for Neuroscience*, *19*(8), 2987–95.

Nogueira, R. G., Jadhav, A. P., Haussen, D. C., Bonafe, A., Budzik, R. F., Bhuva, P., Yavagal, D. R., Ribo, M., Cognard, C., Hanel, R. A., Sila, C. A., Hassan, A. E., Millan, M., Levy, E. I., Mitchell, P., Chen, M., English, J. D., Shah, Q. A., Silver, F. L., Pereira, V. M., Mehta, B. P., Baxter, B. W., Abraham, M. G., Cardona, P., Veznedaroglu, E., Hellinger, F. R., Feng, L., Kirmani, J. F., Lopes, D. K., Jankowitz, B. T., Frankel, M. R., Costalat, V., Vora, N. A., Yoo, A. J., Malik, A. M., Furlan, A. J., Rubiera, M., Aghaebrahim, A., Olivot, J.-M., Tekle, W. G., Shields, R., Graves, T., Lewis, R. J., Smith, W. S., Liebeskind, D. S., Saver, J. L., & Jovin, T. G. (2018). Thrombectomy 6 to 24 Hours after Stroke with a Mismatch between Deficit and Infarct. *New England Journal of Medicine*, *378*(1), 11–21.

Noordergraaf, A. (1978). *Circulatory system dynamics*. Academic Press.

O'Collins, V. E., Macleod, M. R., Donnan, G. A., Horky, L. L., van der Worp, B. H., & Howells, D. W. (2006). 1,026 Experimental treatments in acute stroke. *Annals of Neurology*, *59*(3), 467–477.

Okada, Y., Copeland, B. R., Mori, E., Tung, M. M., Thomas, W. S., & del Zoppo, G. J. (1994). P-selectin and intercellular adhesion molecule-1 expression after focal brain ischemia and reperfusion. *Stroke*, *25*(1), 202–11.

Orgado, J. M., Fernández-Ruiz, J., & Romero, J. (2009). The endocannabinoid system in neuropathological states. *International review of psychiatry (Abingdon, England)*, *21*(2), 172–80.

Ostrowski, R. P., Schulte, R. W., Nie, Y., Ling, T., Lee, T., Manaenko, A., Gridley, D. S., & Zhang, J. H. (2012). Acute Splenic Irradiation Reduces Brain Injury in the Rat Focal Ischemic Stroke Model. *Translational Stroke Research*, *3*(4), 473–481.

Ovbiagele, B., & Nguyen-Huynh, M. N. (2011). Stroke epidemiology: advancing our understanding of disease mechanism and therapy. *Neurotherapeutics : the journal of the American Society for Experimental NeuroTherapeutics*, *8*(3), 319–29.

Pacher, P., Batkai, S., & Kunos, G. (2006). The endocannabinoid system as an emerging target of pharmacotherapy. *Pharmacol Rev*, *58*(3), 389–462.

Palazuelos, J., Aguado, T., Pazos, M. R., Julien, B., Carrasco, C., Resel, E., Sagredo, O., Benito, C., Romero, J., Azcoitia, I., Fernandez-Ruiz, J., Guzman, M., & Galve-Roperh, I. (2009). Microglial CB2 cannabinoid receptors are neuroprotective in Huntington's disease excitotoxicity. *Brain*, *132*(11), 3152–3164.

Pandey, R., Mousawy, K., Nagarkatti, M., & Nagarkatti, P. (2009). Endocannabinoids and immune regulation. *Pharmacological research : the official journal of the Italian Pharmacological Society*, *60*(2), 85–92.

Panikashvili, D., Simeonidou, C., Ben-Shabat, S., Hanus, L., Breuer, A., Mechoulam, R., & Shohami, E. (2001). An endogenous cannabinoid (2-AG) is neuroprotective after brain injury. *Nature*, *413*(6855), 527–31.

Panina-Bordignon, P., Mazzeo, D., Lucia, P. D., D'Ambrosio, D., Lang, R., Fabbri, L., Self, C., & Sinigaglia, F. (1997). Beta2-agonists prevent Th1 development by selective inhibition of interleukin 12. *The Journal of clinical investigation*, *100*(6), 1513–9.

Parker, L. C., Whyte, M. K. B., Dower, S. K., & Sabroe, I. (2005). The expression and roles of Toll-like receptors in the biology of the human neutrophil. *Journal of Leukocyte Biology*, *77*(6), 886–892.

Parmentier-Batteur, S., Jin, K., Mao, X. O., Xie, L., & Greenberg, D. A. (2002). Increased severity of stroke in CB1 cannabinoid receptor knock-out mice. *The Journal of neuroscience : the official journal of the Society for Neuroscience*, *22*(22), 9771–5.

Pazos, M. R., Mohammed, N., Lafuente, H., Santos, M., Martínez-Pinilla, E., Moreno, E., Valdizan, E., Romero, J., Pazos, A., Franco, R., Hillard, C. J., Alvarez, F. J., & Martínez-Orgado, J. (2013). Mechanisms of cannabidiol neuroprotection in hypoxic–ischemic newborn pigs: Role of 5HT1A and CB2 receptors. *Neuropharmacology*, *71*, 282–291.

Pendlebury, S. T., & Rothwell, P. M. (2009). Prevalence, incidence, and factors associated with pre-stroke and post-stroke dementia: a systematic review and meta-analysis. *The Lancet Neurology*, *8*(11), 1006–1018.

Pennypacker, K. R., & Offner, H. (2015). The role of the spleen in ischemic stroke. *Journal of cerebral blood flow and metabolism : official journal of the International Society of Cerebral Blood Flow and Metabolism*, *35*(2), 186–7.

Perry, V. H., Bell, M. D., Brown, H. C., & Matyszak, M. K. (1995). Inflammation in the nervous system. *Current opinion in neurobiology*, *5*(5), 636–41.

Pertwee, R G. (2006). The pharmacology of cannabinoid receptors and their ligands: an overview. *International Journal of Obesity*, *30*, S13–S18.

Pertwee, R G. (2008). The diverse CB1 and CB2 receptor pharmacology of three plant cannabinoids: delta9-tetrahydrocannabinol, cannabidiol and delta9-tetrahydrocannabivarin. *British journal of pharmacology*, *153*(2), 199–215.

Pertwee, R G, Howlett, A. C., Abood, M. E., Alexander, S. P. H., Di Marzo, V., Elphick, M. R., Greasley, P. J., Hansen, H. S., Kunos, G., Mackie, K., Mechoulam, R., & Ross, R. A. (2010). International Union of Basic and Clinical Pharmacology. LXXIX. Cannabinoid receptors and their ligands: beyond CB_1 and CB_2. *Pharmacological reviews*, *62*(4), 588–631.

Pertwee, Roger Guy. (2004, July 20). The pharmacology and therapeutic potential of cannabidiol. . Kluwer Academic/Plenum Publishers.

Petty, M. A., & Lo, E. H. (2002). Junctional complexes of the blood-brain barrier: permeability changes in neuroinflammation. *Progress in neurobiology*, *68*(5), 311–23.

Pisanti, S., & Bifulco, M. (2018). Medical *Cannabis* : A plurimillennial history of an evergreen. *Journal of Cellular Physiology*.

Pittman, R. N. (2011). *Regulation of Tissue Oxygenation*. *Regulation of Tissue Oxygenation*. Morgan & Claypool Life Sciences.

Poltorak, A., He, X., Smirnova, I., Liu, M. Y., Van Huffel, C., Du, X., Birdwell, D., Alejos, E., Silva, M., Galanos, C., Freudenberg, M., Ricciardi-Castagnoli, P., Layton, B., & Beutler, B. (1998). Defective LPS signaling in C3H/HeJ and C57BL/10ScCr mice: mutations in Tlr4 gene. *Science (New York, N.Y.)*, *282*(5396), 2085–8.

Prass, K., Meisel, C., Höflich, C., Braun, J., Halle, E., Wolf, T., Ruscher, K., Victorov, I. V, Priller, J., Dirnagl, U., Volk, H.-D., & Meisel, A. (2003). Stroke-induced immunodeficiency promotes spontaneous bacterial infections and is mediated by sympathetic activation reversal by poststroke T helper cell type 1-like immunostimulation. *The Journal of experimental medicine*, *198*(5), 725–36.

Pryce, G., Ahmed, Z., Hankey, D. J. R., Jackson, S. J., Croxford, J. L., Pocock, J. M., Ledent, C., Petzold, A., Thompson, A. J., Giovannoni, G., Cuzner, M. L., & Baker, D. (2003). Cannabinoids inhibit neurodegeneration in models of multiple sclerosis. *Brain*, *126*(10), 2191–2202.

Raborn, E. S., Marciano-Cabral, F., Buckley, N. E., Martin, B. R., & Cabral, G. A. (2008). The Cannabinoid Delta-9-tetrahydrocannabinol Mediates Inhibition of Macrophage Chemotaxis to RANTES/CCL5: Linkage to the CB2 Receptor. *Journal of Neuroimmune Pharmacology*, *3*(2), 117–129.

Rafols, J. (2015). Control of the brain microcirculation following traumatic brain injury and stroke. *Brain Circulation*, *1*(2), 146.

Rafols, J. A., Kreipke, C. W., & Petrov, T. (2007). Alterations in cerebral cortex microvessels and the microcirculation in a rat model of traumatic brain injury: a correlative EM and laser Doppler flowmetry study. *Neurological Research*, *29*(4), 339–347.

Reggio, P. H. (2002). Endocannabinoid structure-activity relationships for interaction at the cannabinoid receptors. *Prostaglandins, leukotrienes, and essential fatty acids*, *66*(2–3), 143–160.

Reid, D. M., Perry, V. H., Andersson, P. B., & Gordon, S. (1993). Mitosis and apoptosis of microglia in vivo induced by an anti-CR3 antibody which crosses the blood-brain barrier. *Neuroscience*, *56*(3), 529–33.

Richard Kasten, K., Tschop, J., Hans Tschop, M., & Curtis Caldwell, C. (2010). The Cannabinoid 2 Receptor as a Potential Therapeutic Target for Sepsis. *Endocrine, Metabolic & Immune Disorders - Drug Targets*, *10*(3), 224–234.

Riegger, T., Conrad, S., Liu, K., Schluesener, H. J., Adibzahdeh, M., & Schwab, J. M. (2007). Spinal cord injury-induced immune depression syndrome (SCI-IDS). *European Journal of Neuroscience*, *25*(6), 1743–1747.

Rincón-Ferrari, M. D., Flores-Cordero, J. M., Leal-Noval, S. R., Murillo-Cabezas, F., Cayuelas, A., Muñoz-Sánchez, M. A., & Sánchez-Olmedo, J. I. (2004). Impact of ventilator-associated pneumonia in patients with severe head injury. *The Journal of trauma*, *57*(6), 1234–40.

Ritter, L. S., Orozco, J. A., Coull, B. M., McDonagh, P. F., & Rosenblum, W. I. (2000). Leukocyte accumulation and hemodynamic changes in the cerebral microcirculation during early reperfusion after stroke. *Stroke*, *31*(5), 1153–61.

Roger, V. L., Go, A. S., Lloyd-Jones, D. M., Adams, R. J., Berry, J. D., Brown, T. M., Carnethon, M. R., Dai, S., de Simone, G., Ford, E. S., Fox, C. S., Fullerton, H. J., Gillespie, C., Greenlund, K. J., Hailpern, S. M., Heit, J. A., Ho, P. M., Howard, V. J., Kissela, B. M., Kittner, S. J., Lackland, D. T., Lichtman, J. H., Lisabeth, L. D., Makuc, D. M., Marcus, G. M., Marelli, A., Matchar, D. B., McDermott, M. M., Meigs, J. B., Moy, C. S., Mozaffarian, D., Mussolino, M. E., Nichol, G., Paynter, N. P., Rosamond, W. D., Sorlie, P. D., Stafford, R. S., Turan, T. N., Turner, M. B., Wong, N. D., Wylie-Rosett, J., & American Heart Association Statistics Committee and Stroke Statistics Subcommittee. (2011). Heart Disease and Stroke Statistics—2011 Update. *Circulation*, *123*(4), e18–e209.

Ross, A. M., Hurn, P., Perrin, N., Wood, L., Carlini, W., Potempa, K., Vandenbark, A. A., & Hurn, P. D. (2007). Evidence of the peripheral inflammatory response in patients with transient ischemic attack. *Journal of stroke and cerebrovascular diseases : the official journal of National Stroke Association*, *16*(5), 203–7.

Ross, R. A., Brockie, H. C., Stevenson, L. A., Murphy, V. L., Templeton, F., Makriyannis, A., & Pertwee, R. G. (1999). Agonist-inverse agonist characterization at CB1 and CB2 cannabinoid receptors of L759633, L759656, and AM630. *British journal of pharmacology*, *126*(3), 665–72.

Rothwell, N. J., & Luheshi, G. N. (2000). Interleukin 1 in the brain: biology, pathology and therapeutic target. *Trends in neurosciences*, *23*(12), 618–25.

Sacerdote, P., Martucci, C., Vaccani, A., Bariselli, F., Panerai, A. E., Colombo, A., Parolaro, D., & Massi, P. (2005). The nonpsychoactive component of marijuana cannabidiol modulates chemotaxis and IL-10 and IL-12 production of murine macrophages both in vivo and in vitro. *Journal of Neuroimmunology*, *159*(1–2), 97–105.

Sacerdote, P., Massi, P., Panerai, A. E., & Parolaro, D. (2000). In vivo and in vitro treatment with the synthetic cannabinoid CP55, 940 decreases the in vitro migration of macrophages in the rat: involvement of both CB1 and CB2 receptors. *Journal of neuroimmunology*, *109*(2), 155–63.

Saïd-Sadier, N., & Ojcius, D. M. (2012). Alarmins, inflammasomes and immunity. *Biomedical journal*, *35*(6), 437–49.

Salameh, A., Mohajer, M. Al, & Daroucihe, R. O. (2015). Prevention of urinary tract infections in patients with spinal cord injury. *CMAJ : Canadian Medical Association journal = journal de l'Association medicale canadienne*, *187*(11), 807–811.

Salgado, D. R., Ortiz, J. A., Favory, R., Creteur, J., Vincent, J.-L., & De Backer, D. (2010). Microcirculatory abnormalities in patients with severe influenza A (H1N1) infection. *Canadian journal of anaesthesia = Journal canadien d'anesthésie*, *57*(10), 940–6.

Sanders, V. M., Baker, R. A., Ramer-Quinn, D. S., Kasprowicz, D. J., Fuchs, B. A., & Street, N. E. (1997). Differential expression of the beta2-adrenergic receptor by Th1 and Th2 clones: implications for cytokine production and B cell help. *Journal of immunology (Baltimore, Md. : 1950)*, *158*(9), 4200–10.

Savinainen, J. R., Saario, S. M., & Laitinen, J. T. (2012). The serine hydrolases MAGL, ABHD6 and ABHD12 as guardians of 2-arachidonoylglycerol signalling through cannabinoid receptors. *Acta physiologica (Oxford, England)*, *204*(2), 267–76.

Saxena, A., Khosraviani, S., Noel, S., Mohan, D., Donner, T., & Hamad, A. R. a. (2014). Interleukin-10 paradox: A potent immunoregulatory cytokine that has been difficult to harness for immunotherapy. *Cytokine*.

Schiffmann, E., Corcoran, B. A., & Wahl, S. M. (1975). N-formylmethionyl peptides as chemoattractants for leucocytes. *Proceedings of the National Academy of Sciences of the United States of America*, *72*(3), 1059–62.

Schirmer-Mikalsen, K., Moen, K., Skandsen, T., Vik, A., & Klepstad, P. (2013). Intensive care and traumatic brain injury after the introduction of a treatment protocol: a prospective study. *Acta Anaesthesiologica Scandinavica*, *57*(1), 46–55.

Schwartz, R. H. (1985). T-Lymphocyte Recognition of Antigen in Association with Gene Products of the Major Histocompatibility Complex. *Annual Review of Immunology*, *3*(1), 237–261.

Schwarz, H., Blanco, F. J., & Lotz, M. (1994). Anadamide, an endogenous cannabinoid receptor agonist inhibits lymphocyte proliferation and induces apoptosis. *Journal of neuroimmunology*, *55*(1), 107–15.

Secomb, T. W. (2017). Blood Flow in the Microcirculation. *Annual Review of Fluid Mechanics*, *49*(1), 443–461.

Seifert, H. A., & Offner, H. (2018). The splenic response to stroke: from rodents to stroke subjects. *Journal of neuroinflammation*, *15*(1), 195.

Sharma, S., Yang, B., Xi, X., Grotta, J. C., Aronowski, J., & Savitz, S. I. (2011). IL-10 directly protects cortical neurons by activating PI-3 kinase and STAT-3 pathways. *Brain research*, *1373*, 189–94.

Shi, K., Wood, K., Shi, F.-D., Wang, X., & Liu, Q. (2018). Stroke-induced immunosuppression and poststroke infection. *Stroke and Vascular Neurology*, *3*(1), 34–41.

Shobha, N., Buchan, A. M., Hill, M. D., & Canadian Alteplase for Stroke Effectiveness Study (CASES). (2011). Thrombolysis at 3–4.5 Hours after Acute Ischemic Stroke Onset – Evidence from the Canadian Alteplase for Stroke Effectiveness Study (CASES) Registry. *Cerebrovascular Diseases*, *31*(3), 223–228.

Shohami, E., Cohen-Yeshurun, A., Magid, L., Algali, M., & Mechoulam, R. (2011). Endocannabinoids and traumatic brain injury. *British journal of pharmacology*, *163*(7), 1402–10.

Shohami, E., Ginis, I., & Hallenbeck, J. M. (1999). Dual role of tumor necrosis factor alpha in brain injury. *Cytokine & Growth Factor Reviews*, *10*(2), 119–130.

Sielenkämper, a. W., Meyer, J., Kloppenburg, H., Eicker, K., & Van Aken, H. V. (2001). The effects of sepsis on gut mucosal blood flow in rats. *European Journal of Anaesthesiology*, *18*, 673–678.

Silva-Herdade, A. S., Andolina, G., Faggio, C., Calado, Â., & Saldanha, C. (2016). Erythrocyte deformability — A partner of the inflammatory response. *Microvascular Research*, *107*, 34–38.

Sim, L. J., Hampson, R. E., Deadwyler, S. A., & Childers, S. R. (1996). Effects of chronic treatment with delta9-tetrahydrocannabinol on cannabinoid-stimulated [35S]GTPgammaS autoradiography in rat brain. *The Journal of neuroscience : the official journal of the Society for Neuroscience*, *16*(24), 8057–66.

Sinha, D., Bonner, T. I., Bhat, N. R., & Matsuda, L. A. (1998). Expression of the CB1 cannabinoid receptor in macrophage-like cells from brain tissue: immunochemical characterization by fusion protein antibodies. *Journal of neuroimmunology*, *82*(1), 13–21.

Soethoudt, M., Grether, U., Fingerle, J., Grim, T. W., Fezza, F., de Petrocellis, L., Ullmer, C., Rothenhäusler, B., Perret, C., van Gils, N., Finlay, D., MacDonald, C., Chicca, A., Gens, M. D., Stuart, J., de Vries, H., Mastrangelo, N., Xia, L., Alachouzos, G., Baggelaar, M. P., Martella, A., Mock, E. D., Deng, H., Heitman, L. H., Connor, M., Di Marzo, V., Gertsch, J., Lichtman, A. H., Maccarrone, M., Pacher, P., Glass, M., & van der Stelt, M. (2017). Cannabinoid CB2 receptor ligand profiling reveals biased signalling and off-target activity. *Nature Communications*, *8*, 13958.

Spits, H., & Malefyt, de W. (1992). Functional Characterization of Human IL-10. *International Archives of Allergy and Immunology*, *99*(1), 8–15.

Spychala, M. S., Honarpisheh, P., & McCullough, L. D. (2017). Sex differences in neuroinflammation and neuroprotection in ischemic stroke. *Journal of Neuroscience Research*, *95*(1–2), 462–471.

Stefano, G. B., Salzet, M., Rialas, C. M., Mattocks, D., Fimiani, C., & Bilfinger, T. V. (1998). Macrophage behavior associated with acute and chronic exposure to HIV GP120, morphine and anandamide: endothelial implications. *International journal of cardiology*, *64 Suppl 1*, S3-13.

Steiner, J., Rafols, D., Park, H. ., Katar, M. ., Rafols, J. ., & Petrov, T. (2004). Attenuation of iNOS mRNA exacerbates hypoperfusion and upregulates endothelin-1 expression in hippocampus and cortex after brain trauma. *Nitric Oxide*, *10*(3), 162–169.

Stoll, G., Jander, S., & Schroeter, M. (2000). Cytokines in CNS disorders: neurotoxicity versus neuroprotection. *Journal of neural transmission. Supplementum*, *59*, 81–9.

Sugiura, T., Kondo, S., Sukagawa, A., Nakane, S., Shinoda, A., Itoh, K., Yamashita, A., & Waku, K. (1995). 2-Arachidonoylglycerol: a possible endogenous cannabinoid receptor ligand in brain. *Biochemical and biophysical research communications*, *215*(1), 89–97.

Sugiura, T., & Waku, K. (2000). 2-Arachidonoylglycerol and the cannabinoid receptors. *Chemistry and physics of lipids*, *108*(1–2), 89–106.

Sun, Y., Alexander, S. P. H., Garle, M. J., Gibson, C. L., Hewitt, K., Murphy, S. P., Kendall, D. A., & Bennett, A. J. (2007). Cannabinoid activation of PPAR alpha; a novel neuroprotective mechanism. *British journal of pharmacology*, *152*(5), 734–43.

Sussman, B. J., & Fitch, T. S. P. (1959). Thrombolysis with fibrinolysin in cerebral arterial occlusion; the role of angiography. *Angiology*, *10*(4), 268–282.

Szabó, C., Thiemermann, C., Wu, C. C., Perretti, M., & Vane, J. R. (1994). Attenuation of the induction of nitric oxide synthase by endogenous glucocorticoids accounts for endotoxin tolerance in vivo. *Proceedings of the National Academy of Sciences of the United States of America*, *91*(1), 271–5.

Takeda, K., Kaisho, T., & Akira, S. (2003). Toll-Like Receptors. *Annual Review of Immunology*, *21*(1), 335–376.

Tanasescu, R., & Constantinescu, C. S. (2010). Cannabinoids and the immune system: an overview. *Immunobiology*, *215*(8), 588–97.

Tao, Y., Li, L., Jiang, B., Feng, Z., Yang, L., Tang, J., Chen, Q., Zhang, J., Tan, Q., Feng, H., Chen, Z., & Zhu, G. (2016). Cannabinoid receptor-2 stimulation suppresses neuroinflammation by regulating microglial M1/M2 polarization through the cAMP/PKA pathway in an experimental GMH rat model. *Brain, Behavior, and Immunity*, *58*, 118–129.

Ternianov, A., Pérez-Ortiz, J. M., Solesio, M. E., García-Gutiérrez, M. S., Ortega-Álvaro, A., Navarrete, F., Leiva, C., Galindo, M. F., & Manzanares, J. (2012). Overexpression of CB2 cannabinoid receptors results in neuroprotection against behavioral and neurochemical alterations induced by intracaudate administration of 6-hydroxydopamine. *Neurobiology of Aging*, *33*(2), 421.e1-421.e16.

Thomas, B. F., Wei, X., & Martin, B. R. (1992). Characterization and autoradiographic localization of the cannabinoid binding site in rat brain using [3H]11-OH-delta 9-THC-DMH. *The Journal of pharmacology and experimental therapeutics*, *263*(3), 1383–90.

Thompson, M. R., Kaminski, J. J., Kurt-Jones, E. A., & Fitzgerald, K. A. (2011). Pattern recognition receptors and the innate immune response to viral infection. *Viruses*, *3*(6), 920–40.

Tosi, M. F. (2005). Innate immune responses to infection. *Journal of Allergy and Clinical Immunology*, *116*(2), 241–249.

Tukhovskaya, E. a, Turovsky, E. a, Turovskaya, M. V, Levin, S. G., Murashev, A. N., Zinchenko, V. P., & Godukhin, O. V. (2014). Anti-inflammatory cytokine interleukin-10 increases resistance to brain ischemia through modulation of ischemia-induced intracellular Ca^{2+} response. *Neuroscience letters*, *571*, 55–60.

Turner, M. D., Nedjai, B., Hurst, T., & Pennington, D. J. (2014). Cytokines and chemokines: At the crossroads of cell signalling and inflammatory disease. *Biochimica et Biophysica Acta (BBA) - Molecular Cell Research*, *1843*(11), 2563–2582.

Unanue, E. R., & Allen, P. M. (1987). The basis for the immunoregulatory role of macrophages and other accessory cells. *Science (New York, N.Y.)*, *236*(4801), 551–7.

Urday, S., Kimberly, W. T., Beslow, L. A., Vortmeyer, A. O., Selim, M. H., Rosand, J., Simard, J. M., & Sheth, K. N. (2015). Targeting secondary injury in intracerebral haemorrhage—perihaematomal oedema. *Nature Reviews Neurology*, *11*(2), 111–122.

van der Drift, A. C., van Noort, J. M., & Krüse, J. (1990). Catheptic processing of protein antigens: enzymic and molecular aspects. *Seminars in immunology*, *2*(4), 255–71.

Van Wagoner, N. J., & Benveniste, E. N. (1999). Interleukin-6 expression and regulation in astrocytes. *Journal of neuroimmunology*, *100*(1–2), 124–39.

Vannucci, R. C., & Vannucci, S. J. (2005). Perinatal hypoxic-ischemic brain damage: evolution of an animal model. *Developmental neuroscience*, *27*(2–4), 81–6.

Vannucci, S. J., & Hagberg, H. (2004). Hypoxia-ischemia in the immature brain. *Journal of Experimental Biology*, *207*(18), 3149–3154.

Varga, R., Wagner, J. A., Bridgen, D. T., & Kunos, G. (1998). Platelet- and machrophage-derived cannabinoids are involved in endotoxin-induced hypotension. *Faseb J*, *12*(11), 1035–1044.

Venketasubramanian, N., Yoon, B. W., Pandian, J., & Navarro, J. C. (2017). Stroke Epidemiology in South, East, and South-East Asia: A Review. *Journal of stroke*, *19*(3), 286–294.

Venturi, L., Miranda, M., Selmi, V., Vitali, L., Tani, A., Margheri, M., De Gaudio, A. R., & Adembri, C. (2009). Systemic Sepsis Exacerbates Mild Post-Traumatic Brain Injury in the Rat. *Journal of Neurotrauma*, *26*(9), 1547–1556.

Viscomi, M. T., Oddi, S., Latini, L., Pasquariello, N., Florenzano, F., Bernardi, G., Molinari, M., & Maccarrone, M. (2009). Selective CB2 Receptor Agonism Protects Central Neurons from Remote Axotomy-Induced Apoptosis through the PI3K/Akt Pathway. *Journal of Neuroscience*, *29*(14), 4564–4570.

Vogelgesang, A., & Dressel, A. (2011). Immunological consequences of ischemic stroke: immunosuppression and autoimmunity. *Journal of neuroimmunology*, *231*(1–2), 105–10.

von Andrian, U. H., Chambers, J. D., McEvoy, L. M., Bargatze, R. F., Arfors, K. E., & Butcher, E. C. (1991). Two-step model of leukocyte-endothelial cell interaction in inflammation: distinct roles for LECAM-1 and the leukocyte beta 2 integrins in vivo. *Proceedings of the National Academy of Sciences of the United States of America*, *88*(17), 7538–42.

Waksman, Y., Olson, J. M., Carlisle, S. J., & Cabral, G. A. (1999). The central cannabinoid receptor (CB1) mediates inhibition of nitric oxide production by rat microglial cells. *The Journal of pharmacology and experimental therapeutics*, *288*(3), 1357–66.

Walter, L., Franklin, A., Witting, A., Wade, C., Xie, Y., Kunos, G., Mackie, K., & Stella, N. (2003). Nonpsychotropic cannabinoid receptors regulate microglial cell migration. *The Journal of neuroscience : the official journal of the Society for Neuroscience*, *23*(4), 1398–405.

Wang, C. X., & Shuaib, A. (2002). Involvement of inflammatory cytokines in central nervous system injury. *Progress in neurobiology*, *67*(2), 161–72.

Wang, X., Feuerstein, G. Z., Xu, L., Wang, H., Schumacher, W. A., Ogletree, M. L., Taub, R., Duan, J. J.-W., Decicco, C. P., & Liu, R.-Q. (2004). Inhibition of Tumor Necrosis Factor- -Converting Enzyme by a Selective Antagonist Protects Brain from Focal Ischemic Injury in Rats. *Molecular Pharmacology*, *65*(4), 890–896.

Wang, X., Siren, A. L., Liu, Y., Yue, T. L., Barone, F. C., & Feuerstein, G. Z. (1994). Upregulation of intercellular adhesion molecule 1 (ICAM-1) on brain microvascular endothelial cells in rat ischemic cortex. *Brain research. Molecular brain research*, *26*(1–2), 61–8.

Warrington, R., Watson, W., Kim, H. L., & Antonetti, F. R. (2011). An introduction to immunology and immunopathology. *Allergy, Asthma & Clinical Immunology*, *7*(S1), S1.

Westendorp, W. F., Nederkoorn, P. J., Vermeij, J.-D., Dijkgraaf, M. G., & de Beek, D. van. (2011). Post-stroke infection: A systematic review and meta-analysis. *BMC Neurology*, *11*(1), 110.

Westendorp, W. F., Vermeij, J.-D., Vermeij, F., Den Hertog, H. M., Dippel, D. W., van de Beek, D., & Nederkoorn, P. J. (2012a). Antibiotic therapy for preventing infections in patients with acute stroke. *Cochrane Database of Systematic Reviews*, (1).

Westendorp, W. F., Vermeij, J.-D., Vermeij, F., Den Hertog, H. M., Dippel, D. W., van de Beek, D., & Nederkoorn, P. J. (2012b). Antibiotic therapy for preventing infections in patients with acute stroke. In P. J. Nederkoorn (Ed.), *Cochrane Database of Systematic Reviews*. Chichester, UK: John Wiley & Sons, Ltd.

Westendorp, W. F., Vermeij, J.-D., Zock, E., Hooijenga, I. J., Kruyt, N. D., Bosboom, H. J. L. W., Kwa, V. I. H., Weisfelt, M., Remmers, M. J. M., ten Houten, R., Schreuder, A. H. C. M. (Tobien), Vermeer, S. E., van Dijk, E. J., Dippel, D. W. J., Dijkgraaf, M. G. W., Spanjaard, L., Vermeulen, M., van der Poll, T., Prins, J. M., Vermeij, F. H., Roos, Y. B. W. E. M., Kleyweg, R. P., Kerkhoff, H., Brouwer, M. C., Zwinderman, A. H., van de Beek, D., Nederkoorn, P. J., & PASS investigators. (2015). The Preventive Antibiotics in Stroke Study (PASS): a pragmatic randomised open-label masked endpoint clinical trial. *The Lancet*, *385*(9977), 1519–1526.

Witting, A., Walter, L., Wacker, J., Moller, T., & Stella, N. (2004). P2X7 receptors control 2-arachidonoylglycerol production by microglial cells. *Proceedings of the National Academy of Sciences*, *101*(9), 3214–3219.

Wolach, B., Sazbon, L., Gavrieli, R., Broda, A., & Schlesinger, M. (2001). Early immunological defects in comatose patients after acute brain injury. *Journal of neurosurgery*, *94*(5), 706–11.

Wong, P., Laxton, V., Srivastava, S., Chan, Y. W. F., & Tse, G. (2017). The role of gap junctions in inflammatory and neoplastic disorders (Review). *International journal of molecular medicine*, *39*(3), 498–506.

Wood, T. B., Spivey, W. T. N., & Easterfield, T. H. (1899). III.—Cannabinol. Part I. *J. Chem. Soc., Trans.*, *75*(0), 20–36.

Xie, J., Xiao, D., Xu, Y., Zhao, J., Jiang, L., Hu, X., Zhang, Y., & Yu, L. (2016). Up-regulation of immunomodulatory effects of mouse bone-marrow derived mesenchymal stem cells by tetrahydrocannabinol pre-treatment involving cannabinoid receptor CB2. *Oncotarget*, *7*(6), 6436–

47.

Xin, J., Wainwright, D. a, Mesnard, N. a, Serpe, C. J., Sanders, V. M., & Jones, K. J. (2011). IL-10 within the CNS is necessary for CD4+ T cells to mediate neuroprotection. *Brain, behavior, and immunity*, *25*(5), 820–9.

Yanaba, K., Bouaziz, J.-D., Matsushita, T., Tsubata, T., & Tedder, T. F. (2009). The Development and Function of Regulatory B Cells Expressing IL-10 (B10 Cells) Requires Antigen Receptor Diversity and TLR Signals. *The Journal of Immunology*, *182*(12), 7459–7472.

Yanagisawa, M., Kurihara, H., Kimura, S., Tomobe, Y., Kobayashi, M., Mitsui, Y., Yazaki, Y., Goto, K., & Masaki, T. (1988). A novel potent vasoconstrictor peptide produced by vascular endothelial cells. *Nature*, *332*(6163), 411–415.

Yu, S.-J., Reiner, D., Shen, H., Wu, K.-J., Liu, Q.-R., & Wang, Y. (2015). Time-Dependent Protection of CB2 Receptor Agonist in Stroke. *PloS one*, *10*(7), e0132487.

Zaheer, S., Kumar, D., Khan, M. T., Giyanwani, P. R., & Kiran, F. (2018). Epilepsy and Cannabis: A Literature Review. *Cureus*, *10*(9), e3278.

Zarruk, J. G., Fernández-López, D., García-Yébenes, I., García-Gutiérrez, M. S., Vivancos, J., Nombela, F., Torres, M., Burguete, M. C., Manzanares, J., Lizasoain, I., & Moro, M. A. (2012). Cannabinoid Type 2 Receptor Activation Downregulates Stroke-Induced Classic and Alternative Brain Macrophage/Microglial Activation Concomitant to Neuroprotection. *Stroke*, *43*(1), 211–219.

Zelasko, S., Arnold, W. R., & Das, A. (2015). Endocannabinoid metabolism by cytochrome P450 monooxygenases. *Prostaglandins & other lipid mediators*, *116–117*, 112–23.

Zhang, Ji, Hoffert, C., Vu, H. K., Groblewski, T., Ahmad, S., & O'Donnell, D. (2003). Induction of CB2 receptor expression in the rat spinal cord of neuropathic but not inflammatory chronic pain models. *The European journal of neuroscience*, *17*(12), 2750–4.

Zhang, Jing, Shi, K., Li, Z., Li, M., Han, Y., Wang, L., Zhang, Z., Yu, C., Zhang, F., Song, L., Dong, J.-F., La Cava, A., Sheth, K. N., & Shi, F.-D. (2018). Organ- and cell-specific immune responses are associated with the outcomes of intracerebral hemorrhage. *The FASEB Journal*, *32*(1), 220–229.

Zhang, M., Martin, B. R., Adler, M. W., Razdan, R. K., Jallo, J. I., & Tuma, R. F. (2007). Cannabinoid CB(2) receptor activation decreases cerebral infarction in a mouse focal ischemia/reperfusion model. *Journal of cerebral blood flow and metabolism : official journal of the International Society of Cerebral Blood Flow and Metabolism*, *27*(7), 1387–96.

Zheng, H., Cao, N., Yin, Y., & Feng, W. (2017). Stroke recovery and rehabilitation in 2016: a year in review of basic science and clinical science. *Stroke and vascular neurology*, *2*(4), 222–229.

Zheng, W., ZhuGe, Q., Zhong, M., Chen, G., Shao, B., Wang, H., Mao, X., Xie, L., & Jin, K. (2013). Neurogenesis in adult human brain after traumatic brain injury. *Journal of neurotrauma*, *30*(22), 1872–80.

Zhou, X., He, X., & Ren, Y. (2014). Function of microglia and macrophages in secondary damage after spinal cord injury. *Neural regeneration research*, *9*(20), 1787–95.

Zhou, Z., Peng, X., Insolera, R., Fink, D. J., & Mata, M. (2009). Interleukin-10 provides direct trophic support to neurons. *Journal of neurochemistry*, *110*(5), 1617–27.

Zierath, D., Shen, A., Stults, A., Olmstead, T., & Becker, K. J. (2017). Splenectomy Does Not Improve Long-Term Outcome After Stroke. *Stroke*, *48*(2), 497–500.

Zygun, D. A., Zuege, D. J., Boiteau, P. J. E., Laupland, K. B., Henderson, E. A., Kortbeek, J. B., & Doig, C. J. (2006). Ventilator-associated pneumonia in severe traumatic brain injury. *Neurocritical care*, *5*(2), 108–14.